**U.S. Department of Energy**
**1000 Independence Avenue, S.W.**
**Washington, D.C. 20585-0121**

# FY 2002

# Progress Report for Combustion and Emission Control for Advanced CIDI Engines

**Energy Efficiency and Renewable Energy**
**Office of FreedomCAR and Vehicle Technologies**

**Approved by Gurpreet Singh**

**November 2002**

# CONTENTS

# INDEX OF PRIMARY CONTACTS



(click on a person or page number to go to the corresponding report)

# I. INTRODUCTION

## Developing Advanced Combustion and Emission Control Technologies

Gurpreet Singh
Team Leader
Engine and Emission-Control Technologies

On behalf of the Department of Energy's Office of FreedomCAR and Vehicle Technologies, we are pleased to introduce the Fiscal Year (FY) 2002 Annual Progress Report for the Advanced Combustion and Emission Control Research and Development (R&D) Activity. This Activity is focused primarily on the compression ignition, direct injection (CIDI) engine, an advanced version of the commonly known diesel engine, which is used in both light- and heavy-duty vehicles. Extending the use of CIDI engines to light-duty vehicles (especially pickups, vans, and sport utility vehicles) has the potential to significantly improve new vehicle fuel economy and directly addresses the National Energy Policy recommendation to increase the fuel economy of new vehicles without negatively impacting the U.S. automotive industry.

This introduction serves to outline the nature, current progress, and future directions of the Combustion and Emission Control R&D Activity for advanced CIDI engines. Together with DOE National Laboratories and in partnership with private industry and universities across the United States, DOE engages in high risk research and development that provides enabling technology for fuel efficient and environmentally-friendly light- and heavy-duty vehicles. The work conducted under this Activity relies on the DOE Advanced Petroleum-Based Fuels (APBF) Program to provide on-going reformulated diesel fuel developments and to enable meeting our out-year objectives. (The APBF Program is described in a separate report.)

Ken Howden
CIDI Technology
Development Manager

Combustion and Emission Control R&D activities are sharply focused on improving emission control technologies to maintain the high fuel efficiency of CIDI engines while meeting future emission standards. Until the EPA light-duty Tier 2 regulations take effect in 2004 and the heavy-duty engine emission standards take effect in 2007, CIDI engines will be able to meet emissions regulations through enhanced combustion alone. It is now clear that CIDI engines for both light- and heavy-duty vehicles will need exhaust emission control devices in order to meet both the oxides of nitrogen ($NO_x$) and particulate matter (PM) emissions regulations. This situation is analogous to the early 1970s, when gasoline vehicles transitioned to catalytic emission control devices. Both $NO_x$ and PM emission control devices will have to achieve conversion efficiencies of 80 to 95 percent to meet the emission standards for both light-duty vehicles and heavy-duty engines.

Kevin Stork
CIDI Technology
Development Manager

The Environmental Protection Agency (EPA), in their June 2002 report on the progress towards development of the technology to meet the 2007 heavy-duty engine emission regulations[1], cited this Activity as one of their primary sources of information. The Combustion and Emission Control R&D Activity addresses the

1. "Highway Diesel Progress Review," Environmental Protection Agency report EPA420-R-02-016, June 2002, available from http://www.epa.gov/air/caaac/.

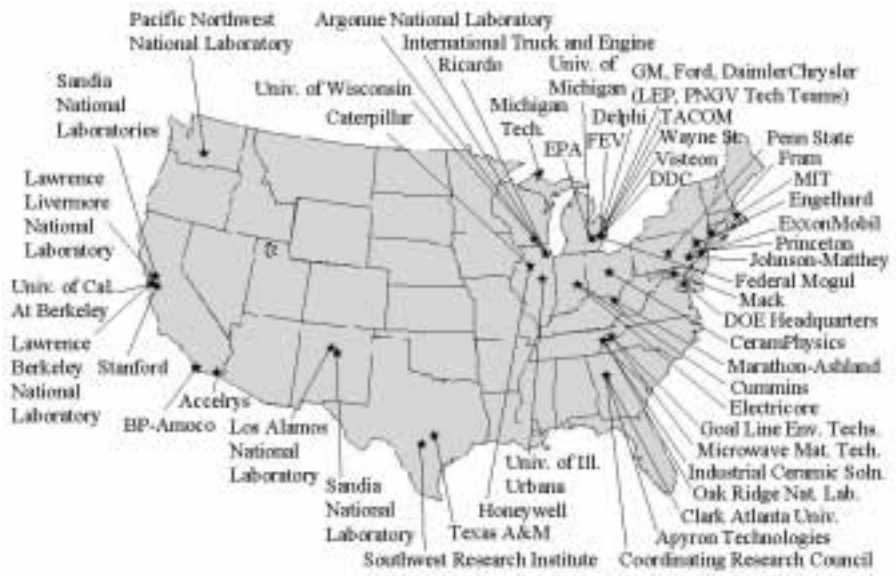


Combustion and Emission Control for Advanced CIDI Engines Activity Participants

fundamental CIDI emission control issues in a cooperative manner with the U.S. automotive industry to assure that the necessary technology is ready and available to implement.

The Combustion and Emission Control R&D Activity for advanced CIDI engines supports the government/industry FreedomCAR partnership through its technology research projects. Today's CIDI engines achieve impressive thermal efficiency; however, in order to meet future emissions standards, advancements in clean combustion, emission control technology and diesel fuels are necessary. The DOE Light Truck goal is to increase the fuel efficiency of light trucks by 35 percent by 2004, while meeting Tier 2 emission standards. Because the emission challenges facing CIDI engines are very similar for both light- and heavy-duty vehicle applications, this Activity has been designed to develop technologies capable of addressing both.

The Advanced Combustion and Emission Control R&D Activity explores the fundamentals of combustion, how emissions are formed, and advanced methods for reducing those emissions to acceptable levels. Testing and modeling are important elements of the Activity and enable us to evaluate potential technology and validate technology selection and direction. By working at the forefront of these new technologies in cost-sharing arrangements with industry, we hope to enhance the knowledge base that can be used by our automotive partners and suppliers (engine manufacturers, catalyst companies, etc.) to develop highly efficient CIDI engines with emissions that meet future standards.

A Dodge Dakota Pickup with a DDC 4.0 Liter CIDI Engine having 63% higher Fuel Economy than its Gasoline Counterpart

## Challenges

Much progress continues to be made on CIDI emission control technology. To control $NO_x$, absorber catalysts, selective catalytic reduction (SCR), and non-thermal plasma catalysts are all potential candidates.

The reduction efficiency of absorber catalysts continues to improve, with steady-state efficiencies at optimum temperatures exceeding 90% routinely. The temperature range for which these catalysts are active continues to broaden. Even so, many improvements are needed before absorbers will be considered to be viable for commercial applications. These include: the ability to maintain high conversion efficiencies over the full useful life of the vehicle; the ability to "bounce back" following exposure to high-sulfur fuels; the ability to reduce $NO_x$ effectively over transient operating conditions; the development of effective desulfurization procedures and/or sulfur traps; minimization of the fuel required during regeneration and desulfurization; the ability to package the catalysts into volumes that will fit within the spaces available on vehicles; identification of how to best integrate absorbers with PM devices; and the ability to manufacture these devices at prices that will be acceptable to consumers.

A Dodge Durango with a Cummins V6 CIDI Engine having 53% higher Fuel Economy than its Gasoline Counterpart

SCR catalysts using urea as a reductant are showing very good performance and are claimed to be less sensitive to sulfur than absorber catalysts. The largest hurdle to using urea-SCR is that a completely new distribution system would be needed to supply urea to the vehicles that use it. A system to co-fuel both diesel fuel and urea using one coaxial hose has been demonstrated. However, no proposal has been offered as to how to prevent users from operating their vehicles without urea or to assure that urea will be available at all the refueling facilities. Infrastructure issues aside, urea-SCR catalysts still have characteristics that need improvement before wide-spread commercialization. One of these issues is "ammonia slip" (ammonia leaves the catalyst without being reacted). While small amounts of ammonia emissions are not deemed to be detrimental to air quality or health, they are undesirable because of their odor. Urea also causes emissions such as alkyl nitrate compounds, which are not present when using only hydrocarbon fuels.

Non-thermal plasma (NTP) systems continue to make significant progress in terms of $NO_x$ reduction efficiency and reduced energy requirements. These improvements have come about through discovery of more efficient and durable catalysts, innovative placement of these catalysts in conjunction with the plasmas, and a better understanding of the reactions occurring on the catalysts. A unique advantage of NTP is that the plasma causes a significant reduction in PM (20-30%). While this reduction does not appear to be sufficient to obviate the need for a PM device, it certainly opens the possibility for a smaller and less costly PM device. Another advantage of some NTP catalysts is that they are quite tolerant of sulfur from the fuel and lubricating oil. A potential problem with some NTP systems is that they can emit $N_2O$, which is a strong greenhouse gas. Current work on NTP is focused on how to combine these synergist components in a manner that will make NTP fully competitive with $NO_x$ absorbers and urea-SCR catalysts.

The advancement of emission control devices has highlighted the need for reliable, durable, and low-cost sensors to control these devices while in use. There is great need for $NO_x$ sensors in multiple applications, and

ammonia sensors for urea-SCR systems. Sensors are also needed to control and optimize the use and regeneration of PM emission control devices.

Through the process of measuring PM emissions from CIDI engines, and devising control systems, much is being learned about PM, not only in terms of mass emissions, but size distribution and toxicity. Recent developments show that CIDI engines using ultra-low sulfur fuel and PM emission control devices have PM emissions similar in mass to gasoline vehicles, and much less than gasoline high emitters (white and black smoking vehicles). Little difference has been found between the toxicity of PM from gasoline and diesel vehicles per unit mass, but the PM from high-emitters (gasoline or diesel) is more toxic than the PM from properly maintained vehicles. This suggests that CIDI vehicles with PM emission control devices may pose no greater health risk than comparable gasoline vehicles. There now is also evidence that new CIDI engines do not form more nanoparticles than older engines - nanoparticles appear to be formed primarily from hydrocarbons (mostly from lubricating oil) and sulfur (from the fuel and lubricating oil). The challenge is to use this knowledge effectively in the design of PM emission control devices, and to educate the public about these positive findings.

## Accomplishments

In FY 2002, significant progress was made on emission control subsystems that would enable CIDI-engine-powered passenger cars and light-duty trucks to meet Tier 2 emission standards. Improved catalyst formulations are allowing $NO_X$ absorbers to be effective over a wider range of temperatures (with most of the improvements occurring at the lower end of the temperature range). The efficiency of NTP systems continues to improve while their energy requirement decreases. Also, NTP systems have been found to significantly reduce PM emissions (though not enough to meet the standards). Urea-SCR systems have undergone extensive optimization during the past year and are being tested for durability. More is being learned about how exhaust gas recirculation (EGR) can reduce $NO_X$ emissions without increasing PM emissions. Work

**Current Status and Technical Targets for CIDI Engine Technology Development[a]**

| Characteristics | Units | Calendar year | | |
|---|---|---|---|---|
| | | 2002 Status | 2004 | 2010 |
| Emission control cost[b] | $/kW | TBD | 4 | 3 |
| Exhaust emission control device volume | L / L[c] | 4 | 2 | 1.5 |
| $NO_x$ emissions (full useful life) | (g/mile) | 0.15 | 0.07 | 0.03 |
| PM emissions (full useful life) | (g/mile) | 0.015 | 0.01 | 0.01 |
| Durability | hrs | <500 | 1000 | 5000[d] |
| Fuel Economy Penalty due to Emission Control Devices[e] | (%) | 6-10 | <8 | <5 |

[a]Targets are for a small passenger car using advanced petroleum-based fuels with 15 ppm sulfur content; all targets must be met simultaneously.
[b]High-volume production: 500,000 units per year.
[c]Liter per liter of engine displacement.
[d]Representative of full-useful-life durability for light-duty vehicles.
[e]Energy used in the form of reductants derived from the fuel, electricity for heating and operation of the devices, and any other energy demand including things that reduce engine efficiency, such as increased exhaust backpressure.

towards practical $NO_x$ sensors continues to advance, setting the stage for optimal control of $NO_x$ conversion devices. More detailed characterization of combustion processes is further reducing engine-out emissions and forming the foundation for the development of advanced combustion technologies such as homogeneous charge compression ignition. Regenerative PM filtration devices are in advanced development, with several fleet tests completed. The accompanying table shows current progress relative to the Activity 2004 and 2010 Technical Targets. What the table does not show is that while progress is being made towards the Technical Targets, attaining acceptable CIDI emission control device durability may pose a more significant hurdle than previously anticipated, even with 15 ppm sulfur content fuel, because of the contribution of consumed lubricating oil to $SO_2$ in the exhaust, and because of the difficulty of assuring all diesel fuel will have less than 15 ppm sulfur. Projects on sulfur traps have been initiated during the past year to address this concern.

## DDC Demonstrates Low $NO_x$ and PM Over the FTP Transient Cycle Using a Small Passenger Car Test Vehicle

Detroit Diesel Corporation (DDC) has completed the second year of a 36-month project to develop CIDI engine emission control technologies that meet future emission regulations. Progress during the second year has included refinement of their "CLEAN Combustion©" strategies to lower engine-out emissions, development of an integrated $NO_x$ (urea-SCR) and PM emission control system, application of that system to a small passenger car test vehicle, testing of that vehicle over the transient FTP Cycle, and completion of limited catalyst aging tests. The development of an integrated $NO_x$ and PM emission control system for light-duty truck applications using the 4.0-liter DDC DELTA engine is also progressing. The application of CLEAN Combustion© and the development of the integrated emission control system allowed the light-duty passenger car to progress from emission standards of Tier II Bin 9 to Tier II Bin 3, a highly significant achievement over the transient FTP Cycle. Similar development using the 4.0-liter DDC DELTA engine is showing reductions of 89% for $NO_x$ and 93% for PM over the transient hot-505 cycle (less demanding than the FTP Cycle). The DDC team has achieved their intermediate performance and emissions milestones related to engine and emission control system technologies. The ultimate integration of these technologies into a prototype light-duty truck demonstrating 2007+ Tier 2 emissions and performance targets remains as a challenging target for future R&D efforts.

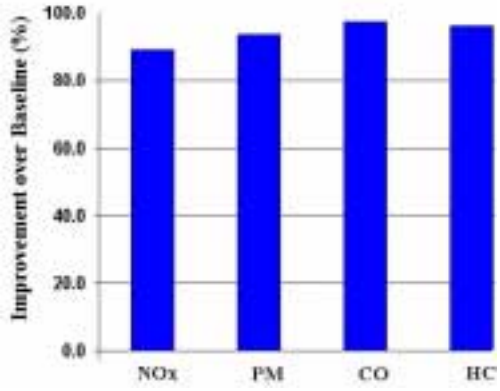


Emissions Reductions of the DDC DELTA 4.0-liter Engine from Application of CLEAN Combustion© and an Unoptimized Integrated Emission Control System

## Cummins Advances the Efficiency and Durability of Their Integrated $NO_x$ and PM Diesel Emission Control System

Cummins has completed the second year of a 36-month project to develop an integrated CIDI engine emission control system based on an $NO_x$ absorber and catalyzed PM filter. Progress during the second year has included development of a new absorber formulation that has extended operation to temperatures 100°C cooler than before which has increased $NO_x$ conversion to 87% over a simulated FTP Cycle. They were also

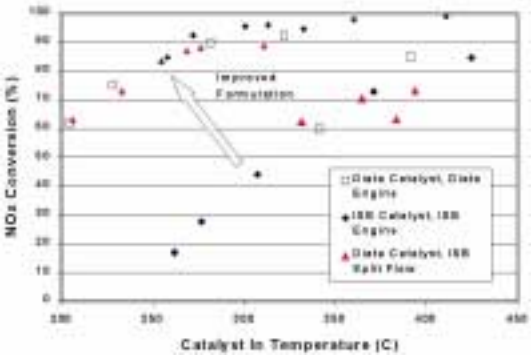


Cummins Improved Catalyst Formulation Has Significantly Improved $NO_x$ Conversion at Low Temperatures

able to reduce the fuel consumption penalty of regeneration down to 3% at cruise conditions. An offline regenerable $SO_x$ trap with sufficient capacity to trap almost 100% of the fuel- and oil-derived sulfur for greater than 20,000 miles has been demonstrated, and work is in progress to increase the operation interval to more than 30,000 miles. Spectroscopic techniques were applied to understand the underlying chemical reactions over the catalyst surface during $NO_x$ trapping and regeneration periods to obtain a fundamental understanding of absorber storage capacity and degradation mechanisms. In the coming year, Cummins plans to further refine this system and test it on the highway and over the transient FTP Cycle.

## Ford Demonstrates a Pathway for Light-Duty Trucks to Achieve Tier II Bin 5 Standards Using Urea-SCR

Ford Motor Company has initiated a project to develop and demonstrate a highly efficient exhaust emission control system for light-duty CIDI engines to meet 2007 Tier II Bin 5 emission standards (0.07 g/mi $NO_x$, 0.01 g/mi PM) with minimal fuel economy penalty and greater than 5,000 hours of durability. (Tier II standards require 90+% $NO_x$ and PM conversion.) Ford modeled two urea-SCR systems, but neither system by itself is predicted to meet the 90% $NO_x$ conversion target required to meet Tier II standards. More rapid heating of the SCR catalyst is needed to reach higher activity sooner. Initial tests using a Ford F-250 light-duty truck yielded only 65% $NO_x$ conversion efficiency over the transient FTP Cycle. Results indicate that the injection system needs to more effectively distribute the reductant to the entire SCR catalyst to achieve higher conversion efficiencies. Ford believes that rapid warm-up of the exhaust system during a cold-start is key to achieving 90+% $NO_x$ conversions required to meet the light-duty Tier II Bin 5 standards. Further optimization of the aqueous urea injection strategy and hardware is also required to allow full utilization of the urea reductant by the SCR catalyst, thus improving $NO_x$ conversion. Continued research on $NO_x$ and $NH_3$ sensors is needed for better selectivity and durability of the emission control devices.

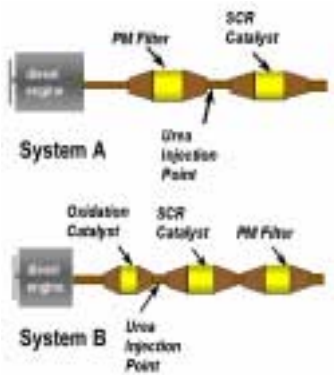


SCR Systems Explored by Ford

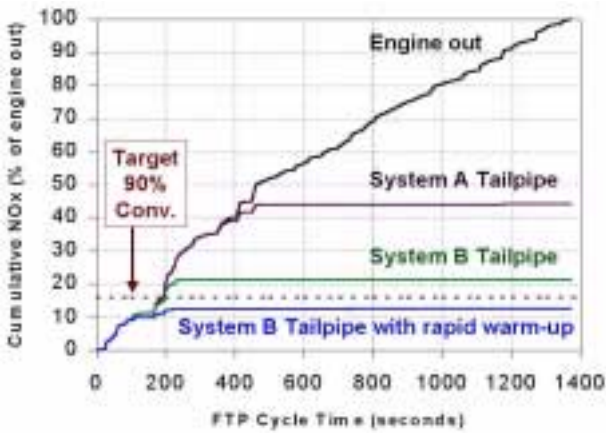


Predicted System Efficiencies

## Pacific Northwest National Laboratory Advances NTP Technology Using a "Cascade Reactor" Approach

Pacific Northwest National Laboratory (PNNL) and its Cooperative Research and Development Agreement (CRADA) partners from Ford, General Motors and DaimlerChrysler have been developing a plasma-assisted catalyst system that is showing great promise for treating emissions of $NO_x$ and PM from the exhaust of CIDI engine-powered vehicles. PNNL has invented a new conceptual plasma/catalyst system that offers the promise of achieving the 90% $NO_x$ reduction targets with significantly reduced input power

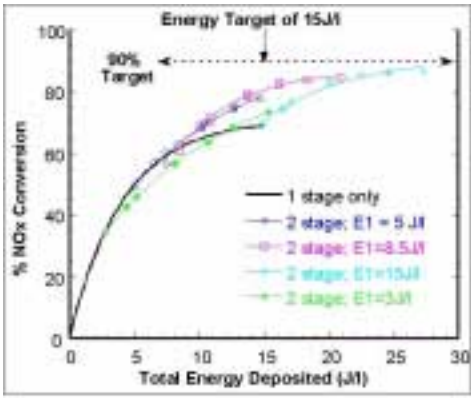


The Benefit of the Cascade Reactor is Increased $NO_x$ Conversion with Equal Energy Input

requirements. This system uses two plasma catalysts in series in a "Cascade Reactor." High $NO_x$ conversions have been demonstrated over a wide temperature range on simulated diesel exhaust. Furthermore, high conversions have been demonstrated in engine tests utilizing real diesel exhaust and diesel fuel as the added reductant. The results obtained in the last year provide good evidence that the overall activity targets of 90% $NO_x$ reduction with less than a 5% fuel-economy penalty are within reach.

## Pacific Northwest National Laboratory Develops an Integrated NTP $NO_x$ and PM Emission Reduction System

Pacific Northwest National Laboratory (PNNL) and its CRADA partner Delphi Automotive Systems have developed an integrated NTP catalyst and particulate filter system for PM and $NO_x$ reduction. $NO_x$ reduction levels as high as 100% were demonstrated to be possible with a plasma assisted catalysis system during pilot-scale reactor testing. On-vehicle steady-state conditions with a sub-scale prototype system achieved 50% peak $NO_x$ reduction, with an 8% total fuel consumption penalty (5% due to electrical demand and 3% for supplemental HC injection). One of the significant breakthroughs this last year was the discovery of a new method to apply power to the plasma reactor, which requires only 25% of the energy needed for the typical AC power supply system. The development of a compact and efficient pulsed power supply will be a major focus for next year's activities.


Sub-Scale Prototype System Used for On-Vehicle Testing

## Researchers Make Significant Advancements Towards Practical $NO_x$ Sensors

$NO_x$ sensors are needed to control regeneration of $NO_x$ emission control devices, and at present, no commercial $NO_x$ sensors exist. Researchers at Lawrence Livermore National Laboratory, Oak Ridge National Laboratory, Delphi Corporation, and CeramPhysics are all developing $NO_x$ sensors. The challenges facing commercial $NO_x$ sensors include response time, sensitivity, selectivity, durability, packaging, and cost. Each of these contractors is using a slightly different approach to $NO_x$ sensor design and construction. Prototype sensors will soon be available for testing.

Proposed Mock-Up of Delphi $NO_x$ Sensor

## Oak Ridge National Laboratory Explores the Use of EGR to Lower Engine-Out $NO_x$

While much activity is ongoing to develop emission control devices to remove $NO_x$, it is possible to significantly reduce $NO_x$ leaving the engine by application of exhaust gas recirculation (EGR). Oak Ridge National Laboratory (ORNL) is conducting two projects on EGR, one to explore the ultimate potential of EGR to reduce engine-out $NO_x$, and the other to develop a measurement methodology to measure EGR distribution

within the intake system of an engine. ORNL researchers found that with proper application of EGR, $NO_x$ could be reduced much more than typically believed without detrimental impacts on particulate emissions and fuel consumption. However, for the maximum benefits to be achieved, EGR must be distributed evenly among the engine cylinders. ORNL has developed a measurement methodology that does this with a high degree of accuracy. Work is continuing by ORNL to identify new combustion regimes using EGR that exhibit the desirable properties of simultaneous low $NO_x$ and PM emissions. Further analysis of the extensive data collected during this investigation is expected to improve the understanding of these new combustion regimes and reveal information to exploit these conditions further for improved emissions.

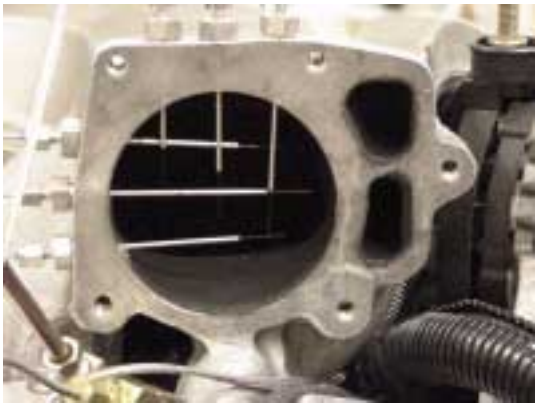

Measurement of EGR Distribution in a Diesel Engine Intake Manifold

## Microwave-Regenerated Diesel Particulate Filter Initiates 7,000 Mile Durability Test

Industrial Ceramic Solutions has redesigned their microwave-regenerated diesel particulate filter to use a new pleated paper cartridge element that is more durable and achieves significantly lower pressure drop. The new paper cartridge element has only 5% of the pressure drop that the previously used material had. (Lower pressure drop is very desirable because diesel engines lose power and efficiency when exhaust back-pressure increases.) The new particulate filter design has been tested on a vehicle in typical driving conditions for nine months without experiencing any failures. A 7,000 mile track test is soon to be conducted to measure particulate collection efficiency, impact on fuel economy, and overall durability of the system.


Industrial Ceramic Solutions Has Significantly Reduced the Pressure Drop of Their Microwave-Regenerated Particulate Filter

## Sandia National Laboratories Furthers the Ability to Model Combustion Turbulence

Introduction of flow swirl in direct-injection diesel combustion systems is an established technique for reducing engine-out PM emissions and enabling reduced $NO_x$ emissions by permitting injection timing retardation and increasing the combustion system EGR tolerance. Swirl influences PM emissions through two paths: reduced formation of PM and more rapid destruction of the PM formed via enhanced flow turbulence and mixing. In spite of its clear potential for enhancing diesel combustion, the physics of swirl-supported combustion systems is still poorly understood. Sandia National Laboratories (SNL) identified a turbulence production mechanism that significantly enhances late-cycle flow turbulence and may speed the oxidation of unburned fuel and

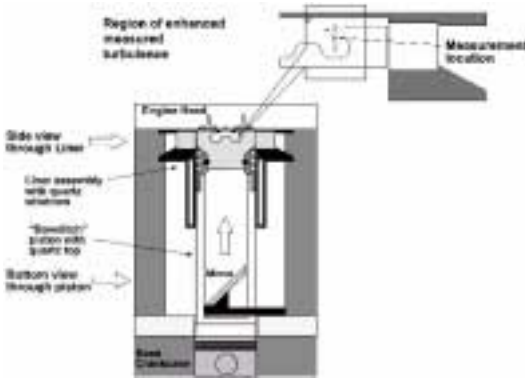


The Sandia Optical Engine Showing the Location of the Turbulence Measurement and Study

PM. Detailed measurements of the characteristics of the turbulence field have clarified the reasons behind the model and will lead to more accurate model predictions. SNL plans to verify the influence of late-cycle turbulence on engine-out emissions of $NO_x$ and PM. They also plan to investigate the interaction of the fuel jets and the mean in-cylinder flow to find conditions for optimal enhancement of turbulence and mixing.

## Argonne National Laboratory Enhances Their X-Ray Fuel Spray Measurement Technique to Include Injection Mass

Using x-radiography, Argonne National Laboratory (ANL) has demonstrated that diesel engine injector fuel sprays are supersonic and that the Mach cone generated by the supersonic sprays can be directly imaged and quantitatively analyzed. Although the manner in which the shock waves affect the atomization of the fuel and the combustion process are currently unknown, the results will likely draw the attention of spray and combustion researchers to investigate their effects. The accuracy of the x-radiographic technique in determining fuel mass was measured using an independent method and was found to have a discrepancy smaller than 5%. Most importantly, in FY 2002, ANL demonstrated that the x-radiography of fuel sprays is possible in a pressurized chamber. More systematic studies of fuel sprays are being conducted and will become the focus of the next few years' research. ANL received the DOE National Laboratory Combustion & Emissions Control R&D Award for this work.

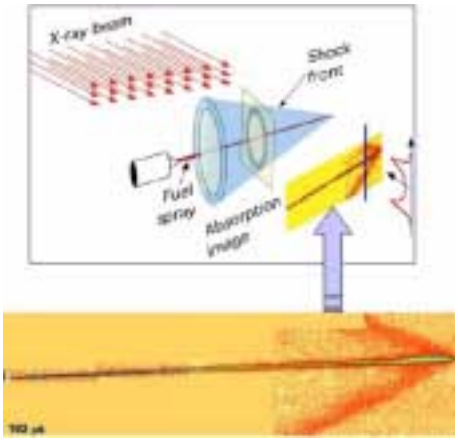


X-Ray Image of a Fuel Spray (bottom) and Schematic of the Apparatus. The Shock Wave is the Image Spreading Out from the Tip of the Fuel Spray.

## Understanding of Homogeneous Charge Compression Ignition is Enhanced and Models are Improved

Homogeneous Charge Compression Ignition (HCCI) engines can have efficiencies as high as CIDI engines, while producing ultra-low emissions of $NO_x$ and PM. HCCI engines can operate on gasoline, diesel fuel, and most alternative fuels. HCCI represents the next major step beyond high-efficiency CIDI engines and has the potential to be less costly because the fuel injection and emission control systems it needs are more basic and less complex. DOE is currently funding research activities at two national laboratories and is co-funding two university-consortium HCCI-research projects with several industry companies. The objective of these projects is to identify the conditions necessary to make HCCI work over the speed and load range of a practical engine. The following are just a few highlights of the HCCI work performed over the past year.

- Lawrence Livermore National Laboratory improved their HCCI combustion models to reduce computation time, predict the effect of cylinder geometry on HCCI combustion, and improve the ability to predict CO emissions (the most difficult HCCI emission to predict).
- Sandia National Laboratories completed a parametric investigation of HCCI performance and emissions over a wide range of intake temperatures, intake pressures, fueling rates, and engine speeds; showed that the high emissions and poor combustion efficiencies at low fuel loads are due to incomplete bulk-gas reactions; and showed that partial charge stratification obtained by late direct fuel injection can substantially improve combustion efficiencies and emissions at low loads without significantly affecting $NO_x$ and smoke.
- Sandia National Laboratories also identified several alternative fuel/tracer mixtures that improve the accuracy of Laser Induced Fluorescence imaging of HCCI combustion and applied vapor-liquid equilibrium theory to successfully model evaporation of simple fuel/tracer mixtures.

- The University of Wisconsin Consortium has developed a combustion control criterion based on the ignition/injection time delay, developed a multidimensional model for early and late injection, demonstrated that HCCI ignition is controlled by effects beyond fuel octane number, formulated computationally efficient methods to incorporate detailed chemistry submodels, and demonstrated HCCI combustion at both very early and very late start-of-injection timings.
- The University of Michigan Consortium demonstrated the use of variable valve actuation to achieve HCCI, developed a thermo-kinetic model of HCCI for rapid computation in engine system simulations, developed a multi-zone model of HCCI operation, obtained benchmark ignition data on simple hydrocarbon fuels, and isolated key elementary chemical reactions important in cool HCCI 'flames.'

## Future Directions

Emission Control Subsystem Technology Development: Research in this area continues to move towards development and testing of complete, integrated systems for meeting future $NO_x$ and PM targets. As designs progress, they are being put to more stringent tests including transient driving cycles with cold-starts. As success with new devices is achieved, the focus will change to getting sufficient durability to meet full useful life requirements. The following are some specific project activities that will be pursued in the coming year.

- DDC will develop and apply the latest generation of aftertreatment systems to the 4.0L engine, refine their CLEAN Combustion© technology and investigate potential to eliminate or reduce the size of aftertreatment devices, and further improve fuel economy and reduce emissions levels.
- Cummins will complete preliminary emission testing of a mobile emission control system on a light-duty vehicle, continue to develop and optimize catalyst formulations for best $NO_x$ and PM conversion efficiency under exhaust temperatures and space velocities consistent with anticipated light-duty applications, and continue to develop and design an offline regenerable sulfur trap to provide sufficient capacity to trap 99+% fuel-oil-derived $SO_x$ with greater than 30,000 miles service interval.
- Ford will install a catalyzed PM filter on the F-250 truck downstream of the SCR system and implement a filter regeneration control strategy, develop onboard diagnostics for identifying possible system malfunctions and to improve the adaptiveness and robustness of the control model, and select the most promising ammonia sensing technology, increase its durability and selectivity in diesel exhaust gas, and develop appropriate control strategies.
- ORNL will examine different $NO_x$ adsorber, CDPF, and DOC configurations, refine strategies to achieve acceptable HC and CO slip, speciate hydrocarbons at the DOC inlet and adsorber inlet; correlate with regeneration strategy, system performance, and develop desulfation strategies, speciate hydrocarbons and measure $H_2S$ and $SO_2$.
- Apyron will scale-up synthesis and processing of adsorbent formulation, work in collaboration with International Truck and Engine Corporation to optimize the sulfur dioxide trap, and develop regeneration protocol for sulfur dioxide adsorbents.

$NO_x$ Catalysts and Sensors: The fundamentals of $NO_x$ catalyst development continue to advance, and several competing designs for $NO_x$ sensors continue to show promise. While tremendous gains have been made in $NO_x$ conversion efficiencies, progress is still needed to widen the effective temperature range, identify more effective and efficient regeneration and desulfurization methods, make $NO_x$ conversion devices more durable to sulfur contamination and thermal stress, and reduce the volume needed to package them.

- As part of the Low Emissions Partnership CRADA, LANL and SNL will continue to synthesize, characterize, and test new catalyst compositions as ammonia SCR catalysts, ORNL will benchmark the performance of a Ford Focus equipped with a urea SCR emissions control system on a chassis dynamometer, and $NO_x$ reduction activity data for promising catalysts will be validated at other national laboratories and the LEP.
- PNNL will continue fundamental mechanistic studies that focus on the surface chemistry of acetaldehyde and $NO_2$ on the active plasma catalyst materials, focus studies of the plasma device on identifying conditions for optimized production of the important reductant materials (aldehydes), identify fate and form of PM following 'treatment' by the plasma reactor, and verify current status of this novel technology by regular full-scale engine tests.
- CeramPhysics will build and test prototype $NO_x$ and dual $O_2$ and $NO_x$ sensors.
- Delphi will continue to refine the electrode materials and performance for $NO_x$ separation, begin to evaluate electronic measurement techniques and define sampling rates, operating temperatures, etc., develop the sensing element structure for ease of manufacture and improved performance, and continue with durability testing of mechanical (2nd generation design) and direct weld (1st generation design) interconnections.

Particle Control Technologies: The technology to reduce PM emissions is better developed than that for $NO_x$ devices. The current emphasis is on making PM emission control devices more durable, reducing impact on fuel consumption, and enabling controlled or continuous regeneration. PM sensors are also needed to assist in controlling regeneration.

- Industrial Ceramic Solutions will test their microwave-regenerated PM filter for 7,000 miles on a closed track and on-road for an additional 20,000 miles. System development and controls will continue to be refined to reduce energy requirements and control regeneration.
- Honeywell will produce their first PM sensors and electronics, and will begin testing them on an engine.

EGR Fundamentals: Measuring and controlling EGR provides a reliable means of reducing engine-out $NO_x$, which in turn reduces the demand placed on $NO_x$ conversion devices.

- Oak Ridge National Laboratory will continue their efforts to identify modes of engine operation where EGR reduces $NO_x$ with little or no impact on PM emissions. They will characterize the PM emissions during high EGR operation.

CIDI Combustion and Model Development: Advancements in fundamental combustion knowledge are useful for reducing emissions and increasing engine efficiency. Improvements in combustion knowledge direct future engine design and identify potential changes in fuels to facilitate emissions reductions.

- Sandia National Laboratories will continue their efforts to more accurately model in-cylinder turbulence and further investigate the interaction of fuel jets and air flow to identify conditions for optimal enhancement of turbulence and mixing. They will also use advanced laser imaging to examine the structure of diffusion flames and investigate other phenomena such as fuel jet wall impingement.
- Argonne National Laboratory will increase the power of their X-ray fuel spray imaging device, test it under pressures representative of diesel engines, and develop models to simulate the spray core and atomization near the injector nozzle.
- Lawrence Livermore National Laboratory will extend their kinetic modeling capabilities to include additional oxygenated compounds to assist in explaining PM production from diesel fuels.
- Argonne National Laboratory will continue to develop the production of small diameter injection holes through application of plating by constructing a forced-circulation system and testing plated injectors for spray characteristics and resistance to deposits.

Homogeneous Charge Compression Ignition: While HCCI could set a whole new paradigm for internal combustion engines, it could also be implemented on near-term engines for reduction in $NO_x$ and PM emissions at the low speeds and light loads typical of highway driving. In the longer term, HCCI could result in a wide range of cleaner and more efficient engines operating on fuels without octane or cetane requirements.

- Lawrence Livermore National Laboratory will build on their results to date to identify ways to achieve cold-starts, extend the operating range of HCCI combustion, and devise additional means of controlling engine speed and load when under HCCI.
- Sandia National Laboratories will investigate the effect of fuels on intake temperature requirements, explore the potential of late-cycle injection for HCCI using diesel fuel, and investigate various partial charge stratification concepts.
- The University of Michigan Consortium will improve their gasoline chemistry models by pursuing chemical kinetic and computational studies, and by conducting shock tube and rapid compression experiments.
- The University of Wisconsin Consortium will implement a high pressure unit injector to assess multiple injection strategies for HCCI, explore the ignition characteristics of diesel fuel through engine experiments, and implement and test efficient methods for including detailed kinetics in multidimensional models.

## Honors and Special Recognitions

- Dennis Siebers of Sandia National Laboratories received the Horning Award from the SAE (Society of Automotive Engineers) for best paper and technical contribution for his research on the evolution of soot in diesel fuel sprays. Dennis also received an award from SAE for excellence in oral presentation and was the invited keynote speaker at ILASS Americas, 15th Annual Conference on Liquid Atomization and Spray Systems (2002) summarizing research on diesel fuel jet development and soot formation processes.
- Mark Musculus of Sandia National Laboratories received SAE Oral Presentation Awards for two of his papers: SAE paper no. 2001-01-1295, 2001, "Diffusion-Flame/Wall Interactions in a Heavy-Duty DI Diesel Engine" and SAE paper no. 2001-01-1296, "Extinction Measurements of In-Cylinder Soot Deposition in a Heavy-Duty DI Diesel Engine."
- Jin Wang and his colleagues at Argonne National Laboratory received the DOE National Laboratory Combustion & Emissions Control R&D Award for their work on imaging of fuel sprays using x-rays. This award is given for outstanding achievement by National Laboratory staff working on advanced CIDI combustion and emissions control R&D. Jin received recognition of his work as an Outstanding Mentor from the Siemens Foundation, and as a Mentor from The College Board.

## Invention Disclosures

- J. B. Green Jr., R. M. Wagner, and C. Stuart Daw, "A Combustion Diagnostic for Active Engine Feedback Control". UT-Battelle is pursuing a patent on this invention disclosure.

The remainder of this report highlights progress achieved during FY 2002 under the Advanced Combustion and Emission Control R&D Activity. The following 41 abstracts of industry and National Lab projects provide an overview of the exciting work being conducted to tackle tough technical challenges associated with CIDI engines, including fuel injection, exhaust gas recirculation, fuel mixing, combustion processes, and catalytic exhaust treatment devices for controlling emissions. We are encouraged by the technical progress realized under this dynamic Activity in FY 2002. We also remain cognizant of the significant technical hurdles that lie ahead, especially those presented for CIDI engines to meet the EPA Tier 2 emission standards and heavy-duty engine standards for the full useful life of the vehicles. In FY 2003, we look forward to working with our industrial and scientific partners to overcome many of the barriers that still stand in the way of delivering advanced technologies for CIDI engines.

Gurpreet Singh
Team Leader,
Engine and Emission-Control Technologies
Office of FreedomCAR and Vehicle Technologies

Kenneth Howden
Office of FreedomCAR and Vehicle Technologies

Kevin Stork
Office of FreedomCAR and Vehicle Technologies

Kathi Epping
Office of FreedomCAR and Vehicle Technologies
(Currently with the Office of Hydrogen, Fuel Cells and Infrastructure Technologies)

# II. EMISSION CONTROL SUBSYSTEM TECHNOLOGY DEVELOPMENT

## A. Demonstration of Integrated $NO_x$ and PM Emission Controls for Advanced CIDI Engines

*Brian Bolton (Primary Contact), Nabil Hakim and Houshun Zhang*
*Detroit Diesel Corporation (DDC)*
*13400 Outer Drive, West*
*Detroit, MI 48239-4001*

*DOE Technology Development Manager: Ken Howden*

*Main Subcontractors: Engelhard Corporation, Iselin, NJ; Michigan Technological University*

This project addresses the following DOE R&D Plan barriers and and tasks:

*Barriers*

A. $NO_x$ Emissions

B. PM Emissions

*Tasks*

4c. Selective Catalytic Reduction Catalysts

5a. Catalyzed Diesel Particulate Filter

6. Prototype System Evaluations

### Objectives

- Demonstrate technologies that will achieve future federal Tier 2 emissions targets.
- Demonstrate production viable technical targets for engine-out emissions, efficiency, power density, noise, durability, production cost, and aftertreatment volume and weight.

### Approach

- Develop and use emerging combustion technologies combined with advanced aftertreatment to pursue integrated engine, aftertreatment and vehicle systems technical targets.
- Develop aftertreatment simulation models for emissions prediction, engine control and total system design.
- Select and evaluate (engine + aftertreatment) system(s) using an integrated experimental and simulation methodology.
- Conduct system performance, emissions and limited durability evaluation.

### Accomplishments

- Developed a first-generation, integrated CIDI engine and emissions-control system for passenger car and light-duty truck applications.

- Demonstrated Tier 2 Bin 3 emissions target over FTP75 on a DaimlerChrysler Neon test vehicle. Achieved combined fuel economy of 63 miles per gallon (integrating FTP75 and highway fuel economy transient cycle test results). Demonstrated feasibility to achieve Tier 2 Bin 8 emissions levels without active $NO_x$ aftertreatment.
- Applied first-generation emissions control system to a sports utility vehicle/light duty truck (SUV/ LDT) 4.0L engine.
- Demonstrated 89% $NO_x$ and 93% particulate matter (PM) reductions over Hot-505 transient engine tests for the 4.0L engine system.
- Refined "CLEAN Combustion©", providing lower engine-out $NO_x$ emissions while simultaneously improving aftertreatment $NO_x$ reduction over transient emissions tests.
- Conducted limited aging tests for selected catalysts and characterized the catalyst performance and emissions.
- Completed digital lab aftertreatment simulation tool milestones related to "stand-alone" model development and selective model validation. New strategies for urea injection control and PM regeneration are emerging.

### Future Directions

- Develop and apply the latest generation of aftertreatment systems to the 4.0L engine. Harvest synergy from other SUV/LDT engine technology programs, including retrofit of latest engine and aftertreatment technology into a SUV/LDT application, addressing the technology scalability issues.
- Refine CLEAN Combustion© technology and investigate potential to eliminate or reduce aftertreatment options to achieve Tier 2 emissions targets for SUV/LDT applications.
- Further improve fuel economy and emissions levels. Develop robust urea injection control and feasible diesel particulate filter (DPF) PM regeneration strategies. Conduct (simulation + hardware) integrated engine-aftertreatment-powertrain-vehicle system testing.

---

## Introduction

DDC is conducting the Low Emissions Aftertreatment and Diesel Emissions Reduction (LEADER) program under a DOE project entitled "Research and Development for Compression-Ignition Direct-Injection Engines (CIDI) and Aftertreatment Subsystem." LEADER is to develop emissions control technologies on vehicles and demonstrate scalability to various vehicle inertia classes. The ultimate objective of this program is to achieve aggressive vehicle emissions targets for 2007 and beyond.

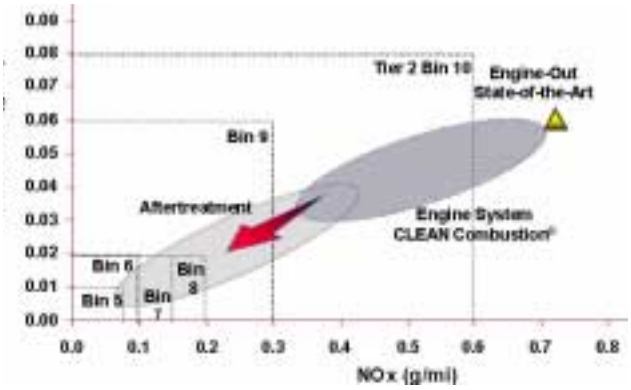


**Figure 1**. Integrated Emissions Reduction Road Map

## Approach

DDC's CLEAN Combustion© strategies have been developed, resulting in substantial advantages over conventional engine $NO_x$-PM trade-off characteristics. In addition, exhaust temperature increase and favorable species generation of CLEAN Combustion© offer an improved environment for aftertreatment integration. Our integrated emissions reduction roadmap is shown in Figure 1. The strategy is to pursue an integrated engine,

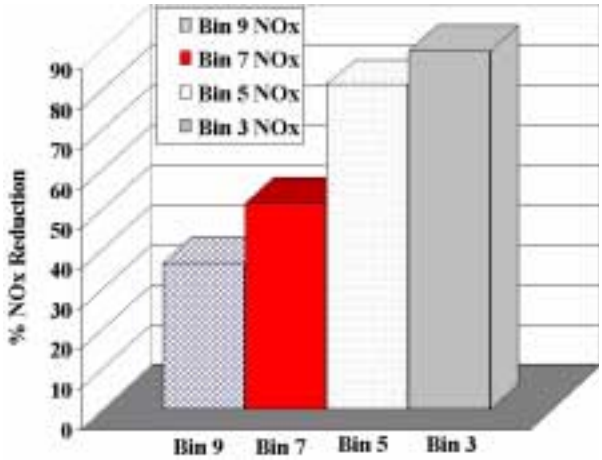


**Figure 2.** Aftertreatment Enhancement Progress Over FTP75

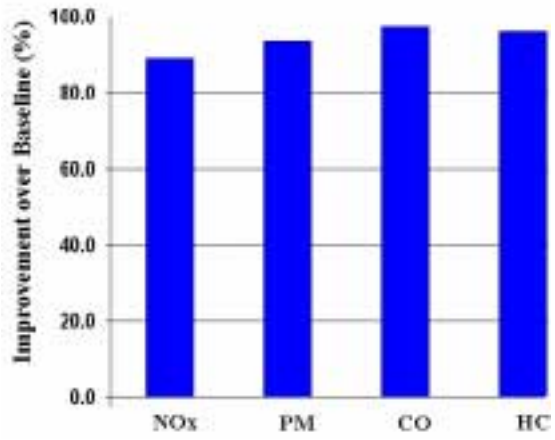


**Figure 3.** Aftertreatment Conversion Efficiency for 4L Engine over Transient Hot 505 Cycles

aftertreatment and vehicle development roadmap using a coupled experimental and simulation labs approach.

## Results

The DDC team implemented a first-generation integrated system into a DaimlerChrysler Neon test vehicle. Figure 2 shows the progression of $NO_x$ reductions made by the application of CLEAN Combustion© to the engine and the addition and optimization of an emission control system. The steady improvement in $NO_x$ reductions approaching 90% allowed this vehicle to progress from Tier 2 Bin 9 to Tier 2 Bin 3, a highly significant achievement for a light-duty diesel passenger car over the FTP75 transient test.

The development of aftertreatment for SUV/ LDT applications is also progressing. Initial integration of aftertreatment hardware with the DDC 4-liter DELTA engine has been completed. Figure 3 shows preliminary results of emissions reduction improvement compared to the baseline engine over the transient Hot-505 cycle. Reductions of 89% of $NO_x$ and 93% of PM are achieved. This aftertreatment technology will be integrated with the latest SUV/LDT engine technology, leveraged from other programs, to pursue minimum emissions performance.

Significant progress has been made in aftertreatment model development. A full suite of 0D, 1D and multi-dimensional (2D, 3D) simulation models has been developed and each model is now being validated on a stand-alone basis. The initial models are being selectively applied to enhance the scalability of technology into the SUV/LDT platform. The stand-alone aftertreatment models are being integrated into the larger engine engineer's development simulation toolbox to expand application into controls, calibration development and vehicle packaging issues.

## Conclusions

Integrating combustion, aftertreatment and vehicle technologies, the DDC team has demonstrated achievement of the project's performance and emissions targets for passenger car applications. DDC is developing new tools to scale the emissions performance to the more challenging SUV/LDT application. It is also noteworthy that these developments and findings have direct application and substantial benefits to the DOE heavy-duty truck engine research and development (R&D) mission.

Intermediate performance and emissions milestones related to engine and aftertreatment technologies have been achieved. The ultimate integration of these technologies into a prototype vehicle demonstrating 2007+ Tier 2 emissions and performance targets remains as a challenging target for future R&D efforts.

# B. Development of Advanced Aftertreatment Subsystem Technologies for CIDI Diesel Engines

*Robert Yu (Primary Contact)*
*Cummins Inc.*
*3540 West 450 South*
*Columbus, IN 47201*

*DOE Technology Development Manager: Ken Howden*

*Subcontractor: Engelhard Corporation, Iselin, NJ*

This project addresses the following DOE R&D Plan barriers and tasks:

*Barriers*

A. $NO_X$ Emissions

B. PM Emissions

*Tasks*

4a. $NO_X$ Adsorber R&D

4f. R&D on Sulfur Trapping Technologies

5a. Catalyzed Diesel Particulate Filter

6. Prototype System Evaluations

## Objectives

- Develop the generic aftertreatment technologies applicable for light-duty vehicle (LDV) and light-duty truck (LDT) engines ranging from 55 kW to 200 kW.
- Develop an optimized and integrated engine/aftertreatment system for a LDT type vehicle, and demonstrate the technology which will enable light-duty diesel engines to meet Federal Tier II emissions with minimum impact on fuel economy. The specific development targets for emissions reduction and fuel injection penalty for the project are:

| | |
|---|---|
| -$NO_X$ conversion efficiency | >90% (hot), >84% (combined) |
| -PM conversion efficiency | >90% (hot), >84% (combined) |
| -Fuel injection penalty over FTP-75 | <5% |
| -Fuel injection penalty at cruise condition | <3% |

## Approach

- Design, test and analyze integrated $NO_X$ and particulate matter (PM) systems.
- Demonstrate a complete exhaust aftertreatment system (EAS) which will enable light-duty diesel engines to meet Federal Tier II emissions with minimum impact on fuel economy.
- Analyze the cost for high-volume production of the aftertreatment system.

## Accomplishments

- The results of preliminary aftertreatment subsystem design and analysis indicate that the best $NO_x$ control approach for LDV and LDT applications is the $NO_x$ adsorber technology. Active lean $NO_x$ and plasma assisted catalytic reduction (PACR) technologies are currently not capable of achieving the high conversion efficiency required to meet Tier-II emissions.
- Progress was made in the development of new adsorber formulation. Engine test results indicate that compared to previous formulations the low side temperature range for $NO_x$ conversion has been extended by 100°C. Greater than 80% $NO_x$ conversion was achieved at 250°C catalyst-in temperature.
- An 87% $NO_x$ conversion efficiency and 94% PM conversion efficiency have been achieved with a breadboard low emission Cummins 5.9 L engine and a Phase II bypass exhaust aftertreatment subsystem (EAS) configuration on the simulated FTP-75 emission cycle. About 7% fuel injection penalty was needed to maintain the $NO_x$ and PM conversion efficiencies at this level. A cold-start test was also performed which achieved about 72% $NO_x$ conversion.
- Progress was made on the bypass regeneration strategy for $NO_x$ adsorbers. The results indicate a 40% to 50% reduction in fuel injection penalty as compared to a full flow regeneration strategy over a simulated FTP-75 emission cycle. Less than 3% fuel injection penalty was achieved at cruise condition.
- With a 15-ppm sulfur diesel fuel and current standard heavy-duty lube oil, the sulfur in the oil can account for up to 50% of the total sulfur in the exhaust. An offline regenerable $SO_x$ trap with sufficient capacity to trap almost 100% fuel- and oil-derived sulfur for greater than 20,000 miles has been demonstrated. Work is in progress to increase the operation interval to more than 30,000 miles.
- The results indicate that the unregulated ammonia emissions can be substantially reduced with an optimum exhaust hydrocarbon (HC) injection strategy.
- A preliminary design and analysis has been completed on PM active regeneration strategy. The more robust catalytic regeneration approach was selected for further development to take advantage of the synergy with the $NO_x$ adsorber system. Microwave system development has been de-emphasized. Initial steady-state and transient testing indicates that a CSF can be regenerated using HC injection.
- Test results continue to indicate that the $NO_x$ conversion as a function of catalyst-in temperature is identical between ISB- and DIATA-size aftertreatment systems. This suggests that a fundamental and "displacement-size" transparent approach can be used for EAS technology development.
- Progress has been made in identifying the best reductant for $NO_x$ adsorber catalysts using reactor studies. Various devices capable of producing the desired reductants, including catalytic partial oxidation (CPO) units and a plasmatron, have been tested in conjunction with an adsorber catalyst to evaluate their feasibility.
- Spectroscopic techniques were applied to understand the underlying chemical reactions over the catalyst surface during $NO_x$ trapping and regeneration periods. In-situ surface probes were useful in providing not only thermodynamic and kinetics information required for model development, but also a fundamental understanding of storage capacity and degradation mechanisms.
- The preliminary LDV aftertreatment system along with the controls and injection system is ready for testing at Argonne National Laboratory (ANL). Temperature data obtained from ANL will be used to optimize the EAS system for the light-duty vehicle.

## Future Directions

- Complete the preliminary emission testing of a mobile EAS system on a light-duty vehicle at ANL.
- Continue to develop and optimize catalyst formulations for best $NO_x$ and PM conversion efficiency under exhaust temperatures and space velocities consistent with anticipated light-duty applications.

- Continue to develop and design an offline regenerable sulfur trap to provide sufficient capacity to trap 99+% fuel- and oil-derived SOx with greater than 30,000 miles service interval.
- Develop and demonstrate $NO_x$ and PM regeneration strategies during FTP-75 and under real life duty cycle operation.
- Develop and optimize the diesel reductant injection system and controls for enrichment during steady-state and transient operations for best aftertreatment performance (conversion efficiency, fuel penalty, and HC slip).
- Design and develop an integrated $NO_x$ and PM system for minimum package size/cost, maximum performance and minimum impact on fuel economy.
- Design and develop an integrated EAS/ISB Engine/LDT system for FTP-75 emissions cycle demonstration along with limited field-testing and provide high volume cost projections.
- Obtain and minimize the impact of the final optimized system on unregulated emissions.
- Obtain transient FTP-75 results on a LDT at ANL.

## Introduction

The key objective of this project is to develop the generic aftertreatment technologies applicable for LDV and LDT engines ranging from 55 kW to 200 kW. This will involve engines with displacements ranging from 1.2 to 6.0 liters. A fundamental and "displacement-size" transparent understanding will be required. Results indicate that the LDV and LDT exhaust operating characteristics can be simulated with the Cummins ISB mule engines. Therefore, most of the aftertreatment subsystem screening will be conducted on the ISB mule engines.

## Approach

In this phase of the project, focus was maintained on $NO_x$ adsorbers as the technology for exhaust aftertreatment. The areas of development included catalyst formulation for high $NO_x$ conversion over an expanded exhaust gas temperature range, catalyst structure for increased exhaust gas residence time on active catalyst sites, and an understanding of the various factors that cause deactivation of the catalyst. Fuel reformulation concepts were investigated to increase the activity of the HCs introduced into the catalyst systems. Even with the availability of 15 ppm sulfur fuels, the development of a sulfur management scheme is critical to prevent catalyst poisoning and deactivation. The application of a sulfur trap that can be regenerated offline or periodically replaced was explored. Due to the low exhaust temperatures in LDV and LDT applications, an active filter regeneration strategy is essential.

PM emissions control was addressed by conducting a design study of various active PM regeneration strategies and selecting the most promising technology for future development. The systems under consideration were conventional burner systems, electrical systems, microwave systems and catalytic burner systems. The chosen technology will need to have high filtration efficiency, low pressure drop, high durability, and synergy with the rest of the aftertreatment system.

Finally, the improved aftertreatment components are being integrated and configured optimally in a system developed for a LDT application. This system will then be calibrated and tested in a controlled environment on a LDT.

## Results

At the start of the project, critical experiments were conducted for different $NO_x$ reduction technologies. Then each technology underwent a selection process as shown in Figure 1. The ranking of $NO_x$ technologies was made against reliability, up-front cost, fuel economy, service interval/serviceability, and size/weight. The results indicated that the best $NO_x$ control approach for LDV and LTD applications is the $NO_x$ adsorber catalyst. Neither active lean $NO_x$ nor PACR technologies are currently capable of achieving the high conversion efficiency required for DOE/FreedomCAR program objectives.

| | Project Emissiongs Target Capacity | Reli-ability | Fuel Economy | Up Font Cost | Service/ Internal Serviceabilty | Size/ Weight | Composite Score |
|---|---|---|---|---|---|---|---|
| Weighting Factor | | 10 | 9 | 9 | 7 | 5 | |
| PACR | No | 3 | 3 | 3 | 3 | 2 | 0* |
| SCRHC | No | 5 | 4 | 5 | 5 | 5 | 0* |
| No Adsorber | Yes | 4 | 5 | 4 | 4 | 4 | 169 |

*Technology not capable of meeting emission standards (5=Best; 1=Worst)

**Figure 1.** Assessment of $NO_x$ Aftertreatment Technologies

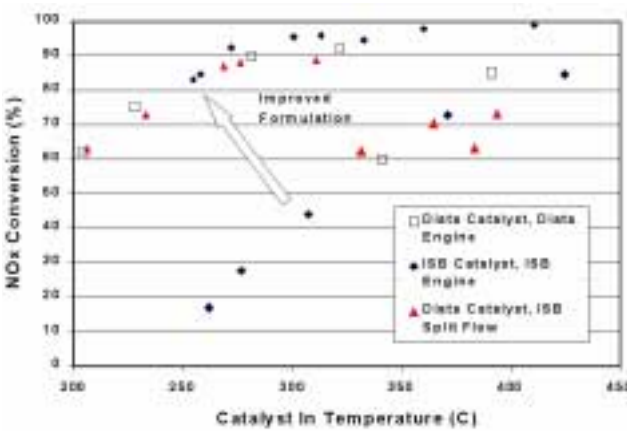


**Figure 2.** $NO_x$ Conversion Efficiency for Improved Catalyst Formulation

After the technology assessment identified $NO_x$ adsorbers as the most promising technology, the program focused on developing this technology. Significant progress was made in adsorber formulation development. Engine test results indicate that the low-side temperature range for $NO_x$ conversion has been extended by 100°C as compared to the previous formulations. Greater than 80% $NO_x$ conversion was achieved at 250°C catalyst-in temperature. Steady-state engine tests using low sulfur fuel (~10 ppm) have shown that greater than 95% $NO_x$ removal can be attained in the temperature range between 275 and 400°C using a repeated cycle of 30 seconds lean absorption followed by a 1 second rich regeneration/reduction at a target exhaust air/ fuel ratio of 9:1. The new formulation results are shown in Figure 2. The results also indicate that the $NO_x$ conversion versus temperature curves are identical between ISB and DIATA aftertreatment systems. This suggests that the EAS technology development is a fundamental and "displacement-size" transparent process.

This improved formulation was incorporated in an adsorber/CSF EAS bypass configuration and tested on the simulated FTP-75 emission cycle. An 87% $NO_x$ conversion efficiency and 94% PM conversion efficiency were achieved with a bread-board low emission ISB engine at about 7% fuel injection penalty. Because of the low exhaust temperatures, 72% $NO_x$ conversion efficiency was obtained for the cold-start cycle. For subsequent hot-start FTP-75 cycles, the $NO_x$ conversion efficiency averaged about 87%. The PM trapping efficiency averaged about 94%. Figure 3 shows the cumulative $NO_x$ conversion efficiency time history of representative hot- and cold-start cycles. At about 200 seconds, there is a drop in the cumulative $NO_x$ efficiency because a period of high space velocity and high $NO_x$ loading occurs when the catalyst temperature is still relatively low. Subsequent regeneration slowly recovers the $NO_x$ conversion efficiency to the final value.

Most of the initial testing of adsorbers was done in full flow. In an attempt to reduce the fuel penalty, the bypass regeneration strategy was investigated next. Figure 4 shows the two exhaust aftertreatment system configurations investigated. For the full-flow configuration, shown at the top in Figure 4, all the engine exhaust flows through the $NO_x$ adsorber during both lean and rich periods. The calculated injected fuel penalty for the breadboard ISB low-$NO_x$ engine over different steady-state operating conditions in the full flow configuration is also shown. One way to reduce fuel penalty associated with $NO_x$ adsorber regeneration is to reduce $O_2$ flow during regeneration. This can be accomplished by using the bypass configuration shown on the bottom in Figure 4. The fuel penalty for the ISB breadboard engine with 20% flow going through the catalyst being regenerated is also shown. Since both bypass legs have to be regenerated in turn, the total fuel penalty is two times the 20% bypass flow, resulting in a fuel penalty 60% lower than using full-flow regeneration. The actual test results indicated a 40%

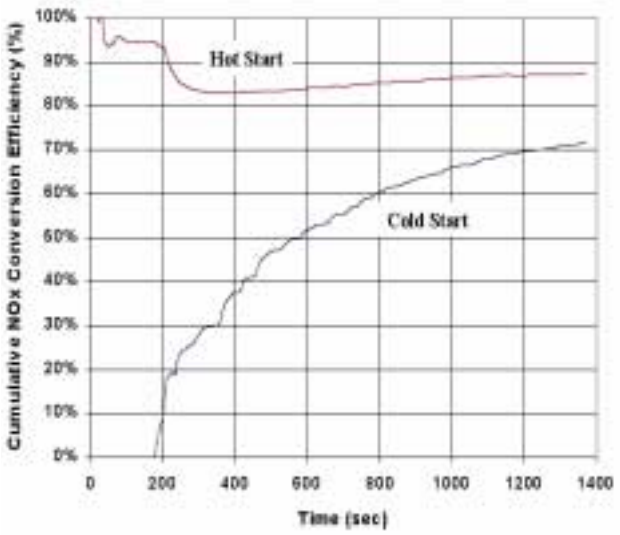


**Figure 3.** Cumulative $NO_X$ Conversion Efficiency over Hot and Cold FTP-75 Cycles for the Bypass Configuration

to 50% reduction in fuel injection penalty as compared to a full-flow regeneration strategy over a simulated FTP-75 emission cycle. The fuel injection penalty was less than 3% at cruise conditions. In addition, tests show that the HC slip after the $NO_X$ adsorber is also lower because the space velocity and fuel injection quantity are both lower during bypass, resulting in a more complete reaction.

As shown previously in Figure 2, the $NO_X$ adsorber catalysts have achieved high $NO_X$ reduction levels using very low sulfur (< 15 ppm) diesel fuels during steady-state conditions. However, the degradation of adsorber performance due to sulfur poisoning remains an issue and needs to be addressed. $SO_X$ competes for active $NO_X$ adsorption sites to form thermodynamically stable compounds. The regeneration of the sulfur-poisoned adsorber requires an extremely high temperature (> 650°C) and rich conditions for an extended period. With a 15 ppm sulfur diesel fuel and current standard heavy-duty lube oil, the sulfur in the oil can account for up to 50% of the total sulfur in the exhaust. There are two paths that are currently being explored for sulfur management by Cummins: (1) the use of a $SO_X$ trap that can be regenerated offline or replaced periodically, and (2) the use of diesel fuel and high temperature to desorb the sulfates from the adsorber. An assessment of each system is summarized below.

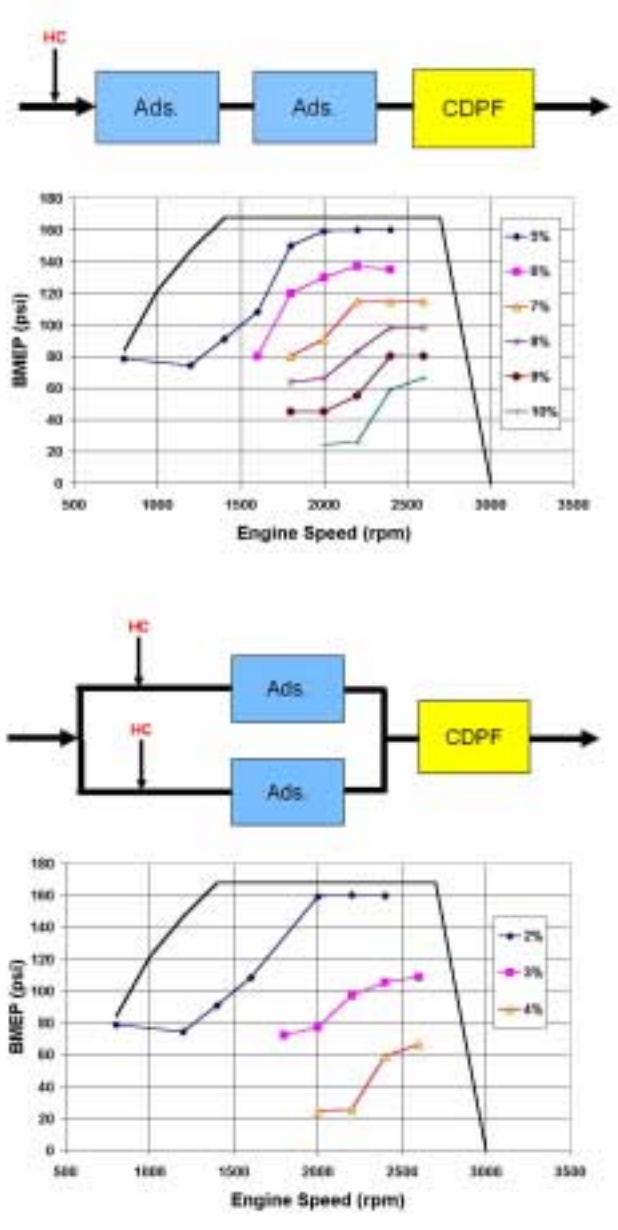


**Figure 4.** $NO_X$ Adsorber Fuel Penalties for the Breadboard ISB Engine: Full-flow Regeneration (top), and 20% Bypass Regeneration (bottom)

Disposable/Offline Regenerable $SO_X$ Trap

- High adsorption capacity for sulfur
- High selectivity toward sulfur adsorption
- No release of secondary emissions from trap

- Usable life of $SO_x$ trap is dependent on sulfur level in fuel and lube oil
- Good protection of adsorber catalyst from sulfur poisoning during misfueling
- Good technology for light-duty applications - small size, low cost, and limited useful life requirement

Desulfation of $NO_x$ Adsorber

- Integrates $NO_x$ and $SO_x$ trapping functions on one catalyst; does not require separate $SO_x$ trap
- Requires on-board high temperature exhaust management to release sulfur from catalyst (> 650$^o$C)
- Incurs additional fuel penalty during desulfation process
- Involves release of secondary emissions (hydrogen sulfide and/or sulfur dioxides) during desulfation
- Catalyst material development requires tradeoff between $NO_x$ storage and conversion, and $SO_x$ storage and release functions, and catalyst thermal durability is compromised

Figure 5 shows the replacement interval for the different capacity $SO_x$ traps having trapping efficiency near 100% all the time (< 10 ppb break-through) for a 6L engine. The current development path uses a formulation containing base metals. A $SO_x$ trap with a 20 gm $SO_2$/liter capacity and an estimated 20,000 mile lifetime before change-out has been demonstrated. Work is in progress to increase the operation interval to more than 30,000 miles. Alternate substrates with high pore volume are being investigated to provide increased capacity.

Throughout the testing, it was also observed that the unregulated ammonia emissions could be substantially reduced with an optimum exhaust HC injection strategy. As shown in Figure 6, significant $NH_3$ spikes can be seen when there is excess HC injection. A portion of the excess HC converts to $NH_3$ while the rest comes out of the EAS as slip. The $NH_3$ emissions decrease substantially when the HC injection is optimized for the same $NO_x$ conversion efficiency. This testing provided evidence that $NH_3$

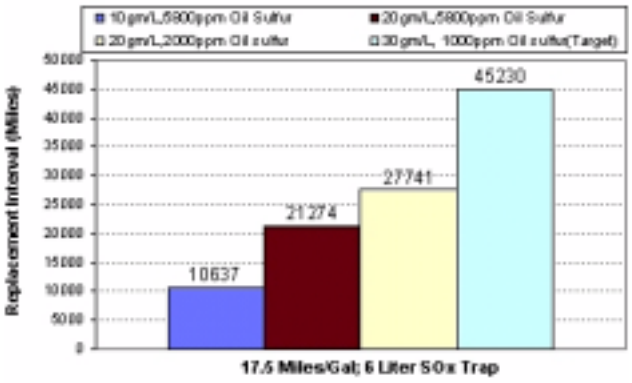


**Figure 5.** $SO_x$ Trap Replacement/Offline Regeneration Interval

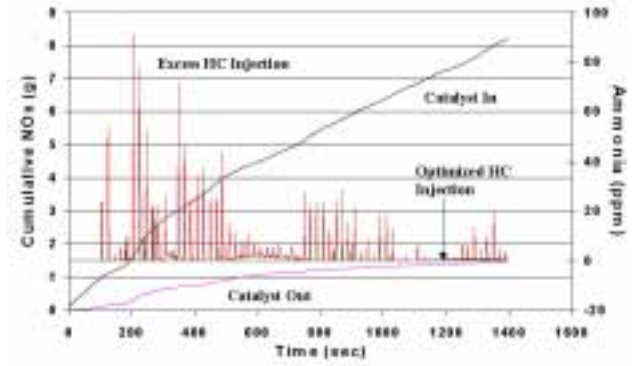


**Figure 6**. Ammonia Slip and HC Injection

does form over the adsorber, but it seems to be a secondary reaction to HC combustion and $NO_x$ reduction. If HC is still left after these reactions, it may react to form $NH_3$. So if the control strategy is well defined to avoid over injection, $NH_3$ formation may not be a problem.

Another major deliverable for the project is reduction in particulate emissions. Efforts were initially directed towards developing a Microwave Assisted Particulate Oxidizer System (MAPOS) using a fibrous media filter. The novelty of microwave heating of diesel particulate traps, and the volumetric heating and selective heating characteristics of microwaves, were the main attractions for its selection over other conventional methods such as electrical and burner systems. A parametric study,involving several key parameters such as microwave power, soot loading, heating

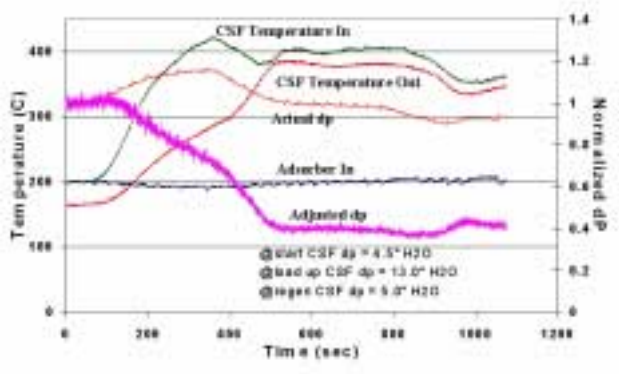


**Figure 7.** Catalyzed Soot Filter Regeneration Using HC Injection

time, regenerative exhaust flow rate and regenerative exhaust temperature, was initiated for developing an effective regeneration strategy. The test results indicated a strong sensitivity/dependence of the regeneration on volumetric flow rate during regeneration. Results also indicated that heating was not uniform as expected and that significant material development is necessary for achieving the much-needed uniform heating. Therefore, at this point the microwave system development has been de-emphasized. In parallel with the MAPOS testing, a preliminary design and analysis on particulate matter (PM) active regeneration strategies was also conducted. The systems under consideration were conventional burner systems, electrical systems, microwave systems, and catalytic burner systems. The systems were evaluated under the following categories: initial cost/size/packaging, reliability/ durability, performance, controls, supplier interaction/system maturity, service/maintenance, and safety. The relative ranking of the systems was done utilizing Pugh Matrix concept, a six-sigma tool. The results indicated that the catalytic burner system stood out compared to the conventional burners, electrical systems, and microwave systems. The focus of the development will be on catalytic burner systems mainly because of their simplicity and their immediate compatibility with engine management, but also because of probable synergistic effects with certain $NO_x$ aftertreatment systems. The initial steady-state results Figure 7 indicate that a catalyzed soot filter (CSF) can be regenerated using HC injection. At the start of the test the CSF was loaded (13" of water delta pressure). Hydrocarbon (diesel

| | Chemical | Thermal | Mechanical |
|---|---|---|---|
| Adsorption | S poisoning (fuel/lube) Lube/ash poisoning Carbonaceous deposits (coking) Condensation/ solubility of metal nitrate | Pt and Metal-Oxide (MO) sintering | Physical breakage |
| Regeneration | Residual nitrate Physical/chemical blockage of pores | Pt-MO interactions MO-support interactions | |
| Conversion | Poison-induced recon-struction of catalyst surface | Pt & MO sintering | |
| Desulfation | Residual sulfate | Pt & MO sintering Pore/surface changes | Thermal Shock |

**Figure 8.** Catalyst Degradation Mechanisms

fuel) was injected upstream of the $NO_x$ adsorber, which raised the system inlet temperature of 200°C to almost 400°C at CSF-in, and the CSF was back to its originally clean condition in less than 10 minutes. Development work to identify the optimized PM reduction strategy continues.

The low temperature encountered in the exhaust for LDV and LDT applications is not only a major hurdle for soot filters but is an issue for adsorbers as well. Light-duty aftertreatment systems need to have the capability to trap and regenerate $NO_x$ at low exhaust temperatures, e.g., <200°C and minimize catalyst degradation during $NO_x$ regeneration and desulfation cycles. Currently, use of diesel fuel as reductant: 1) requires at least 250°C for effective $NO_x$ regeneration; 2) provides the potential for catalyst coking; and 3) may produce local exotherms causing sintering. A more active reductant such as hydrogen provides the low temperature regeneration and eliminates degradation due to coking and sintering. Using a catalytic partial oxidation (CPO) reactor, the feasibility of using diesel fuel to generate the syngas and use it as the reductant was evaluated.

The CPO reactor was connected upstream of the catalyst. During this initial testing, naphtha (carbon number C7- C10) was used to generate the syngas. During the regeneration cycle, the engine exhaust was bypassed 100% and only the reformate (syngas) flowed through adsorber catalyst. The reformate flow rate during $NO_x$ regeneration was

approximately 3 standard cubic feet per minute (SCFM) and was controlled to a temperature of approximately 150°F. Gas Chromatography (GC) analysis showed 30% $H_2$ and 17% CO in the dry reformate. It was encouraging to see that a $NO_x$ conversion of greater than 90% was demonstrated for inlet exhaust temperatures ranging from 148°C to 448°C.

Catalyst durability is the most critical issue for current aftertreatment systems using $NO_x$ adsorber technology. Spectroscopic characterization of the inlet portion of catalyst samples following the time sequence of an engine test revealed important information related to catalyst deactivation. Deactivation of $NO_x$ adsorbers involves many pathways, and sulfur poisoning is possibly the most recognizable one. The degradation pathways that have been identified by this project are summarized in Figure 8.

Surface changes on catalysts can be characterized using differential Diffuse Reflectance mid-Infrared Fourier Transforms (DRIFTs), a subtraction of the spectrum of the fresh sample from the spectrum of an aged sample. Both build-ups and depletions are observed in differential DRIFTs. The assignment of the condensed hydrocarbons can be verified by Raman spectra between the fresh and the aged sample. For aged samples, the fluorescence comes from the aromatic residual of the condensed hydrocarbon species. The intensity ratio between these two carbon bands reflects the aromatic domain size, which is a good indicator of coke formation. Temporal build-ups of nitrates, sulfates and hydrocarbons were also studied. Nitrate build-up seems to slow down after 200 hrs of operation.

Besides a rapid increase at the beginning, the sulfate buildup increases continuously in intensity with time. Further reactions of surface oxy-sulfur species to form pyro- or poly-sulfates may account for the continuous build-ups. The overall build-ups of hydrocarbons also grow with time. However, the non-uniformity of the burning of the injected fuel during operation gives rise to fluctuations in hydrocarbon deposit.

## Conclusions

1. Low side temperature range for $NO_x$ conversion has been extended to achieve greater than 80% $NO_x$ conversion at 250°C catalyst-in temperature.
2. The by pass regeneration strategy for $NO_x$ adsorbers resulted in a 40% to 50% reduction in fuel consumption penalty as compared to a full flow strategy.
3. An off-line regenerable $SO_x$ trap with sufficient capacity to trap almost 100% fuel and oil derived sulfur for greater than 20,000 miles has been demonstrated.
4. The unregulated ammonia emissions were substantially reduced with an optimum HC injection strategy.
5. Plasmatron and CPO, capable of producing the desired reductants, were tested inconjunction with an adsorber to evaluate their feasibility.
6. Spectroscopic techniques were applied to understand the underlying chemical reactions over the catalyst surface during $NO_x$ trapping and regeneration periods.

## FY 2002 Publications/Presentations

1. R. Mital, S. C. Huang, B. J. Stroia, R. C. Yu and C. Z Wan, "A Study of Lean $NO_x$ Technology for Diesel Emission Control," SAE 2002 FL-141

2. Robert Yu, Scott Cole, Brad Stroia, Shyan Huang, Ken Howden, and Steve Chalk, "Development of Diesel Exhaust Aftertreatment System for Tier II Emissions," SAE 2002-01-18673.

3. Howard L. Fang, Shyan Huang, Robert Yu, C. Z. Wan and Ken Howden, "A Fundamental Consideration on $NO_x$ Adsorber Technology for DI Diesel Application," SAE 2002 FFL-205

4. R. Mital, J. Li, S. C. Huang and R. C. Yu "Evaluation of a $NO_x$ Adsorber System on a Light-duty Diesel Vehicle," to be presented at Diesel Engine Emission Reduction Workshop, San Diego, CA, August 2002

# C. Investigation of Sulfur Trap Systems for Protection of Catalytic Emissions Control Devices

*John Storey and Bill Partridge*
*Oak Ridge National Laboratory*
*NTRC*
*2360 Cherahala Blvd.*
*Knoxville, TN 37932*

*DOE Technology Development Manager: Kathi Epping*

This project addresses the following DOE R&D Plan barriers and tasks:

*Barriers:*

A. $NO_x$ Emissions

B. PM Emissions

*Tasks:*

4f. R&D on Sulfur Trapping Technologies

## Objectives

- Investigate the performance and durability of sulfur trap catalysts and the chemical processes involved

## Approach

- Develop Spatially-resolved Capillary Inlet Mass Spectrometry (SpaciMS) $SO_2$ and $H_2S$ diagnostic measurement
- Evaluate two sulfur trap formulations, R1 and R2
- Deploy capillaries at points inside the sulfur trap and at the catalyst entrance
- Measure transient response during adsorption phase and regeneration phase

## Accomplishments

- Developed SpaciMS measurement diagnostic for both $SO_2$ and $H_2S$
- Applied SpaciMS to two full-scale sulfur trap devices and acquired data relevant to $SO_2$ and $H_2S$ formation in the two devices
- Discovered possible intermediate formation of carbonyl sulfide (COS) in R1

## Future Directions

- Resolve sulfur balance in R1 formulation by quantifying intermediate species, believed to be COS
- Characterize fuel reductant usage on a component basis
- Apply SpaciMS to a $NO_x$ adsorber on an engine equipped with post-injection capabilities

## Introduction

$NO_x$ adsorber catalysts provide a promising approach for emissions reduction in the fuel-lean environment of diesel-engine exhaust. However, fuel sulfur remains the biggest barrier to their implementation. Even with fuel sulfur as low as 15 ppm, sulfur poisoning will occur and subsequent desulfurization schemes will be necessary. Sulfur trap catalysts offer the possibility of preventing or attenuating $NO_x$ adsorber poisoning by trapping the $SO_2$ in the exhaust. Issues remain, however, with their effectiveness and durability.

We have previously reported on the use of the SpaciMS to investigate intra-catalyst $NO_x$, $CO_2$, and HCs[1-3]. In this report, we report on the development of $SO_2$ and $H_2S$ measurements with the SpaciMS and the application of the SpaciMS to the measurement of intra-catalyst S species. Two different sulfur-trap formulations were investigated: R1, which produced $H_2S$ and $SO_2$ during regeneration; and R2, which contained a modifier and only produced $SO_2$ during regeneration. The questions we needed to resolve were thus: Does R2 produce $H_2S$ initially and then further oxidize to $SO_2$ within the catalyst? Can we resolve the stoichiometry of the S species involved in regeneration of both sulfur traps? The experiments were designed to answer these questions.

## Approach

Standard mixtures of $SO_2$ and $H_2S$ were used to determine the response of the SpaciMS to these species. $SO_2$ is monitored using mass 64, and $H_2S$ using mass 34. Although $O^{18}O^{16}$ is naturally present in lean exhaust and has mass 34, it was determined that the $H_2S$ is only formed under reducing conditions when oxygen concentrations are very low. Therefore, the SpaciMS was able to detect $H_2S$ in the absence of $O_2$.

A dual-leg system was used to investigate both sulfur trap formulations at EmeraChem, Inc. in Knoxville, Tennessee. Figure 1 is a photograph of the system with the SpaciMS in the foreground, and Figure 2 describes the experimental setup and adsorption/regeneration schedule followed in the texperiment. Note that one capillary was deployed at the exit of each of the eight bricks. The extended adsorption/regeneration schedule allowed for the study of adsorption dynamics and regeneration transients. In addition, sampling for semi-volatile organic species and particulate matter (PM) was performed at the exit of each brick in an attempt to determine the species involved in fuel reforming.

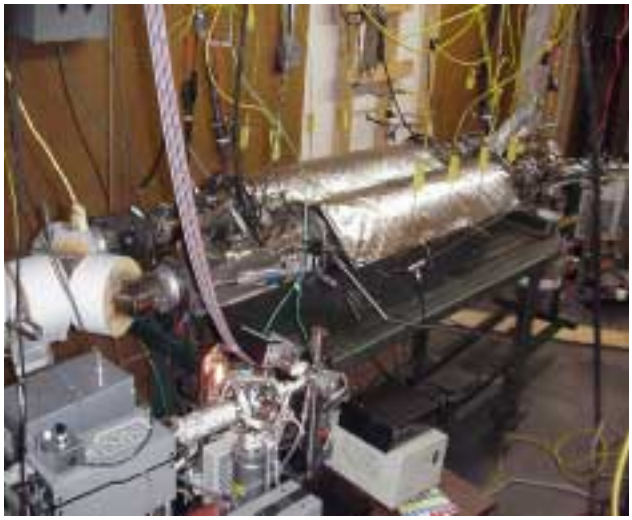

**Figure 1.** Photograph of the Test Catalyst with SpaciMS Instrument in the Foreground

For these experiments, a turbocharged, direct-injected medium-duty diesel engine coupled to an electrical generator provided the exhaust. The sulfur trap was loaded using 150 ppm Diesel Emissions Control-Sulfur Effects (DECSE) fuel for two hours at an exhaust temperature of 320$^{o}$C. This simulates more than 20 hours of operation with 15 ppm S fuel. Regeneration was performed using 3 ppm DECSE fuel for operating the engine and the in-pipe injection system. $SO_2$, $CO_2$, and ($O_2$ + $H_2S$) were measured at each capillary position for an entire 5 minute desorption/regeneration cycle. A PM sample and semi-volatile organic samples were collected at the exits of Bricks 1,4, 5, and 8 (see Figure 2) to see if formulation and residence time had a significant effect on the HC species.

## Results

Figure 3 shows a trace of the the three species, $SO_2$, $CO_2$, and ($O_2$ + $H_2S$), as a function of time during regeneration of catalyst R2. The $O_2$ is depleted, the $CO_2$ increases, and $SO_2$ is released. Note that the majority of the $SO_2$ release occurs during $O_2$ depletion, i.e., under rich conditions.

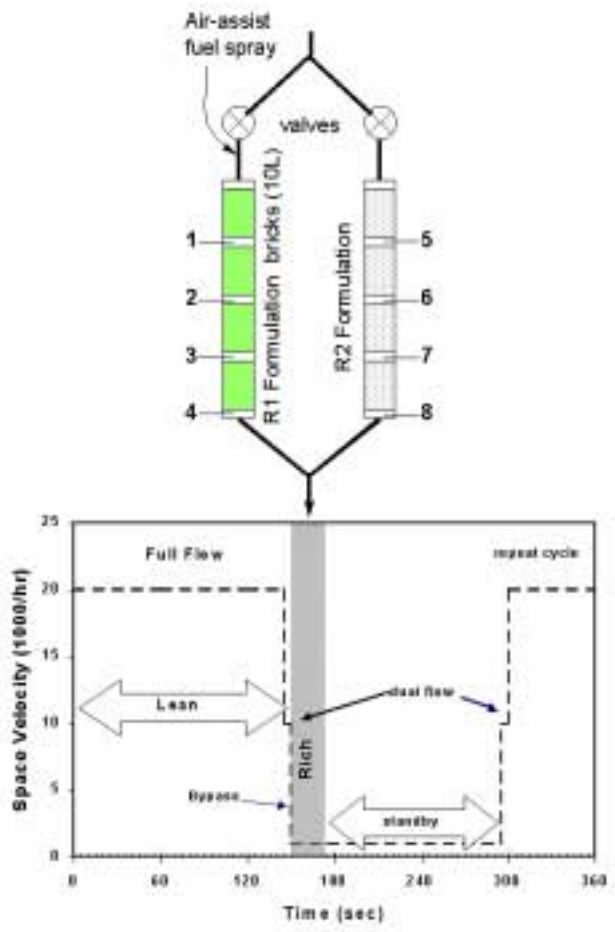


**Figure 2.** Schematic of the catalyst configuration and adsorption/regeneration schedule. Two capillaries were placed at the exit of each of the four monoliths. One side of the dual-path unit contained the R1 sulfur trap, and the other contained the R2 catalyst. Extended adsorption/ regeneration times were used to allow observation of S loading and release.

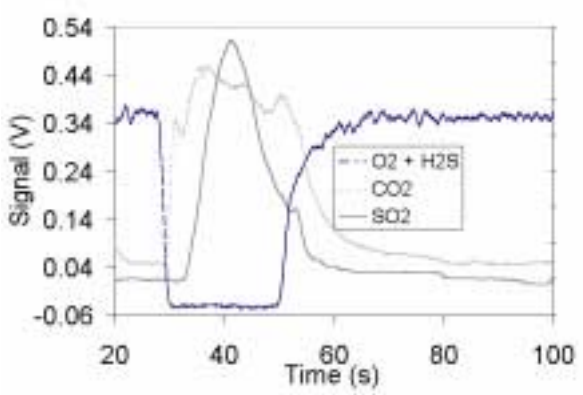


**Figure 3.** Transient emissions as a function of time for capillary 5, after the first monolith in R2, during regeneration. Note that these curves were the same for capillaries 6-8, with the exception of higher $SO_2$, indicating a cumulative release of the stored $SO_2$.

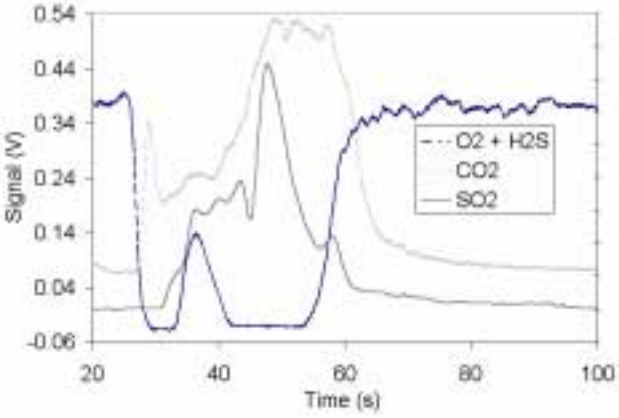


**Figure 4.** Transient emissions as a function of time for capillary 1, after the first monolith in R1, during regeneration. Note that these curves were the same for capillaries 2-4, with the exception of higher $H_2S$ and lower $SO_2$, indicating a cumulative release of the stored S as $H_2S$, and conversion of the released $SO_2$ to $H_2S$.

There is also no evidence of $H_2S$ formation in R2 in any of its four individual bricks.

Figure 4 shows a trace of the same 3 species ($SO_2$, $CO_2$, and ($O_2$ + $H_2S$)) during a regeneration event for catalyst R1. There are some clear differences between Figure 3 and Figure 4. The $O_2$ + $H_2S$ curve shows depletion of $O_2$ at the start of regeneration, and the appearance of $H_2S$ after 30 seconds. $SO_2$ is released concomitantly with $H_2S$, with an additional release at the end of the $H_2S$ pulse. Furthermore, $CO_2$ production has a similar staged behavior - the majority of the $CO_2$ is produced after the $H_2S$ disappears.

In an attempt to resolve the stoichiometry of the S species, the cumulative $H_2S$ and $SO_2$ were plotted as a function of position for both R1 and R2 in Figure 5. Figure 5a shows an increase in $H_2S$ that is ~ 3 times larger than the loss of initial $SO_2$, indicating that some other intermediate S species is responsible

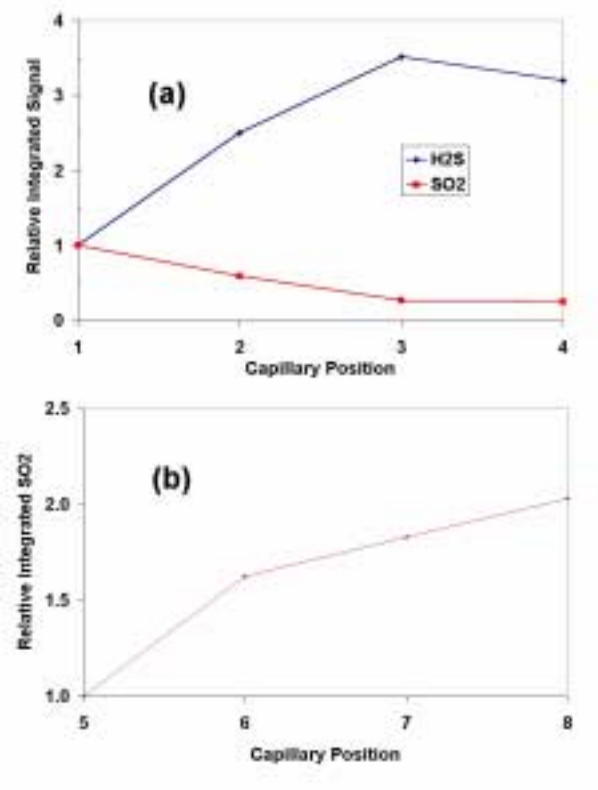


**Figure 5.** Integrated $H_2S$ and $SO_2$ concentrations for the R1 sulfur trap (a) and R2 sulfur trap (b) as a function of position. Note that R2 didn't produce any $H_2S$.

for the additional $H_2S$ formation. In contrast, Figure 5b shows that R2 doesn't form any $H_2S$, and the release of $SO_2$ increases monotonically through the fourth brick.

The cumulative evidence thus points to an intermediate being formed in R1, which we believe is carbonyl sulfide (COS). If this compound forms, it explains the stepped behavior of the $CO_2$ and $SO_2$ formation shown in Figure 4. Further oxidation of COS would lead to increases of $SO_2$ and $CO_2$, which is observed after 40-45 seconds. Furthermore, COS reduction would lead to additional $H_2S$ formation in the downstream bricks, which is shown in Figure 5a.

HC speciation of the gases exiting the first and last bricks for R1 and R2 failed to identify any particular marker for HC reforming products. The fuel HC species were very abundant, but little difference was observed between species produced by either sulfur trap formulation.

## Conclusions

The SpaciMS was applied to investigate intra-catalyst sulfur species for two different sulfur trap formulations. The results showed that the sulfur trap with the modifier, R2, successfully prevented the formation of $H_2S$. In R1, $SO_2$ was shown to be a source of $H_2S$. An additional species, COS, is believed to contribute to $H_2S$ in R1, which would resolve the stoichiometry of the S species.

## References

1. W.P. Partridge, J.M.E. Storey, S.A. Lewis, R.W. Smithwick, G.L. DeVault, M.J. Cunningham, N.W. Currier and T.M. Yonushonis, "Time-Resolved Measurements of Emission Transients by Mass Spectrometry," SAE Paper 2000-01-2552, (2000).

2. W.P. Partridge, J.M.E. Storey, S.A. Lewis, R.W. Smithwick, G.L. DeVault, M.J. Cunningham, N.W. Currier and T.M. Yonushonis, "Resolving $NO_x$-Adsorber Emissions Transients," presented at and published in the proceedings to the DEER Workshop, San Diego, CA, August 2000.

3. John Storey, Bill Partridge, Sam Lewis, Jim Parks, Aaron Watson, Neal Currier and Jason Chen, "Resolving $NO_x$-Adsorber Emission Transients and Sulfur Poisoning using Mass Spectrometry," presented at and published in the proceedings to the FY2001 DOE National Laboratory Merit Review and Peer Evaluation, Knoxville, TN, June 2001.

# D. Effects of Regeneration Conditions on the Performance Of $NO_x$ Adsorber Systems

*C. Scott Sluder (Primary Contact), Brian H. West*
*Oak Ridge National Laboratory*
*2360 Cherahala Blvd*
*Knoxville, TN 37932*

*DOE Technology Development Manager: Kathi Epping*

This project addresses the following DOE R&D Plan barriers and tasks:

*Barriers*

A. $NO_x$ Emissions

B. PM Emissions

*Tasks*

4a. $NO_x$ Control Device R&D

5a. Catalyzed Diesel Particulate Filter

6. Prototype System Evaluations

## Objective

- Investigate the effects of regeneration conditions on performance of $NO_x$ adsorber devices during transient operation.

## Approach

- Conduct chassis-dynamometer evaluations of a 1999 Mercedes A170 CIDI vehicle using an ultra-low sulfur fuel. Perform these evaluations using prototype $NO_x$ adsorbers installed on the vehicle downstream of a lightoff catalyst and a catalyzed diesel particle filter. Utilize reductant-gas injection system for $NO_x$ adsorber regeneration. The gas injection system allows cost-effective manipulation of minimum air:fuel ratio and duration of the rich regeneration events.

## Accomplishments

- Collaborated with the catalyst manufacturers (via Manufacturers of Emission Controls Association, [MECA]) to acquire 5 prototype $NO_x$ adsorbers for this study.
- Conducted multiple hot-start LA-4 cycles for each $NO_x$ adsorber catalyst for a variety of regeneration conditions. Results emphasize importance of controlling $NO_x$ emissions during the "hill 2" portion of the Federal Test Procedure (FTP).
- Presented results at the 2002 CIDI Annual Program Review, Diesel Engine Emissions Reduction Workshop, and SAE Powertrain and Fluid Systems Conference.

## Future Directions

- Project completed, no future plans for on-vehicle, syngas-based regeneration at the Oak Ridge National Laboratory (ORNL). Future plans at ORNL are to utilize these data and experience gained through this study in other $NO_x$ adsorber research at ORNL.

## Introduction

Lean-burn direct-injection engines (both compression-ignition and spark-ignition) offer the potential of significant fuel-efficiency gains over their stoichiometric counterparts. Unfortunately, both of these technologies present nitrogen oxides ($NO_x$) and particulate matter (PM) emissions challenges that must be overcome for these technologies to be commercially viable. While the three-way catalyst has permitted enormous reductions in $NO_x$, carbon monoxide, and hydrocarbons from homogeneous-charge, stoichiometric engines for over 20 years, this technology is not effective for reducing $NO_x$ from lean-burn engines due to the excess oxygen in the exhaust. The $NO_x$ adsorber catalyst is one technology that holds promise for reducing $NO_x$ from lean-burn engines. The $NO_x$ adsorber catalyst will store $NO_x$ during lean operation and can be regenerated periodically by brief rich excursions. Producing these rich excursions in a CIDI engine is one of the challenges to commercialization of this technology. To improve the understanding of the needed regeneration conditions, industry partners recommended utilization of Oak Ridge National Laboratory (ORNL's) synthesis-gas regeneration system. This laboratory tool allows manipulation of exhaust conditions without the costly engineering associated with full-pass engine control and regeneration strategy development.

## Approach

A 1999 Mercedes A170 CDI (Figure 1) was used as the testbed for this project. The Mercedes is equipped with a common-rail, direct-injection, turbocharged diesel engine with exhaust gas recirculation, representing the state-of-the art in commercially available diesel technology. A regeneration system was developed in an earlier activity [1] to allow regeneration of the $NO_x$ adsorber during transient tests without the need for costly and time-consuming engine modifications. The regeneration system utilizes bottled synthesis gas (nominally 2/3 CO, 1/3 $H_2$, with 2% $C_2H_4$) together with the engine exhaust stream to mimic exhaust conditions that could potentially be generated using late-cycle, in-cylinder injection of diesel fuel. Late-cycle injection is a likely means for generating the rich exhaust conditions necessary for actively controlled emissions control technologies.

**Figure 1.** Mercedes A170 Test Vehicle

The hot-start LA-4 cycle was selected as a repeatable transient test for evaluating the different catalysts. Each catalyst was tested in triplicate at each condition. A cold-start LA-4 cycle preceded the first hot-start of each triplicate. The requisite 10-minute soak between the cold and hot cycles was also used between each hot-start to ensure that start-of-test engine, coolant, and exhaust temperatures were always the same.

Each catalyst was evaluated at more than one test condition. Some catalysts were evaluated at numerous minimum air:fuel ratios and regeneration durations. While the initial project plan called for evaluating two catalysts, as more industry partners became aware of the activity, more catalysts were provided. To stay within program resources, not all catalysts were evaluated on all cycles. Also, some of the prototype catalysts were available for only a very short time and had to be returned to the manufacturers.

Properties of the five catalysts are shown in Table 1. Four of the five catalysts were on 400 cell per square inch (cpsi) monoliths, and all monoliths were 5.66 inch diameter x 6 inches long (2.5 liters). A wide range of precious metal loadings were represented, in addition to different adsorbent formulations. All catalysts were provided by

**Table 1. $NO_x$ Adsorber Characteristics**

| Adsorber | Cell Density cells/cm$^2$ (cells/in$^2$) | Precious Metal Loading g/L (g/ft$^3$) | Contains Barium/Alkali Metals? |
|---|---|---|---|
| A | 62 (400) | 5.79 (164) | Yes/Yes |
| B | 62 (400) | 4.24 (1.20) | Yes/No |
| C | 62 (400) | 4.24 (120) | Yes/No |
| D | 62 (400) | 5.79 (164) | Yes/No |
| E | 46 (300) | 3.53 (100) | Unknown/ Unknown |

members of the Manufacturers of Emission Controls Association (MECA).

## Results

The second-by-second integrated $NO_x$ emissions for the Mercedes operating on the hot-start LA-4 cycle with adsorber A installed are shown in Figure 2. All tests in this figure used a fixed regeneration schedule with a 2.0 second rich pulse duration, with variable minimum indicated air:fuel ratio (iAFR). As expected, lowering iAFR improves $NO_x$ reduction performance. Figure 3 shows the integrated $NO_x$ for 3 tests at the richest regeneration condition, 10.2 iAFR, with the same fixed regeneration schedule, but with 1.5, 2.0, and 2.5 second rich pulse duration. Figure 3 shows that at an iAFR of 10.2, the $NO_x$ emissions do not change

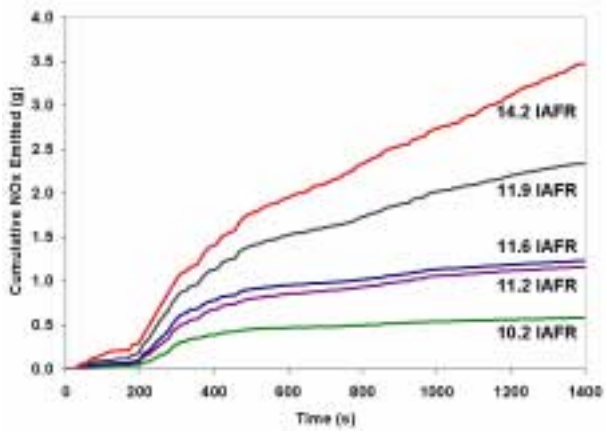


**Figure 2.** Cumulative $NO_x$ Emissions for Catalyst A on Hot-Start LA-4 Cycle for 2.0 Second Generation Schedule at Several Minimum Indicated Air:Fuel Ratios

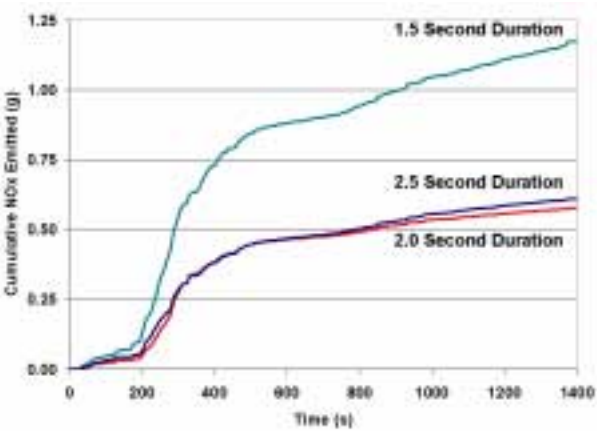


**Figure 3.** Cumulative $NO_x$ Emissions for Catalyst A on Hot-Start LA-4 Cycle at 10.2 iAFR for Variable Rich-Pulse Duration

significantly when rich pulse duration is increased from 2.0 to 2.5 seconds, but nearly double for a decreased duration of 1.5 seconds. These data suggest that rich pulse durations of longer than 2.0 seconds will not yield significant gains in $NO_x$ reduction for adsorber A. The relatively large change in $NO_x$ emissions associated with decreasing the rich pulse duration to 1.5 seconds may be indicative of a transition to an operating regime in which the reduction reaction is a rate-limiting step [2]. Note in Figures 2 and 3 that the period from about 200 - 350 seconds is a relatively high $NO_x$ emission period, regardless of the iAFR or rich pulse duration. This part of the test cycle produced the highest emissions for every adsorber evaluated. Figure 4 shows the LA-4 test cycle and the timing of

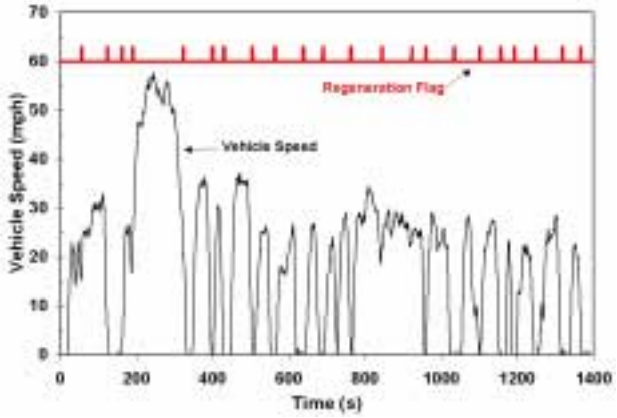


**Figure 4.** LA-4 Driving Cycle with Regeneration Schedule

the regeneration events. Note that "hill 2," or the segment of the test from about 200-350 seconds, is the highest speed portion of the test, with a maximum speed of 56 mph. Maximum speed on the other "hills" is below 35 mph, and the average speed over the whole cycle is below 20 mph. Given the higher loads associated with "hill 2," it is clear why the engine-out $NO_x$ is highest for this portion of the test.

Figure 5 shows the tailpipe (post-$NO_x$ adsorber) $NO_x$ concentration for adsorbers A and B on a hot-start LA-4 cycle. The $NO_x$ slip during regeneration events is sometimes higher than the full-scale (100 ppm) limit for the tailpipe analyzer, as can be seen. There is also slip evident during the lean periods, and there is considerable slip on "hill 2,"as discussed previously. Note that the slip during regeneration is usually higher for adsorber A than for adsorber B, except during "hill 2." The behavior shown in Figure 4 is similar for all of the adsorber, iAFR, and duration combinations that were investigated, except that the magnitude of the slip is different for different cases.

Figure 6 shows an apportionment of the $NO_x$ emissions to three modes: regeneration, the "hill 2" period, and other lean periods during the cycle. The emissions apportioned to "hill 2" do not include emissions due to regeneration during that time; these are included in the regeneration apportionment.

At 10.2 iAFR, it is apparent that slip during lean periods, whether during "hill 2" or during other lean periods, is the best opportunity to reduce $NO_x$ emissions, except perhaps for adsorber E. It is interesting that slip due to regeneration is not necessarily problematic for adsorber B (and perhaps E) on either the 2.0 or the 2.5 second duration, despite the fact that the $NO_x$ reduction for both adsorbers improves very significantly from the 2.0 second to the 2.5 second duration. It is also worth noting that despite apparently large concentration spikes during regeneration, only adsorber E releases a substantial fraction of its $NO_x$ emissions during regeneration.

Maximizing $NO_x$ storage capacity, reducing slip during regeneration, and retaining high CO and HC reduction efficiency represent a trade-off for $NO_x$ adsorbers [3]. For this reason, minimizing $NO_x$ slip

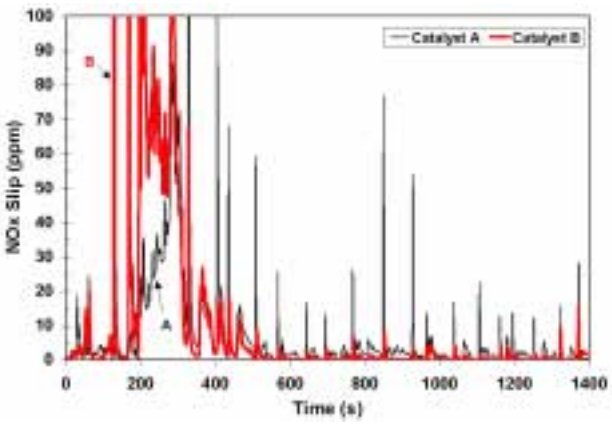


**Figure 5.** Tailpipe $NO_x$ ($NO_x$ slip) for Two catalysts on Hot LA-4 Cycle

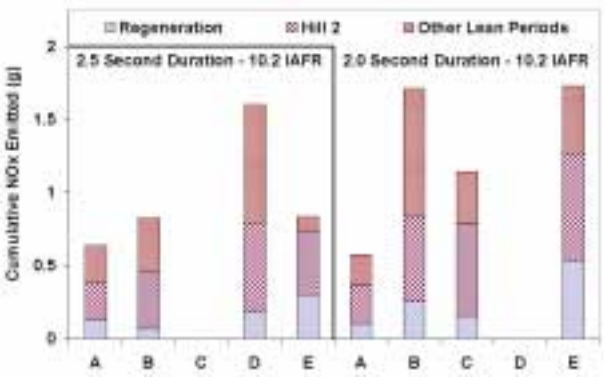


**Figure 6.** Hot LA-4 $NO_x$ Emissions Apportioned to Regeneration, Hill 2, and All Other Lean Periods

during lean periods allows more flexibility during the regeneration event for the same overall $NO_x$ reduction efficiency.

For a more thorough discussion of this work, please refer to the Society of Automotive Engineers Paper on this subject listed below.

## Conclusions

All 5 $NO_x$ adsorbers demonstrated greater than 85% $NO_x$ reduction (when fresh) for a hot LA-4 cycle at some iAFR/duration condition.

For a fixed regeneration schedule on the hot LA-4 test cycle, reducing the iAFR during regeneration events or increasing the duration of the rich pulse can increase the $NO_x$ reduction efficiency of the $NO_x$

adsorbers at the expense of fuel economy penalty and CO and HC emissions.

Catalysts with high $NO_x$ storage capacity yielded the best "hill 2" performance and in general the best overall $NO_x$ reduction efficiency in this study. Reducing $NO_x$ slip during lean periods appears to have more potential to reduce overall $NO_x$ emissions than does reducing slip during regeneration.

## References

1. West, Brian H., and Sluder, C. Scott, "$NO_x$ Adsorber Performance in a Light-Duty Diesel Vehicle," SAE Paper No. 2000-01-2912, Society of Automotive Engineers, 2000.

2. Li, Y., Roth, S., Yassine, M., Beutel, T., Dettling, J., and Sammer, C., "Study of Factors Influencing the Performance of a $NO_x$ Trap in a Light-Duty Diesel Vehicle," SAE Paper No. 2000-01-2911, Society of Automotive Engineers, 2000.

3. Dou, D., and Balland, J., "Impact of Alkali Metals on the Performance and Mechanical Properties of $NO_x$ Adsorber Catalysts," SAE Paper No. 2002-01-0734, Society of Automotive Engineers, 2002.

## FY2002 Publications/Presentations

1. Sluder, C. Scott, and Brian H. West, "Determining the Effects of Regeneration Conditions on the Performance of $NO_x$ Adsorber/DPF Systems," DOE Annual CIDI Review, Argonne, Illinois, May 2002.

2. West, Brian H., and C. Scott Sluder, "Effects of Regeneration Conditions on $NO_x$ Adsorber Performance," Diesel Engine Emission Reduction Workshop, San Diego, CA, August 2002.

3. Sluder, C. Scott, and Brian H. West, "Effects of Regeneration Conditions on $NO_x$ Adsorber Performance," SAE Paper 2002-01-2876, October 2002.

# E. Developing $NO_x$ Adsorber Regeneration Strategies for Diesel Engines (CRADA with International Truck and Engine Corporation)

*Brian H. West (Primary Contact), Mike Kass, John Thomas*
*Oak Ridge National Laboratory*
*2360 Cherahala Boulevard*
*Knoxville, TN 37932*

*DOE Technology Development Manager: Gurpreet Singh*

*Industrial Partner: International Truck and Engine Corporation, Maywood, IL*

This project addresses the following DOE R&D Plan barriers and tasks:

*Barriers*

A. $NO_x$ Emissions

B. PM Emissions

*Tasks*

4a. $NO_x$ Adsorber R&D

4e. R&D on $NO_x$ Reducing Technologies

## Objectives

- Develop $NO_x$ adsorber regeneration and desulfation strategies for diesel aftertreatment systems (including diesel oxidation catalysts and diesel particle filters).
- Improve understanding of role/fate of different exhaust hydrocarbons in advanced diesel aftertreatment systems for several reductant delivery systems. International Truck and Engine Corporation will focus on in-cylinder strategies while Oak Ridge National Laboratory (ORNL) examines in-manifold and in-pipe strategies.

## Approach

- $NO_x$ adsorber regeneration strategies will be developed for several steady-state conditions. Electronic control of intake throttle and exhaust gas recirculation (EGR) valve will be used to lower the air:fuel ratio prior to reductant delivery.
- System performance will be measured for a variety of regeneration conditions. Hydrocarbon speciation and other advanced ORNL analytical tools will be used to improve understanding of the system.

## Accomplishments

- Developed PC-based system for transient electronic control of intake throttle, EGR valve, wastegate, and reductant (fuel) delivery in-manifold (pre-turbo) and/or in-pipe (after turbo).
- Commissioned motoring dynamometer with digital transient control.
- Achieved >90% $NO_x$ reduction in steady-state modes for first aftertreatment system [diesel oxidation catalyst (DOC), catalyzed diesel particulate filter (CDPF), $NO_x$ adsorber].

### Future Directions

- Refine strategies to achieve acceptable HC and CO slip.
- Re-examine same engine modes with different aftertreatment *system* (presence/size of DOC, CDPF location, adsorber formulation, etc).
- Speciate hydrocarbons at DOC inlet and adsorber inlet; correlate with regeneration strategy, system performance.
- Develop desulfation strategies, speciate hydrocarbons and measure $H_2S$ and $SO_2$.

---

## Introduction

The phase-in of Environmental Protection Agency (EPA) light-duty Tier 2 emissions regulations begins in 2004; in 2009 they will be fully phased-in, requiring on the order of 90% reduction in $NO_x$ and particulate matter (PM) from current levels. More stringent heavy-duty standards take effect in 2007, and requiring about 90% reduction in $NO_x$ and PM. The $NO_x$ adsorber catalyst is a promising technology to help meet these stringent new $NO_x$ standards, but there are many open issues that must be resolved prior to commercialization. The (lean-burn) diesel engine does not readily run rich, but rich exhaust conditions are required to regenerate the $NO_x$ adsorber catalyst. While producing the rich exhaust in itself is a challenge, doing so can also potentially cause durability problems, excessive fuel consumption, and excess HC and/or CO emissions. Additionally, the $NO_x$ adsorber catalyst is very sensitive to sulfur in the exhaust, so effective sulfur management schemes must be developed that will ensure full useful life of the aftertreatment systems. This Cooperative Research and Development Agreement (CRADA) aims to help resolve some of the problems and unknowns with the $NO_x$ adsorber technology.

## Approach and Results

International Truck and Engine will pursue late-cycle, in-cylinder injection of fuel to achieve rich exhaust conditions for adsorber regeneration. Complementary experiments at ORNL will focus on in-manifold (pre-turbo) and in-pipe (after turbo) fuel injection. ORNL has developed a PC-based controller for transient electronic control of EGR valve position, intake throttle position, and actuation of fuel injectors in exhaust manifold and downstream pipe locations (Figure 1). Aftertreatment systems

**Figure 1.** In-Manifold Fuel Injection for $NO_x$ Adsorber Regeneration

consisting of different diesel oxidation catalysts and $NO_x$ adsorbers in conjunction with catalyzed diesel particle filters will be evaluated for a variety of regeneration strategies at steady-state conditions. The first system (utilizing a small DOC) has been fabricated, and initial strategy development has been completed. Reductions of $NO_x$ in excess of 90% have been achieved in steady-state modes, as shown in Figure 2. As this work is being done under a CRADA, the data herein are CRADA-protected, hence the lack of y-axis data values. Further experiments will focus on other loads and speeds, and more detailed gas and particulate measurements for the refined regeneration strategies.

## Conclusions

$NO_x$ adsorber catalysts and diesel particle filters have potential to help diesel engines meet future

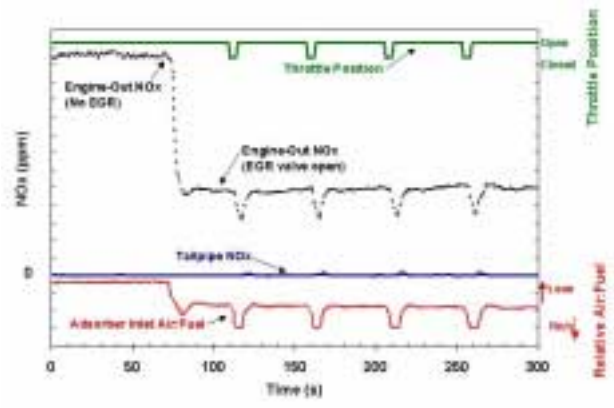


**Figure 2.** Engine-out and Tailpipe $NO_x$ Emissions for Quasi-Steady Operation with Electronic Control of Throttle, EGR, and In-Pipe Fuel Injection (data values omitted for CRADA protection)

light- and heavy-duty emissions standards. Achieving the requisite reductions with acceptable fuel penalties and HC and CO emissions are challenges being addressed in this project.

# F. Developing an Exhaust Gas Sulfur Trap for CIDI Engines

*Leslie Story (Primary Contact)*
*Apyron Technologies, Inc*
*4030 F, Pleasantdale Road*
*Atlanta, GA 30314*

*Mark Mitchell*
*Department of Chemistry*
*Clark Atlanta University*
*223 James P. Brawley Drive, SW*
*Atlanta, GA 30314*

*Svetlana Iretskaya*
*Apyron Technologies, Inc*
*4030 F, Pleasantdale Road*
*Atlanta, GA 30314*

*DOE Technology Development Manager: Kenneth Howden*

*Industrial Partner: International Truck and Engine Corporation, Melrose Park, IL*

This project addresses the following DOE R&D Plan barriers and tasks:

*Barriers*

A. $NO_x$ Emissions

B. PM Emissions

*Tasks*

4f. R&D on Sulfur Trapping Technologies

## Objectives

- Determine important compositional parameters of solid adsorbent for sulfur dioxide removal and optimize adsorbent formulation for removal of sulfur dioxide from exhaust gas.
- Develop test and optimize a regenerable sulfur dioxide trap for commercialization.

## Approach

- Evaluate promising solid adsorbent formulations for their capacity and rate of sulfur dioxide adsorption as well as their ability to be regenerated.
- Test the most promising sulfur dioxide adsorbents for sulfur dioxide capacity using a simulated exhaust gas mixture in a laboratory flow-reactor system.
- Develop, in consultation with engineers at International Truck and Engine Corporation, the initial design for the adsorbent to be used on the engine.
- Conduct the engine tests in collaboration with engineers at International Truck and Engine Corporation.
- Prepare initial sulfur dioxide trap for engine trials, using optimized adsorbent formulation and design parameters.

- Establish baseline sulfur dioxide adsorption capacity/profile under typical engine operating conditions.
- Determine sulfur dioxide adsorption capacity for a series of engine operating conditions, based on requirements of downstream $NO_x$ adsorber.
- Develop regeneration protocol based on results from engine tests.
- Utilize accelerated aging to assess durability of sulfur dioxide trap.
- Finalize sulfur dioxide trap specifications for commercial production.

### Accomplishments

- Synthesized, characterized, and tested new sulfur dioxide adsorbent formulations.
  - Optimized the "active ingredient/promoter/support" combination for sulfur dioxide adsorption capacity at typical exhaust gas temperatures.
  - Evaluated the optimized adsorbents in simulated exhaust gas to determine breakthrough and post-breakthrough performance under realistic flow conditions.
- Demonstrated the ability of the adsorbents to be regenerated without losing significant adsorption capacity.
- Developed initial design for exhaust gas sulfur dioxide trap, procured materials for formulation, and have begun preparing initial adsorbents for engine tests.
- Have made contact with engineering personnel and have set up the procedure for "canning" the adsorbent for initiation of the engine tests.

### Future Directions

- Scale up synthesis and processing of adsorbent formulation.
- Work in collaboration with International Truck and Engine Corporation to optimize the sulfur dioxide trap.
- Develop regeneration protocol for sulfur dioxide adsorbents.

---

## Introduction

One of the primary environmental concerns associated with diesel engines is their emission of nitrogen oxides ($NO_x$), precursors to ozone formation. Technologies exist that effectively reduce $NO_x$ emissions, but these emission control devices are poisoned by sulfur. One of the technologies that is currently being developed for CIDI engine emission control is a combination consisting of a $NO_x$ adsorber/catalyst preceded by a regenerable sulfur trap.

The objective of this work is to develop a sulfur trap that, when placed upstream of a $NO_x$ adsorber, would completely adsorb $SO_x$ from the exhaust gas and prevent poisoning of the $NO_x$ adsorber by sulfur. Apyron Technology's patented Advanced Material Synthesis Technology (AMST) had been used to synthesize a new sulfur dioxide adsorbent which shows superior regenerable $SO_x$ adsorption capacity over a wide range of temperatures and space velocities.

## Approach

Several sets of adsorbents were prepared and tested to compare their rates of $SO_2$ adsorption, and their adsorption and regeneration capacities using the CAHN thermogravimetric analysis system (TGA) shown in Figure 1. Most experiments were conducted at 150$^o$C and at 400$^o$C to evaluate the performance of the materials at the low and high ends of the temperature range of CIDI engine exhaust gases.

The TGA experiments allowed us to select the most promising materials, which were then tested in the flow reactor system. Two modifications of the flow reactor system were used in this study: a four-

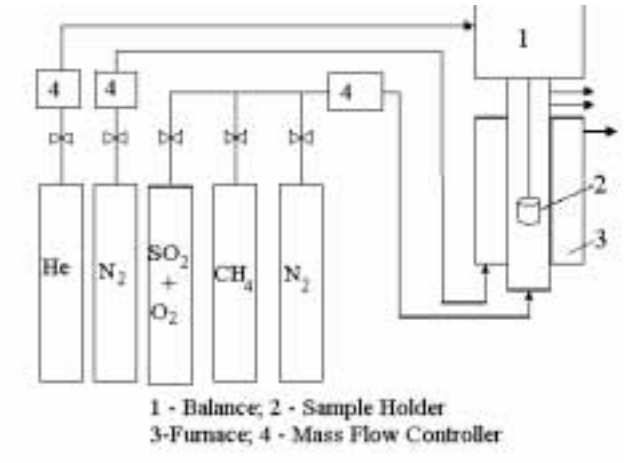


**Figure 1.** Experimental System to Study $SO_2$ Adsorption (CAHN TG-151 TGA)

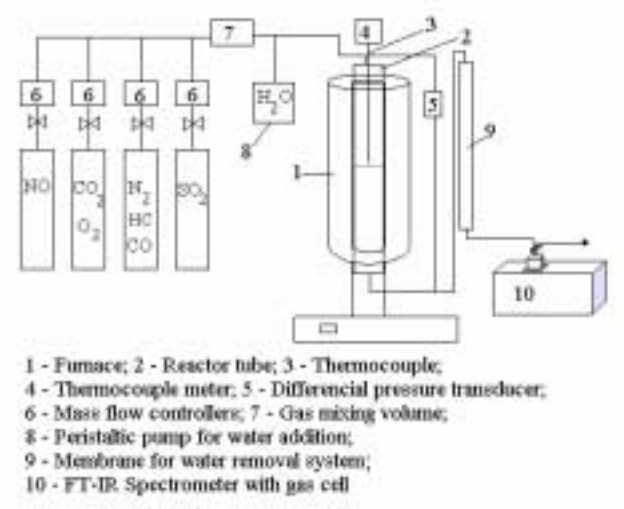


**Figure 2.** Flow Reactor System to Study $SO_2$ Adsorption from Simulated Exhaust Gas in the Presence of Water Vapor

tube reactor system to run comparative tests, and a single tube reactor system equipped with a peristaltic pump to introduce water vapor into the reaction gas mixture. The testing system with the water pump is shown in Figure 2. The TGA experiments and most of the comparative flow-reactor tests were performed using a simple sulfur dioxide gas mixture: 0.3% $SO_2$, 2-3% $O_2$, with the balance being He or $N_2$. When the preliminary experiments reduced the number of adsorbents to the best four, we began using a simulated exhaust gas mixture: 25 ppm $SO_2$, 300 ppm NO, 150 ppm CO, 35 ppm $C_3H_6$, 9.2% $CO_2$, 6.5% $O_2$, balance $N_2$. The experiments using the simulated exhaust gas mixture were run according to the temperature/space velocity matrix shown in Table 1, which was designed based on the recommendations of personnel from International Truck & Engine Corporation.

| | | Temperature, $^oC$ | | | | |
|---|---|---|---|---|---|---|
| | | 100 | 200 | 300 | 400 | 500 |
| Space Velocity, $h^{-1}$ | 20,000 | X | | X | | |
| | 40,000 | | X | X | | |
| | 60,000 | | | X | X | |
| | 80,000 | | | X | | X |

**Table 1.** Matrix of Flow Reactor Experiments for $SO_2$ Adsorption from Simulated Exhaust Gas

## Results

The screening and testing protocol resulted in the selection of a material that showed a high rate of adsorption and large capacity for sulfur dioxide at the target temperatures as well as excellent regeneration properties. Figure 3 presents the weight gains shown by an adsorbent during a long-term, 50 cycle adsorption/regeneration test using the TGA. The first 35 adsorption/regeneration cycles were carried out at 400$^o$C, and the last 15 at 500$^o$C. Regeneration was performed by heating the sample in flowing methane at 600$^o$C and maintaining that temperature

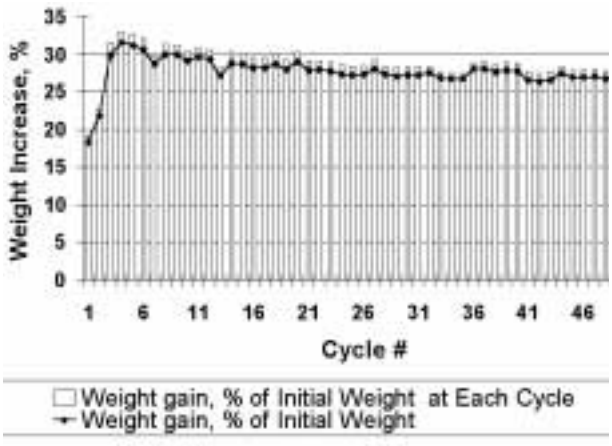


**Figure 3.** Weight Gain ($SO_2$/$SO_3$ uptake) as a Function of the Number of Adsorption/ Regeneration Cycles

for 5 minutes. One can see that sample showed virtually no loss of adsorption capacity during the 50-cycle experiment.

Flow reactor tests of the four most promising materials were conducted according to the experimental matrix presented in Table 1. The tests indicated that all the materials had very high selectivity for $SO_2$ adsorption. Some NO to $NO_2$ and CO to $CO_2$ conversions were observed at higher temperatures, as well as some oxidation of the propylene that was added to simulate unburned fuel. Table 2 presents a typical outlet gas mixture before $SO_2$ breakthrough was observed.

| Space Velocity, $h^{-1}$ | Temperature, $^oC$ | $SO_2$ | NO | $NO_2$ | CO | $C_3H_6$ |
|---|---|---|---|---|---|---|
| 20,000 | 100 | 0 | 300 | 0 | 150 | 30 |
| | 300 | 0 | 280 | 20 | 90 | 0 |
| 40,000 | 200 | 0 | 300 | 0 | 150 | 10 |
| | 300 | 0 | 285 | 15 | 115 | 0 |
| 60,000 | 300 | 0 | 292 | 8 | 115 | 0 |
| | 400 | 0 | 215 | 85 | 20 | 0 |
| 80,000 | 300 | 0 | 298 | 2 | 115 | 0 |
| | 500 | 0 | 260 | 40 | 0 | 0 |

**Table 2.** Typical Concentrations of Outlet Gases (ppm) Prior to $SO_2$ Breakthrough

The observed $SO_2$ breakthrough times varied with temperature and space velocity. In general, the amounts of $SO_2$ adsorbed by the adsorbents before sulfur dioxide slip was observed were proportional to temperature and inversely proportional to space velocity.

The best performer of the four materials tested using simulated exhaust gas was then tested in the presence of 5% water vapor at 300$^o$C and a space velocity of 60,000 $h^{-1}$. Figure 4 presents the sulfur dioxide concentration in the exhaust gas stream as a function of time on stream for the sample in dry and wet simulated exhaust gas. One can see from Figure 4 that the adsorbent actually showed superior performance in the presence of 5% water vapor, with the time before $SO_2$ breakthrough increasing by approximately 50% with water vapor in the stream. This observation of the effect of water vapor on $SO_2$

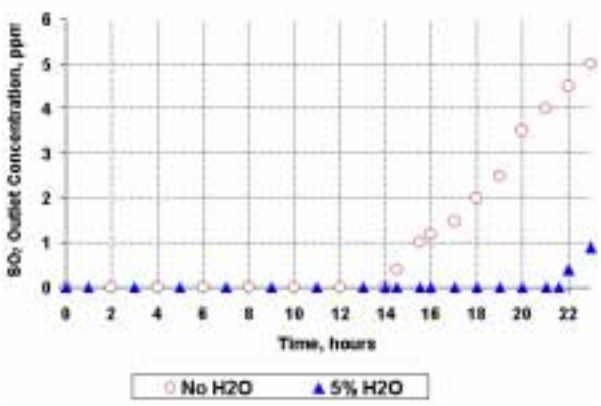


**Figure 4.** Flow Reactor Experimental Results

adsorption capacity was confirmed by several subsequent experiments using slight modifications of the adsorbent formulation.

## Conclusions

We have developed and optimized the formulation for use in the sulfur dioxide trap. The material shows excellent flow behavior in simulated flue gas that improves when water vapor is added to the gas stream. The material shows excellent regeneration behavior, showing virtually no loss in adsorption capacity over 50 adsorption/regeneration cycles. We have begun preparing the material to be used in the initial engine tests and have made arrangements to have the adsorbent "canned" for fitting onto the engines for testing at International Truck and Engine Corporation facilities.

# G. Advanced CIDI Emission Control System Development

*Christine Lambert and Robert Hammerle (Primary Contact)*
*Ford Research Laboratories*
*P.O. Box 2053, MD 3179, SRL*
*Dearborn, MI 48121*

*DOE Technology Development Manager: Ken Howden*

*Main Subcontractors: FEV Engine Technology, Inc., Auburn Hills, MI; ExxonMobil Research and Engineering Company, Paulsboro, NJ*

This project addresses the following DOE R&D Plan barriers and tasks:

*Barriers:*

A. $NO_x$ Emissions

B. PM Emissions

C. Cost

*Tasks:*

4c. Selective Catalytic Reduction Catalysts

5a. Catalyzed Diesel Particulate Filter

6. Prototype System Evaluations

## Objectives

- Develop and demonstrate a highly efficient exhaust emission control system for light-duty CIDI engines to meet 2007 Tier II Bin 5 emissions standards (0.07 g/mi $NO_x$, 0.01 g/mi PM) with minimal fuel economy penalty and greater than 5000 hours of durability. Tier II Bin 5 standards require 90+% conversion of both $NO_x$ and particulate matter (PM).

## Approach

- Establish baseline emission control system.
- Conduct parallel engine dynamometer and vehicle testing.
- Continue research to identify the most active and durable catalysts and PM filters.
- Continue research to determine the most selective and durable exhaust gas sensors.
- Choose a very low-sulfur diesel fuel to represent fuel of 2007 and beyond.

## Accomplishments

- Project began in July 2001. FEV subcontract was completed in August 2001. ExxonMobil subcontract was completed in May 2002.
- Initial systems analysis was completed, and selective catalytic reduction (SCR) using aqueous urea was chosen as the baseline emission control system due to its potential for very high $NO_x$ reduction with minimal fuel economy penalty across a wide range of driving conditions.
- A prototype diesel light-truck engine, installed on a dynamometer at FEV, achieved steady-state $NO_x$ conversions of up to 98%.

- Engine-out emissions data were collected on a Ford F-250 truck equipped with a similar mid-sized diesel engine. The baseline emission control system using SCR and aqueous urea injection achieved 65% $NO_x$ conversion over the FTP cycle.
- A second vehicle equipped with a smaller engine and a similar urea SCR system has shown 80+% $NO_x$ conversion and accumulated 20,000 on-the-road miles.
- The importance of an upstream oxidation catalyst was demonstrated in the laboratory using an NO/ $NO_2$ feedgas mixture. Durable 90% $NO_x$ conversion was achieved.

### Future Directions

- Investigate the effects of aging on an upstream oxidation catalyst.
- Install a catalyzed PM filter on the F-250 truck downstream of the SCR system and implement a filter regeneration control strategy.
- Enhance the model-based control for $NO_x$ reduction by using ammonia ($NH_3$) surface coverage on the SCR catalyst.
- Develop onboard diagnostics for identifying possible system malfunctions and to improve the adaptiveness and robustness of the control model.
- Incorporate aqueous urea injection into a computational fluid dynamics (CFD) model.
- Review system costs and determine ways to decrease cost if necessary.
- Develop more durable and selective $NO_x$ sensors.
- Select the most promising ammonia sensing technology, increase its durability and selectivity in diesel exhaust gas, and develop appropriate control strategies.
- Investigate concepts for onboard delivery of aqueous urea and its specifications.

## Introduction

Reducing PM and $NO_x$ emissions are primary concerns for diesel vehicles required to meet 2007 Federal Tier II and California LEV II emission standards (Table 1). These standards represent a 90-95% reduction from current Federal Tier I diesel standards.

**Table 1.** 2007 Emission Standards (passenger cars and light-duty vehicles)

| Standard (g/mi) | *50k mi* | | *120k mi* | |
|---|---|---|---|---|
| | $NO_x$ | PM | $NO_x$ | PM |
| LEV II | 0.05 | --- | 0.07 | 0.01 |
| Tier II, Bin 5 | 0.05 | --- | 0.07 | 0.01 |

The high oxygen content of diesel exhaust makes onboard $NO_x$ control complicated. The available technologies for high $NO_x$ reduction in lean environments include SCR, in which $NO_x$ is continuously removed through active reductant injection over a catalyst, and lean $NO_x$ traps (LNT), which are materials that adsorb $NO_x$ under lean conditions and require periodic regeneration under rich conditions to reduce $NO_x$ to $N_2$. The technology with the most potential to achieve 90+% $NO_x$ conversion with minimal fuel economy penalty is SCR with an ammonia-based reductant such as aqueous urea. Ammonia-SCR has been used extensively for stationary source $NO_x$ control [1]. Its high selectivity and reactivity with $NO_x$ in high $O_2$ environments makes SCR attractive for diesel diesel vehicle use.

The main reactions are shown below:

*urea decomposition:*

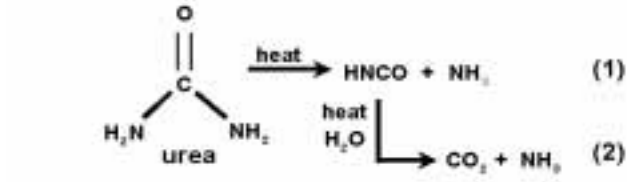


*$NO_x$ reduction:*

$$4NO + 4NH_3 + O_2 \longrightarrow 4N_2 + 6H_2O \quad (3)$$

$$6NO_2 + 8NH_3 \longrightarrow 7N_2 + 12H_2O \quad (4)$$

$$2NH_3 + NO + NO_2 \longrightarrow 2N_2 + 3H_2O \quad (5)$$

Compared to ammonia, aqueous urea is much more convenient for customers to handle. Feasibility has been proven by past work at Ford [2], Volkswagen [3] and Mack Truck [4].

Control of diesel PM is accomplished with a periodically regenerated ceramic filter. The filter may be washcoated with precious metal to help oxidize HC and collected soot. A diesel oxidation catalyst (DOC) may also be placed upstream of the filter to further aid in filter regeneration.

## Approach

Supplier catalysts are tested in a laboratory flow reactor and ranked for fresh and aged conversion levels. Full-size monoliths of the most promising formulations are installed in the engine dynamometer and onboard the vehicle and tested in parallel. All testing is conducted with very low sulfur fuel (4 ppm by weight). Modeling is used to help choose the catalyst configuration with the highest potential to meet the emission standards. CFD analysis is used to model the distribution of exhaust flow through the catalysts and optimize system design. Since cold-start plays an important role in emission control system functionality, special emphasis is placed on rapid warm-up strategies. Appropriate exhaust gas sensors and control strategies are used for durable system function.

## Results

A typical conversion curve for reduction of $NO_x$ with $NH_3$, using a base metal/zeolite catalyst, is shown in Figure 1. Using NO-only feedgas for $NO_x$, over 90% conversion is achieved at a catalyst temperature of 250°C and is maintained until 550°C. With 50% of the NO replaced by $NO_2$, known as "fast SCR" [5], the 90% conversion window begins at less than 200°C. This wide temperature window for very high $NO_x$ conversion makes ammonia-SCR a good choice for light-duty diesel vehicle applications.

Figures 2 and 3 show baseline system choices for Tier II $NO_x$ and PM control. In System A (Figure 2), a catalyzed PM filter is located upstream of the SCR catalyst to take full advantage of heat produced by the engine to oxidize HC, CO and soot. However,

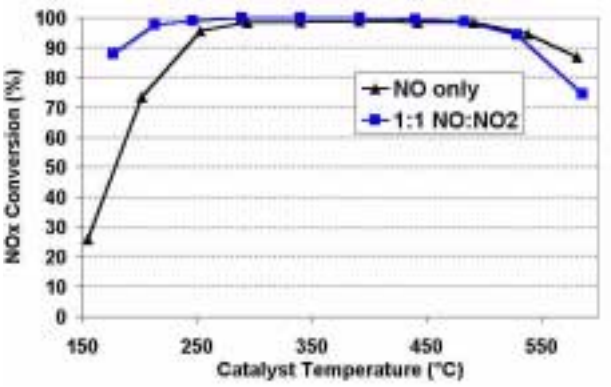


**Figure 1.** $NO_x$ Conversion vs Catalyst Temperature [Laboratory flow reactor; Base metal/zeolite SCR catalyst; Feedgas conditions: 14% $O_2$, 4.5% $H_2O$, 5% $CO_2$, 350 ppm $NO_x$, 350 ppm $NH_3$, balance $N_2$; Space velocity: 30000 $h^{-1}$]

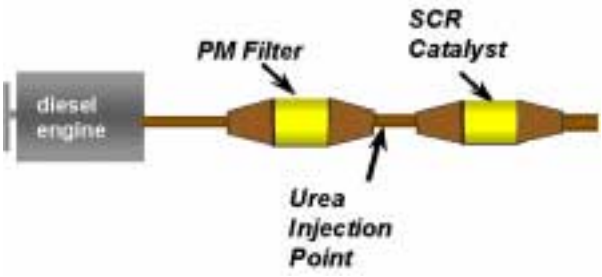


**Figure 2.** System A. PM Trapping Function is Placed Closest to the Engine

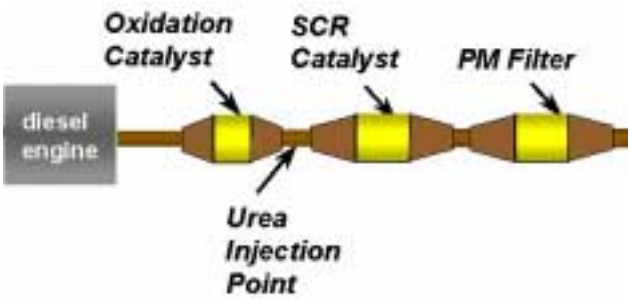


**Figure 3.** System B. Oxidation and $NO_x$ Reduction Functions are Placed Closest to the Engine

the SCR catalyst takes longer to heat up and is more susceptible to damage by large exotherms generated in the filter. It is advantageous to reverse the order of the components to achieve higher SCR catalyst temperatures and convert more $NO_x$ earlier in the test

cycle, as shown by System B (Figure 3). An oxidation catalyst close to the engine is required to oxidize HC and CO, followed by urea injection and SCR. The downstream PM filter can trap soot at any operating temperature and can also oxidize ammonia that slips past the SCR catalyst. System B, however, requires additional heat to regenerate the filter, resulting in a higher fuel economy penalty.

Predicted $NO_x$ efficiencies for Systems A and B are shown in Figure 4. Neither system by itself is predicted to meet the 90% $NO_x$ conversion target required to meet Tier II standards. More rapid heating of the SCR catalyst is needed to reach higher activity sooner. Figure 4 assumes an extra 50°C can be added to the system during the first 30 seconds.

An F-250 truck with a mid-sized prototype diesel engine was tested with an oxidation catalyst, aqueous urea injection system, and an SCR catalyst based on System B configuration. A maximum $NO_x$ conversion over the FTP of 65% was achieved using a baseline aqueous urea injection strategy in conjunction with a $NO_x$ sensor. Results indicate that the injection system needs to more effectively distribute the reductant to the entire SCR catalyst. Another vehicle equipped with a similar emission control system achieved over 80% $NO_x$ conversion on the FTP. The increased conversion was assumed to be due to more effective reductant use.

$NO_x$ sensors used onboard the truck and engine dynamometer were modified to address thermal microcracking occurring during excessive diesel exhaust cooling. The modification increased response times slightly but were still within the usable range for this application. Research on a lower cost, less complex $NO_x$ sensor was initiated. Several different sensing technologies for selective detection of $NH_3$ in the exhaust gas were investigated. These included resistive sensors based on thin film zeolites and molybdenum oxide ($MoO_3$), as well as silicon carbide-based (SiC) semiconducting devices and zirconia electrochemical elements. Although all of these technologies showed promise for selective $NH_3$ detection, they each demonstrate severe limitations (drift, durability, reproducibility, etc.) and require further development.

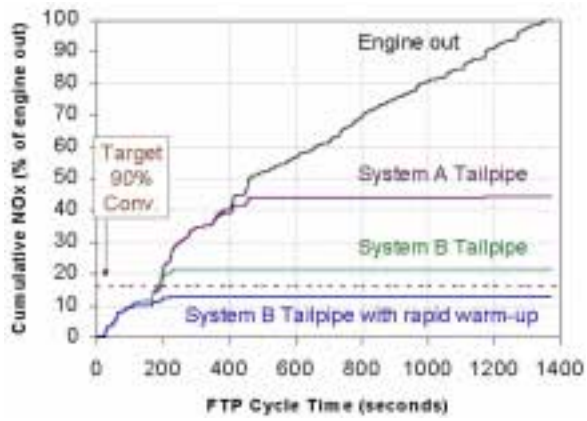


**Figure 4.** Predicted System Efficiencies

## Conclusions

Rapid warm-up of the exhaust system during a cold-start is key to achieving 90+% $NO_x$ conversions required to meet the light-duty Tier II Bin 5 standards. Further optimization of the aqueous urea injection strategy and hardware is required to allow full utilization of the reductant by the SCR catalyst, thus improving $NO_x$ conversion. Continued research on $NO_x$ and $NH_3$ sensors is needed for better selectivity and durability.

## References

1. R.M. Heck and R.J. Farrauto, "Catalytic Air Pollution Control," Van Nostrand Reinhold, New York, 1995.

2. H. Luders, R. Backes, G. Huthwohl, D.A. Ketcher, R.W. Horrocks, R.G. Hurley, and R.H. Hammerle, "An urea lean $NO_x$ catalyst system for light duty diesel vehicles," SAE 952493.

3. W. Held, A. Konig, T. Richter, L. Puppe, "Catalytic $NO_x$ reduction in net oxidizing exhaust gas," SAE 900496.

4. W.R. Miller, J.T. Klein, R. Mueller, W. Doelling, J. Zuerbig, "The development of urea-SCR technology for US heavy duty trucks," SAE 2000-01-0190.

5. M. Koebel, G. Madia, M. Elsener, "Selective catalytic reduction of NO and $NO_2$ at low

temperatures," Catalysis Today 73 (2002) 239-247.

## FY 2002 Publications/Presentations

1. Christine K. Lambert, Paul M. Laing,Robert H. Hammerle, "Using Diesel Aftertreatment Models to Guide System Design for Tier II Emission Standards", SAE 2002-01-1868.

2. David Kubinski, Richard Soltis, Jacobus Visser and Michael Parsons, "Detection of $NH_3$ using a YSZ-based potentiometric sensor with a tungsten oxide electrode." Proceedings of Electrochem. Soc. Meeting, San Fran., CA, Sept. 2-7, 2001.

3. R. E. Soltis, K. E. Nietering, D. Kubinski, "Non-ideal behavior of zirconia-based $NO_x$ sensors under reducing conditions", 9th International Meeting on Chemical Sensors in Boston, July 7-10, 2002.

# III. $NO_x$ CATALYSTS AND SENSORS

## A. Catalytic Reduction of NOx Emissions for Lean-Burn Engine Technology

*Timothy J. Gardner (Primary Contact)*
*Sandia National Laboratories (SNL)*
*Materials Chemistry Department*
*P.O. Box 5800, MS 1349*
*Albuquerque, NM 87185*

*Ralph N. McGill*
*Oak Ridge National Laboratory (ORNL)*
*National Transportation Research Center*
*2360 Cherahala Boulevard*
*Knoxville, TN 37932*

*Kevin C. Ott*
*Los Alamos National Laboratory (LANL)*
*Chemistry Division*
*Actinides, Catalysis, and Separations Group , MS J514*
*Los Alamos, NM 87545*

*DOE Technology Development Manager: Kathi Epping*

*CRADA Partners: Low Emissions Technologies Research and Development Partnership (LEP), (Member Companies: DaimlerChrysler Corporation, Ford Motor Company, and General Motors Corporation)*

This project addresses the following DOE R&D Plan barriers and tasks:

*Barriers*

A. $NO_x$ Emissions

C. Cost

*Tasks*

4c. Selective Catalytic Reduction Catalysts

### Objective

- Develop new catalyst technology to enable CIDI engines to meet Environmental Protection Agency (EPA) Tier II emission standards with minimal impact on fuel economy.

### Approach

- Discovery and development of new catalyst materials for reducing $NO_x$ emissions in lean-burn exhaust environments by greater than 90% in the 200 to 400°C temperature range using ammonia as a reductant. Materials for study include:
  - Hydrous Metal Oxide (HMO) or other oxide-supported catalysts; and
  - Microporous materials-supported catalysts, including zeolites.

- Evaluation of new catalyst materials in both bulk powder and monolith forms, including short-term durability testing under hydrothermal conditions and in the presence of $SO_2$.
- Scale-up of synthesis and processing of promising catalyst formulations to enable fabrication of prototype catalytic converters for CIDI engine dynamometer testing.
- Technology transfer of most promising catalyst formulations and processes to designated catalyst suppliers via the Low Emissions Technologies Research and Development Partnership (LEP).

## Accomplishments

- LANL completed the transition from hydrocarbon to ammonia selective catalytic reduction (SCR) catalyst testing. Thirty catalyst powders were screened for fresh catalyst activity, 6 for hydrothermal stability, and 5 for $SO_2$ aging. All zeolite-supported catalysts tested to date meet or exceed the LEP staged catalyst acceptance protocol.
- Preliminary data from LANL catalyst screening has determined that more stringent test conditions are needed to discriminate among the various zeolite-supported base metal catalyst powders.
- Initial LANL results on $NO_x$ and $NH_3$ storage showed that ammonium nitrate forms at temperatures less than 190°C for zeolite-supported base metal catalyst powders. Ammonium nitrate is thermally decomposed on heating from 150-250°C to produce $NH_3$, $N_2O$, and $N_2$. This behavior is in contrast to oxide-supported catalyst powders, which do not show significant ammonium nitrate formation.
- After significant ammonia SCR catalyst screening efforts (145 catalysts to date), SNL performed extensive short-term durability (26 catalysts to date) and $SO_2$ aging (8 catalysts to date) evaluations of non-vanadia catalyst formulations with promising fresh catalyst activity. Four non-vanadia catalyst formulations (powder form) that passed all criteria in the LEP staged catalyst acceptance protocol were identified.
- One of the non-vanadia SNL catalyst formulations was fabricated on a monolith core, showing excellent catalyst activity relative to supplier benchmark catalysts.
- SNL developed promoter phases that enhanced the fresh catalyst activity, short-term durability, and $SO_2$ tolerance of oxide-supported catalyst powders.
- SNL performed comparison studies showing the superiority of the ion exchangeable silica-doped hydrous titanium oxide (HTO:Si) supports relative to either $TiO_2$ or $Al_2O_3$ supports for these new ammonia SCR catalyst formulations (powder form).
- Both LANL and SNL filed patent disclosures on new ammonia SCR catalyst formulations.
- LANL had one journal paper accepted for publication on zeolite-based lean $NO_x$ catalysts (hydrocarbon SCR). SNL presented three papers on hydrocarbon or ammonia SCR catalysts, published one internal report on hydrocarbon SCR, and submitted two journal papers on hydrocarbon SCR. One Society of Automotive Engineers (SAE) technical paper on ammonia SCR was also published by SNL.

## Future Directions

- LANL and SNL will continue to synthesize, characterize, and test new catalyst compositions as ammonia SCR catalysts.
- LANL will perform more detailed studies of $NO_x$ and $NH_3$ storage and release phenomena, specifically comparing oxide- and zeolite-supported catalysts.
- Further testing of catalysts beyond the requirements of the LEP staged catalyst acceptance protocol will be performed by both LANL and SNL. These tests will be done to further discriminate $NO_x$ reduction activity differences among catalysts of various composition. This will include testing the

effects of space velocity, $NO/NO_2$ ratio, low-level concentrations of hydrocarbons, and $SO_3$ on the $NO_x$ reduction performance of ammonia SCR catalysts.

- LANL and SNL will continue short-term hydrothermal stability and $SO_2$ aging tests using the LEP-defined acceptance criteria.
- Microstructural analysis of LANL and SNL catalysts will be continued at ORNL.
- $NO_x$ reduction activity data for promising catalysts will be validated at other national laboratories and the LEP. Technology transfer activities for promising non-vanadia catalyst formulations will be initiated.
- ORNL will benchmark the performance of a Ford Focus equipped with a urea SCR emissions control system on a chassis dynamometer, paying special attention to unregulated emissions and the emissions profiles for the various emissions control system components.
- ORNL will initiate a study of low temperature urea decomposition in an exhaust system. A comparison of catalyst performance will be made between urea solution and gaseous ammonia injection as the reductant. Other control studies will also be included, which may involve LANL characterization efforts as well.

---

## Introduction

This multi-partner effort involves separate CRADAs between three national laboratories (Los Alamos National Laboratory [LANL], Oak Ridge National Laboratory [ORNL], and Sandia National Laboratories [SNL]) and the Low Emissions Technologies Research and Development Partnership (LEP, composed of DaimlerChrysler Corporation, Ford Motor Company, and General Motors Corporation). Each of these CRADAs is scheduled to run through 2003. The project addresses reduction of CIDI engine $NO_x$ emissions using exhaust aftertreatment - identified as one of the key enabling technologies for CIDI engine success. The overall CRADA efforts are currently focused on the development of urea/ammonia selective catalytic reduction (SCR) processes for reducing $NO_x$ emissions, specifically targeting the selection of appropriate catalyst materials to meet the exhaust aftertreatment needs of light- and medium-duty diesel engines. Infrastructure issues notwithstanding, this process has the greatest potential to successfully attain the > 90% $NO_x$ reduction required for CIDI engines to meet the new EPA Tier II emission standards scheduled to be phased in starting in 2004. Unless otherwise explicitly stated, all results reported herein refer to catalyst formulations in powder form. As our project advances, we hope to expand our efforts to include catalyst evaluation in monolith form. This goal will be facilitated via technology transfer between the national laboratories and the LEP and its designated catalyst suppliers.

Los Alamos National Laboratory (LANL) Efforts

During FY02, work at LANL was focused on completing the transition from the use of hydrocarbons to ammonia as reductant for the ongoing research into the selective catalytic reduction of $NO_x$ in CIDI engine exhaust. LANL's history of participation in this CRADA has centered on the use of microporous catalysts, particularly zeolite-based catalysts using base metals as the active component. With over 900 different microporous materials in the LANL lean $NO_x$ catalyst library, our effort in FY02 has been to downselect a representative number for initial screening, short-term durability, and $SO_2$ aging tests under ammonia SCR conditions that have been described earlier (see FY01 Annual Progress Report). A cross section of zeolite-supported catalysts were chosen having different pore topologies and diameters, with ion exchange used to load a variety of base metal ions. During FY02 we have performed activity testing on 30 different zeolite-supported catalyst powders from the LANL library. This testing also included evaluation of five separate preparations of one specific catalyst powder formulation in order to determine the reproducibility of both catalyst synthesis and bench top reactor operation. Of the 30 total catalysts, we have tested 6 for short-term durability (hydrothermal aging). Of these 6, we have tested 5 for $SO_2$ aging.

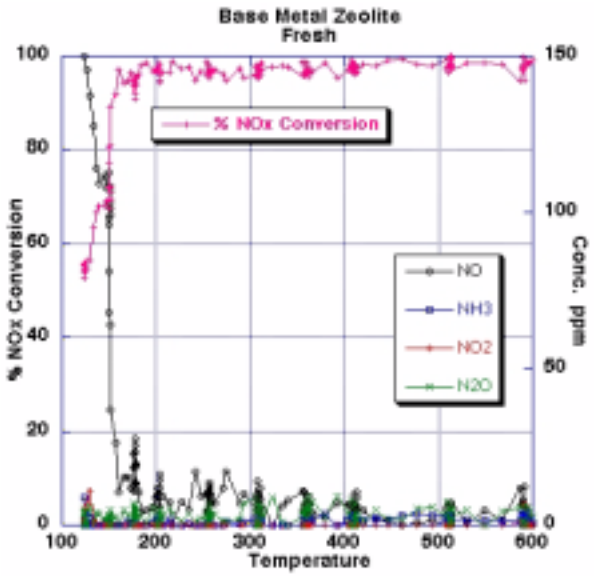


**Figure 1.** Ammonia SCR $NO_x$ Activity Test under Standard Test Conditions for a Fresh Zeolite-Supported Base Metal Catalyst

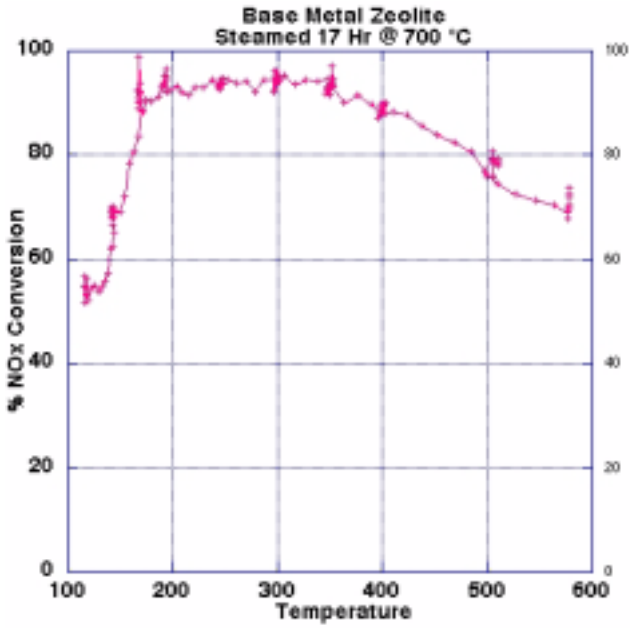


**Figure 2.** Ammonia SCR $NO_x$ Activity Test under Standard Test Conditions for a Zeolite-Supported Base Metal Catalyst Powder Tested after Being Steamed for 17 h at 700°C

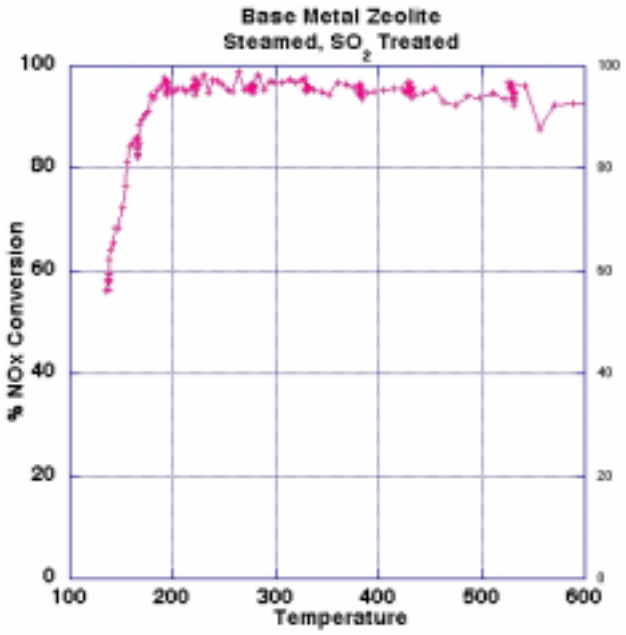


**Figure 3.** Ammonia SCR $NO_x$ Activity Test under Standard Test Conditions for a Zeolite-Supported Base Metal Catalyst Powder Tested after $SO_2$ Aging (15 ppm $SO_2$ in 10% steam for 16 h at 350°C)

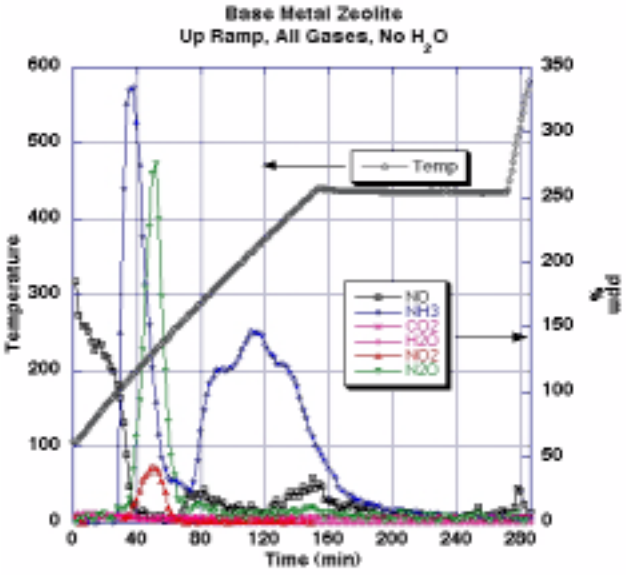


**Figure 4.** Upramp test following the downramp test shown in Figure 1 for a zeolite-supported base metal catalyst powder. Data indicate the decomposition of adsorbed ammonium nitrate at temperatures of ~200°C up to 250°C.

The results of these screening studies have indicated that under the test conditions prescribed by our LEP CRADA collaborators, the zeolite-supported catalyst powders meet or exceed the 90% $NO_x$ conversion efficiency test between 200 and 400°C, and also pass both the short-term durability test (16 h at 600°C) and $SO_2$ aging test (16 h exposure to 15 ppm $SO_2$ at 350°C). In fact, of those catalysts tested for short-term durability, all of them also passed the criterion even after being exposed to 5-10% steam at 700°C. Examples of the fresh catalyst screening, short-term durability, and $SO_2$ aging test results over one zeolite-supported base metal catalyst powder are shown in Figures 1, 2, and 3, respectively.

Under these test conditions, all of the different zeolite-supported catalyst powder materials tested to date have yielded results similar to those shown in Figure 1. While these test results are exciting, they imply that we need to define more stringent test conditions such that we can discriminate among the different catalyst formulations. Future studies will be directed towards altering our test parameters to allow for better discrimination in catalyst performance. These parameters are increased space velocity, varying the $NO/NO_2$ ratio in the feed, increased time and temperature of the short-term durability (hydrothermal aging) test, and increased concentration of $SO_2$ in the $SO_2$ aging test. We are also considering altering the test for aging to use $SO_3$ rather than $SO_2$, a condition that may better reflect the speciation of $SO_x$ downstream of a diesel oxidation catalyst. Another parameter that may be added to the test matrix is the addition of CO and hydrocarbons to the feed to simulate the conditions where a diesel oxidation catalyst has either not achieved light-off conditions, or has suffered a loss in activity because of poisoning. With the development of these more stringent test conditions, we will then be able to select the best catalyst formulations for further development and/or transfer to the LEP and its designated catalyst suppliers for their testing and development.

We have also obtained preliminary results on $NO_x$ and $NH_3$ storage and release from one of these zeolite-supported base metal catalyst powders. At temperatures below approximately 190°C, $NO_x$ is stored on these materials as ammonium nitrate

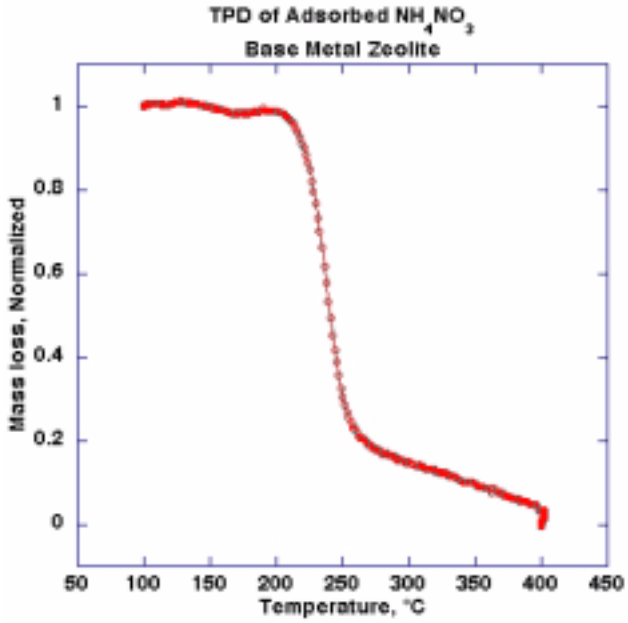


**Figure 5.** Desorption of Ammonium Nitrate from a Zeolite-Supported Base Metal Catalyst Powder with Increasing Temperature

($NH_4NO_3$). Upon subsequent heating of the catalyst to 150-250°C, the adsorbed $NH_4NO_3$ thermally decomposes to a mixture of mainly $NH_3$ and $N_2O$ (see Figure 4). Gas chromatographic analysis also indicates the evolution of $N_2$ during this process (data not shown). Higher temperatures result in the desorption of stored ammonia. Thermogravimetric analysis (see Figure 5) performed under similar conditions leads to a similar conclusion that the decomposition of bound $NH_4NO_3$ is responsible for the evolution of gases upon increasing the temperature of the catalyst. Preliminary results at both SNL and LANL indicate that oxide-supported catalysts do not store $NO_x$ as $NH_4NO_3$ under typical operating conditions, a significant deviation in behavior compared to the zeolite-supported catalysts. We will be following up on these observations during the next year, as well as, studying in greater detail the similarities and differences in storage phenomena on oxide- and zeolite-supported catalysts.

Oak Ridge National Laboratory (ORNL) Efforts

ORNL's continuing role in this project has been to provide characterization of catalyst performance, both in bench scale reactor testing and in an engine

laboratory, in addition to microstructural evaluation of catalysts using electron microscopy.

In the short term, we plan to do experiments with one of Ford's urea SCR Focus vehicles. We will "benchmark" its performance on the chassis dynamometer, with special attention to the unregulated emissions. To the extent possible, we will examine the emissions profiles between components of the exhaust emission control system to gain an understanding of the intermediate emissions.

Starting in FY03, we will begin to study the phenomena associated with urea decomposition in the exhaust system with a particular emphasis on the low temperature regime where urea decomposition can be incomplete. This investigation will be accomplished in the engine lab using both aqueous urea and ammonia for comparison. A second, associated experiment will investigate the adsorption and desorption of urea by the catalyst by impregnating materials with urea and measuring the ammonia released during a subsequent desorption cycle (LANL may also participate in this effort).

Sandia National Laboratories (SNL) Efforts

This year we continued our ammonia SCR catalyst screening efforts, specifically focusing on the identification of non-vanadia SCR catalyst compositions that meet $NO_x$ reduction activity requirements. Vanadia-based catalyst formulations, although possessing high activity, durability, and resistance to $SO_2$ aging, are undesirable due to potential volatility issues associated with catalyst use in exhaust aftertreatment applications. Included within our recent efforts were catalyst development studies to improve promising formulations with respect to short-term durability and $SO_2$ aging requirements, as well as efforts to prepare promising catalyst formulations in monolith core form.

Various numbers of catalyst formulations have advanced through different stages of the testing matrix (LEP staged catalyst acceptance protocol) as shown in Table 1. These numbers represent the testing of experimental bulk catalyst powders only and do not include any catalyst testing in monolith core form (supplier benchmark catalysts or experimental SNL-fabricated monoliths). Relative to FY01 efforts, more effort in FY02 was spent evaluating the short-term durability and $SO_2$ aging of promising catalyst formulations. As these tests require a considerable amount of reactor unit time relative to simple fresh catalyst screening tests, fresh catalyst screening efforts were correspondingly decreased in FY02.

**Table 1.** Summary of FY01-FY02 SNL Ammonia SCR Catalyst Powder Development Efforts

| | # of Catalysts Tested | | # of Catalysts Meeting Activity Criteria[+] | |
|---|---|---|---|---|
| Stage of Testing Matrix | FY02 | Total[^] | FY02 | Total[^] |
| Fresh (Degreemed) Catalyst | 57 | 145 | 26 | 39 |
| Short-Term Durability[*] | 22 | 26 | 7 | 10 |
| $SO_2$ Aging[*] | 7 | 8 | 4 | 5 |

[+] Catalyst acceptance criteria defined as > 90% $NO_x$ conversion over the 200-400$^o$C temperature range.

[^] Total is defined as FY01 + FY02.

[*] Using primary decision points defined as follows: short-term durability (600$^o$C/16 h/full exhaust gas mix [no $SO_2$]) and $SO_2$ Aging (350$^o$C/24 h/ full gas mix [20 ppm $SO_2$, no $NH_3$]). See FY01 Annual Progress Report for a description of the full exhaust gas mix and $SO_2$ aging gas mix compositions.

A total of five different catalyst powders have passed the LEP staged catalyst acceptance protocol. One catalyst is representative of a supported vanadia-based composition; this catalyst has been deselected from further consideration due to volatility concerns. The other four catalysts consist of different active base metal and promoter components (two distinctly different catalyst formulations denoted Catalyst A [with or without promoter] and Catalyst B [with or without promoter]). In many respects, the success of these catalyst formulations can be attributed to the recent development of promoter phases that enhance fresh catalyst activity, short-term durability, and $SO_2$ tolerance relative to the performance of the supported-base metal active phase alone. Rigorous comparisons of the effect of the catalyst support (HTO:Si vs. $TiO_2$ vs. $Al_2O_3$) were made with one of these catalyst formulations (Catalyst B with promoter). Figure 6 shows the fresh catalyst activity and short-term durability performance of Catalyst B without promoter (HTO:Si support, powder form). Although the fresh catalyst activity and 600°C hydrothermal aging results are very close to the acceptance criteria (> 90% $NO_x$ conversion between 200 and 400°C, see dotted line in Figure 6 used as a

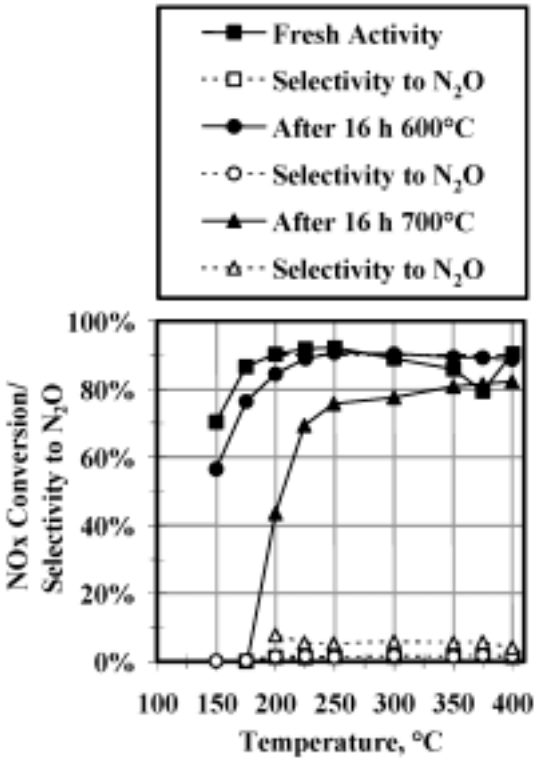


**Figure 6.** $NO_x$ Conversion and $N_2O$ Selectivity Profiles for Catalyst B (HTO:Si support, no promoter, powder form) in Its Fresh State and after Short-Term Durability Experiments at 600 and 700°C

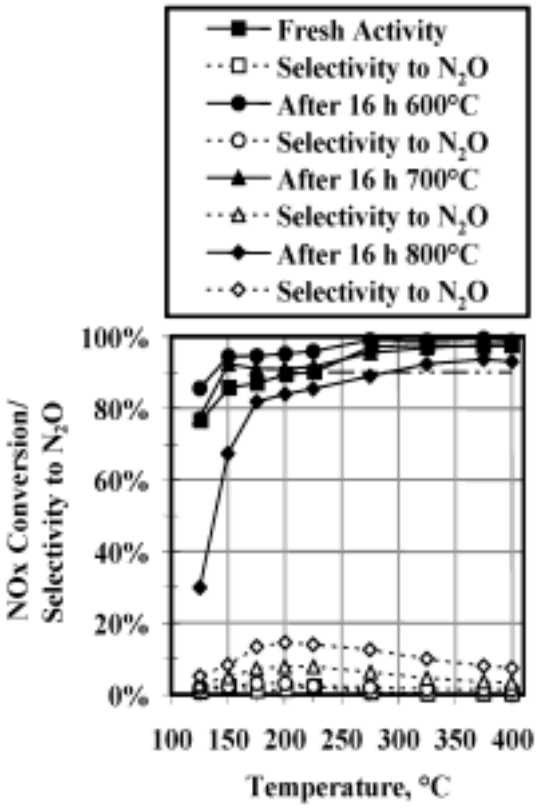


**Figure 7.** $NO_x$ Conversion and $N_2O$ Selectivity Profiles for Catalyst B (HTO:Si support, with promoter, powder form) in Its Fresh State and after Short-Term Durability Experiments at 600, 700, and 800°C

reference), significant deactivation occurs for this catalyst during hydrothermal aging at 700°C.

The effect of a promoter phase on improving fresh catalyst activity and short-term durability performance is shown in Figure 7. In addition to improving fresh catalyst activity (particularly at low temperature), the promoter phase significantly improves the resistance to catalyst deactivation during hydrothermal aging for Catalyst B. Note that the results for Catalyst B with promoter after 800°C hydrothermal aging are superior to those of Catalyst B without promoter after 700°C aging (see Figure 6). A slight increase in $N_2O$ selectivity is observed with increasing hydrothermal aging temperature, possibly consistent with sintering of the active phase component of the Catalyst B formulation.

Figure 8 shows that the Catalyst B with promoter formulation (HTO:Si support) shows no significant deactivation after 48 h of $SO_2$ aging at 350°C. The high level of catalyst activity over a wide temperature range demonstrates, along with the short-term durability data shown in Figure 7, that this catalyst satisfies all requirements in the LEP staged catalyst acceptance protocol.

One important question to answer in the overall catalyst development effort is whether the SNL ion exchangeable hydrous metal oxide supports offer performance advantages relative to commercial catalyst support materials. For fresh catalysts in powder form, it was found that the SNL HTO:Si support offers distinct advantages with respect to the Catalyst B (with promoter) formulation dispersed on several commercial catalyst support materials. Figure 9 shows fresh catalyst activity and short-term durability results obtained for a Catalyst B (with promoter) formulation on a commercial $TiO_2$ (Sachtleben Hombikat). By comparing Figures 7

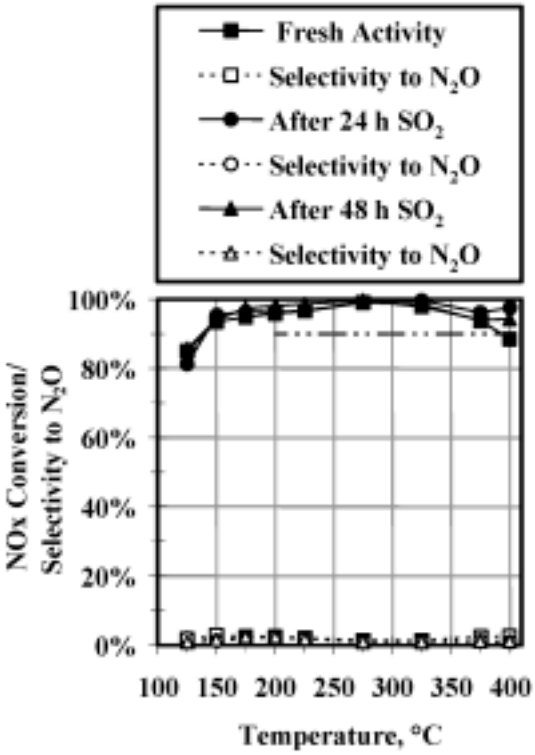


**Figure 8.** $NO_x$ conversion and $N_2O$ selectivity profiles for Catalyst B (HTO:Si support, with promoter, powder form) in its fresh state and after $SO_2$ aging experiments at 350°C for 24 h and 48 h

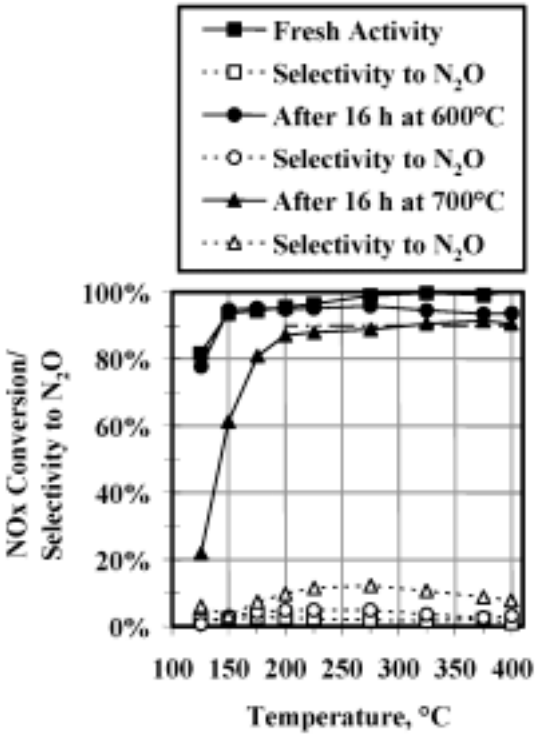


**Figure 9.** $NO_x$ Conversion and $N_2O$ Selectivity Profiles for Catalyst B (Commercial Sachtleben Hombikat $TiO_2$ support, with promoter, powder form) in Its Fresh State and after Short-Term Durability Experiments at 600 and 700°C

and 9, it can be observed that the HTO:Si-supported Catalyst B (with promoter) formulation is more resistant to hydrothermal aging than the equivalent $TiO_2$-supported formulation. Specifically, hydrothermal aging of the HTO:Si-supported Catalyst B (with promoter) at 800°C is nominally equivalent to hydrothermal aging of the $TiO_2$-supported Catalyst B (with promoter) at 700°C.

A second commercial support material, $Al_2O_3$ (γ-form), was also evaluated with the equivalent Catalyst B (with promoter) formulation. In this case, the HTO:Si-supported Catalyst B (with promoter) was found to possess both better low temperature activity and improved resistance to $SO_2$ poisoning relative to the $Al_2O_3$-supported material (catalysts in powder form). Figure 10 shows the fresh catalyst activity of the $Al_2O_3$-supported Catalyst B (with promoter) relative to the activity obtained after $SO_2$ aging for 24 h. Unlike the Catalyst B (with promoter) formulation on the HTO:Si support, which showed no observable deactivation due to $SO_2$ aging over 48 h at 350°C (see Figure 8), a slight deactivation was observed after 24 h of $SO_2$ aging at 350°C for the equivalent catalyst formulation on the $Al_2O_3$ support. Examination of the low temperature portion of the $NO_x$ conversion profiles in Figures 8 and 10 clearly shows the superior low temperature performance of the HTO:Si-supported Catalyst B (with promoter) material.

The HTO:Si-supported Catalyst B (with promoter) formulation is the most promising bulk powder catalyst evaluated to date for ammonia SCR performance. We therefore have begun preliminary experiments to evaluate this formulation in monolith core form using the direct coating method developed as part of previous monolith coating activities. Using the direct coating method, an alumina-coated cordierite is soaked in the organometallic soluble intermediate to provide a precursor to the ion exchangeable silica-doped hydrous titanium oxide

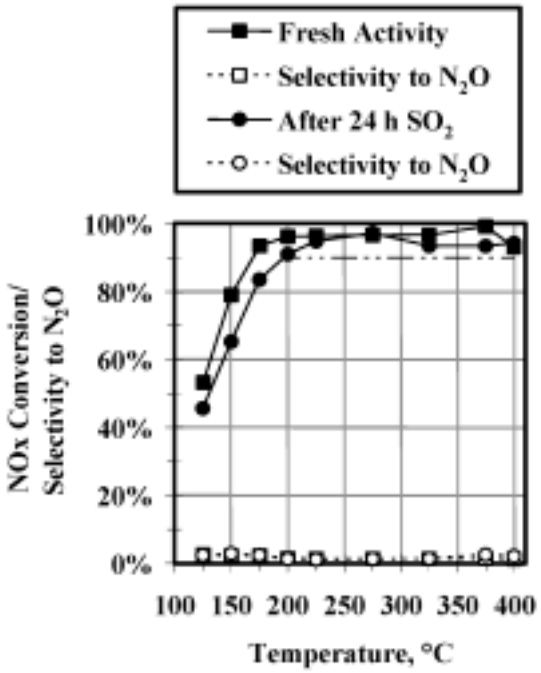


**Figure 10.** $NO_x$ Conversion and $N_2O$ Selectivity Profiles for Catalyst B ($Al_2O_3$ support, with promoter, powder form) in Its Fresh State and after $SO_2$ Aging Experiments at 350°C for 24 h and 48 h

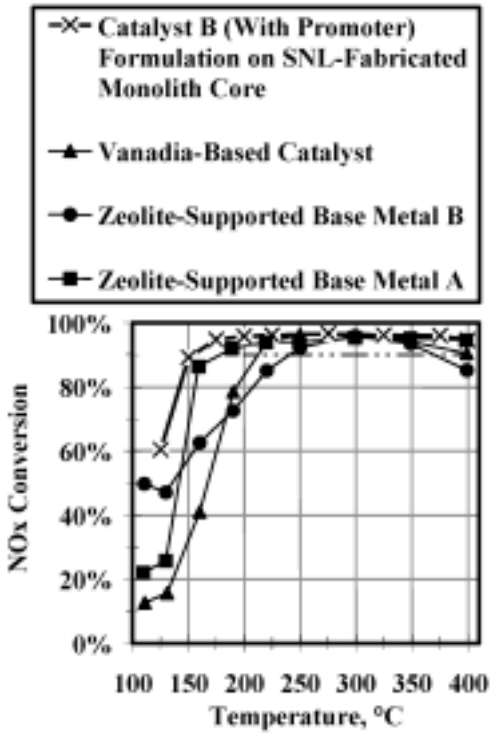


**Figure 11.** $NO_x$ conversion profiles for fresh supplier benchmark catalysts, as well as an experimental SNL non-vanadia catalyst formulation (HTO:Si-supported Catalyst B with promoter). All catalysts shown were tested in monolith core form.

(HTO:Si) coating. Following atmospheric hydrolysis of the soluble intermediate coating and drying, the monolith itself is put through the ion exchange and/or other subsequent processes to add promoter and/or active metal phases. An example of fresh catalyst activity test results for the Catalyst B (with promoter) formulation relative to supplier benchmark materials in monolith core form is shown in Figure 11. All of the catalysts shown in Figure 11 show good to excellent ammonia SCR activity between 200 and 400°C. The zeolite-supported base metal A catalyst exhibits the best low temperature (<200°C) performance of the supplier benchmark materials. The initial efforts at producing the HTO:Si-supported Catalyst B (with promoter) formulation in monolith core form yielded excellent results. This catalyst has fresh catalyst activity at least as good as the best supplier material over the entire temperature range of interest. In particular, high ammonia SCR activity in the 150-200°C range is desirable for both light- and medium-duty CIDI exhaust applications. Hydrothermal and $SO_2$ aging studies will now be initiated for the Catalyst B (with promoter) formulation in monolith core form.

In addition to continuing our catalyst screening efforts to identify other non-vanadia SCR catalyst compositions that meet $NO_x$ reduction activity requirements, tests will be conducted in an effort to further discriminate between the five bulk powder catalyst compositions that have passed the LEP staged catalyst acceptance protocol. Possible efforts include monolith core evaluation of these promising formulations, systematic variation of the $NO/NO_2$ ratio, increasing space velocity, increasing $NO_x$ concentration, and testing the effect of hydrocarbons and/or CO on ammonia SCR catalyst performance. Initial efforts have been made to facilitate testing of the HTO:Si-supported Catalyst B (with promoter) formulation by the LEP and LANL. Once our laboratory test data has been validated, this material

may be considered for technology transfer to the LEP and its designated catalyst suppliers. A Sandia Technical Advance (patent disclosure) has been filed on these new unpromoted and promoted base metal/ HTO:Si catalyst formulations.

## References

1. T. J. Gardner, R. N. McGill, K. C. Ott, and M. J. Royce, "Catalytic Reduction of $NO_x$ Emissions for Lean-Burn Engine Technology," in 2001 Annual Progress Report: Combustion and Emission Control for Advanced CIDI Engines, U.S. Department of Energy, Office of Transportation Technologies, November, 2001, pp. 38-50.

## Presentations/Publications/Patents

1. T. J. Gardner, L. I. McLaughlin, D. L. Mowery, and R. S. Sandoval, "Preparation Effects on the Performance of Silica-Doped Hydrous Titanium Oxide (HTO:Si)-Supported Pt Catalysts for Lean-Burn $NO_x$ Reduction by Hydrocarbons," Sandia Report, SAND2002-0085, Sandia National Laboratories, Albuquerque, NM, January, 2002, 48 pages.

2. T. J. Gardner, L. I. McLaughlin, D. L. Mowery-Evans, and R. S. Sandoval, "Reduction of $NO_x$ Emissions for Lean-Burn Engine Technology," Presentation at the 2002 National Laboratory CIDI and Fuels R&D Review, Argonne, IL, May 14, 2002.

3. K. C. Ott, N. C. Clark, J. A. Rau, "Reduction of $NO_x$ Emissions for Lean-Burn Engine Technology," Presentation at the 2002 National Laboratory CIDI and Fuels R&D Review, Argonne, IL, May 14, 2002.

4. T. J. Gardner, L. I. McLaughlin, D. L. Mowery-Evans, and R. S. Sandoval, "Development of Ammonia/Urea SCR Catalysts for Mobile Diesel Engine Exhaust Aftertreatment," Presented at the 3rd DOE 2000 National Laboratory Catalysis Research Conference, Richland, WA, May 23, 2002.

5. T. J. Gardner, L. I. McLaughlin, D. L. Mowery-Evans, and R. S. Sandoval, "Ammonia/Urea Selective Catalytic Reduction (SCR) for Mobile Diesel Engines: Influence of Exhaust Parameters," Presented at SAE Future Car Congress, Arlington, VA, June 3, 2002.

6. K. C. Ott, N. C. Clark, J. A. Rau, "Hysteresis in Activity of Microporous Lean $NO_x$ Catalysts in the Presence of Water Vapor", accepted for publication in Catalysis Today.

7. T. J. Gardner, L. I. McLaughlin, D. L. Mowery-Evans, and R. S. Sandoval, "Selective Catalytic Reduction of $NO_x$ by Hydrocarbons in Lean-Burn Exhaust Environments," submitted for publication to Applied Catalysis.

8. T. J. Gardner, L. I. McLaughlin, D. L. Mowery-Evans, and R. S. Sandoval, "The Effect of Sodium Content on the Performance of Silica-Doped Hydrous Titanium Oxide (HTO:Si)-Supported Pt Catalysts for Lean-Burn $NO_x$ Reduction by Hydrocarbons. Part 1. Effects of Catalyst Preparation and Test Mode," submitted for publication to Applied Catalysis.

9. K. C. Ott and N. C. Clark, "Catalyst and Process for Preparation of Catalysts for Lean Burn Engine Exhaust Abatement", U. S. Patent Disclosure, January, 2002.

10. T. J. Gardner, L. I. McLaughlin, and D. L. Mowery-Evans, "Unpromoted and Promoted Base Metal/HTO:Si Catalysts with Enhanced Activity, Durability, and Sulfur Tolerance for Selective Catalytic Reduction of $NO_x$ via Ammonia/Urea," Sandia Technical Advance (U.S. Patent Disclosure), July, 2002.

# B. Electrochemical $NO_x$ Sensor for Monitoring Diesel Emissions

*L. Peter Martin (Primary Contact), Ai-Quoc Pham*
*Lawrence Livermore National Laboratory*
*P.O. Box 808, MS L-353*
*Livermore, CA 94551-0808*

*DOE Technology Development Manager: Nancy Garland*

This project addresses the following DOE R&D Plan barriers and tasks:

Barriers

A. $NO_x$ Emissions

B. PM Emissions

*Tasks*

2a. Advanced Sensors and Controls

## Objectives

- Develop an electrochemical $NO_x$ sensor for CIDI exhaust gas monitoring
- Fabricate 1st generation laboratory prototype for sensitivity/selectivity testing at Ford Research Laboratory
- Continue investigation of materials and sensing mechanism to optimize performance

## Approach

- Utilize an ionic ($O^{2-}$) conducting ceramic as an electrolyte and mechanical support (substrate)
- Use colloidal spray deposition to apply metal oxide electrodes to the electrolyte substrate
- Evaluate electrode materials and processing conditions for sensitivity and response time
- Test operating modes, i.e. potentiometric and amperometric, to optimize performance
- Demonstrate stability and cross-sensitivity with interfering gas

## Accomplishments

- Developed a potentiometric sensor with high $NO_2$ response, negligible NO sensitivity, and fast response time at 700°C
- Identified a current-biased mode of potentiometric operation giving the best NO sensitivity and response speed (~27 mV at 500 ppm NO, 10% $O_2$, 650°C, 1.5 s response)
- Selected electrode materials for the current-biased NO sensor

## Future Directions

- Investigate sensor stability and oxygen sensitivity
- Send 1st generation laboratory prototype sensor to Ford for sensitivity/selectivity testing
- Continue to investigate electrode materials/microstructure
- Design and build integrated (self-heated) prototype sensor
- Perform fundamental investigation to identify NO sensing mechanism

## Introduction

The most promising NO sensors for exhaust gas monitoring are based on ionically conducting solid state electrochemical devices [1, 2]. These devices typically consist of a solid ceramic electrolyte onto which two or more metal or metal-oxide electrodes are deposited, and can they be operated in either potentiometric or amperometric modes. Significant progress has been made towards the development of deployable sensors using yttria-stabilized zirconia (YSZ) as the electrolyte and catalytically active metal oxides as the sensing electrodes [3]. However, improvements are still needed in sensitivity, response time, reliability, and cross-sensitivity.

The current work is directed towards the development of a fast, high sensitivity electrochemical $NO_x$ sensor. Target operating parameters for the proposed sensor are (as per discussions with Ford collaborators) sensitivity to the total $NO_x$ content in the range of 1-1000 ppm, operating temperature >600°C, and response time equal to 1 second or less. The elevated operating temperature is to insure compatibility with a possible conversion catalyst which will convert the total $NO_x$ to one species, probably NO. In addition, the sensor should be simple and reliable, and cross-sensitivity with other oxidizing/reducing gas should be minimized. It should be noted that the relative merits of $NO_2$ versus NO selective sensors are not clear at the present time.

## Approach

The approach is to develop a sensor using catalytic metal oxide electrodes on a solid ionic conductor electrolyte. Similar technology has been widely investigated for various gas sensing applications and has been successfully developed for use as exhaust gas oxygen sensors. The current effort approaches the problem by the application of novel materials and fabrication processes designed to optimize electrode microstructures. In addition, a potentially novel mode of operation has been identified which yields enhanced NO response amplitude and speed.

Sensors were prepared by spray deposition of metal oxide electrodes onto YSZ electrolyte substrates, followed by sintering at 1000-1100°C. $NO_x$ sensing experiments were performed in a quartz tube inside a furnace. All tests were performed using 500 ppm NO or $NO_2$ in 10% $O_2$, balance $N_2$, at a flow rate of 1000 ml/min. The configuration of a typical sensor and test apparatus are shown schematically in Figure 1. All tests were performed in the temperature range of 600-700°C.

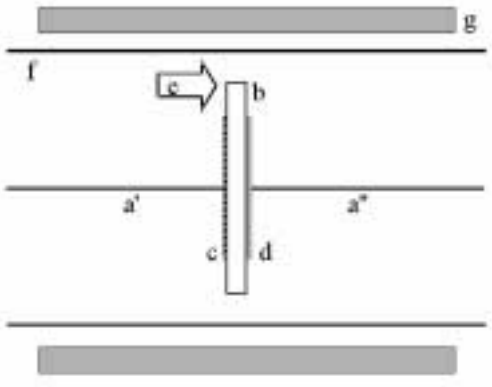


**Figure 1.** Schematic of the experimental test set up showing: a', a") wire leads, b) YSZ electrolyte, c) metal oxide electrode, d) Pt or metal oxide electrode, e) test gas flow, f) quartz tube, and g) furnace hot zone.

## Results

Figure 2 shows the mixed potential response from a sensor using a composite YSZ/doped-lanthanum manganate sensing electrode and a Pt metal reference electrode. The data show a baseline near 0 mV when the gas stream is composed of 10% $O_2$ with balance $N_2$ at 700°C, and a response in excess of 40 mV when 500 ppm $NO_2$ is introduced. The 90% recovery (turn-off) time for this sensor is 2.5 seconds, which approaches the target 1 second (the data points in all Figures are spaced 0.5 seconds apart). The sharp peaks at the beginning of each response result from a transient overpressure when the $NO_2$ is introduced into the gas stream. The sensor has negligible NO sensitivity, making it highly selective to $NO_2$. It was observed that potentiometric sensors which gave reasonable sensitivity to NO at temperatures >600°C for example, sensors with $NiCr_2O_4$ as the sensing electrode had recovery times which were much too

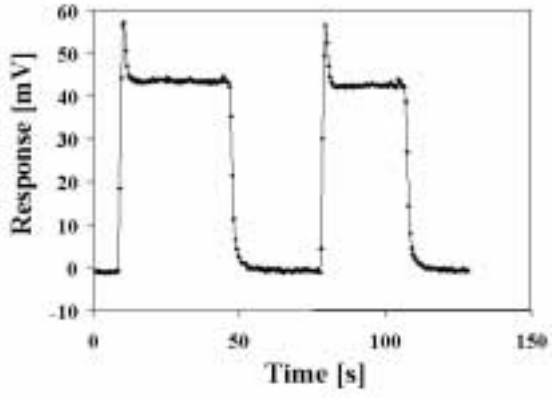


**Figure 2.** Potentiometric response of a $NO_2$ sensor, operated at 700°C, with a composite sensing electrode (YSZ and doped-lanthanum manganate). The gas contains 10% $O_2$ and 500 ppm $NO_2$.

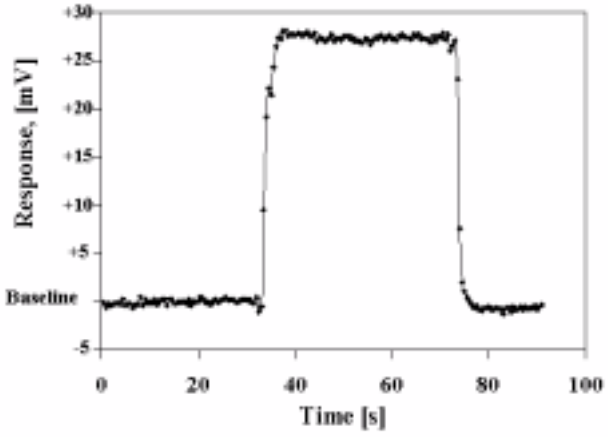


**Figure 3.** Response of the current-biased sensor to 500 ppm NO in 10% $O_2$ at 650°C. The sensor uses a $NiCr_2O_4$ sensing electrode and a composite reference electrode.

long (>10 seconds). Thus, alternate modes of operation were investigated.

Since the electrochemical sensing mechanisms for the $NO_x$ species involve oxidation/reduction reactions, it is logical to think that one could modify the kinetics, and perhaps speed up the response, by appropriately biasing the sensor electrodes. Other investigators have attempted to correlate the gas composition with the current resulting from a fixed potential-bias across the electrodes. In the 10% $O_2$ environment, however, this biasing causes a high $O_2$ pumping current which overwhelms the $NO_x$ sensing response. To correct for this high $O_2$ current, it is generally necessary to pump out the oxygen from the sample gas stream, for example using a YSZ pump. This contributes to the complexity of the sensor, and it raises concerns relating to the possible decomposition of the $NO_x$ during the pumping operation. We have developed a related technique in which a fixed current, rather than a fixed potential, is applied between the sensing and reference electrodes. The potential required to maintain this current is then measured and correlated to the gas composition. Figure 3 shows data from a sensor using a $NiCr_2O_4$ sensing electrode and a YSZ/doped-lanthanum manganate reference electrode at 650°C. The response is +27 mV when 500 ppm NO is introduced into the gas stream, and the 90% recovery time is 1.5 seconds. It is interesting to note the positive sign of the response, which is indicative of the reduction of NO and is consistent with the direction of bias of the electrodes. Under the current-biasing conditions shown in Figure 3, the sensor has high $NO_2$ sensitivity (~3x the NO sensitivity).

It is possible, by operating under different biasing conditions, to make the sensor shown in Figure 3 insensitive to $NO_2$. Under those conditions, the sign of the response becomes negative, indicating that the sensor response comes from the oxidation of NO to $NO_2$. Thus, changing the biasing can actually change the operating mechanism of the sensor. In addition, the sensitivity nearly doubles (to 45 mV for 500 ppm NO) but the response time becomes slower (90% recovery increases to 7 seconds).

## Conclusions

We have developed a potentiometric $NO_2$ sensor with high sensitivity, selectivity, and speed at 700°C. We have developed an alternative mode of operation for NO detection which utilizes a current-bias across the electrodes. This mode of operation gives good NO sensitivity (~27 mV at 500 ppm NO) and response speed (1.5 s) when operated at 650°C in 10% $O_2$. When operated under different biasing conditions, this mode of operation gives enhanced NO response and negligible $NO_2$ sensitivity at the expense of response time. To the best of our knowledge, this mode of operation has not been reported in the literature pertaining to

electrochemical $NO_x$ sensors. Continued investigation is necessary to optimize performance, quantify cross sensitivity, and establish stability of the sensor.

## FY 2002 Publications/Presentations

1. L. P. Martin, Q. Pham, and R. S. Glass, "Electrochemical $NO_x$ Sensor for Monitoring CIDI Vehicle Emissions," presented at National Laboratory CIDI and Fuels R&D Merit Review and Peer Evaluation, Argonne, IL, May 14, 2002.

2. L. P. Martin, Q. Pham, and R. S. Glass, "Effect of $Cr_2O_3$ Electrode Morphology on the NO Response of a Stabilized Zirconia Sensor," submitted to Sensors and Actuators B (June, 2002).

## References

1. F. Menil, V. Coillard, and C. Lucat, "Critical review of Nitrogen Monoxide Sensors for Exhaust Gases of Lean Burn Engines," Sensors Actuators B 67 (2000) 1-23.

2. N. Miura, G. Lu, and N. Yamazoe, "Progress in Mixed-Potential Type Devices Based on Solid Electrolyte for Sensing Redox Gases," Solid State Ionics 136-137 (2000) 533-542.

3. T. Ono, M. Hasei, A. Kunimoto, T. Yamamoto, and A. Noda, "Performance of the $NO_x$ Sensor Based on Mixed Potential for Automobiles in Exhaust Gases, JSAE Review 22 (2001) 49-55.

# C. $NO_x$ Control and Measurement Technology for Heavy-Duty Diesel Engines

*Bill Partridge (Primary Contact)*
*Oak Ridge National Laboratory (ORNL)*
*NTRC*
*2360 Cherahala Blvd.*
*Knoxville, TN 37932*

*Tom Yonushonis*
*Cummins, Inc.*
*1900 McKinley Avenue*
*Columbus, IN 47201*

*DOE Technology Development Manager: Gurpreet Singh*

This project addresses the following DOE R&D Plan barriers and tasks:

*Barriers*

A. $NO_x$ Emissions

C. Cost

*Tasks*

4. $NO_x$ Control Device R7D

4d. Advanced $NO_x$ Reducing Systems

## Objectives

- Advance the development of $NO_x$ aftertreatment systems for diesel engines by quantifying their detailed chemical processes to identify barriers and improvement strategies.

## Approach

- Develop advanced measurement capabilities to elucidate relevant aspects of $NO_x$-aftertreatment performance with improved resolution and/or sensitivity.
- Apply the Spatially-resolved Capillary Inlet Mass Spectrometer (SpaciMS) to investigation of gas-phase species dynamics, including $NO_x$ slip and desorption and reductant reforming, in bench-scale and full-scale devices.

## Accomplishments

- Developed magnetic-sector based SpaciMS for quantifying hydrogen spatio-temporal distributions throughout an operating catalyst.
- Developed instrument, based on Laser-Induced Phosphorescence (LIP), for resolving spatio-temporal temperature distributions within a catalyst.

## Future Direction

- Apply the $H_2$-SpaciMS and LIP instruments to study reductant generation and usage associated with $NO_x$ adsorber regeneration.

## Introduction

$NO_x$-adsorber catalysts provide a promising approach for emissions reduction in the fuel-lean environment of diesel-engine exhaust. $NO_x$-adsorber systems have a finite capacity to store $NO_x$ emissions by forming surface nitrogen species at active catalyst sites. These systems are periodically regenerated to restore capacity by injecting pulses of reductant, which causes the stored $NO_x$ to be desorbed and reduced, ideally to $H_2O$, $CO_2$, and $N_2$. Because of its availability, diesel fuel is a convenient reductant, but it requires reforming to produce secondary species such as $H_2$ and CO that are believed to be more efficient reductants. In-cylinder injection of diesel fuel via a late injection and in-pipe injection are the most common ways of introducing a reductant.

High-speed instruments capable of temporally resolving the transient emissions associated with the fundamentally dynamic $NO_x$ adsorber process are required to develop and optimize these promising emissions control strategies. Minimally- or non-invasive diagnostics might allow for intra-channel probing of the catalyst chemistry to quantify the axial distribution of participating species, $NO_x$ loading, reductant reforming, sulfur poisoning and desulfation. Such information is critical to understanding the detailed catalyst chemistry, identifying rate limiting steps, specifying device size and aspect ratio, and optimizing washcoat formulation to improve storage, reforming, regeneration, and sulfur tolerance performance.

## Approach and Results

### $H_2$-SpaciMS Instrument

The $H_2$-SpaciMS has been developed to quantify spatio-temporal distributions of hydrogen. It can also characterize the multiple exhaust constituents now routinely investigated with the original quadrupole-based SpaciMS, including $NO_x$, $O_2$, $CO_2$, $H_2S$, $SO_2$ and various hydrocarbon fragments. The $H_2$-SpaciMS is shown in Figure 1, and is based on a VTI Odyssey magnetic-sector mass spectrometer. VTI has worked closely with ORNL to improve the base instrument. Calibration scans were used to assess the performance of the new instrument relative to the original SpaciMS. The

**Figure 1.** The $H_2$-SpaciMS is based on a magnetic-sector MS, and has the same portability characteristics of the original instrument.

instrument response to nitric oxide was used as a benchmark because of our extensive experience measuring this species. The original SpaciMS routinely provided linear NO response with four-9s correlation coefficient, and a 2-sigma detection limit of 11 ppm based on $2\sigma$(0 ppm NO)Signal(1000 ppm NO)/$\sigma$(1000 ppm NO). In the first quarter of FY2002, the $H_2$-SpaciMS had good linearity but an NO detection limit of 800 ppm, indicating a requisite 70 X improvement just to match the benchmark. By the beginning of the third quarter of FY2002, this improved performance had been achieved; the $H_2$-SpaciMS demonstrates linear NO response with four-9s correlation coefficient, and a 2-sigma detection limit of 17 ppm. The hydrogen response of the $H_2$-SpaciMS is shown in Figure 2, and indicates excellent linearity with six-9s correlation coefficient, and a 2-sigma detection limit of 5 ppm. This is very good performance and should be more than adequate for mapping $H_2$ generation and usage through a regenerating $NO_x$ adsorber.

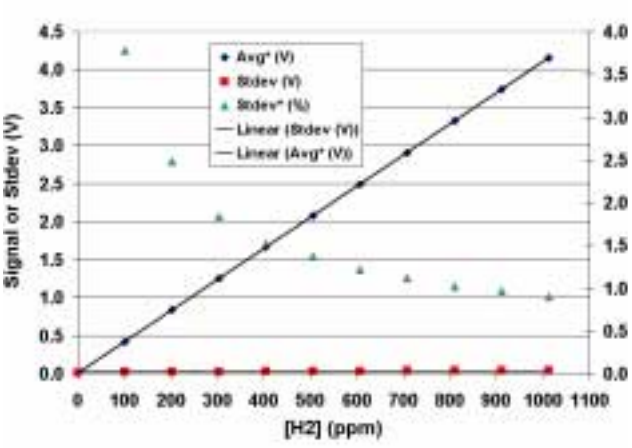


**Figure 2.** Response of the $H_2$-SpaciMS to hydrogen in terms of signal and standard deviation. This data indicates six-9s linearity and a 5-ppm 2-sigma detection limit.

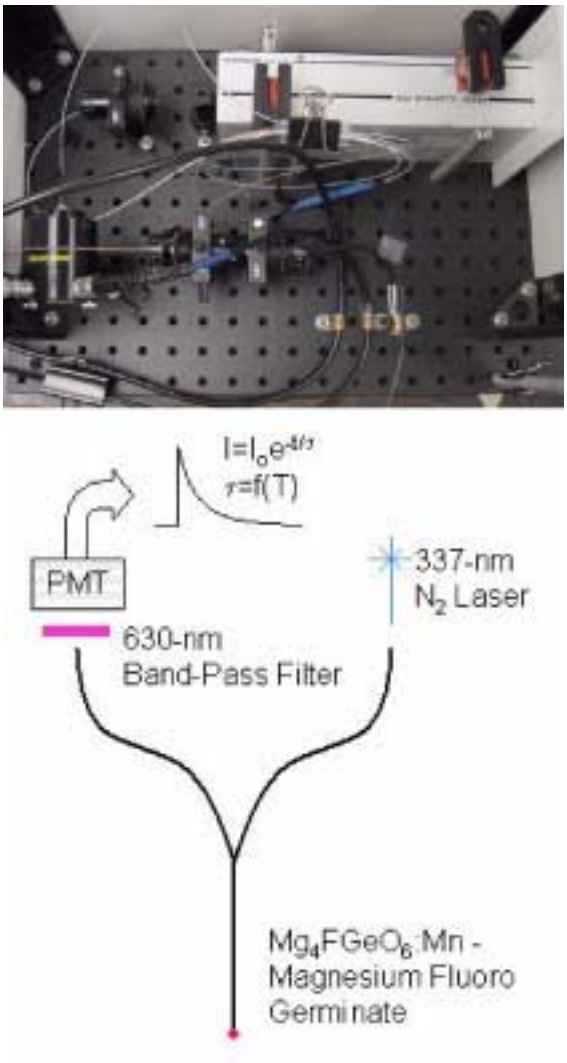


**Figure 3.** Photograph of the LIP instrument showing the nitrogen laser, fiber coupler and PMT (top); Schematic of the LIP instrument (bottom)

Phosphor Thermography Instrument

The Laser-Induced Phosphorescence (LIP) instrument has been developed to quantify spatio-temporal temperature distributions throughout an operating catalyst. It is based on the temperature-dependent phosphorescence lifetime of rare-earth-doped ceramic phosphors, as described by Allison and Gillies [1]. The instrument photograph and schematic are shown in Figure 3. A 337-nm laser is injected into one (pump) leg of a fiber coupler to excite the phosphor which is deposited on the tip of a gold-coated bare fiber. The gold coating allows for high-temperature applications up to 750°C. The phosphor is excited by the laser to long-lived excited states which decay via phosphorescence in the 650-nm range. Some of the phosphorescence is captured by the same optical fiber used to deliver the pump light, and is directed to a second (detection) leg of the fiber coupler. The light emitted from the fiber coupler's detection leg is filtered to reject pump light at 337 nm, and is detected via a photomultiplier tube (PMT). The phosphorescence signal displays an exponential decay with a time constant, t, proportional to temperature, as shown in Figure 3. The PMT signal waveform is monitored at 400 kHz and analyzed via a LabView program to actively determine the phosphorescence time constant. The time constant measurements can be made at rates up to ca. 1.8 Hz. Figure 4 shows a calibration curve, which is used to convert the phosphorescence time constant to temperature. Temperature gradients are resolved by translating the phosphor tip.

The LIP instrument has been applied to quantify spatio-temporal temperature distributions throughout an EmeraChem $NO_x$ adsorber catalyst during regeneration. A 1-inch diameter catalyst core (200 cells/in$^2$) was housed in a quartz tube and heated in a tube furnace to 250°C. This catalyst was exposed to a mixture of 11% $O_2$ in $N_2$ at a space velocity of 25,000 exchanges/hr. Reductant (9.98% ethylene,

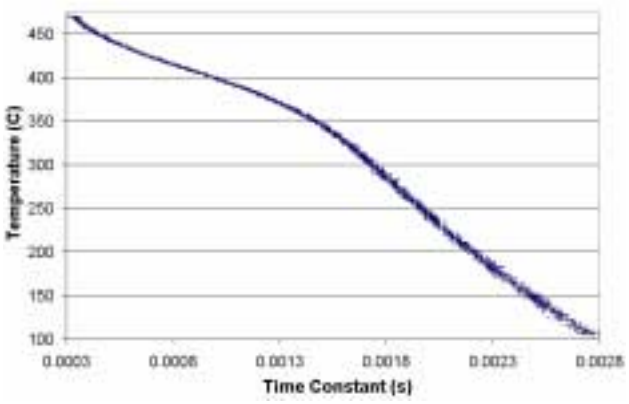


**Figure 4.** LIP calibration curve used to convert the phosphorescence time constant to temperature.

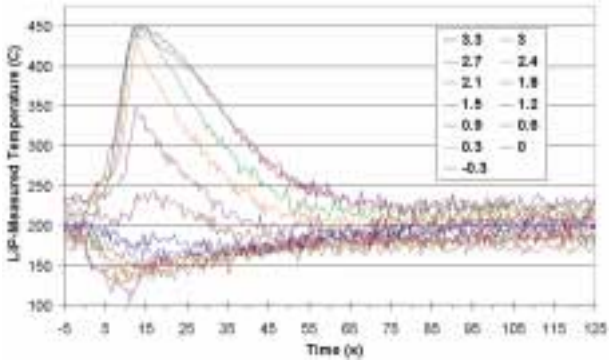


**Figure 5.** Spatially resolved temperature transients throughout a $NO_x$ adsorber catalyst, associated with reductant injection, measured using the LIP instrument.

0.21% $N_2$, CO balance) was injected for a 12-s duration on a 125-s period. LIP temperature measurements were made every 0.3-in throughout the 3-in long catalyst core by translating a 140-µm outside diameter phosphor-tipped optical fiber through one of the central channels. The ratio of channel to fiber area for this setup is 210 to mitigate flow occlusion associated with the fiber. The resulting temperature distributions are shown in Figure 5, where the reductant pulse started at time 0, and curves 0 and 3.0 represent behavior at the entrance and exit faces of the catalyst, respectively. Temperature transients were measured throughout the catalyst as well as 0.3 inches upstream and downstream of the catalyst. Figure 5 indicates noticeable cooling on the order of 50°C in the region of the catalyst entrance face associated with the unheated reductant injection. There is some gradual gas heating up to 1.8 inches into the catalyst, which is likely due to heat transfer from the bulk monolith. Catalyst light-off occurs around 2 inches into the core, as inferred by the dramatic temperature increases at locations in the back third of the core. Peak temperatures of approximately 450°C are reached at the back end of the catalyst. Such temperature data is invaluable, along with SpaciMS measured species distributions, to the detailed understanding and modeling of catalyst processes.

## Conclusions and Future Plans

The $H_2$-SpaciMS and LIP instruments will be applied in late FY2002 and FY2003 to study reductant generation and usage throughout an operating $NO_x$ adsorber catalyst.

Minimally invasive analytical techniques capable of resolving spatio-temporal temperature and gas-phase species (including $H_2$, $NO_x$, $O_2$, $CO_2$, HC and $H_2S$) distributions within an operating catalyst are critical to establishing a detailed understanding of catalyst performance. Without such detailed information, model development and materials improvement to overcome existing performance barriers will be severely limited. The SpaciMS and LIP instruments, developed in a DOE sponsored CRADA between Cummins and ORNL, provide these requisite analytical techniques. Moreover, these diagnostics are readily transportable, which allows for applications at industrial sites.

## References

1. Allison, S. W. and Gillies, G. T. (1997). 'Remote Thermometry with thermographic phosphors: Instrumentation and applications,' Rev. Sci. Instrum. 68 (7), 2615-2650.

# D. Evaluation of $NO_x$ Sensors for Heavy Duty Vehicle Applications

*Michael D. Kass (Primary Contact), Ned E. Clapp, Jr., Ron L. Graves, and Tim Armstrong*
*Oak Ridge National Laboratory*
*2360 Cherahala Blvd.*
*Knoxville, TN 37932*

*DOE Technology Development Managers: Gurpreet Singh and Kevin Stork*

*CRADA Partner: Ford Motor Company, Dearborn, MI*

This project addresses the following DOE R&D Plan barriers and tasks:

*Barriers*

A. $NO_x$ Emissions

C. Cost

*Tasks*

2a. Advanced Sensors and Controls

## Objective

- Characterize the performance of $NO_x$ emission sensors and identify potential areas of improvement.

## Approach

- Develop a bench device to evaluate sensor performance under controlled conditions.
- Evaluate the flow characteristics of the test rig to determine baseline performance.
- Perform sensor evaluation by monitoring controller output.
- Extract the pumping currents from the NGK $NO_x$ sensor.
- Utilize discoveries to improve sensor response.

## Accomplishments

- Successfully measured $NO_x$ pumping current under transient operation.
- Performed preliminary analysis of $NO_x$ pumping current signature.

## Future Directions

- Evaluate performance of prototype emission sensors as they become available.

## Introduction

Urea selective catalytic reduction (SCR) and $NO_x$ adsorber systems are being investigated as devices to reduce $NO_x$ emissions from diesel engines. Optimization of these devices on an automotive platform will likely require feedback control. The availability of emission sensors is limited; in fact, the only currently available $NO_x$ sensors are those manufactured by NGK (the electronic controls to operate the device were developed by Siemens). Before any $NO_x$ sensor can be integrated into an emission control system, its performance must be accurately assessed to determine its range of operation and response.

The overall objective of this study is to characterize the performance of emission sensors and identify potential areas of improvement. To accomplish this objective, a test apparatus and

methodology for controlled evaluations were developed. For the NGK $NO_x$ sensor, the pumping current signature has been evaluated under transient conditions and analyzed to determine if an advanced filter algorithm could be applied to improve sensor response.

The NGK $NO_x$ sensor design consists of two cells with diffusion barriers. Exhaust enters the first cell, where it is thermally decomposed into NO and elemental oxygen. The oxygen present in the exhaust is pumped out of the first cell to levels approaching 10 ppm. The current generated by pumping out the oxygen from Cell 1 is transformed into a voltage by the controller to become the $O_2$ signal output for the device. The NO present in Cell 1 moves through a diffusion barrier to Cell 2. In Cell 2, the NO is decomposed into elemental nitrogen and oxygen on a rhodium electrode. The current generated by pumping $O_2$ out of Cell 2 is used to provide the $NO_x$ output signal of the device.

## Approach

A bench-scale rig was developed in order to measure the transient response of selected $NO_x$ (or oxygen) emission sensors. During FY2001, a fourth generation NGK $NO_x$ sensor was evaluated using the bench rig. The response of the device was measured and determined to be temperature dependent. During FY2002, a preliminary study was undertaken to determine if the $NO_x$ pumping current of the NGK sensor could be measured under transient operation. However, because no additional prototype emission sensors were made available for evaluation, the project was idled while further plans were being developed.

## Results

A fourth generation NGK $NO_x$ sensor was characterized in the sensor evaluation bench-rig developed at ORNL. A group of 8 wires connects the sensor hardware to the controller. The line providing the $NO_x$ pumping current was identified, and a high-speed picoammeter was spliced directly into this line. The picoammeter was set up to float the current signal to enable direct measurement of the current without interference. A photograph showing the key components is shown in Figure 1.

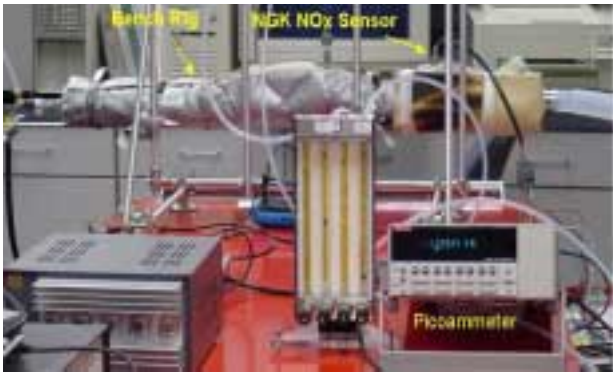


**Figure 1.** Bench Rig for Emission Sensor Evaluation

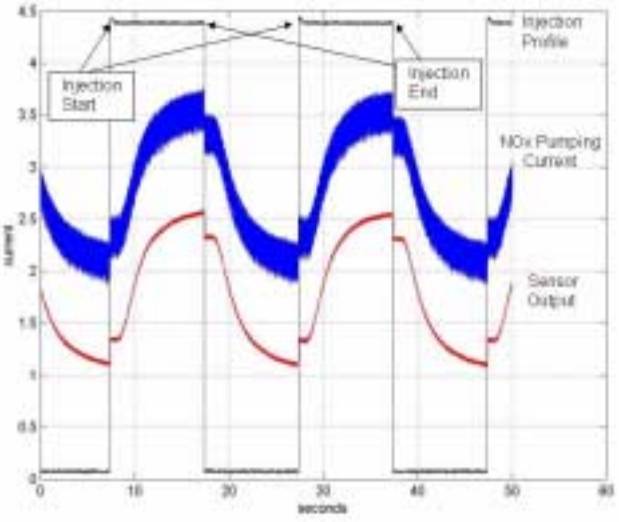


**Figure 2.** $NO_x$ Pumping Current and Controller Output Transient Result

Nitrogen was flowed through the bench rig at 10 liters per minute. An injection flow of 1000 ppm NO (balance nitrogen) was pulsed into the nitrogen stream at a pulse width of 10 seconds and a frequency of 0.05 Hz. The $NO_x$ pumping current was measured simultaneously with the controller output using a high-speed data acquisition system. The square wave injection profile is presented along with the $NO_x$ pumping current signature (as measured using the picoammeter) and the controller output in Figure 2. Comparison of the two signatures shows that the pumping current signal is noisy compared to sensor output. Further analysis revealed that at the start and end of each injection, the pumping current rises or drops sharply, while the

sensor output lags noticeably. The lag in $NO_x$ output was improved through the application of a smoothing function to the $NO_x$ pumping current. However, further experimental testing and analysis is needed in order to understand the how the controller filter performs under a variety of operating conditions.

## Conclusions

There were no new emission sensors (either commercially available or prototype) to be evaluated in the ORNL bench rig during FY2002. Preliminary measurements were performed on the NGK $NO_x$ sensor to measure the pumping current during transient operation. The current measurements were made using a high-speed picoammeter. Preliminary analysis shows that the noise of the pumping current signature is filtered to provide the sensor output. However, the controller output response is noticeably slower than the original pumping current during large step changes in NO concentration. A smoothing function was applied to the pumping current signature and was able to improve upon the response relative to the output signal.

# E. Plasma Catalysis for $NO_x$ Reduction from Light-Duty Diesel Vehicles

*Stephan Barlow, Ja-Hun Kwak, Chuck Peden (Primary Contact), and Russ Tonkyn*
*Pacific Northwest National Laboratory*
*P.O. Box 999, MS K8-93*
*Richland, WA 99353*

*DOE Technology Development Managers: Kathi Epping and Patrick Davis*

*CRADA Partner: Low Emissions Technologies Research and Development Partnership*
*(LEP - Member Companies: Ford Motor Company, General Motors, and DaimlerChrysler Corporation)*
*John Hoard (Primary Contact)*
*Ford Scientific Research Lab*
*P. O. Box 2053, MD 3179, Dearborn, MI 48121-2053*

*Byong Cho and Steven Schmieg, General Motors R&D Center*
*David Brooks, DaimlerChrysler Technology Center*

*This project also includes a plasma-reactor materials development effort with:*

*Steve Nunn*
*Oak Ridge National Laboratory*
*P.O. Box 2008, MS 6087*
*Oak Ridge, TN 37831-6087*

This project addresses the following DOE R&D Plan barriers and tasks:

*Barriers*

A. $NO_x$ Emissions

B. PM Emissions

C. Cost

*Tasks*

4b. Non-thermal Plasma R&D

5e. R&D on PM Reducing Technologies

## Objective

- Develop a novel plasma/catalyst $NO_x$ reduction and particulate matter (PM) aftertreatment system that will achieve 90% $NO_x$ reduction using less than 5% of the engine power on a compression ignition direct injection (CIDI) engine.

## Approach

- Synthesize and characterize new catalysts. A highly active and stable plasma catalyst material is critical to meeting the project goals.
- Measure plasma/catalyst activity in simulated and real exhaust.
- Through more fundamental mechanistic studies, identify the important reaction intermediates and the rate-limiting reactions in a plasma/catalyst system. Use this information to guide the catalyst synthesis efforts.

- Design and construct prototype plasma/catalyst reactor systems.
- Evaluate prototype reactor systems for emission ($NO_x$ and PM) reduction performance, energy efficiency, and durability.
- Utilize ORNL ceramic processing capabilities to simplify the design of the plasma reactor portion of the emission control device.

### Accomplishments

- Five weeks of engine testing conducted at FEV facility in Pontiac, MI.
- Sixty to seventy percent $NO_x$ reduction demonstrated in engine tests using diesel fuel as the reductant.
- Additional engine testing also occurring at General Motors (GM).
- New system concept ("Cascade Reactor") shown to reduce input energy requirements for equivalent levels of $NO_x$ reduction. Patent filed.
- Eleven papers published, 6 with PNNL as lead authors. Sixteen presentations made at scientific meetings including Diesel Engine Emissions Reduction Workshop (DEER) and Society of Automotive Engineers (SAE) conferences. Four new invention disclosures (to date, 2 of these filed for patents), and 1 patent still being prosecuted.
- Established and initiated (now routine) use of facilities for in-situ Fourier Transform Infrared Laboratory (FTIR) mechanistic studies.
- Nitrogen and carbon balance continue to be routinely obtained in our laboratory measurements.
- Joint studies of catalysts for light- and heavy-duty diesel vehicles were initiated with researchers on the DOE-funded Pacific Northwest National Laboratory (PNNL)/Caterpillar CRADA.
- 2001 CIDI Combustion and Emission Control Program Special Recognition Award received. 2001 R&D 100 Award for Catalysts Invented at PNNL.

### Future Directions

- Continue fundamental mechanistic studies that focus on the surface chemistry of acetaldehyde and $NO_2$ on the active plasma catalyst materials.
- Focus studies of the plasma device on identifying conditions for optimized production of the important reductant materials (aldehydes) identified in the mechanistic studies.
- Continue development of catalyst materials with higher activity and improved durability utilizing a 'structured' search guided, in part, by the results from our mechanistic studies.
- Identify fate and form of PM following 'treatment' by the plasma reactor. This will follow-up our recent results showing considerable reduction of PM by a plasma device.
- Iterate on production methods and form of plasma reactor ceramic parts produced by ORNL with testing performed at PNNL on PNNL plasma reactor designs. Verify current status of this novel technology by regular full-scale engine tests. The next scheduled tests will occur in the early fall of this year (2002). Engine tests will also continue to be carried out at GM.

---

## Introduction

In this project, we have been developing a novel plasma/catalyst technology for the remediation of $NO_x$ under lean (excess oxygen) conditions, specifically for compression ignition direct injection (CIDI) diesel engines that have significant fuel economy benefits over conventional stoichiometric gasoline engines. Our previous work has shown that a non-thermal plasma in combination with an appropriate catalyst can provide $NO_x$ emission reduction efficiency of 60-80% using a simulated diesel exhaust [1]. Based on these levels of $NO_x$ reduction obtained in the lab, a simple model was

developed in this project that allows for the estimation of the fuel economy penalty that would be incurred by operating a plasma/catalyst system [2]. Results obtained from this model suggest that a 5% fuel economy penalty is achievable with the then current (FY2000) state-of-the-art catalyst materials and plasma reactor designs.

Figure 1 is a conceptual schematic of a plasma/ catalyst device. Also shown is our current best understanding of the role of the various components of the overall device for reducing $NO_x$ from the exhaust of a CIDI engine. In this last year, we have continued to focus on (1) improving the catalyst and plasma reactor efficiencies for $NO_x$ reduction, (2) studies to reveal important details of the reaction mechanism(s) that can then guide our catalyst and reactor development efforts (focus 1), and (3) evaluating the performance of prototype systems on real engine exhaust. While studies of the effects of the plasma on PM in real diesel engine exhaust is meant to be part of the project, this year we did not conduct any experiments along these lines due to the major effort required to carry out the engine testing (focus 3).

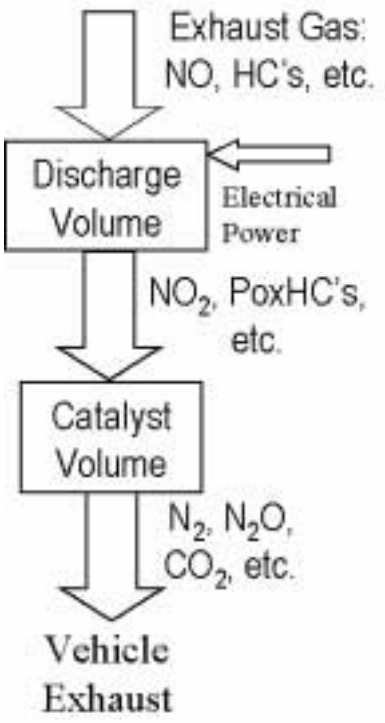


**Figure 1.** Schematic of a Two-Step Discharge/ Catalyst Reactor Used for Reducing $NO_x$ and PM from the Exhaust of CIDI engines.

## Approach and Results

Our catalyst development efforts in FY2002 have continued to focus on 1) the 'optimum' cation substitution (type and amount) into zeolite-Y; 2) whether the zeolite structure is necessary for creating the 'active catalytic sites,' and if, "yes", what is the 'optimum' structure; and 3) whether the addition of other metal-dopants, reported to be good partial hydrocarbon oxidation catalysts, could increase the yield of desirable aldehyde species. For example, in Figure 2 we show the $NO_x$ conversion over a variety of alkali-metal and alkaline-earth exchanged Y-zeolite catalysts that address issue 1). As can be seen in the figure, Ba-Y is clearly the best of this series of materials, displaying both the highest activity and a wide temperature 'window'. To understand this behavior, we have initiated studies that utilize FTIR spectroscopy to identify important details of the reaction mechanism. We have already obtained sufficient data this year to submit a first manuscript to a peer-reviewed journal on our work [3]. In Figure 3, we show FTIR spectra obtained following $NO_2$ adsorption on three alkali-metal exchanged Y zeolites, LiY, KY, and CsY. Interestingly, the spectra for LiY is considerably different than that obtained for the other two catalysts. These results may help explain the qualitatively different activity profile for LiY shown in Figure 2.

Our plasma reactor development work this year has consisted of three main activities. 1) As part of 'work-in-kind', DaimlerChrysler arranged for the evaluation of a commercial 'plasma reactor' (ozonizer) design in engine tests that took place at FEV in Auburn Hills, MI, in January. The results provided important insights into the performance and stability of this commercial design relative to the prototype designs developed in this project. 2) In collaboration with PNNL (S. Barlow), Steve Nunn at ORNL has been refining the design and fabrication of ceramic parts for a plasma reactor in order to reduce part number and complexity. Prototype parts manufactured at ORNL were assembled into a reactor and tested at PNNL this year. The prototype plasma reactor pictured in Figure 4 demonstrates that a uniform plasma can be generated. Further characterization of this prototype reactor will be

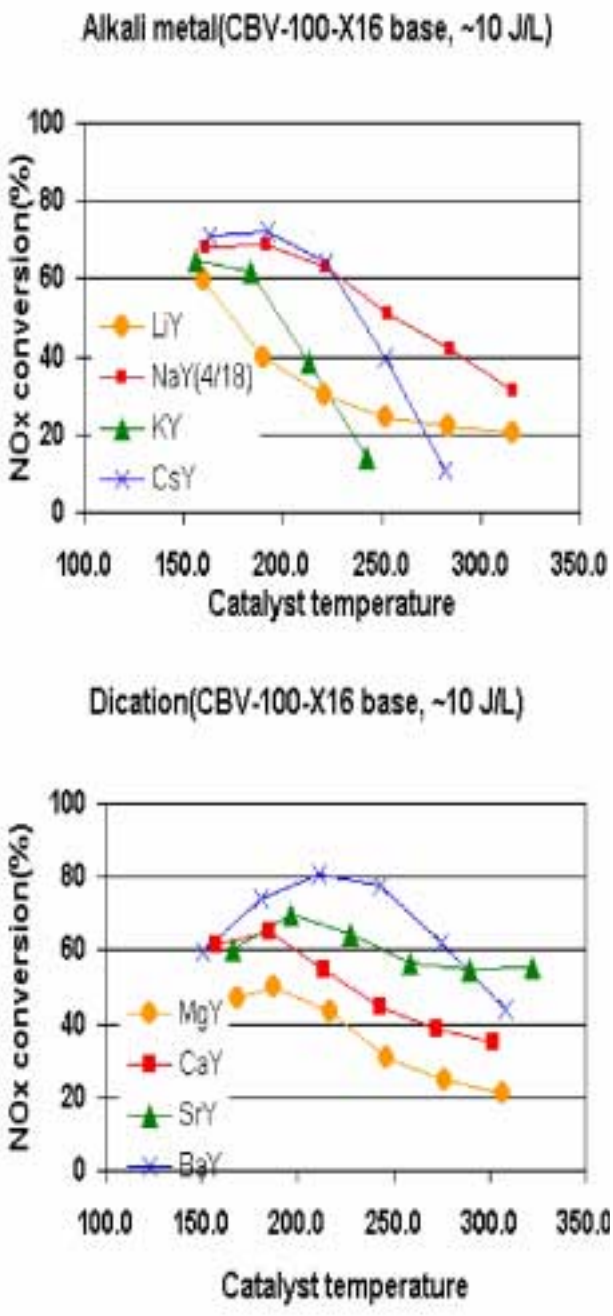


**Figure 2.** Plasma-assisted $NO_x$ conversion levels over a variety of alkali-metal and alkaline earth substituted zeolite Y catalyst materials as a function of exhaust gas temperature. Reactions were run at gas flow rates that yield a 12,000 hr-1 SV, and with a plasma-reactor energy of 10 J/L. The simulated diesel exhaust gas feed was 8% $O_2$, 2% $H_2O$, 210 ppm NO, 520 ppm ($C_3$) $C_3H_6$, balance

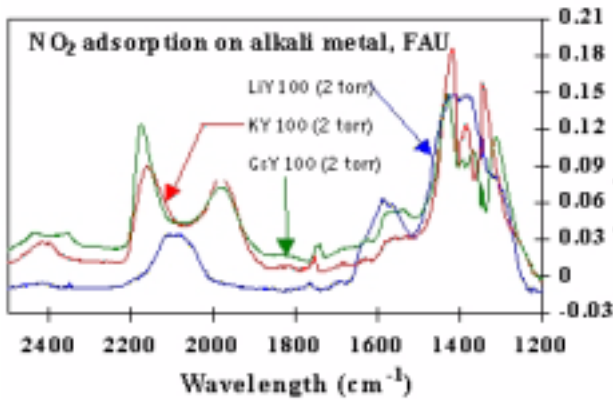


**Figure 3.** FTIR Spectra Taken for $NO_2$ Adsorption on a Number of Alkali-Metal Substituted Y-zeolites at Room Temperature

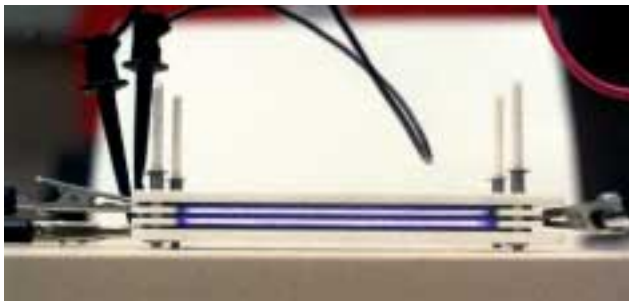

**Figure 4.** Picture of a Prototype Plasma Reactor Utilizing Ceramic Parts Manufactured at ORNL by Steve Nunn.

carried out this next year. 3) As reported in last year's annual report, PNNL has invented a new conceptual plasma/catalyst system that offers the promise of achieving the 90% $NO_x$ reduction targets with significantly reduced input power requirements. A patent was submitted for this invention in September of 2001. In our prior studies of the extent of $NO_x$ conversion versus plasma energy and oxygen and propene concentration, we observed an exponential approach to a limiting value. While we continue to search for more efficient catalysts, the implication is that there is an upper bound to the possible $NO_x$ conversion regardless of the energy input or gas composition. Unfortunately, for all the materials we have tested, that limit is below our 90% target. Consequently, we proposed that a multiple stage treatment strategy, whereby two or more plasma-catalyst reactor stages are utilized in series,

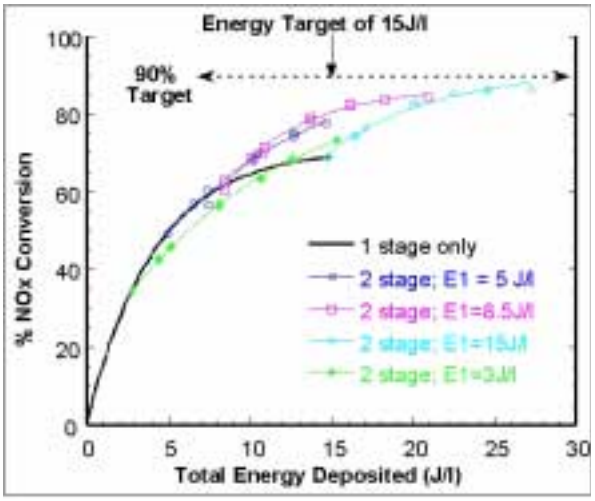


**Figure 5.** Comparison of the % $NO_x$ conversion vs. total energy deposited by 1 (solid line) or 2 (dashed lines) plasmas. Gas composition was 6% O2, 2% $H_2O$, 600 ppm $C_3H_6$, 200 ppm NO with balance $N_2$. The flow rate was 2 slm, and the catalysts were held at 170°C.

can increase the maximum $NO_x$ conversion obtainable. Furthermore, modeling of this concept has shown that the method can reduce the energy and/or hydrocarbon requirements for a fixed conversion efficiency [4]. Figure 5 [5] provides the data obtained this year that demonstrates the validity of the new concept, results that are fully consistent with modeling of the reactor. Note that the data are plotted versus total energy deposited, whether by one or two plasma regions. The target of 90% is shown for comparison, as is our nominal goal of 15 J/l deposited plasma energy. For the two-plasma data, the power into the first plasma was fixed while the power into the second one was varied. At moderate to high power into the first plasma, the additional plasma stage enhances the overall $NO_x$ removal performance. At relatively high power, the use of a second reactor is apparently justified. From the figure, above 10 J/l or so, delivering extra power to the plasma is best done using the second plasma. Judging from the figure it seems entirely possible that 90% conversion could be reached by a third plasma region.

Engine testing of prototype plasma/catalyst devices is an important element of our project to

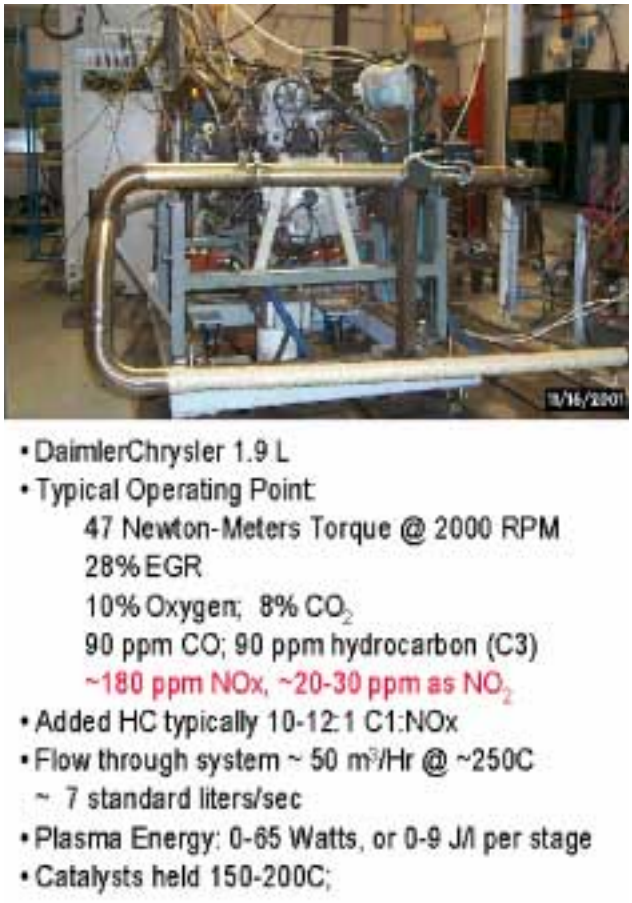


**Figure 6.** Comparison of the % $NO_x$ conversion vs. total energy deposited by 1 (solid line) or 2 (dashed lines) plasmas. Gas composition was 6% $O_2$, 2% $H_2O$, 600 ppm $C_3H_6$, 200 ppm NO with balance $N_2$. The flow rate was 2 slm, and the catalysts were held at 170°C.

provide a 'calibration' of where the technology is relative to the alternatives, and with respect to meeting the overall goals of the project. We have previously described the first of these engine tests (at ORNL) that demonstrated as much as 50% reduction with an estimated total fuel economy penalty of 6% (see FY2000 annual report). Despite these very promising results, there were a large number of experimental ambiguities that suggested even better performance. For this reason, we designed a vastly improved and flexible test unit that was used in engine dynamometer testing in Detroit last November. The overall goals of the tests are as follows. 1) Determine where we really are on an actual system using our "best available technology". Notably, we attempted to remove most of the

ambiguities from prior ORNL tests. Figure 6 shows the engine parameters and a picture of our device attached to the diesel engine dyno at FEV. Excellent overall activity was observed even when utilizing diesel fuel as the added reductant necessary to carry out plasma catalysis. To assess the progress of these engine tests, we directly compared the results to those obtained at ORNL. Figure 7 shows this comparison. In the figure, underlined text indicates areas in which the FEV test was more demanding than the ORNL tests. As can be seen, in most cases the recent FEV tests provided more challenges to the plasma catalysis concept. Despite this, overall performance was excellent, including the observation that approximately 60% $NO_x$ conversion was obtained using a realistic (diesel fuel) reductant have initiated new experiments designed to determine the fate of PM from the exhaust of a CIDI engine after passing through the oxidizing region of a non-thermal plasma reactor. We have set up instrumentation to carefully measure the number and size distribution of PM emitted from a Yanmar L70AE, 300cc, 4-cycle diesel generator, and described the first results in last year's annual report where we observed a sizable reduction in PM that was proportional to the input energy of the plasma reactor. In this next year, we plan to focus our studies on the identification of the fate of the PM. In particular, an important question is whether this observed PM reduction is due to electrostatic precipitation or if, indeed, the PM is more fully oxidized (ideally to $CO_2$).

## Conclusions

PNNL and its LEP CRADA partners from Ford, General Motors and DaimlerChrysler have been developing a plasma-assisted catalyst system that is showing great promise for treating emissions of $NO_x$ and PM from the exhaust of CIDI engine-powered vehicles. High $NO_x$ conversions have been demonstrated over a wide temperature range on simulated diesel exhaust. Furthermore, high conversions have been demonstrated in engine tests utilizing real diesel exhaust and diesel fuel as the added reductant. The results obtained in the last year provide good evidence that the overall project targets of 90% $NO_x$ reduction with less than a 5% fuel-economy penalty are within reach.

| | ORNL | FEV |
|---|---|---|
| Space Velocity (over all Catalysts) | 12,500/hr | 7,200/hr (but catalyst volume not nearly filled) |
| Soot Filter? | No | Yes |
| Catalyst Temperature | Likely Optimum | 160-180C |
| Power Delivered to Plasma Reactors | Not measured but estimated to be high | Not measurable but probably not nearly as high |
| Catalyst | BaY | NaY |
| Reductant | Propylene | Fischer-Tropsch Diesel |
| Coatings | PNNL | Johnson/Matthey |
| $NO_x$ Conversion | 60% | 60% |
| Stable Activity? | Deactivated Over Time | Seams Reasonably Stable |

**Figure 7.** Comparison of FEV Test Results to ORNL Test Results

## References

1. A.G. Panov, R.G. Tonkyn, M.L. Balmer, C.H.F. Peden, A. Malkin, and J.W. Hoard, "Selective Reduction of $NO_x$ in Oxygen Rich Environment with Plasma-Assisted Catalysis: Role of Plasma and Reactive Intermediates", SAE 2001-01-3513, and references therein.

2. J. Hoard, P. Laing, M.L. Balmer, and R. Tonkyn, "Comparison of Plasma-Catalyst and Lean $NO_x$ Catalyst for Diesel $NO_x$ Reduction", SAE 2000-01-2895.

3. J. Szanyi, "Adsorption and Reaction of $NO_2$ and $CH_3CHO$ on Na-Y, FAU: an in-Situ FTIR Investigation", Journal of Catalysis, submitted for publication.

4. S.E. Barlow, R.G. Tonkyn, J. Hoard and W. Follmer, "Cascade Processing of $NO_x$ by Two-Step Discharge/Catalyst Reactors", SAE 2001-01-3509.

5. (a) R.G. Tonkyn, and S.E. Barlow, "Multi-Step Discharge/Catalyst Processing of $NO_x$ in Synthetic Diesel Exhaust", SAE 2001-01-3510; (b) R.G. Tonkyn, S.E. Barlow, and J.W. Hoard "Reduction of $NO_x$ in Synthetic Diesel Exhaust via Two-Stage Plasma-Catalysis Treatment", Applied Catalysis B, submitted for publication.

## List of Publications


1. J. W. Hoard, R. G. Tonkyn, M. L. Balmer, and A. G. Panov, "Plasma-Catalysis for Diesel $NO_x$ Emissions: Technology Overview", Proceedings of the 2nd Asia-Pacific International Symposium on the Basics and Application of Plasma Technology, Kaohsiung, Taiwan, ROC, 18-20 April 2001.

2. J.W. Hoard, T.J. Wallington, R.L. Bretz, and A. Malkin, "Products and Intermediates in Plasma-Catalysis of Simulated Diesel Exhaust", Proceedings of the 3rd International Symposium on Non-thermal Plasma Technology for Pollution Control, April 23-27, 2001 (Cheju Island, Republic of Korea).

3. J.W. Hoard, "Plasma-Catalysis During Temperature Transient Testing", Proceedings of the 2001 DEER Workshop, Portsmouth, VA, August, 2001.

4. S. Yoon, R.G. Tonkyn, A.G. Panov, A.C. Ebeling, S.E. Barlow, and M.L. Balmer, "An Examination of the Role of Plasma Treatment for Lean $NO_x$ Reduction Over Sodium Zeolite Y and Gamma Alumina. Part 1: Plasma assisted $NO_x$ reduction over NaY and $Al_2O_3$", Catalysis Today 72 (2002) 243.

5. S. Yoon, R.G. Tonkyn, A.G. Panov, A.C. Ebeling, S.E. Barlow, and M.L. Balmer, "An Examination of the Role of Plasma Treatment for Lean $NO_x$ Reduction Over Sodium Zeolite Y and Gamma Alumina. Part 2: Formation of Nitrogen", Catalysis Today 72 (2002) 251.

6. A.C. Ebeling, A.G. Panov, D.E. McCready, and M.L. Balmer, "Characterization of Acid Sites in Ion-exchanged and Solid State-exchanged Zeolites", SAE 2001-01-3571.

7. J. Hoard, A. Panov, R. Tonkyn, M.L. Balmer, and S. Schmieg, "Products and Intermediates in Plasma-Catalyst Treatment of Simulated Diesel Exhaust", SAE 2001-01-3512.

8. A.G. Panov, R.G. Tonkyn, M.L. Balmer, C.H.F. Peden, A. Malkin, and J.W. Hoard, "Selective Reduction of $NO_x$ in Oxygen Rich Environment with Plasma-Assisted Catalysis: Role of Plasma and Reactive Intermediates", SAE 2001-01-3513.

9. S.J. Schmieg, B.K. Cho, and S.H. Oh, "Hydrocarbon Reactivity in a Plasma-Catalyst System: Thermal Versus Plasma-Assisted Lean-$NO_x$ Reduction", SAE 2001-01-3565.

10. S.E. Barlow, R.G. Tonkyn, J. Hoard and W. Follmer, "Cascade Processing of $NO_x$ by Two-Step Discharge/Catalyst Reactors", SAE 2001-01-3509.

11. R.G. Tonkyn, and S.E. Barlow, "Multi-Step Discharge/Catalyst Processing of $NO_x$ in Synthetic Diesel Exhaust", SAE 2001-01-3510.

12. R.G. Tonkyn, S.E. Barlow, and J.W. Hoard, "Reduction of $NO_x$ in Synthetic Diesel Exhaust via Two-Stage Plasma-Catalysis Treatment", Applied Catalysis B, submitted for publication.

13. J.W. Hoard, T.J. Wallington, R.L. Bretz, and A. Malkin, "Relative Importance of O(3P) Atoms and OH Radicals in Hydrocarbon Oxidation during the Non-thermal Plasma Treatment of Diesel Exhaust", to be submitted for publication.

14. J. Szanyi, "Adsorption and Reaction of $NO_2$ and $CH_3CHO$ on Na-Y,FAU: an in-Situ FTIR Investigation", Journal of Catalysis, submitted for publication.


## List of Presentations

1. M.L. Balmer-Millar, S. Barlow, A. Ebeling, A. Panov, C. Peden, R. Tonkyn, S. Yoon, J. Hoard, B. Cho, S. Schmieg, D. Brooks, and S. Nunn, "Plasma Catalysis for $NO_x$ Reduction from Light-Duty Diesel Vehicles", presentation at the DOE CIDI Engine Combustion, Engine Control, and Fuels R&D Review, Knoxville, TN, June, 2001.

2. J.W. Hoard, "Plasma-Catalysis During Temperature Transient Testing", presentation at the DEER Workshop, Portsmouth, VA, August, 2001.

3. J.W. Hoard, "Plasma-Catalysis for Diesel $NO_x$ Reduction", presentation for the Natural Sciences

and Engineering Research Council of Canada, March, 2002.

4. J. Hoard, A. Panov, R. Tonkyn, M.L. Balmer, and S. Schmieg, "Products and Intermediates in Plasma-Catalyst Treatment of Simulated Diesel Exhaust", presentation at the SAE Spring Fuels and Lubes Meeting, Reno, NV, May, 2002.

5. A.G. Panov, R.G. Tonkyn, M.L. Balmer, C.H.F. Peden, A. Malkin, and J.W. Hoard, "Selective Reduction of $NO_x$ in Oxygen Rich Environment with Plasma-Assisted Catalysis: Role of Plasma and Reactive Intermediates", presentation at the SAE Spring Fuels and Lubes Meeting, Reno, NV, May, 2002.

6. S.J. Schmieg, B.K. Cho, and S.H. Oh, "Hydrocarbon Reactivity in a Plasma-Catalyst System: Thermal Versus Plasma-Assisted Lean-$NO_x$ Reduction", presentation at the SAE Spring Fuels and Lubes Meeting, Reno, NV, May, 2002.

7. S.E. Barlow, R.G. Tonkyn, J. Hoard and W. Follmer, "Cascade Processing of $NO_x$ by Two-Step Discharge/Catalyst Reactors", presentation at the SAE Spring Fuels and Lubes Meeting, Reno, NV, May, 2002.

8. R.G. Tonkyn, and S.E. Barlow, "Multi-Step Discharge/Catalyst Processing of $NO_x$ in Synthetic Diesel Exhaust", presentation at the SAE Spring Fuels and Lubes Meeting, Reno, NV, May, 2002.

9. S. Barlow, A. Ebeling, C. Peden, R. Tonkyn, J. Hoard, B. Cho, S. Schmieg, D. Brooks, and S. Nunn, "Plasma Catalysis for $NO_x$ Reduction from Light-Duty Diesel Vehicles", presentation at the DOE CIDI Engine Combustion, Engine Control, and Fuels R&D Review, Argonne, IL, May, 2002.

10. J.W. Hoard,, A.G. Panov, M.L. Balmer-Millar, R.G. Tonkyn, C.H.F. Peden, "Hydrocarbon and Aldehyde Reductants in Plasma-Catalytic $NO_x$ Conversion in Lean Exhaust", presentation at the 24th Annual Spring Symposium of the Michigan Catalysis Society, Flint, MI, May 2002.

11. J.W. Hoard, "Plasma-Catalyst System Evaluations by Thermal Cycles", presentation at the 24th Annual Spring Symposium of the Michigan Catalysis Society, Flint, MI, May 2002.

12. J.W. Hoard, S.E. Barlow, R.G. Tonkyn "Cascade Processing on $NO_x$ in Lean Exhaust", presentation at the 24th Annual Spring Symposium of the Michigan Catalysis Society, Flint, MI, May 2002.

13. A.G. Panov, R.G. Tonkyn, M.L. Balmer, C.H.F. Peden, A. Malkin, and J.W. Hoard, "Selective Reduction of $NO_x$ in Oxygen Rich Environment with Plasma-Assisted Catalysis: Role of Plasma and Reactive Intermediates", presentation at the 3rd DOE National Laboratory Catalysis Conference, Richland, WA, May, 2002.

14. R.G. Tonkyn, S.E. Barlow, and J.W. Hoard "$NO_x$ Removal in Diesel Exhaust using a Cascaded Two-Step Plasma/Catalysis Treatment", presentation at the 3rd DOE National Laboratory Catalysis Conference, Richland, WA, May, 2002.

15. J. Szanyi, "The Adsorption and Reaction of NO2 and $CH_3CHO$ on Na-Y,FAU: an FTIR Study", presentation at the 3rd DOE National Laboratory Catalysis Conference, Richland, WA, May, 2002.

16. C. S. Lee, J.-H. Kwak, and C.H.F. Peden, "Characterization and Testing of Alkali- and Alkaline Earth-Cation Exchanged Y Zeolites", presentation at the 3rd DOE National Laboratory Catalysis Conference, Richland, WA, May, 2002

## Special Recognitions and Awards/Patents Issued

1. 2001 DOE CIDI Combustion and Emission Control Program Special Recognition Award, May 2001.

2. R&D 100 Award from Research and Development Magazine for the invention and development of new catalysts for a plasma/catalysis lean-NOx reduction technology, October, 2001.

# F. Non-Thermal Plasma System Development: Integrated PM and $NO_x$ Reduction

*Darrell Herling (Primary Contact), John Frye, Mark Gerber, Del Lessor, Monty Smith*
*Pacific Northwest National Laboratory*
*902 Battelle Blvd., MSIN: P8-35*
*Richland, WA 99352*

*DOE Technology Development Manager: Gurpreet Singh*

*CRADA Partner: Delphi Automotive Systems*
*Joe Bonadies*
*Delphi Engine & Chassis Systems*
*1601 N. Averill Avenue*
*Flint, MI 48556*
*M/C 485-220-065 Drop N*

This project addresses the following DOE R&D Plan barriers and tasks:

*Barriers*

A. $NO_x$ Emissions

B. PM Emissions

C. Costs

*Tasks*

4b. Non-termal Plasma R&D

5e. R&D on PM Reducing Technologies

## Objectives

- Develop an integrated non-thermal plasma (NTP) assisted catalyst and particulate filter system for PM and $NO_x$ reduction in a heavy-duty diesel vehicles
- Reduce particulate matter (PM) by an average of 90% and $NO_x$ by an average of 80% on emissions test cycle
- Design a system that is compact, robust and tolerant to sulfur and other impurities
- Achieve the target of 3% fuel economy penalty and minimum impact on vehicle operation

## Approach

- Development of NTP system for PM reduction
  - Develop and demonstrate a regeneration strategy for DPF based on using oxidants produced in plasma
  - Demonstrate and characterize direct oxidation of PM in plasma; establish appropriate reactor design and operating conditions
- Develop a durable and compact NTP reactor design
  - Use modeling to describe the plasma characteristics and influential parameters of the plasma, and to analyze the physical design

  - Conduct experiments to obtain a better understanding of plasma chemistry and influential parameters that affect performance, and validate models
- Develop energy efficient power supply and control system architecture for plasma reactor
- Develop effective and robust selective $NO_x$ catalyst
  - Investigate metal-metal oxide catalysts for plasma assisted $NO_x$ reduction
  - Develop catalyst formulations/material synthesis and evaluate their performance

### Accomplishments

- Performed sub-scale (2.0 liter engine) prototype system evaluation trials on engine and chassis dynamometer and showed >50% $NO_x$ reduction under steady-state conditions
- Evaluated the use of late cycle diesel fuel injection for HC addition
- Demonstrated 50% direct oxidation of PM within the plasma reactor and regeneration of a DPF by plasma produced by-products at 280°C
- Tested new catalyst formulations that showed increase in $NO_x$ reduction performance over a wider range of temperatures, with peak reduction efficiency of 100% (SGB)
- Developed a "clean-up" catalyst (oxidation catalyst) to reduce residual CO and HC after the NTP-catalyst systems that achieves 85-90% efficiency down to 150°C
- Discovered and tested an alternative power supply strategy, which showed significant energy savings of up to 75% over typical alternating current (AC) system

### Future Directions

- Continue to investigate the operating conditions of the short-pulse power strategy and develop a commercial-ready power supply
- Further investigate late-cycle fuel injection parameters to determine if a higher level of aldehyde production is possible (needed to improve catalyst performance)
- Investigate methods to increase PM destruction in plasma
- Integrate plasma into soot filter (or close coupling) and investigate catalyzed filter for enhanced PM oxidation and/or $NO_x$ reduction

---

## Introduction

The objective of this Cooperative Research and Development Agreement (CRADA) project is to develop an integrated NTP assisted catalyst and diesel particulate filter (DPF) system for PM and $NO_x$ reduction in heavy-duty diesel vehicles, with an average of 90% PM and 80% $NO_x$ reduction over an emissions driving cycle. The CRADA partners are the DOE, PNNL, and Delphi Automotive Systems - Delphi Engine & Chassis Systems, Innovation Center. The goal of the CRADA partner is to develop the NTP-catalysis technology to a commercial-ready emission control device for new vehicles and retrofits. A schematic of the processing steps in the NTP-DPF-catalyst emission control system and the nature of the $NO_x$ and PM at each intermediate point is shown in Figure 1.

## Approach

The approach taken for this project addresses four key areas associated with technical development needs for a plasma assisted soot filter and catalysis aftertreatment device that will reduce PM and $NO_x$ emissions from heavy-duty diesel engines. The development activities for each task area utilize a combination of analytical and structural modeling, surface science and analytical/physical chemistry, and experimentation to better understanding the physiochemical phenomena that occurs within each component of the aftertreatment system.

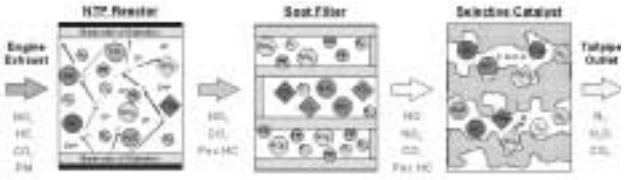

**Figure 1.** Conceptual schematic of an NTP assisted-DPF-catalyst exhaust aftertreatment system. The state of $NO_x$ and PM emissions are shown for each stage of the system.

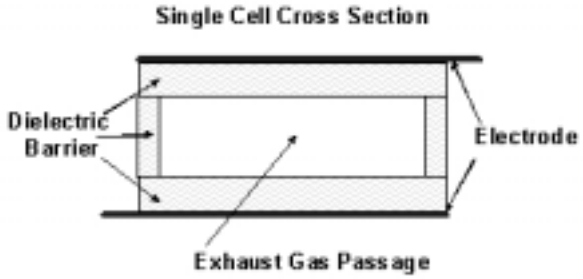


**Figure 2.** Single Cell Parallel Plate NTP Reactor

## Results

The FY02 project activities focused on investigation and development of five technical aspects of the NTP assisted-DPF-catalyst technology: 1) perform prototype engine tests to establish the current level of on-vehicle performance; 2) increase the understanding of plasma and catalyst chemistry and the influence of hydrocarbon type/ amount; 3) improve $NO_x$ catalyst performance; 4) quantify the direct PM oxidation in the plasma region and DPF regeneration; and 5) improve plasma reactor durability and decrease power requirements.

Plasma Reactor Development

Reactor development included expanding the capabilities of the plasma-chemistry models and uses of these models to predict and analyze plasma performance under various operating conditions. The improvements to the models consisted of expanding the chemical database to include secondary reactions, a more complete list of back reactions, and more accurate kinetic rate data. The modeling provided great insight to the influential parameters of the plasma and allowed analysis of the physical design and energy deposition. In fact, the modeling work discovered a significant amount of wasted energy in the form of nonproductive gas heating that occurs.

**Figure 3.** Prototype plasma reactor for a 2.0 liter engine. Dimensions: length 82 mm; width 160 mm; height 90 mm; weight 2.9 kg.

Based on modeling activities and experimental trials, it was decided that Delphi will pursue the parallel plate, dielectric barrier discharge reactor design for their final commercial product. This design is comprised of flat electrodes that are located on opposing sides of the exhaust gas passage, as shown in Figure 2, with alumina dielectric barriers used to suppress arcing between the electrodes. Figure 3 shows a prototype plasma reactor for a 2.0 liter engine ready for installation and full-scale testing.

Besides the influence of physical design parameters on performance, the modeling and experimental studies also showed that the exhaust gas species and concentrations can also play a significant role in the energy requirements and NO oxidation efficiency, particularly at high exhaust-gas temperatures. From previous modeling of the plasma physics, coupled with the gas-phase chemistry for NO to $NO_2$ conversion, it was found that the production and availability of $RO_2$ and $HO_2$ species are key components in the NO to $NO_2$ conversion reaction sequence. The reaction rates between NO and $RO_2$ species are extremely fast, and by maximizing the hydrocarbon amount and type, the production of these species is increased. Figures 4 and 5 show simulated gas bench (SGB) test results

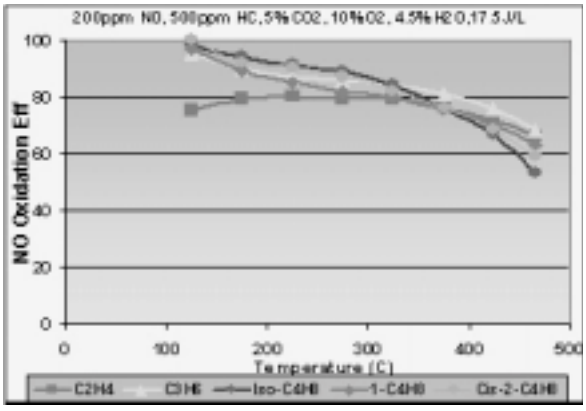


**Figure 4.** Plasma Reactor Efficiency as a Function of Unsaturated Hydrocarbon Type and Exhaust Gas Temperature

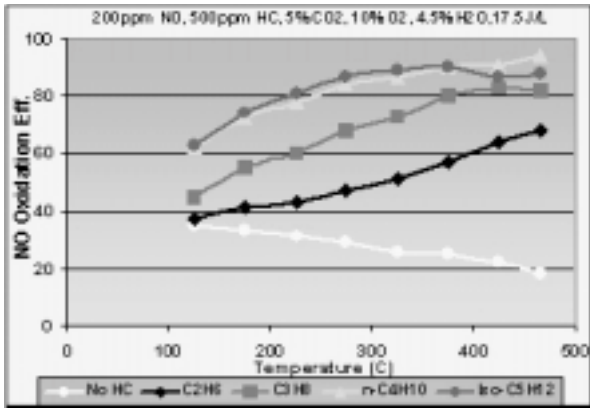


**Figure 5.** Plasma Reactor Efficiency as a Function of Temperature with Various Saturated Hydrocarbon Types

based on various alkene and alkane hydrocarbon (HC) species in the gas feed. The effects of HC species are important to understand and consider when determining the optimum operating environment for plasma aftertreatment. Unsaturated HCs are more active for NO conversion at lower temperatures, while saturated HCs are more active for NO conversion at higher temperatures. The length of the HC chain governs the effectiveness of the HC for NO to $NO_2$ conversion, and branched HC chains exhibit the same NO to $NO_2$ conversion efficiency as the parent chain. The combination of saturated and unsaturated HCs broadens the temperature window for efficient conversion.

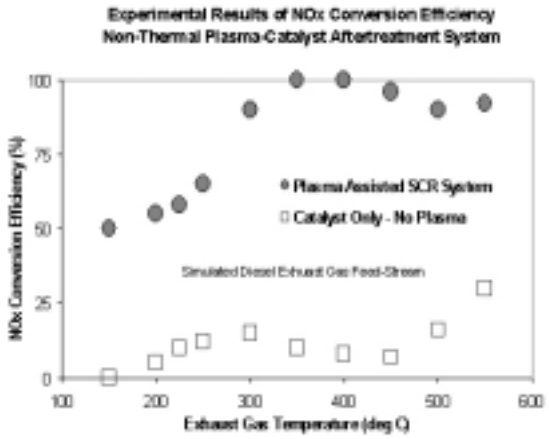


**Figure 6.** Experimental results of the catalyst performance run on a simulated gas bench. Gas mixture: 200 ppm $NO_x$, 500 ppm $C_3H_6$, 7% $CO_2$, 10% $O_2$, 5% $H_20$, balance $N_2$. Space velocities: plasma: 1 M/hr, catalyst: 25 k/hr.

$NO_x$ Catalyst Material Development

Enhancement of the catalyst performance was realized through modifications of the original catalyst material. The first improvement is an extension of operating temperature range, which was achieved by applying a second catalyst material suited for lower temperature $NO_x$ reduction. This second catalyst is a metal doped aluminosilicate structure, which provides $NO_x$ reduction at temperatures primarily below 300°C, and is used in conjunction with the alumina based material. For bench-scale and engine testing, two washcoated monoliths were used, one with the aluminosilicate and the other with the alumina. Results from tests run with a mixture of both catalyst materials washcoated on one monolith were not favorable.

The improved catalyst hybrid was tested in the laboratory on a SGB pilot-scale reactor, as well as with actual engine tests. Results from SGB testing, shown in Figure 6, indicate $NO_x$ conversion efficiency as high as 100%. This high efficiency is a result of the alumina based material, which is active at temperatures from 300°C to 550°C, and the contribution at the lower temperatures is primarily due to the aluminosilicate material. The best performance was achieved when the catalyst set was used in conjunction with the plasma, again confirming that the plasma processing is necessary to

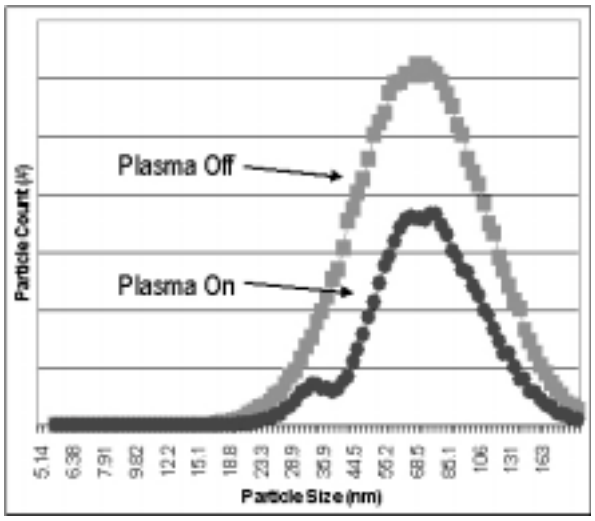


**Figure 7.** Particle size distribution from scanning mobility particle sizer (SMPS) data shows a reduction in TPM with plasma processing. Particulate source: 1.9 liter common-rail DI diesel.

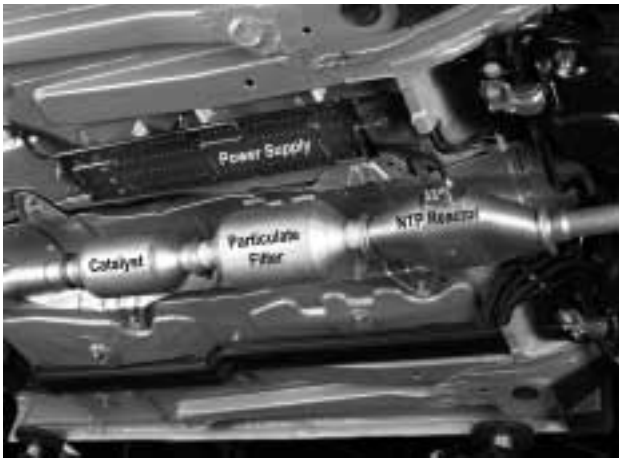


**Figure 8.** Sub-scale Prototype System Used to Evaluate System Components On-Car and With Engine Dynamometer Testing

produce the active reductant species like acetaldehyde. Figure 6 shows the results with and without the plasma processing. Also, aging tests with 20 ppm $SO_2$ in the feedstream revealed only a 5% decrease in activity over 100-hour period.

Particulate Reduction and DPF Regeneration

Since a plasma-based device requires electrical power, which places an additional energy burden on the vehicle, it is desirable to obtain the most value from such an aftertreatment system as possible. This CRADA project is investigating alternative uses of the plasma, beyond just $NO_x$ reduction, to develop a system that can also reduce PM emissions. The focus for PM reduction with plasma technology this last year was to demonstrate and characterize the direct oxidation of PM in the plasma region and to demonstrate a regeneration strategy for DPF based on using oxidants produced in plasma.

An experimental study was conducted that demonstrated the direct oxidation of particulate matter within the plasma reactor. The same plasma reactor used for $NO_x$ reduction was used and operated at the same power levels for the PM reduction study. The experimental results show a 47-54% reduction in particulate mass over various engine speeds, and the average change in the particle size distribution curves due to the plasma processing is shown in Figure 7. In some specific operating conditions, PM reduction levels as high as 95% were observed. However, this was at conditions where the plasma power was at its peak and particulate transport rate through the plasma region was relatively low. This condition allows for a significant increase in particle resonance time in the plasma and interaction with oxidants, hence processing more of the PM.

In order to enhance the PM reduction capability over what is achievable with just the direct oxidation in the plasma, a DPF was added to the system. The concept is to utilize the oxidants produced by the plasma, $NO_2$, $O\cdot$ and $O_2(a^1\Delta)$, to regenerate the particulate filter. These species are good oxidizers, and even though the $O\cdot$ and $O_2(a^1\Delta)$ are short lived, they are transportable over short distances from the plasma to the filter, and therefore can enhance filter regeneration.

Experiments were conducted on an engine dyno with a plasma-DPF prototype device to qualify the benefits of using a plasma reactor to produce the oxidants in-situ for filter regeneration. With the assistance of the plasma reactor the pressure drop across the DPF unit was decreased over time, which indicated that regeneration was occurring. Furthermore, with at least 120 ppm of total HC output from the engine, adequate regeneration took

place at temperatures as low as 280°C. The study was conducted at steady-state engine operating conditions, and subsequent testing is still required to determine the performance level under transient conditions.

Prototype Testing

In order to validate the performance of the plasma-catalysis system, it is necessary to conduct prototype system tests under real-life operating conditions. Therefore, engine dynamometer and vehicle testing was conducted to establish the level of performance of the current system design. A sub-scale plasma-DPF-catalyst prototype system was fabricated for and tested on a 2.0 liter lean-burn diesel engine. A picture of the prototype system installed on the test vehicle is shown in Figure 8. The testing was conducted on a chassis dynamometer utilizing the European MVEG (ECE+EUDC cycles) driving cycle and emissions test protocol (on-line and dilution tunnel/emissions bag collection data).

The average NO to $NO_2$ conversion efficiency achieved over the driving cycle for the plasma reactor was 90%. This is reasonably good performance, since the THC from the engine is only about 100 ppm at the peak exhaust gas temperature of 450$^{o}$C. Figure 9 shows the plasma reactor conversion efficiency during the MVEG test. Also during vehicle testing, the engine management system (EMS) was set-up to provide additional HC to the exhaust system through a late-cycle fuel injection step. Based on vehicle testing data, the fuel penalty associated with supplemental fuel injection was measured at 3%.

Based on previous studies, it has been determined that acetaldehyde is the most efficient reductant that can be used with the catalyst. However, the aldehyde formation with real engine exhaust, even with late-cycle fuel injection, is lower than the SGB testing with propene as the exclusive HC reductant. Because of this, the steady-state catalyst peak $NO_x$ reduction performance was only 50%.

In order to produce the maximum amount of acetaldehyde possible, it is desirable to have as much propene or higher molecular weight unsaturated HC entering the plasma reactor as possible. Figure 10

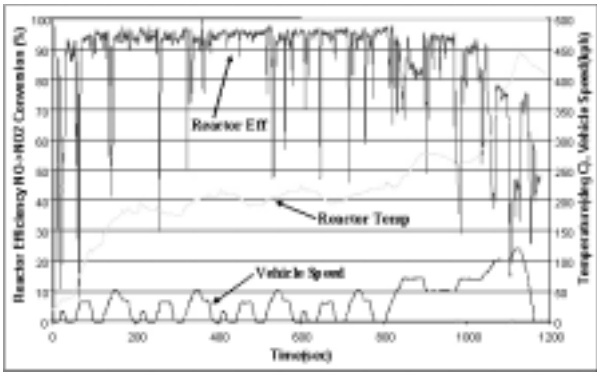


**Figure 9.** Plasma reactor efficiency over driving cycle. Testing was conducted with vehicle powered by 2.0 liter engine, and late-cycle injection was controlled via the engine management system.

shows the amount of acetaldehyde produced from the plasma when diesel is injected versus propene injected just ahead of the plasma device. Future development work will focus on how the propene and iso-butene concentrations can be increased with the late-cycle diesel fuel injection method.

Power Supply and Control System Development

Delphi has developed an AC voltage power supply specifically designed for use with the parallel plate plasma reactor construction. The output is rated at a maximum of 1 kW and the electrical conversion efficiency from a 12 V DC source to a maximum of 6.5 kV AC is ~90%. The integrated power controller regulates the applied plasma reactor power to the minimum that is needed to maintain >90% NO to $NO_2$ conversion efficiency given the engine operating conditions and $NO_x$ level.

Based on the vehicle testing, the peak energy consumption for the AC system is 17 J/L, which is about a 5% fuel economy penalty for a light-duty diesel vehicle. However, modeling work and experimental validation has shown that a large fraction of the AC power goes directly into nonproductive heating (>95%), and very little energy is actually needed for the desired electrochemistry. Further modeling results showed that the power consumption can be reduced by using a short-pulse power system, because the fraction of current carried by electrons ($f_e$) is much closer to 1 versus <0.5 for the AC system. Testing with a specifically designed

pulsed power, under the proper electrical conditions, has shown much lower energy requirement at 4.5 J/L, or 25-30% of the AC system. The lower power requirement means less impact on fuel economy, which is expected to be about 1-2% due to the additional electrical demand for the pulsed power system versus 5% for the AC system.

## Conclusions

$NO_x$ reduction levels as high as 100% were demonstrated to be possible with a plasma assisted catalysis system during pilot-scale reactor testing. Vehicle steady-state testing using a sub-scale prototype system achieved 50% peak $NO_x$ reduction, with an 8% total fuel penalty (5% due to electrical demand and 3% for supplemental HC injection). $NO_x$ reduction was demonstrated to be possible with reductant provided by late cycle diesel fuel injection, but the results were limited by a less than desirable level of aldehyde production. In addition to demonstrating $NO_x$ reduction through the NTP system was shown to be effective for particulate reduction; direct PM oxidation in the plasma, as well as DPF regeneration utilizing the oxidative species produced upstream in the plasma.

One of the significant breakthroughs this last year was the discovery of a new method to apply power to the plasma reactor, which requires only 25% of the energy needed for the typical AC power supply system. The development of a compact and efficient pulsed power supply will be a major focus for next year's activities.

## Awards and Recognition

In October 2001, R&D Magazine awarded a coveted R&D100 Award to PNNL, Ford Motor Company, and Delphi Automotive Systems for the development of catalyst materials that when used in conjunction with a non-thermal plasma device achieve a high level of $NO_x$ reduction. The work under this CRADA contributed to catalyst material development, which won the R&D100 Award.

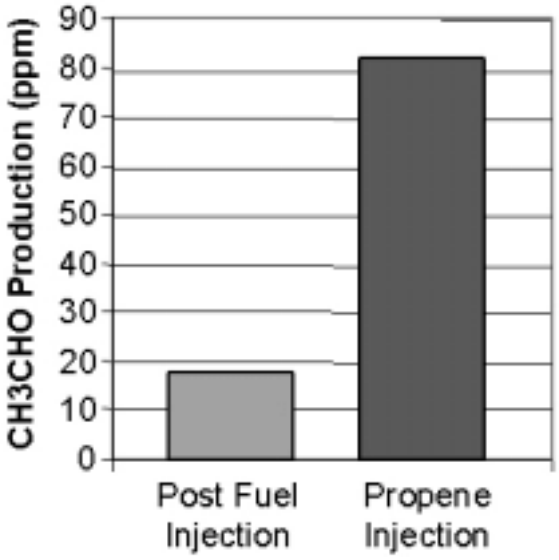


**Figure 10.** On-Vehicle Acetaldehyde Produced from the Plasma when Diesel is Injected versus when Propene is Injected Just Ahead of the Plasma Device

# G. Plasma-Facilitated Reduction of $NO_x$ for Heavy-Duty Emissions Control

*Christopher L. Aardahl (Primary Contact)*
*Pacific Northwest National Laboratory*
*P.O. Box 999, MS K8-93*
*Richland, WA 99352*

*DOE Technology Development Manager: Gurpreet Singh*

This project addresses the following DOE R&D Plan barriers and tasks:

*Barriers*

A. NOx Emissions

B. PM Emissions

C. Costs

*Tasks*

4b. Non-termal Plasma R&D

5e. R&D on PM Reducing Technologies

## Objective

- Develop an exhaust aftertreatment system that will achieve 90% $NO_x$ reduction using 3-5% of the engine fuel consumption of a heavy-duty diesel engine.

## Approach

- An aftertreatment system involving a non-thermal plasma reactor in conjunction with a catalytic reactor is being developed to reduce $NO_x$ emissions from heavy-duty engines. In this endeavor, a partnership between Pacific Northwest National Laboratory (PNNL) and Caterpillar Inc. has been formed. PNNL is responsible for plasma system design, process engineering, plasma bench testing, and catalyst development and characterization. Caterpillar is responsible for catalyst development and characterization, lean-$NO_x$ bench testing, and engine cell testing.

## Accomplishments

- A steady-state engine test was completed (end of 2001) on a slipstream from a Caterpillar 3126B engine. Results show $NO_x$ removal efficiencies from 40 - 95% depending on engine load and speed conditions, the temperature of the catalysts, the formulation of the catalyst, and the reducing agent used.
- Optimization of Ag/γ-alumina catalysts was completed for a variety of reducing agents. Results show optimal formulation is dependent on hydrocarbon speciation.
- The use of co-promoters for Ag/γ-alumina catalyst formulations was initiated. Formulation is complete, and testing of these new catalyst formulations is ongoing.
- The investigation of plasma-based reforming of fuel was initiated. It has been demonstrated that it may be possible to produce ammonia from hydrocarbon fuel. Partial oxidation is also being investigated.

- A catalyst exchange program with the Low Emissions Partnership (LEP) (USCAR) Plasma-Catalysis Cooperative Research & Development Agreement (CRADA) has shown that combination of light-duty and heavy-duty catalysts results in significant synergy.
- An examination of catalyst materials using $^{27}Al$ nuclear magnetic resonance (NMR) was performed. Results show that aluminum coordination in the γ-alumina has a significant impact on activity.

### Future Directions

- Continue to examine plasma-based reforming as a way to produce oxygenates or ammonia on-board a vehicle from diesel fuel.
- Continue to investigate copromoter formulations for increased activity.
- Continue to develop a mechanistic understanding of $NO_x$ reduction in a plasma-catalytic system. Focus in FY03 will be on Diffuse reflectance infrared Fourier transform (DRIFT) and Raman spectroscopy using in situ techniques to identify reactive intermediates on the surface of catalysts.
- Optimize catalyst formulations into support architectures that are suitable for on-vehicle use (monoliths or ceramic foams). Examine methods to increase performance at high space velocity.

---

## Introduction

Non-thermal plasma assisted catalysis (PAC) is an effective method for reducing $NO_x$ emissions in diesel exhaust; however, further advances in plasma system efficiency and catalyst development are needed for vehicle applications. Research in FY02 has focused on an extensive set of laboratory and engine experiments, process engineering, and formulation activities. Formulation has focused on Ag/doped γ-alumina and, in particular, on optimizing this material for PAC using a variety of hydrocarbons. We are also developing new formulations based on copromoters. In these materials, γ-alumina is doped with two metals in an effort to develop synergistic functionality in the catalyst. We have also initiated two high profile tasks in the CRADA. The first is a catalyst exchange with the LEP CRADA, where mixtures of light-duty and heavy-duty catalysts are used to broaden the applicable temperature range of the PAC technology. The second activity is based around plasma reformation of hydrocarbons in order to produce oxygenates and other more reactive molecules for aftertreatment needs.

## Results

To date, over 150 catalysts have been screened for $NO_x$ reduction activity. More than 30 base materials have been examined, and the synthesis of γ-alumina through sol-gel routes has been optimized to produce high $NO_x$ reduction. The addition of promoters such as Silver (Ag), Stannium (Sn), and Indium (In) further enhance reduction. The current test stand can operate up to 600°C with simulated exhaust streams. Simulated exhaust is composed of $N_2$, $O_2$, $H_2O$, NO, $NO_2$, CO, $CO_2$, and $SO_2$. Thus far, conversions exceeding 95% have been obtained on our bench configuration.

Work in FY02 started with the completion and analysis of data collected during a steady-state engine test at Caterpillar Inc. that took place in the Summer and Fall of 2001 (CAT 4126B Engine). Results showed high activity at space velocities below 35,000 $k/hr^{-1}$ (80-95% $NO_x$ reduction), but performance degraded significantly at space velocities above 50,000 $k/hr^{-1}$ (reduction dropped to 40%). Comparison of lab data obtained using simulated exhaust and data obtained using the 4126B engine showed good agreement. Data taken at 10,000 $k/hr^{-1}$ are shown in Figure 1. Here, the bottom axis refers to the catalyst-reducing agent combination.

Another important aspect of our work in FY02 was the optimization of Ag/γ-alumina formulations for a variety of reducing agents. In FY01, we showed that alcohols and aldehydes showed increased ability to reduce $NO_x$ over γ-alumina based materials when compared to non-oxygenated

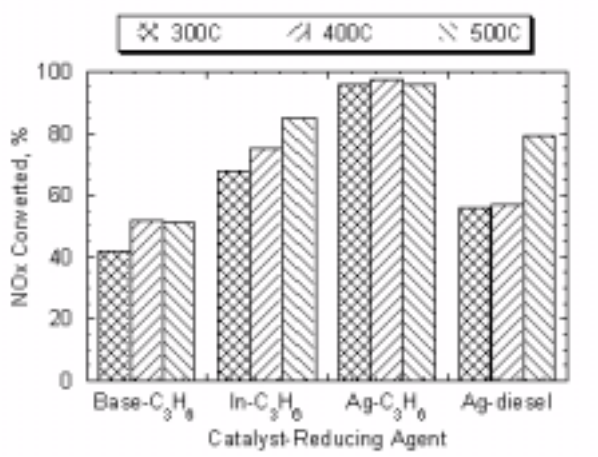


**Figure 1.** Engine Test Results for Catalyst-Reducing Agent Combinations

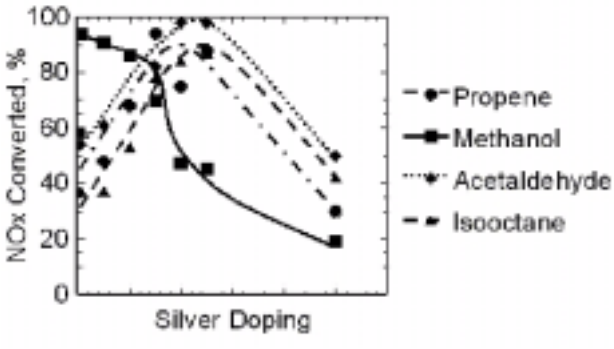


**Figure 2.** Trends of Conversion versus Silver Doping Level for Four Hydrocarbons

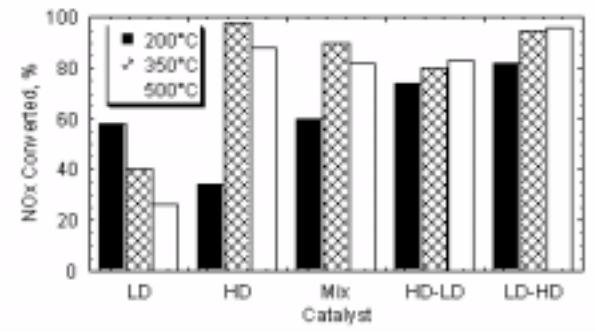


**Figure 3.** $NO_X$ Conversion Data Obtained on Catalyst Mixtures

hydrocarbons such as propylene and isooctane. This data was taken at constant silver loading. In FY02 the focus was to determine whether optimal silver loading changed with hydrocarbon speciation. Figure 2 shows that silver level does have an impact. For the hydrocarbons tested, high activity was obtained in all cases. Even fuel-type hydrocarbons such as isooctane performed well using modified catalyst formulations. The general trend suggests that higher silver loading is required for hydrocarbons that are not oxygenated. For reactive compounds such as methanol, highest conversion was obtained on the undoped base material.

Two significant new tasks have commenced during FY02. First, catalysts have been exchanged between PNNL's Caterpillar CRADA and PNNL's LEP CRADA. There are four goals that the combined teams hope to accomplish: broadening of the active temperature range for PAC, collection of transient data on the catalysts, analysis of lean-$NO_x$ behavior on the combination, and N-balance for the combination. This effort is well underway. Some preliminary data is shown in Figure 3, where $NO_x$ conversion is shown, for 5 different set-ups: light-duty (LD) catalyst alone, heavy-duty (HD) catalyst alone, a mixture of LD and HD, HD followed by LD, and LD followed by HD. As expected, LD and HD show activity at low and high temperature, respectively. The mix shows broadening of the temperature window, but significant enhancements are observed when the catalysts are staged with LD first. Experiments to determine why this is the case are still in progress.

The other significant new task is focused on plasma reforming. It is well known that plasmas partially oxidize hydrocarbon, and it is now believed that this aspect of the plasma operation is at least as beneficial as the conversion of NO to $NO_2$ for the plasma-facilitated de$NO_x$ process. The question remains, however, whether plasmas could be used to do significant scale partial oxidation and/or nitridation. Early results show that plasma can form ammonia from $H_2$ and $N_2$ mixtures. We have also demonstrated that ammonia can be formed from hydrocarbon and $N_2$, but the degree to which this occurs is still being examined. We have also initiated experiments on partial oxidation in an attempt to produce alcohols and aldehydes from fuels. Results to determine efficacy of plasma reforming are expected in early FY03.

## Conclusion

Analysis of data from the FY01 engine test has been completed. Results show that improvements still need to be made. Lessons learned from this test have led to new avenues for catalyst development, including the examination of optimal doping levels of silver on γ-alumina. The Ag/γ-alumina catalyst has now been optimized for a range of hydrocarbons. New tasks focused on catalyst exchanges with the LEP CRADA and plasma reforming have been initiated and are already producing promising results.

## Publications and Presentations

1 Rappe, K. G., Aardahl, C. L., Habeger, C. F., Tran, D. N., Delgado, M. A., Wang, L.-Q., Park, P. W., and Balmer, M. L. (2001) Plasma-facilited SCR of $NO_x$ in heavy-duty diesel exhaust. Paper 2001-01-3570, SAE: Warrendale, PA.

2. Park, P. W., Rockwood, J. E., Boyer, C. L., Ragle, C., Balmer-Millar, M. L., Aardahl, C. L., Habeger, C. F., Rappe, K. G., Tran, D. N., and Delgado, M. A. (2001) Lean-$NO_x$ and plasma catalysis over γ-alumina for heavy-duty diesel applications. Paper 2001-01-3569, SAE: Warrendale, PA.

3. Wang, L.-Q., Aardahl, C. L., Rappé, K. G., Tran, D. N., Delgado, M. A., and Habeger, C. F. (2002) Solid-state 27Al NMR investigation of plasma-facilitated $NO_x$ reduction catalysts. J. Mater. Res., in press.

4. Aardahl, C. L., Habeger, C. F., Rappe, K. G., Tran. D. N., Delgado, M. A., Park, P. W., and Balmer, M. L. (2001) Reduction of $NO_x$ by plasma-facilitated catalysis: an update on the PNNL-Caterpillar CRADA on heavy-duty emissions reduction. Proc. 2001 Diesel Engine Emissions Reduction Workshop, Portsmouth, VA. US Department of Energy, Washington, DC.

5. Park, P.W., Boyer, C. L., Ragle, C. Balmer, M. L., Aardahl, C. L., Habeger, C. F., Rappe, K. G., and Tran, D. N. (2001) Development of catalytic materials for non-thermal plasma aftertreatment. Proc. 2001 Diesel Engine Emissions Reduction Workshop, Portsmouth, VA. US Department of Energy, Washington, DC.

6. C. L. Aardahl "Plasma-facilited SCR of $NO_x$ in heavy-duty diesel exhaust." Presented at the SAE Spring Fuels and Lubricants Meeting, Reno, NV. May 6-9, 2002.

7. C. L. Aardahl "Plasma-facilitated $NO_x$ control for heavy duty diesel engines." Presented at the

8. FY 2002 DOE National Laboratory Merit Review and Peer Evaluation on CIDI Engine Combustion, Emission Control, and Fuels R&D, Argonne National Laboratory, Argonne, IL. May 14-16, 2002.

9. C. L. Aardahl "Plasma-facilitated catalysis: de$NO_x$ for heavy-duty diesel emissions reduction." Invited talk at the University of Washington, Chemical Engineering Department, Seattle, WA. May 20, 2002.

10. C. L. Aardahl "Plasma-facilitated catalysis: de$NO_x$ for heavy-duty diesel emissions reduction." Presented at the National Laboratory Catalysis Meeting, Pacific Northwest National Laboratory, Richland, WA. May 22-23, 2002.

# H. Material Support for Nonthermal Plasma Diesel Engine Exhaust Emission Control

*Stephen D. Nunn (Primary Contact)*
*Materials Processing Group*
*Oak Ridge National Laboratory, P.O. Box 2008, M/S 6087*
*Oak Ridge, TN 37831*

*ORNL Technical Advisor: David Stinton*

*DOE Technology Development Manager: Nancy Garland*

This project addresses the following DOE R&D Plan barriers and tasks:

*Barriers*

A. $NO_x$ Emissions

B. PM Emissions

*Tasks*

4b. Non-thermal Plasma R&D

## Objectives

- Identify appropriate ceramic materials, develop processing methods, and fabricate complex-shaped ceramic components that will be used in Pacific Northwest National Laboratory (PNNL)-designed nonthermal plasma (NTP) reactors for the treatment of diesel exhaust gases.
- Fabricate and ship components to PNNL for testing and evaluation in prototype NTP reactors.
- Develop a component design and establish a fabrication procedure that can be transitioned to a commercial supplier.
- Assemble and test a prototype NTP reactor on a laboratory diesel engine.

## Approach

- Evaluate commercially viable forming methods to fabricate complex-shaped ceramic components that meet PNNL design specifications.
- Modify processing as needed to accommodate material and design changes.
- Evaluate bonding and sealing materials for preparing assemblies of the ceramic components.
- Investigate metallization materials and processes to apply electrodes to the ceramic components.

## Accomplishments

- Modified the processing procedure for fabricating the ceramic components to improve reliability and simplify the production.
- Identified a sealing glass composition for joining together the ceramic components that are used in the NTP reactor assembly.

- Initiated plans to conduct functional testing of the NTP reactor on a 1.7 liter diesel engine in an engine test cell.

### Future Directions

- Finalize the selection of sealing materials to bond and seal the various ceramic and metal components of the NTP reactor into a complete assembly for functional testing.
- In collaboration with PNNL, select a NTP reactor design for assembly and testing to determine the operational performance of the device.
- Fabricate an NTP reactor assembly and test the device in a diesel engine exhaust gas stream.

---

## Introduction

NTP reactors have shown great potential as an effective means for eliminating unwanted exhaust gas emissions from diesel engines. In particular, the NTP reactor is very effective in reducing $NO_x$. Researchers at PNNL are developing new, proprietary design configurations for NTP reactors that build on past experimental work. To improve the effectiveness, these designs include ceramic dielectric components having complex configurations. Oak Ridge National Laboratory (ORNL) has extensive experience in the fabrication of complex ceramic shapes, primarily based on prior work related to developing ceramic components for gas turbine engines. The ORNL expertise is being utilized to support PNNL in its development of the new NTP reactor designs.

## Approach

Collaborative discussions between ORNL and PNNL are used to establish new ceramic component designs for improved NTP reactors. Meeting NTP reactor design objectives is balanced with the limitations of ceramic manufacturability to arrive at a new component configuration. The ceramic processing facilities and expertise at ORNL are then used to establish fabrication capabilities and to produce components for testing at PNNL. This is an iterative process as both parties gain more knowledge about fabricating the components and about their performance in NTP reactor tests. The ultimate goal is to identify a design which performs well and which can be readily produced by a commercially viable process.

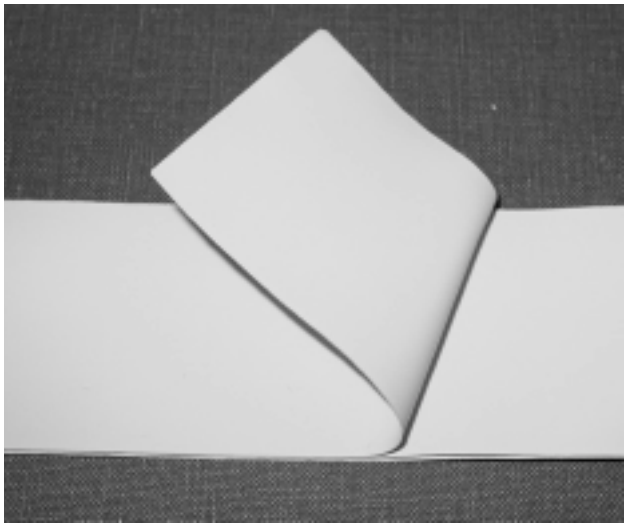

**Figure 1**. Photograph of Pieces of the Tape Cast Ceramic Material Showing the Flexibility of the Unfired Tape

## Results

In the early stages of this project, complex-shaped ceramic components were fabricated by the gelcasting process. Although these parts performed well in laboratory tests, it was decided that the fabrication process was too complicated to be feasible for commercial production. A new fabrication process was developed that uses commercially available tape cast ceramic materials. In the green state (unfired), the ceramic tape is flexible as shown Figure 1. The tape can be shaped and laminated to form the ceramic dielectric components for the NTP reactor. This is illustrated in Figure 2, where grooves have been formed in the

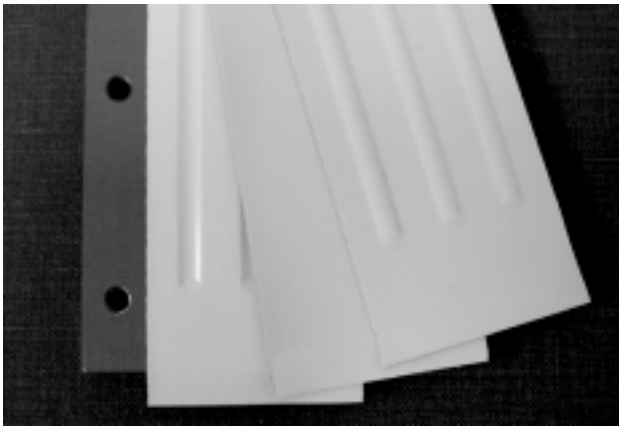

**Figure 2.** Examples of Formed and Flat Tape Segments Illustrating How They Are Assembled to Form the Ceramic Dielectric Components

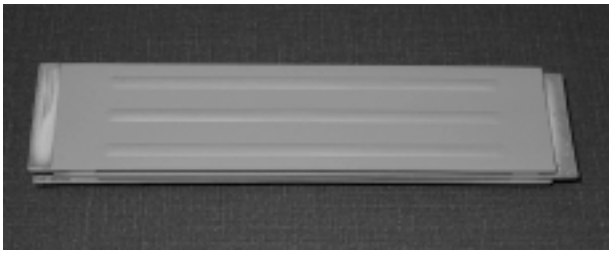

**Figure 3.** Sintered Dielectric Plates Assembled in a Stack with Individual Plates Separated by Alumina Ceramic Spacers

outer layers that will be laminated with flat tape layers to form the final assembly. Using a flat core is a modification of the original process that simplifies fabrication and improves yield. Silver electrodes are applied to the inside of the grooved areas and then extended to the outside of one end of the assembly. A stack of sintered components is shown in Figure 3. The individual dielectric plates are separated by alumina ceramic spacers to produce a precise gap between the plates.

In the NTP reactor assembly, the ceramic components will be fixed in place in a metal housing, with ceramic spacers being used to maintain the separation between the individual plates. To form the assembly, a bonding and sealing material is needed to fix the ceramic components in position and to form a gas tight seal to contain the exhaust gases. The bonding/sealing material must be an electrical


**Figure 4.** Test Assembly for Evaluating Bonding and Sealing of the NTP Reactor Component Materials

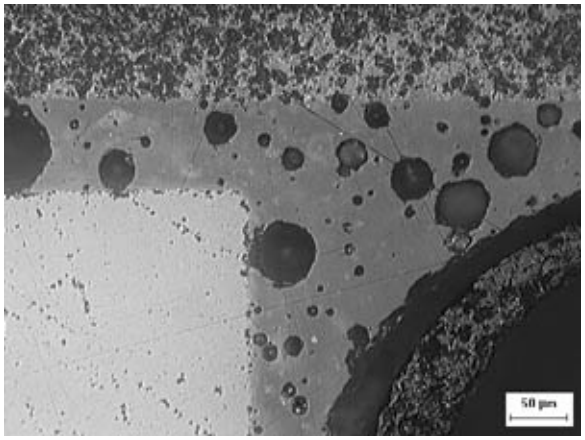

**Figure 5.** Micrograph showing the adhesive bond between the dielectric material (top) and the spacer (lower left). A smooth fillet has formed where the outer portion of the two materials join (center) forming a gas-tight seal. Bar equals 50 microns.

insulator and must have an appropriate thermal expansion match to maintain a tight bond during thermal cycling. Several glass compositions have been evaluated for use in joining the various components. An example of a test sample is shown in Figure 4, where pieces of the dielectric ceramic and the spacer are bonded in a sandwich. A photomicrograph of the bond is shown in Figure 5. The glass wets and bonds the materials together and forms a fillet of material at the outer surface to make a gas-tight seal. Additional testing will be required to identify an appropriate bonding material to join the ceramic components to the metal housing.

Plans are now being made to make a complete NTP reactor during the coming fiscal year and to conduct tests of the performance of the device on a 1.7 liter diesel engine, in an engine test cell.

## Conclusions

The ceramic dielectric component fabrication procedure was modified to simplify production of parts for the NTP reactors. The new procedure should lower cost and improve reliability and yield of the components. A sealing glass was identified for joining together the ceramic components of the NTP reactor, but additional testing is needed to find a material that will bond the ceramics to the metal housing of the reactor.

# I. Small, Inexpensive Combined $NO_x$ and $O_2$ Sensor

*William N. Lawless (Primary Contact) and C.F. Clark, Jr.*
*CeramPhysics, Inc.*
*921 Eastwind Drive, Suite 110*
*Westerville, OH 43081*

*DOE Technology Development Manager: Kenneth Howden*

This project addresses the following DOE R&D Plan barriers and tasks:

*Barriers*

A. $NO_x$ Emissions

C. Cost

*Tasks*

2a. Advanced Sensors and Controls

## Objectives

- Demonstrate the $NO_x$ sensing capability of a small amperometric zirconia sensor made by capacitor-manufacturing-methods and containing Rh or Pt/Rh electrodes.
- Demonstrate a dual amperometric sensor containing oxygen-sensing layers and $NO_x$-sensing layers and embedded Pt leads.
- Demonstrate that both oxygen and $NO_x$ can be measured with a device based on a zirconia tube containing an oxygen sensor and a dual oxygen/$NO_x$ sensor.
- Supply prototype sensors and microprocessors to potential users.

## Approach

- Make and evaluate $NO_x$ sensors.
- Design and evaluate dual $O_2$ and $NO_x$ sensors.
- Build microprocessor controllers for the sensors.
- Build and test $O_2$ and $NO_x$ sensors enclosed in a zirconia tube to control and measure the free oxygen content.
- Provide sensors to potential users for evaluation.

## Accomplishments

- Purchase of raw materials by the sensor manufacturer.
- Assembly of equipment for testing with $NO_x$.
- Measurement of sensitivity of $O_2$ sensors to $NO_x$.

## Future Directions

- Testing of $NO_x$ sensors.
- Testing of dual $O_2$ and $NO_x$ sensors.

## Introduction

The measurement of the oxygen partial pressure in exhaust gases has long been recognized as an important diagnostic for the efficient combustion of fossil fuels. In recent years the importance of $NO_x$ in exhaust gases has gained increasing attention for emissions control, and regulatory agencies at both the state and federal levels have mandated reductions in $NO_x$ levels.

## Approach

This project builds on a successful DOE project to manufacture and test a miniature, amperometric, zirconia oxygen sensor. In this project, a small multilayer ceramic structure is made using standard ceramic capacitor processing techniques. The layers are made of zirconia, an oxygen conducting material, and are separated by platinum electrodes with controlled porosity. A constant voltage is applied to the sensor and the amperometric current through the sensor is a direct measure of the oxygen in the surrounding atmosphere.

The same structure and techniques will be used to manufacture a $NO_x$ sensor, except that Rh or Pt/Rh electrodes will be used to catalyze the $NO_x$. The sensor will measure oxygen released from the $NO_x$. It will be necessary to separately measure and correct for the free oxygen in the surrounding gas.

## Results/Future Directions

The first major step in the project is for the sensor manufacturer, MRA Laboratories, to make multilayer sensors using Rh and Pt/Rh electrodes. To manufacture these sensors, it is necessary for them to purchase zirconia powder and Rh powder, which required a large initial outlay of funds. Project funds sufficient for this purchase were not authorized until a few months after the project start date. After the funds were authorized, there were further delays in obtaining the raw materials from the suppliers. MRA has now received all materials and will deliver the first batch of sensors in the near future.

In preparation for receiving these sensors, test equipment has been assembled and tested at CeramPhysics. This equipment includes an electrochemical $NO_x$ sensor which will be used as a standard to calibrate the $NO_x$ sensors produced in this project.

Tests on oxygen sensors from the companion DOE project indicate that these sensors are insensitive to $NO_x$. This is a necessary condition for a successful dual sensor. A $NO_x$ sensor will measure the combined oxygen from $NO_x$ catalysis and the residual oxygen in the surrounding atmosphere. Measuring the residual oxygen content separately with a sensor insensitive to $NO_x$ will allow for an exact determination of the $NO_x$.

# J. $NO_x$ Sensor for Direct Injection Emission Control

*David B. Quinn (Primary Contact), Earl W. Lankheet (Principal Investigator)*
*Delphi Corporation*
*MC 485-220-065*
*1601 N. Averill Ave.*
*Flint, MI 48556*

*DOE Technology Development Manager: Kenneth Howden*

*Main Subcontractor: Electricore, Inc. Indianapolis, IN*

This project addresses the following DOE R&D Plan barriers and tasks:

*Barriers*

A. $NO_x$ Emissions

C. Cost

*Tasks*

2a. Advanced Sensors and Controls

## Objective

- Develop an electronics control circuit for the $NO_x$ sensor.
- Develop the packaging for the electronic controller.
- Develop the sensing element structure based on integrating zirconia and alumina ceramics and planar element technology.
- Develop the interconnection method to carry power and signal to and from the $NO_x$ measurement device.
- Develop the necessary materials and process refinements in support of the ceramic sensing element.

## Approach

- Use alumina and zirconia ceramic tapes and thick film screen printed pastes to form the necessary control and measurement cells. Integrate the heater on the co-fired substrate.
- Make generous use of sample test coupons to select electrode materials, pump and chamber configuration, and optimal operating temperature.
- Develop sensing element cell configuration based on modeling and confirmation gas bench testing.
- Use set-based concurrent engineering (SBCE) to develop at least 2 different techniques to interconnect the power and signal wires to the sensing element substrate. Use accelerated engine and environmental testing to establish the optimum interconnection approach.
- Use existing sensor packaging technology to house and protect the sensing element.

### Accomplishments

- Developed several sample coupons with various cell configurations used for pump and measurement electrode screening.
- Demonstrated ideal separation performance on an electrode material, but this performance was limited to very low oxygen concentrations.
- Showed that a small addition of gold into the platinum electrodes severely reduces the oxygen transport capacity of the electrodes.
- Fully characterized the impedance and temperature behavior of sensing element cells.
- Designed and began testing a mechanical interconnection system.
- Successfully demonstrated direct welding of single and multiple (gang) nickel-coated copper wires to platinum substrate pads achieving an average tensile pull strength value of 11 lbs.

### Future Directions

- Continue to refine the measurement techniques and define sampling rates, operating temperatures, etc.
- Develop the sensing element structure for ease of manufacture and improved performance.
- Continue with durability testing of mechanical (2nd generation design) and direct weld (1st generation design) electrode materials and performance for $NO_x$ separation.
- Begin to evaluate electronic interconnections and determine the need for passivation.

---

## Introduction

This project strives to develop the remaining technology needed to deliver a robust $NO_x$ sensor for use in closed-loop control of $NO_x$ emissions in lean-burn, particularly CIDI engine technologies. At least two applications for $NO_x$ sensors have been identified: (1) engine-out $NO_x$ control, requiring a high $NO_x$ range of zero to 1500 ppm $NO_x$, and (2) aftertreatment control and diagnostics, requiring a low $NO_x$ range, less than about 100 ppm $NO_x$.

This activity builds on existing and developing Delphi technology in multi-layer and exhaust sensor ceramics, as well as work performed under a separate Cooperative Research and Development Agreement (CRADA) with Pacific Northwest National Laboratory (PNNL).

## Approach

The Delphi-led team will leverage the electrochemical planar sensor technology that has produced stoichiometric planar and wide range oxygen sensors as the basis for development of a $NO_x$ sensor. Zirconia cell technology with an integrated heater will provide the foundation for the sensor structure. The re-use of proven materials and packaging technology will help to ensure a cost-effective approach to the manufacture of this sensor.

The electronics technique and interface is considered to be an area where new strategies need to be employed to produce higher signal/noise (S:N) ratios of the $NO_x$ signal with emphasis on signal stability over time for robustness and durability.

Packaging the electronics requires careful design and circuit partitioning so that only the necessary signal conditioning electronics are coupled directly in the wiring harness, while the remainder are situated within the electronic control module (ECM) for durability and costs reasons.

The sensing element will be based on the amperometric method utilizing integrated alumina and zirconia ceramics. Precious metal electrodes will be used to form the integrated heater as well as the cell electrodes and leads. Inside the actual sensing cell structure, it is first necessary to separate $NO_x$ from the remaining oxygen constituents of the exhaust, without reducing the $NO_x$. Once separated, the $NO_x$ will be measured using a second cell. Various test sample coupons will be designed and

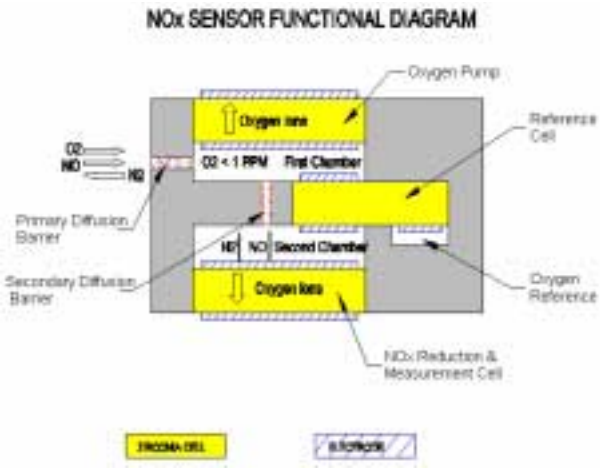


**Figure 1.** Functional Diagram of a $NO_x$ Sensor

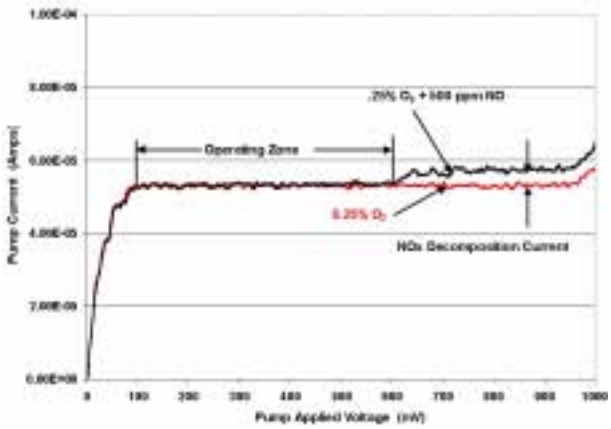


**Figure 2.** CV Curve of an Ideal Behavior $NO_x$ Electrode

constructed to facilitate material selection and refinement as well as cell, diffusion barrier, and chamber development.

The sensing element substrate could have 6 to 8 interconnections. To facilitate a robust durable connection, at least two techniques will be evaluated using the SBCE approach. One technique will be mechanical, while the second will be a metallurgical connection. Due to the anticipated low $NO_x$ signal levels, there may also be a need to "passivate" the lead interconnections to obtain the necessary isolation and durability. Materials and process refinements will play an important role in the development of this sensor and are integrated into this project accordingly.

## Results

Figure 1 shows the functional diagram of a $NO_x$ sensor. This structure consists of layers of zirconia and alumina ceramics with appropriate electrode materials constructed to yield three distinct cells. In the first oxygen separation cell, the incoming exhaust sample is separated by means of pumping oxygen so that only $NO_x$ components are remaining. The second cell is used to monitor and control the first cell. The third cell is for the measurement of the $NO_x$ in the exhaust sample by means of reducing the $NO_x$ and monitoring the corresponding low current levels that result. The integrated heater and other structure are not shown for clarity.

Using an element structure similar to that in the function diagram shown, a voltage can be applied to the pump cell and the current can be monitored to produce a cyclic voltammetry (CV) curve like that of Figure 2. One series is plotted where background oxygen is the only gas being measured. When 500 ppm $NO_x$ is added to the sampled gas, a second series is plotted. This graph shows the behavior of an ideal $NO_x$ sensor electrode. At lower applied voltages, the electrode in the pump cell does not reduce the $NO_x$ component. At higher voltages, both the $NO_x$ and the oxygen are reduced. Once the oxygen is separated and removed from the exhaust sample, the measurement of $NO_x$ concentration can be made. This separation behavior is required over the full range of operating conditions, and needs to be very stable over time. The results from Figure 2 show excellent behavior, but this has only been obtained at very low oxygen concentration levels with corresponding low oxygen pumping current levels. At higher oxygen concentration levels (>0.1%), the pump cell can not effectively pump all of the oxygen, leaving some oxygen to confuse the measurement cell, resulting in an inaccurate measurement.

Figure 3 plots the electrode current capacity versus temperature for candidate $NO_x$ separation and measurement electrodes fabricated using a thick film printing method. Two of the electrodes tested contained low levels of gold, 0.3 and 0.5%

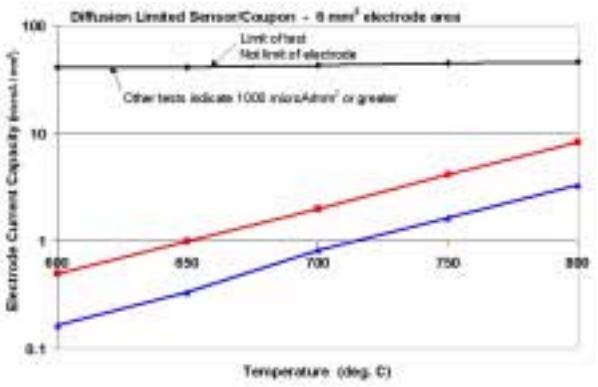


**Figure 3.** Current Capacity of Electrodes with Au Doping

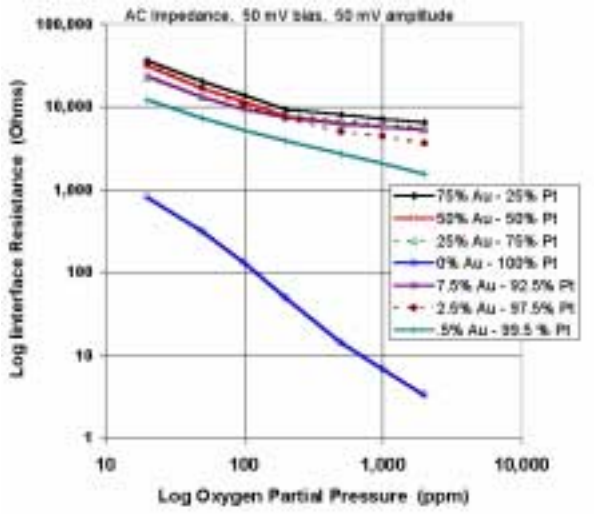


**Figure 4.** Coupon Sputtered Electrode Impedance @ 650°C

respectively. Gold has been found to suppress $NO_x$ reduction at low applied voltages. It can be seen that even low-level additions of gold significantly reduce the electrode current capacity. This explains the electrode problem with separation of $NO_x$ at higher oxygen concentration levels.

The impact of gold addition to platinum electrodes was also studied with sputter deposited thin film electrodes. The sputtering process provided an easy means of obtaining a wide range of gold concentrations. Figure 4 plots the significant increase in electrode interface impedance that occurs when gold is added to the platinum. Even a small

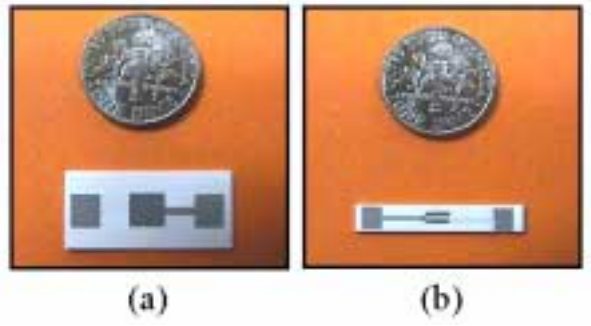


**Figure 5.** Development Sample Test Coupons (a) open faced, and (b) diffusion limited

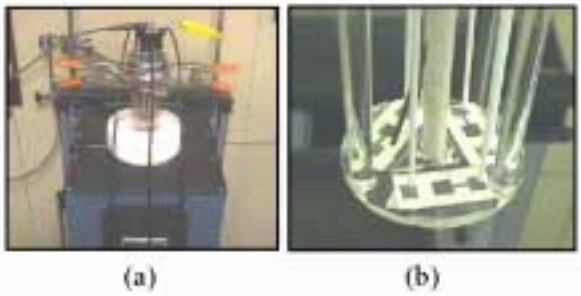


**Figure 6.** Sample Coupons Mounted in a Gas Bench Test Fixture (a) gas bench furnace, (b) Quartz fixture showing sample coupons

amount (such as 0.5% Au) is seen to increase the impedance by 50 times. This would also reduce the oxygen pumping capacity of the cell by a factor of 50.

Continued electrode material refinements are being made to enhance the robustness and stability of this separation effect and are the focus of the research using sample coupons shown in Figure 5, which are routinely tested in a gas bench using the fixture shown in Figure 6.

Figure 7 shows the proposed assembly package to house the sensing element. This assembly package is very similar to that of other planar sensor element housings that have been proven to be durable to the exhaust environment and cost effective to manufacture. There are several package areas where plans call for tailoring the design to meet the new requirements imposed by the $NO_x$ sensor. The

**Figure 7.** $NO_x$ Sensor Assembly Package

interconnection area needs to effectively house and protect the signal and power connections to the substrate. Due to real estate issues, it is necessary to have very compact and effective terminations/ interconnections. The low signal levels of the $NO_x$ sensor may also require that the terminal lead and interconnection area be "passivated" or protected, so that each signal wire is fully isolated from the next.

Figure 8 illustrates the pre-consolidation step that enables the 19-strand wire to be formed into a rectangular shape to facilitate welding. Figure 9 shows the wire/platinum pad interface from a polished cross section as seen by optical microscopy. Tensile tests on ultrasonically welded lead wires to the platinum pads have yielded average pull strengths of 11 lbs.

## Conclusions

Sample coupons and mule sensing elements have been fabricated that demonstrate $NO_x$ can be separated from background oxygen, albeit at low concentration levels of oxygen. Tests have shown that gold doping of the platinum electrodes reduces the oxygen pumping capacity of the cells to a much larger degree than expected. This information will be used to modify the sensor design.

Feasibility of direct welding of wires to the substrate has been demonstrated. This can have a significant impact on both assembly cost and the durability of the interconnection. Further development with this technique will be needed to perfect its use.

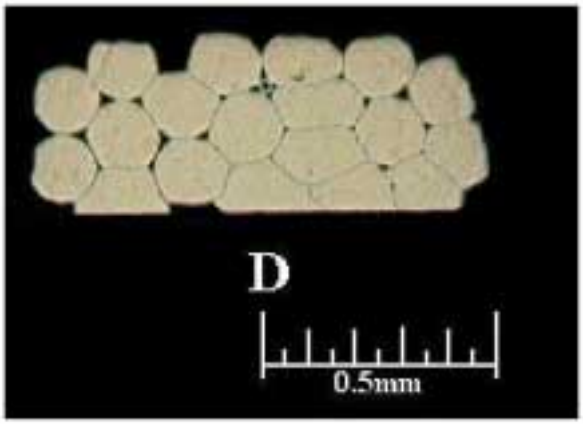


**Figure 8.** Wire Pre-Consolidation Prior to Welding

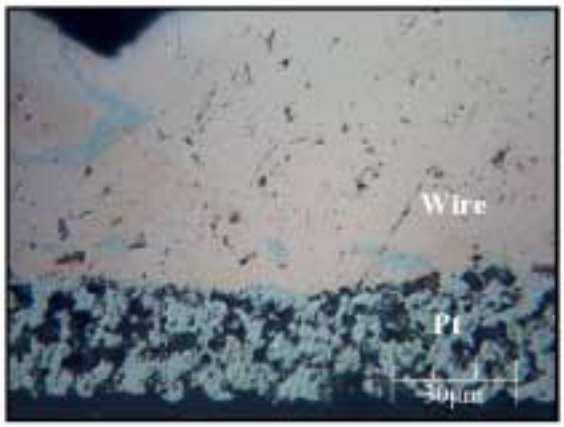


**Figure 9.** Welded Wire - Platinum Pad Interface

# IV. PARTICULATE CONTROL TECHNOLOGIES

## A. Materials Improvements and Durability Testing of a Third Generation Microwave-Regenerated Diesel Particulate Filter

*Dick Nixdorf (Primary Contact)*
*Industrial Ceramic Solutions, LLC*
*1010 Commerce Park Drive, Suite I*
*Oak Ridge, TN 37830*

*DOE Technology Development Managers: Kathi Epping and Nancy Garland*

*ORNL Technical Advisor: David Stinton*

*Subcontractors: Transportation Research Center, Lydall Technical Papers, Northrop Gruman Electron Devices, Lubrizol Corporation*

This project addresses the following DOE R&D Plan barriers and tasks:

*Barriers*

B. PM Emissions

C. Cost

*Tasks*

5c. Microwave Regenerating Diesel Particulate Filter

### Objectives

- Develop and test a pleated ceramic fiber filter to significantly reduce engine backpressure over that achieved by conventional particulate filters.
- Design, fabricate and road test a particulate filter system that will microwave regenerate at all engine operating conditions.
- Conduct a 7,000-mile vehicle controlled track test of the microwave filter system with periodic emissions analysis to demonstrate filter durability.
- Provide filter durability, fuel penalty and particulate removal efficiency data from the diesel vehicle testing.

### Approach

- Conduct papermaking, pleating and filter cartridge testing to establish an acceptable prototype pleated filter cartridge.
- Use finite element analysis of microwave fields and laboratory air flow/microwave heating tests to design the vehicle-ready test system
- Validate the filter system's particulate removal efficiency on a stationary diesel engine test cell.
- Install and road test the improved microwave filter system on a 7.3-liter diesel vehicle.

- Conduct a 7,000 mile controlled track test of the filter system, including microwave regeneration at various operating conditions and Federal Test Procedure (FTP) emissions testing to verify filter durability during and after the test sequence.

### Accomplishments

- A microwave-regenerated filter system was installed and road tested on 1.9-liter Volkswagen Jetta vehicle for 200 miles and six filter microwave cleanings (the Jetta testing was abandoned due to engine and exhaust system defects on the vehicle unrelated to this work).
- A pleated ceramic fiber filter cartridge was developed and demonstrated to accomplish 1/20th the exhaust backpressure as that of a conventional wall-flow particulate filter.
- The ICS ceramic fiber filter cartridge has been tested for over nine months on the Ford 7.3-liter truck, under standard highway driving conditions, with no failure of materials.
- A pleated filter cartridge system, capable of regenerating at any engine operating condition, for road testing on a 7.3-liter Ford F-250 truck was designed and laboratory tested.
- The pleated filter system will be tested in a 7,000-mile track test in October/November 2002.

### Future Directions

- Integrate the microwave filter particulate matter (PM) control unit with $NO_x$, hydrocarbon, and CO emission devices to develop a total system approach to meet Environmental Protection Agency (EPA) Tier II emissions.
- Continue on-road testing on the 7.3-liter Ford truck for an additional 20,000 miles, under high-load conditions, to extend the durability performance database.
- Enlist exhaust system, catalyst, engine, and vehicle manufacturers in a joint product development effort to move toward 2004 commercialization of the microwave-regenerated particulate filter.
- Work with microwave suppliers and materials companies to further harden the microwave and filter media components of the pleated filter microwave system against vibration and exhaust forces.

---

## Introduction

Most current diesel engine particulate filter technologies depend on a catalyst to assist in the regeneration of the filter. Catalyst technology requires a minimum exhaust temperature of approximately 300°C to be effective. Small and medium size diesel engines rarely achieve this exhaust temperature. The microwave-regenerated particulate filter (Mw-DPF) has been developed to provide the required particulate removal efficiencies and regenerate at low exhaust temperatures. A catalyst can be easily applied to the Mw-DPF to allow regeneration at higher exhaust temperatures without microwave assistance. The Mw-DPF is a viable answer to the low-temperature urban driving cycle where the catalyst technologies are ineffective (see Figure 1). Engine backpressure, created by particulate filters, reduces engine performance and fuel economy. The ICS pleated ceramic fiber filter demonstrates $1/20^{th}$ of the backpressure on the engine as that exhibited by the standard wall-flow filter (see Figure 2). This device will provide a major breakthrough for those vehicle manufacturers concerned with engine performance caused by wall-flow particulate filters.

## Approach

The ceramic fiber wall-flow filter was tested on a Ford F-250 7.3-liter CIDI truck, under routine highway driving conditions, for approximately 2,000 miles over a period of several months to demonstrate filter durability. The truck filter was removed and microwave-regenerated in the laboratory to understand the effects of microwave heating on the particulate loaded cartridge.

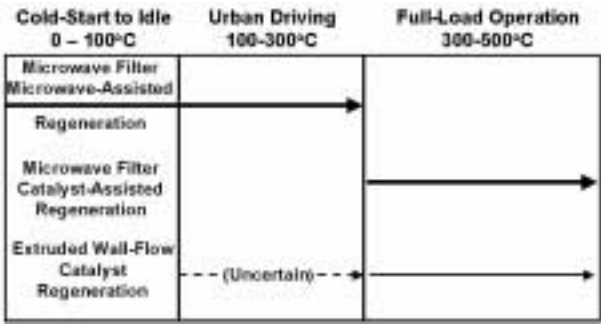


**Figure 1.** Mw-DPF Particulate Filter Regeneration at all Engine Operating Conditions

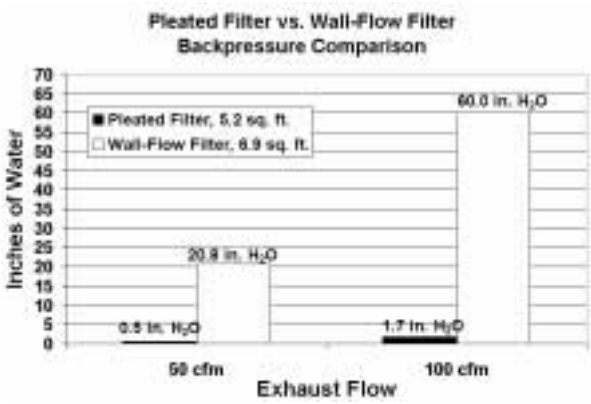


**Figure 2.** Exhaust Backpressure of the ICS Pleated Filter Cartridge vs. Conventional Wall-Flow Filters

A second major project for 2002 was installation of a ceramic fiber, wall-flow microwave filter system on a 1.9-liter TDI Volkswagen Jetta vehicle for a 7,000-mile track test. Microwave regenerations were to be conducted at engine idle conditions. The Volkswagen Jetta, equipped with an on-board microwave regeneration system, was driven for approximately two hundred highway miles with six idle condition regenerations conducted. The Jetta vehicle exhibited two pre-existing severe mechanical problems. The exhaust gas recirculation (EGR) valve was uncontrollable, opening and closing at random during the engine idle microwave regenerations.

This condition resulted in unacceptable exhaust flow variations during the microwave regenerations. During stationary engine testing at Oak Ridge National Laboratory (ORNL) on an identical 1.9-liter TDI engine, three hours were required to load the filter cartridge at normal engine speeds. The same size cartridge on the Volkswagen vehicle was found to load in less than one hour. The second problem was high inorganic ash accumulation in the filter, probable due to several years of being parked, as well as previous testing of unusual fuels and lubricants. ICS and DOE agreed that conducting the expensive track testing on such an unreliable test vehicle was counter-productive. Therefore, the 7,000-mile track testing was transferred to the Ford F-250 7.3-liter truck.

During the test vehicle change, ICS was able to complete the development of a low-backpressure pleated filter cartridge, to replace the wall-flow design, for the 7,000-mile durability track testing. The pleated filter system being prepared for the Ford truck will allow microwave regeneration at conditions other than engine idle, which is a significant requirement by the diesel engine manufacturers. ICS is currently testing the microwave-heating properties of this system in the laboratory. In early July, particulate emissions testing will be conducted on the pleated filter on a 1.7-liter Mercedes engine at ORNL. In October, the 7,000-mile track test will begin at the Transportation Research Center in East Liberty, Ohio. The data from this test will verify system durability using filter efficiency performance in FTP chassis dynamometer testing and will accurately measure the fuel penalty of the Mw-DPF.

## Results

Data verifying the durability of the filter cartridge in the Ford truck highway testing is shown in Figure 3, showing the slow rate of cleaned-filter backpressure increases on the same filter over a nine-month period. That testing is still proceeding on the same ceramic fiber filter cartridge with no apparent mechanical damage to the filter cartridge.

The ability of the microwave to clean a particulate-loaded filter to within 95% - 100% of its clean condition has been demonstrated in engine testing for the last three years. Similar results of microwave regeneration on the Volkswagen Jetta vehicle are shown in Figure 4. The design of the new pleated ceramic fiber filter cartridge is displayed in Figure 5. The commercialization plan for the pleated


**Figure 3.** Backpressure Increases on a Single ICS Fiber Filter during Nine Months of Semi-Continuous Loadings and Cleanings on a Ford 7.3-liter CIDI Vehicle

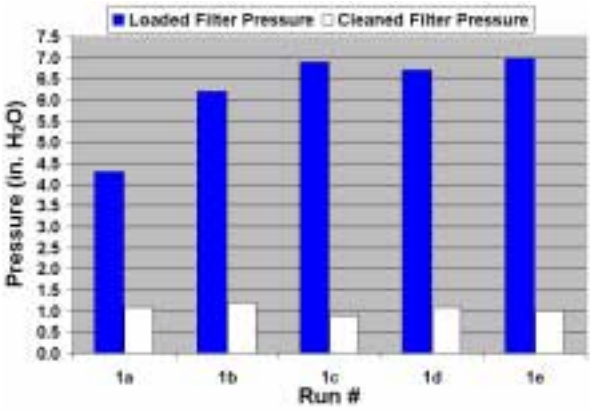


**Figure 4.** Microwave Filter Cleaning Efficiency Using the On-Board System of the Volkswagen Jetta Vehicle

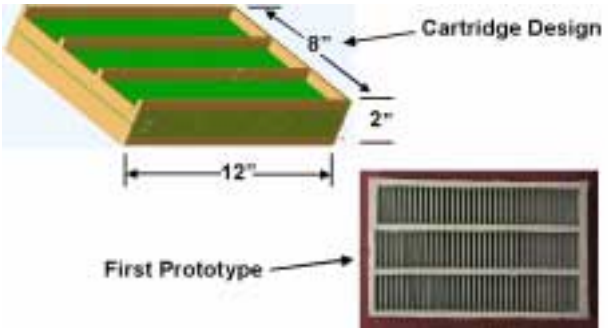


**Figure 5.** ICS Pleated Ceramic Fiber Particulate Filter Cartridge Cassette

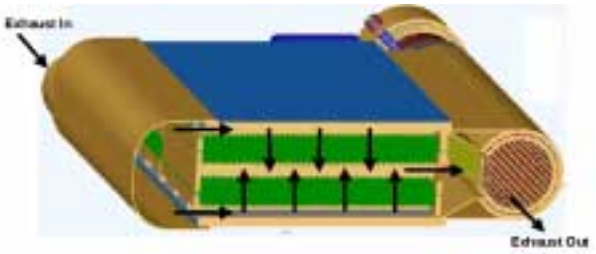


**Figure 6.** ICS Pleated Particulate Filter System Microwave Regeneration Design

**Figure 7.** On-board Generator to Supply Power to the Microwave System for the Mw-DPF on the Ford 7.3-liter Test Truck

filter is to produce the same size cassette for all vehicles, using multiple cassettes as the engine size increases. The design of the pleated particulate filter system as shown in Figure 6 will accomplish microwave regeneration at all engine conditions. The on-board generator supplying power to the microwave system on the Ford truck is shown in Figure 7. The new uniform-sized pleated cassette concept, with multiple cassettes as engine size increases, will maintain the price of the Mw-DPF below that of current particulate control technologies, while providing significant advantages in engine backpressure. Materials improvements in

the ceramic fiber filter system have continued in 2002, including filter media burst strength increases from the 6 psi goal achieved in 2001 to 10 psi in 2002. The application of an inexpensive silicon carbide coating to the filter cartridge has improved the microwave heating ability as well as its corrosion resistance. The use of silicon carbide structural members to frame the pleated filter also insures stability during high temperature excursions.

## Conclusions

Filter backpressure and the ability to regenerate a particulate filter at low exhaust temperatures are significant issues to diesel engine manufacturers preparing to meet EPA emission standards. Laboratory and stationary engine testing of the ceramic fiber microwave-regenerated filter system has shown meaningful progress in those areas. The 7,000-mile track test on the Ford 7.3-liter vehicle will begin durability verification. Continuation of the development of the pleated cassette system in 2003 will lead to a commercially viable product for mobile sources by 2004.

## FY 2002 Publications/Presentations

1. Nixdorf, R., "In-Situ Microwave Cleaning of Silicon Carbide Fiber Filtration Media", TechTextile Symposium North America, Atlanta, GA, April 2002.

# B. Diesel Particle Scatterometer

*Arlon Hunt (Primary Contact), Ian Shepherd, and John Storey*
*Lawrence Berkeley National Laboratory, 70-108*
*University of California, Berkeley, 94720*

*Oak Ridge National Laboratory Contact: John Storey*

*DOE Technology Development Manager: Kathi Epping*

This project addresses the following DOE R&D Plan barriers and tasks:

*Barriers*

B. PM Emissions

*Tasks*

2. Sensors and Controls

## Objectives

- Develop and use the Diesel Particle Scatterometer (DPS) for real-time diesel particle size and property measurements
- Extend diesel particle scatterometer (DPS) capabilities in time, sensitivity, and application
- Interpret optical properties of particles
- Commercialize instrument

## Approach

- Measure angle-dependent polarized laser light scattering from diesel exhaust particles, including the scattering intensity (millisecond response) and two polarization transformations
- Model soot scattering as: spheres - Mie scattering theory to fit data, porous particles - check validity using coupled dipole model of particle clusters
- Determine size distribution and the compositional information using the absorptive and refractive properties (n, k) of soot

## Accomplishments

- Upgraded and improved the software analysis package
- Received the Energy100 award for DPS development
- Developed improved AC and DC calibration techniques
- Completed upgrade of the system to operate with an ultraviolet (UV) laser
- Carried out comparison measurements with another light scattering instrument
- Reached agreement with an instrument company to commercialize the DPS

## Future Directions

- Design next generation instrument

- Develop a more "user friendly" software package
- Pursue tech transfer of the DPS with Sierra Instruments, Inc.

---

## Introduction

To determine the characteristics of diesel exhaust particles requires new instrumentation that can provide real-time information on diesel particulates including their size distribution, composition and morphology. Previous instruments typically require particle collection or operate too slowly to monitor particle characteristics during transients. To address these problems, we have developed a new instrument, the Diesel Particle Scatterometer (DPS) for real-time diesel particle size and property measurements. We have designed, built and compared the DPS with other instruments and techniques for measuring diesel particulates. Presently we are operating two instruments, one at Lawrence Berkeley National Laboratory (LBNL) and one at Oak Ridge National Laboratory (ORNL).

## Approach

The DPS is an optical light scattering instrument that measures the intensity and polarization of laser light scattered from particles in a diesel exhaust stream. One DC and two AC signals are measured by each of 13 detectors arrayed around the exhaust stream. The data stream is obtained by the synchronous detection of the polarized light that is modulated at a 50 kHz rate by a polarization modulator. The three angle-dependent polarization transformations that describe the light scattering; $S_{11}$, $S_{34}$, and $S_{12}$, are fit by Mie scattering calculations using a Levenburg-Marquardt optimization program. The results are plotted as a size distribution, and the refractive and absorptive optical properties of the particles are pre recorded along with diagnostics to indicate the contribution of the various detectors. The absorptive component of the index of refraction gives a measure of the elemental carbon content of the exhaust particles. An important advantage of the instrument is its rapid response time; it has been tested at greater than 1 Hz data acquisition rate. This speed allows for the measurement of engine transients and even cylinder-to-cylinder variations.

## Results

Two DPS instruments were designed and built at LBNL and have been operating at LBNL, ORNL and other locations. Operating experience with the instruments has provided information that has led to a number of improvements to the instruments this year. In addition, results from another light scattering instrument were compared with the results from the DPS. This comparison led to a careful examination of the instrument calibration and to a new set of improved calibration techniques. These activities established the instrument operation on a solid basis and led to technology transfer activities toward commercialization of the DPS.

The software associated with the DPS is extensive and complex, including both data acquisition and analysis. Several major improvements were made and a number of minor "bugs" eliminated. The output display was enhanced to show the relative contributions to the results from the various detectors. To verify the instrument operation, the DPS and another older single detector scanning polar nephelometer were operated simultaneously. Comparison indicated that better calibration of the DC and two AC sensitivities for each of the 13 detectors was needed. New calibration techniques and improvement of the polarization optics resulted in better comparisons and fits to the experimental data that are more robust. In interactions with the Sierra Instruments, Inc., a need was expressed to have a more compact measurement head that could be placed very close to the dilution system they manufacture. A new design has been proposed, and work on the individual components has been initiated. Sierra Instruments has agreed to commercialize the DPS pending trials at the Caterpillar test facility. Those tests will take place in the summer of 2002 and should lead to the commercial development of the DPS within about one year.

The work commenced last year on the coupled-dipole modeling of random, porous diesel soot

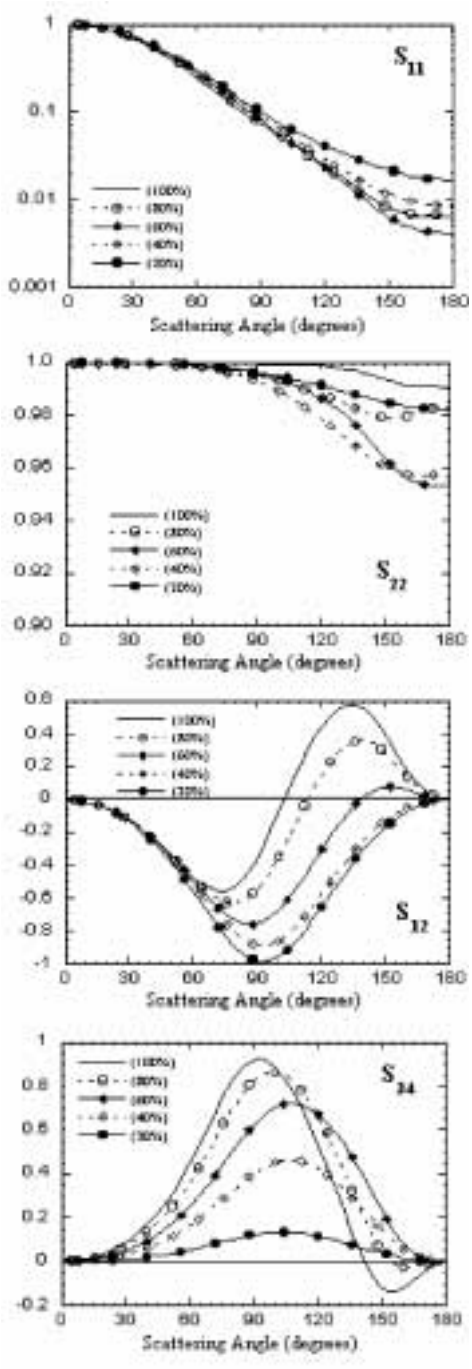


**Figure 1.** Results of a series of coupled-dipole calculations of the scattering matrix elements for sphere with a size parameter of 1.76. Dipoles were removed from the lattice by random selection and the matrix elements recalculated. A density of 100% is a sphere with a completely filled lattice.

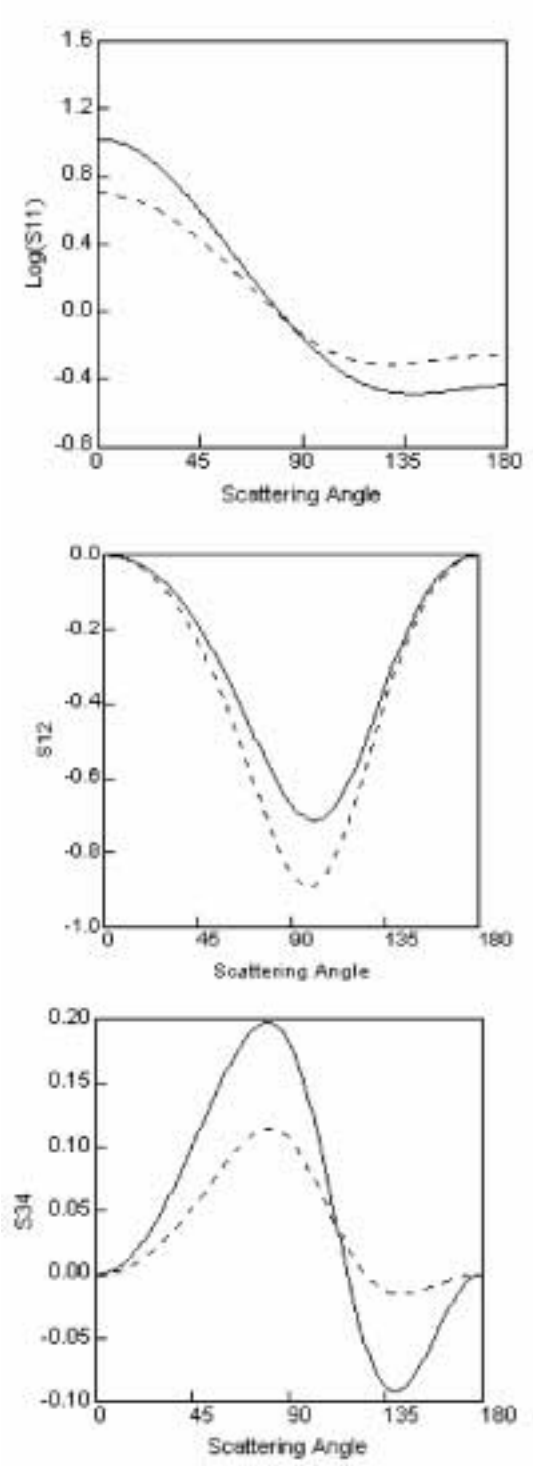


**Figure 2.** Comparison of angular scattering at 355 and 532 nm for a distribution with mean=120 nm, σ=3.8 and ref index=1.49-0.084i. Dashed line=532 nm. Solid line=355 nm.

particles has been completed and an archival paper has been written. A typical result from a set of coupled-dipole simulations is shown in Figure 1. Results such as these are very useful for interpreting experimental results. The coupled-dipole model has proved to be a powerful tool for gaining insight into the effects of particle morphology on scattering properties.

The incorporation of an argon-ion ultra-violet laser into the system has been completed this year. The use of this continuous wave (CW) laser at 355 nm wavelength significantly enhances the sensitivity of the system to smaller particle sizes compared to the CW YAG laser, at 532 nm, used in our previous studies. This may be illustrated by comparing, in Figure 2, the scattering patterns predicted at the two wavelengths for a particle size distribution that was observed experimentally. These results show the markedly increased sensitivity of the instrument at the shorter wavelength. In $S_{34}$, for example, which at the small particle limit is zero, shows a much larger modulation of the angular scattering at 355 nm. This approach provides more robust fits using the Mie model that significantly extends the instrument capability.

## Conclusions

This year was largely involved with instrument testing, improving the calibration, and perfecting the software. Incorporation of the UV laser into the instrument was also completed. Sierra Instruments has stated their intention to commercialize the instrument and combine it with their patented dilution system.

## References/Publications

1. P. Hull, I.G. Shepherd and A.J. Hunt, "Modeling Light Scattering from Diesel Soot Particles", submitted to Applied Optics, 2002.
2. A.J. Hunt, I.G. Shepherd and J. Storey, "Diesel Particle Scatterometer," 2001 Annual Report Office of Advanced Automobile Technologies, Washington, DC.
3. A.J. Hunt, M.S. Quinby-Hunt, I.G. Shepherd, "Polarized Light Scattering for Diesel Exhaust Particulate Characterization," Proc. of the Diesel Engine Emissions Reduction Workshop, DOE/ EE-0191 1999.
4. A.J. Hunt, M.S. Quinby-Hunt, I.G. Shepherd, "Diesel Exhaust Particle Characterization by Polarized Light Scattering," SAE Transactions 982629, LBNL-43695.
5. A.J. Hunt, I.G. Shepherd, M.S. Quinby-Hunt and J.M. Storey, "Size and Morphology Studies of Diesel Exhaust Particles using Polarized Light Scattering," 5th International Congress on Optical Particle Sizing, Minneapolis, MN, August 10-13, 1998.

# C. Optical Diagnostic Development for Exhaust Particulate Matter Measurements

*Peter O. Witze (Primary Contact)*
*Combustion Research Facility, Sandia National Laboratories*
*PO Box 969, MS 9053*
*Livermore, CA 94550-0969*

*DOE Technology Development Manager: Kathi Epping*

This project addresses the following DOE R&D Plan barriers and tasks:

*Barriers*

B. PM Emissions

*Tasks*

2. Sensors and Controls

## Objectives

- Develop real-time, engine-out particulate matter (PM) diagnostics for measuring size, number density volume fraction, aggregate characterization, volatile fraction, and metallic-ash species and concentration.
- Transfer resulting technology to industry.

## Approach

- Laser-induced incandescence (LII) will be used to measure the soot volume fraction and primary particle size.
- Simultaneous measurements of LII and elastic light scattering (ELS) will be used to obtain the following PM aggregate parameters using the Rayleigh-Debye-Gans polydisperse fractal aggregate (RDG-PFA) approximation:
  - particle volume fraction
  - diameter of primary particles
  - number density of primary particles
  - geometric mean of the number of primary particles per aggregate
  - geometric standard deviation of the number of primary particles per aggregate
  - mass fractal dimension
  - radius of gyration of the aggregated primary particles
- Laser-induced desorption with elastic light scattering (LIDELS) will be used to measure the volatile fraction of the PM.
- Laser-induced breakdown spectroscopy (LIBS) will be used to measure metallic-ash species and concentration.
- A scanning mobility particle sizer (SMPS) will be used as the reference standard for particle size distributions.
- Off-the-shelf components are used to build a measurement system that can be easily duplicated by industry partners.
- Artium Technologies Inc., Los Altos Hills, CA, will commercialize the resulting technology.

### Accomplishments

- A mobile, high-energy laser diagnostics (HELD) instrument has been built for off-site use by industrial collaborators. Initial application is scheduled for late September, 2002, at the Vehicle Emissions Laboratory at General Motors (GM) R&D in Warren, MI.
- Real-time LIDELS measurements of the volatile fraction of diesel PM have been obtained for load and EGR sweeps.
- Time-resolved LII measurements of PM volume fraction have been obtained for engine startup/ shutdown and EGR and throttle transients, and have been compared with SMPS measurements.
- A collaborative investigation of the effects of EGR on PM was conducted with the Combustion Research Group at the National Research Council (NRC) of Canada.
- A Particulate Matter Collaboratory web page has been established as a part of the DOE Diesel Collaboratory Project. Initial members include Sandia and NRC.
- A phone-modem network connection has been established between Sandia's turbocharged direct injection (TDI) diesel engine laboratory and Artium Technologies, Inc. for the development of a commercial LII instrument.

### Future Directions

- Continue the collaboration with Artium toward commercialization of an LII system for PM measurements. Their prototype instrument is scheduled for delivery to Sandia in September, 2002.
- Continue collaborations with industry (Ford and GM) for their on-site use of the HELD instrument.
- Develop laser-induced breakdown spectroscopy (LIBS) as a technique for identifying metallic ash species and measuring their relative concentrations.
- Develop experimental and modeling capability for RDG-PFA approximation for aggregate characterization.
- Extend the LIDELS technique to enable time-resolved measurements (~10 Hz data rate) from its current real-time performance of approximately one minute per measurement.

---

## Introduction

LII is a well-established technique for the measurement of PM volume fraction and primary particle size; it has been applied to both stationary burner flames and diesel engine combustion. Light from a high-energy pulsed laser is used to quickly heat the PM to its vaporization point, resulting in gray-body radiation that is proportional to the PM volume fraction; the cooling rate of the PM following laser heating is a measure of primary particle size. Simultaneous measurement of ELS from the particles at several discrete angles relative to the incident laser beam can be used to obtain additional information regarding the characteristics of PM aggregates using the RDG-PFA approximation.

LIDELS is a new technique we have developed for the real-time measurement of the volatile fraction of diesel PM. Laser energy is used to desorb the volatile matter from the diesel PM, and ELS measurements obtained before and after desorption give the volatile fraction. Conventional procedures require collection on filter paper and subsequent analysis. Several hours to several days are required to obtain a measurement. Our current LIDELS procedure requires approximately one minute to obtain a measurement, but an equipment upgrade will permit 10 Hz data rates.

LIBS is a fairly well-established technique for measuring metallic ash. A focused laser beam is used to ionize the ash, resulting in atomic emissions that identify the secies and their concentrations.

A single HELD instrument can perform all of the above tasks. Its main advantages over conventional PM measurement techniques are that it can be applied in any environment (e.g., hot or cold,

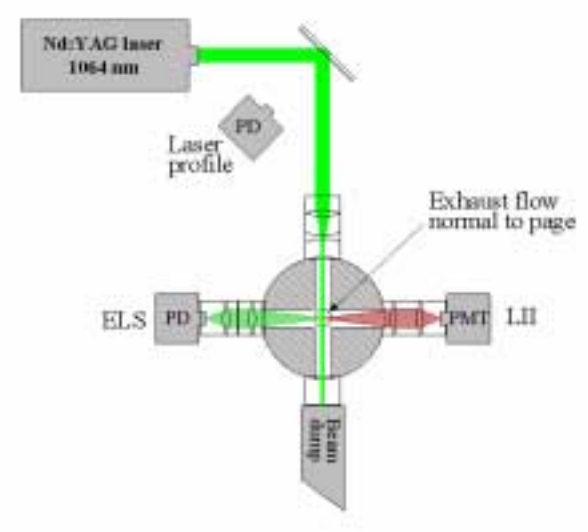


**Figure 1.** Schematic of a HELD Experimental Setup

**Figure 2.** Photograph of the HELD

undiluted or diluted, etc.), it responds in real time, and it is very sensitive to low PM concentrations (e.g., the lower limit for LII is estimated to be one part per trillion).

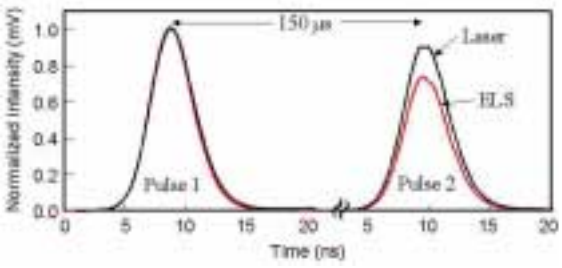


**Figure 3.** Double-pulse LIDELS technique. The two laser pulses are separated by 150 s.

## Approach

A schematic of the HELD experimental setup is shown in Figure 1 for simultaneous measurements of LII and ELS. The collimated beam of a pulsed Nd:YAG laser (1064 nm) is passed through the exhaust flow sampled through an optical cell. Three measurements are simultaneously obtained with fast photodetectors: 1) Incident temporal profile of the laser pulse, detected from diffuse scattering of a mirror; 2) LII signal, detected with a photomultiplier tube with spectral response from 300-650 nm; 3) ELS, detected through an interference bandpass filter centered at 1064 nm.

The complete HELD system is contained on a mobile cart of dimensions 2'x4' as shown in Figure 2. The only external connections required for use are the sample line for the diesel exhaust, a return vent line, and 110 V power. The laser and data-acquisition oscilloscope are both PC controlled, providing essentially "hands-off" operation.

## Results

The main accomplishment this year was the development and demonstration of the LIDELS technique for measuring the volatile fraction of diesel PM. LIDELS uses two laser pulses of comparable energy, separated in time by an interval sufficiently short to freeze the flow field (see Figure 3), to measure the change in PM volume caused by laser-induced desorption of the volatile fraction. The first laser pulse produces ELS that gives the volume of the total PM, and also deposits the energy to desorb the volatiles. ELS from the second pulse gives the system volume of the remaining solid portion of the PM, and the ratio of these two measurements is the

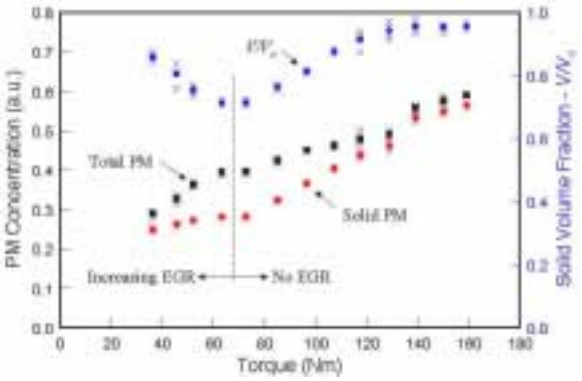


**Figure 4.** LIDELS measurements for a load sweep at 1500 rpm. The crosses indicate four repeats of the measurements, and the solid symbols

quantitative solid volume fraction. Calibration is required for the individual total PM and solid fraction to be quantitative.

LIDELS measurements for a load sweep are shown in Figure 4. The utilization of EGR specified by the engine control module is indicated in the figure, with EGR used for loads less than approximately 70 Nm; at the lowest load point the EGR amount is approximately 28%. The solid fraction measurements reveal a distinct minimum of 0.72 at the load point where the EGR was turned off. At the lowest load, with EGR, the solid fraction is 0.86, and at the highest loads the data asymptote to 0.96.

## Conclusions

Our double-pulse LIDELS technique appears to be robust, exhibiting good repeatability and consistency. We have demonstrated its applicability by performing a load sweep on a turbocharged direct-injection diesel engine. The measurements presented show all of the expected trends, but future work will be required to validate an inherent assumption that the change in scattering cross section between the two pulses is due mainly to changes in particle size and not particle properties.

## FY 2002 Publications/Presentation

1. Witze, P. O., "Real-Time Measurement of the Volatile Fraction of Diesel Particulate Matter Using Laser-Induced Desorption with Elastic Light Scattering (LIDELS)," International Energy Agency Task Leaders Meeting, Trondheim, June 23-26, 2002.

2. Witze, P. O., "High-Energy Pulsed-Laser Diagnostics for the Measurement of Diesel Particulate Matter,", GM R&D Seminar, Warren, May 17, 2002.

3. Witze, P. O., "High-Energy Pulsed-Laser Diagnostics for the Measurement of Diesel Particulate Matter,", Ford SRL Seminar, Dearborn, May 16, 2002.

4. Witze, P. O., "High-Energy Pulsed-Laser Diagnostics for the Measurement of Diesel Particulate Matter," National Laboratory CIDI and Fuels R&D Merit Review & Peer Evaluation, Argonne, May 13-15, 2002.

5. Witze, P. O., "Real-Time Measurement of the Volatile Fraction of Diesel Particulate Matter Using Laser-Induced Desorption with Elastic Light Scattering (LIDELS)," SAE Spring Fuels & Lubricants Meeting, Reno, May 6-9, 2002.

6. Witze, P. O., "Qualitative Laser-Induced Incandescence Measurements of Particulate Emissions During Transient Operation of a TDI Diesel Engine," SAE Spring Fuels & Lubricants Meeting, Reno, May 6-9, 2002.

7. Witze, P. O., "High-Energy Pulsed-Laser Diagnostics for the Measurement of Diesel Particulate Matter," DOE/OATT Midyear Review, Livermore, March 27, 2002.

8. Witze, P. O., "High-Energy Pulsed-Laser Diagnostics for the Measurement of Diesel Particulate Matter," Sandia/FE/EPRE Sensor Workshop, Livermore, February 20, 2002.

9. Witze, P. O., "High-Energy Pulsed-Laser Diagnostics for the Measurement of Diesel Particulate Matter," Cross-cut Diesel CRADA Meeting, Livermore, January 16-17, 2002.

10. Axelsson, B. and Witze, P. O., "Qualitative Laser-Induced Incandescence Measurements of Particulate Emissions During Transient Operation

of a TDI Diesel Engine," SAE Paper 2001-01-3574, October, 2001.

11. Witze, P. O., "Real-Time Measurement of the Volatile Fraction of Diesel Particulate Matter Using Laser-Induced Desorption with Elastic Light Scattering (LIDELS)," SAE Paper 2002-01-1685, May, 2002.

# D. Particulate Matter Sensor for Diesel Engine Soot Control

*David Sandquist (Primary Contact)*
*Honeywell Inc.*
*MN14-3B35*
*12001 State Highway 55*
*Plymouth, MN 55441*

*DOE Technology Development Manager: Kenneth Howden*

*Main Subcontractors: University of Minnesota, Minneapolis, MN and Honeywell Control Products, Freeport, IL*

This project addresses the following DOE R&D Plan barriers and tasks:

*Barriers*

B. PM Emissions

*Tasks*

2a. Advanced Sensors and Controls

## Objectives

- Develop diesel engine exhaust particulate matter (PM) sensor prototypes that have low cost, high speed, reliability, and are compatible with the harsh operational environment of diesel engines.
- Install the sensor prototypes in an appropriate engine and compare test results to results of other reference instrumentation output.
- Use test results to improve sensor concepts and to develop compatible sensor packages.
- Develop associated sensing electronics and signal processing hardware.
- Demonstrate prototype sensor to the DOE.

## Approach

The project has three main steps in order to accomplish the research:

- PM Sensor Development S We will design and build several prototypes of PM sensors utilizing high-temperature metal rings, disks, or screens, with commercially available glass or ceramic electrical feed-through. We will develop different readout electronic circuits to measure the ionization, charge, current, or capacitance, as well as other parameters such as temperature. Results from sensor testing of the various sensing concepts will be analyzed and compared to reference instrumentation.
- Sensor Testing S We will establish a diesel engine testbed that will include $O_2$, $NO_x$, and PM reference instrumentation, in addition to other instrumentation. A data acquisition system will be established that will be used to record the testing results for further data analysis. These tests will be conducted at the University of Minnesota's Center for Diesel Research and will utilize equipment from their Particle Measurement Laboratory. Gas concentration and particle size distribution information will be recorded to compare to sensor test results.

- Sensor Packaging S Staff members of Honeywell Labs and Sensing and Controls Division will develop suitable sensor packages for the PM sensors. Packaging materials should provide protection to the sensor as well as the ability to withstand the harsh operational environment. Sensor packages will be exposed to high temperatures and corrosive and potentially condensing environments. Destructive and nondestructive testing of the sensor package will be completed.

### Accomplishments

- The program has just been kicked off at the writing of this report. Initial sensor development has begun with quantifying the approaches using quality function deployment (QFD) methods.

### Future Directions

- As part of the Sensor Development task, we will conclude the QDF task and begin development of the sensors and electronics.
- After development of the sensors and electronics, we will begin testing the devices at the diesel engine testbed facility at the University of Minnesota.

---

## Introduction

Emission regulations worldwide emphasize reducing fine particulate matter emissions. Recent studies have shown that fine particles are more strongly linked with adverse health effects than are larger particles, and engines are an important source of fine particles.

Particles in the nuclei mode and in the accumulation appear to be formed by different mechanisms. Accumulation mode particles are primarily carbonaceous and are associated with rich combustion and poor subsequent oxidation during the engine cycle. Most nuclei mode particles are not even formed until the exhaust dilutes and cools. They consist of a complex, poorly understood mix of sulfuric acid and partially burned fuel and lubricating oil. Formation of these two types of particles likely occurs under different engine operating conditions with heavy loads favoring carbonaceous accumulation mode particles and light loads most likely favoring the formation of vapor phase precursors of nuclei mode particles. These precursors may not undergo gas to particle conversion until the exhaust cools and dilutes in the atmosphere.

In order to meet future emission standards, future diesel engines will have to be fitted with sophisticated combusion controls systems and, almost certainly, an aftertreatment system including particle filters or traps. An effective exhaust particulate sensor would not only lead to a reduction of particulate emissions from the engine itself, but would also make traps and other aftertreatment devices more feasible. Particulate traps are now commercially available and are likely to be applied in high volume in the future. They are large, expensive and impose a significant fuel economy penalty. The particulate sensor would help reduce the amount of particulate matter created. Thus the particulate trap could be either smaller or regenerated less often.

## Approach

Solid particles present in diesel engine exhaust carry a significant electrical charge (Kittelson et al., 1986a; 1986b, Moon, 1984). Several types of sensors based on measurement of particle charge will be investigated for possible further development.

The sensors to be investigated include an ionization sensor, an image charge sensor, and sensors based on AC conductance and capacitance of the exhaust.

An ionization sensor responds by collection of the net charge present on particles in the exhaust stream. This principle offers simplicity and fast response, but the required collection of electrically conducting carbonaceous particles on electrode surfaces leads to fouling.

An image charge sensor develops a mirror charge by surrounding the normal flow of charged exhaust particles within a cylindrical electrode (Collings et al., 1986; Kittelson and Collings, 1987). This method has fast response and has been demonstrated as a sensing technology for feedback engine control (Hong, et al. 1987: Hong and Collings, 1990).

The PM sensor concepts we propose use one or more electrodes installed in the diesel engine exhaust as detailed in Figure 1. The electrodes must remain electrically isolated. Additional electrodes might be used for direct particle charging. Alternatively, a second sensing electrode could also be utilized to form a guard ring.

Figure 1(a) utilizes an electrically isolated sensing electrode to monitor the ionization or charge transported by soot particles generated in the combustion process. An electrical circuit monitors the signal levels from the sense electrode. Figure 1(b) is an alternative approach utilizing another electrode, which can either be used as a guard ring or a control electrode as detailed in Figure 1(c).

Another approach to sensing these particles would rely on probing the exhaust with a variable frequency AC signal. One implementation would be a capacitive probe. Another implementation would be to set up a resonant circuit.

The signal processors for these approaches vary from a simple current monitor or voltage monitor to a more complex resonant circuit to measure the impedance or capacitance of the exhaust gas stream.

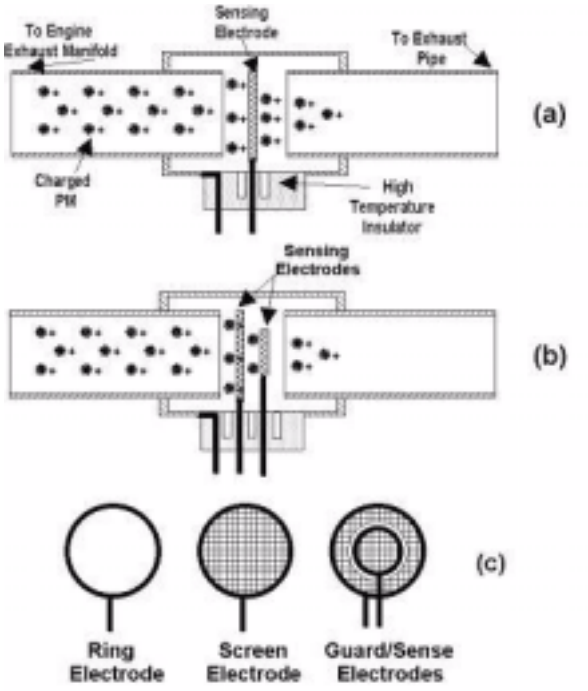


**Figure 1.** Different Particle Matter Sensor Concepts

## Conclusions/Future Directions

There are several approaches available to detect particulate matter in diesel engine exhaust. We are in the process of evaluating each of the approaches to select which approaches to develop based on feasibility, robustness, cost, and manufacturability.

# V. EGR FUNDAMENTALS

## A. Extending Exhaust Gas Recirculation Limits in CIDI Engines

*Robert M. Wagner (Primary Contact) and Johney B. Green, Jr.*
*Oak Ridge National Laboratory*
*2360 Cherahala Boulevard*
*Knoxville, TN 37932*

*DOE Technology Development Manager: Kathi Epping*

*CRADA Partner: Ford Motor Company, Dearborn, MI*
*Ford Investigators: John Hoard, Lee Feldkamp, and Tony Davis*

This project addresses the following DOE R&D barriers and tasks:

*Barriers:*

A. $NO_x$ Emissions

C. Cost

*Tasks:*

2. Sensors and Controls

4d. Advanced $NO_x$ Reducing Systems

### Objectives

- Reduce engine-out $NO_x$ emissions by 50% or more with a minimal penalty for particulate matter (PM) emissions.
- Lower the performance requirements for post-combustion emissions controls.

### Approach

- Characterize emissions and combustion in a modern light-duty common rail CIDI engine under extreme exhaust gas recirculation (EGR) conditions.
- Identify potential operating regimes for reduced $NO_x$ and minimal PM penalty.
- Evaluate correlations between existing engine sensors and pressure/emissions signals to develop virtual PM/$NO_x$ sensor concept to detect combustion quality.

### Accomplishments

- Performed extensive experiments under high EGR conditions on a Mercedes 1.7-L, turbocharged, common rail, four-cylinder CIDI engine.
- Performed detailed analysis of emissions and combustion data from recent experiments.
- Explored the potential for recovery of fuel penalty associated high EGR operation.
- Continued diagnostic tool development using data from recent experiments.

### Future Directions

- Continue analysis and interpretation of recent data.

- Continue exploring the potential for recovering fuel penalty.
- Conduct parametric study of HC emissions under high EGR conditions.
- Investigate higher loads in more detail.

## Introduction

This activity builds on previous collaborations between ORNL and Ford under a Cooperative Research And Development Agreement (CRADA ORNL 95-0337). The effort has progressed from examining combustion instabilities in spark-ignition engines to examining relationships between EGR, combustion, and emissions in CIDI engines. Information from CIDI engine experiments, data analysis, and modeling are being employed to identify and characterize new combustion regimes where it may be possible to simultaneously achieve significant reductions in $NO_x$ and PM emissions. These data are also being used to develop an on-line combustion diagnostic (virtual sensor) to make cycle-resolved combustion quality assessments for active feedback control. Extensive experiments on a Mercedes 1.7-L engine with full-pass control have led to the identification of two operating strategies which yield simultaneous reductions in $NO_x$ and PM emissions. Efforts for the remainder of the year will focus on continued data analysis and further development of the virtual sensor concept under the recently identified new combustion regime.

## Approach

Actual EGR utilization in production engines is typically less than optimal because of high HC and PM emissions under high EGR conditions. Until recently, it was believed that PM continues to increase with increasing EGR rate. ORNL has identified combustion regimes where simultaneous reductions in $NO_x$ and PM are achieved under high EGR conditions with air-fuel ratios lean of stoichiometric. Extensive experiments were performed in these regimes to improve the understanding of the combustion process and to explore strategies for reducing the fuel penalty associated with operation in these regimes. The information gathered during these on-going experiments is also being used in the development of diagnostic tools (virtual sensors) for characterizing combustion quality on a cycle-by-cycle basis to provide active, real-time feedback for predictive control. This type of control may be necessary for effective operation in these regimes.

## Results

Extensive experiments were performed on a Mercedes 1.7-L CIDI engine under extremely high EGR conditions. The engine at ORNL is equipped with full-pass control of electronic throttle, EGR valve, and fueling parameters. Regulated steady-state emissions and PM size and mass were measured in each individual exhaust runner as well as after the turbocharger. In-cylinder pressure data were also recorded for each cylinder on a crank-angle resolved basis. Two approaches were explored for reducing engine-out $NO_x$ with minimal PM penalty at high EGR levels. Approach one (A1) involves sweeping EGR rate until the EGR valve is fully open and then using an intake throttle to further increase EGR rate. Approach two (A2) involves sweeping EGR rate until the EGR valve is fully open and then retarding injection timing (main and pilot) while maintaining the EGR valve in the fully open position.

Approach one emissions results are shown in Figure 1 for an engine set point of 1500 rpm and 2.6 bar brake mean effective pressure (BMEP). Figure 1 shows a steady decrease in $NO_x$ with increasing EGR rate and a significant increase in HC and brake specific fuel consumption (BSFC) at the higher EGR conditions. The trend in PM is more complicated and increases until an EGR rate of approximately 44% and then decreases sharply. The increase in BSFC and HC correspond to this sharp decrease in PM. In other words, there is a fuel penalty associated with the reduction in PM emissions. Although not shown, the air-fuel ratio was lean for all EGR levels and reached a minimum of 22 for the highest EGR rate shown. The PM-$NO_x$ trade-off curve shown in Figure 2 is considerably different than the "classic" curve where PM continues to increase with decreasing $NO_x$. The decrease in PM mass is accompanied by a decrease in PM size and concentration as shown in Figure 3. PM mass and

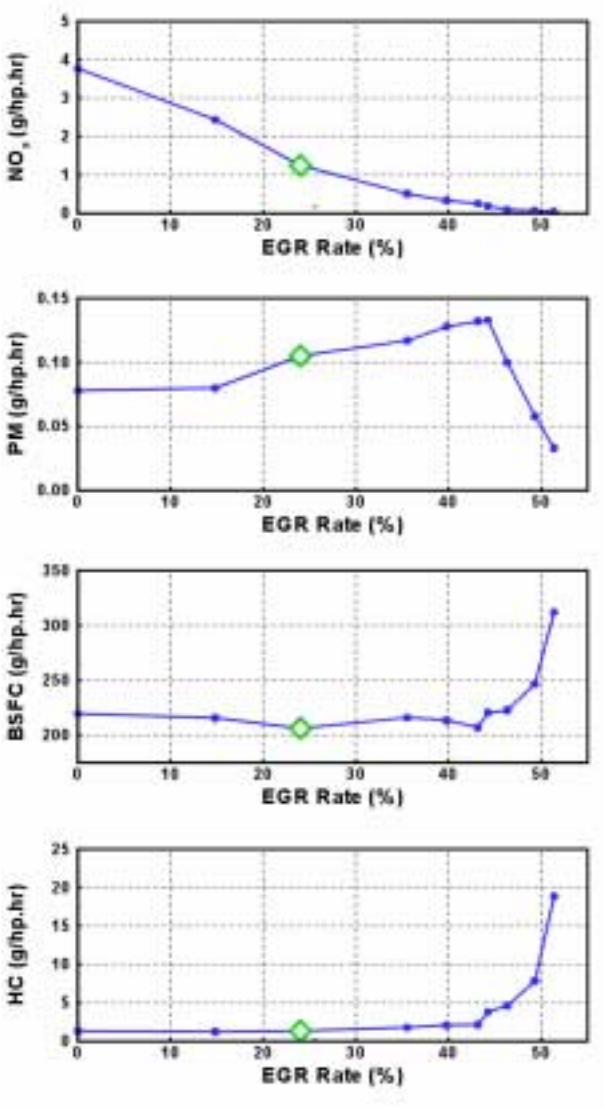


**Figure 1.** Simultaneous low $NO_x$ and low PM were observed at higher EGR rates using intake throttling (A1). Intake throttling starts at an EGR rate of 44% (1500 rpm, 2.6 bar BMEP). The diamond symbol corresponds to the production condition.

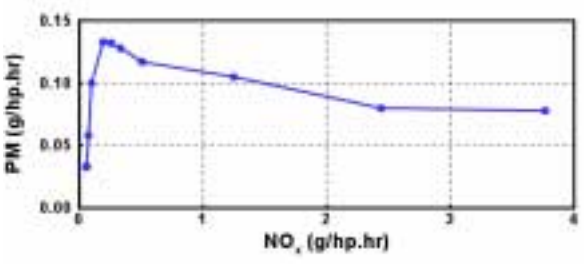


**Figure 2.** Not so "classic" PM and $NO_x$ tradeoff was observed using approach A1 (1500 rpm, 2.6 bar BMEP).

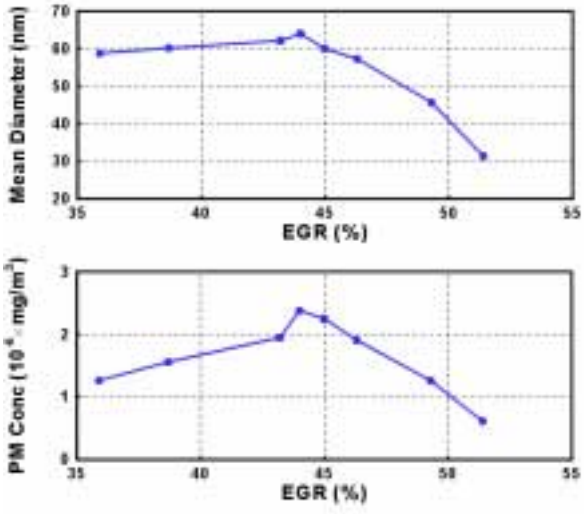


**Figure 3.** Particulate size and concentration decreased at very high EGR levels (1500 rpm, 2.6 bar BMEP).

size information for individual cylinders are shown in Figure 4 for four EGR rates. Cylinder four shows significantly more PM mass than the other three cylinders for lower EGR conditions. This imbalance appears to recede with increasing EGR rate.

Example heat release rate profiles are shown in Figure 5 for A1 and the same engine conditions represented in Figures 1 through 4. Significant differences in the profiles are not visible until the EGR rate exceeds 45%. At this point, the maximum heat release rate decreases and is accompanied by an increase in the combustion duration. This shift occurs over the period of decreasing PM and is accompanied by a decrease in Indicated Mean Effective Pressure (IMEP) and an increase in the Coefficient of Variation (COV) in IMEP as shown in Figure 6.

Emissions trends for A2 are shown in Figure 7 and were very similar to those seen for A1. Recall A2 involved retarding injection timing with the EGR valve in the fully open position. Although not

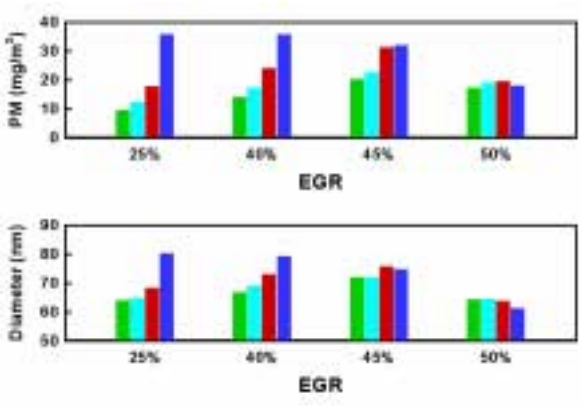


**Figure 4.** Cylinder-to-cylinder variations in PM emissions decreased at higher EGR levels (1500 rpm, 2.6 bar BMEP).

| | EGR (%) | SOI ($^{o}$ATDC) | BSFC (g/hp.hr) | $NO_x$ (g/hp.hr) | PM (g/hp.hr) | HC (g/hp.hr) | Exh Temp ($^{o}$C) | Recovery Approach |
|---|---|---|---|---|---|---|---|---|
| Production | 14 | -5 | 257 | 2.20 | 0.13 | 3.19 | 202 | NA |
| A1 | 47 | -7 | 253 | 0.24 | 0.07 | 6.28 | 224 | Adv Timing |
| A2 | 43 | 0 | 269 | 0.25 | 0.04 | 8.92 | 251 | Increased Rail Press |

**Table 1.** BSFC Penalty Recovery in Low $NO_x$ and Low PM Combustion Regime

shown, the heat release rate profiles were similar to those seen for A1. The most significant difference corresponded to the pilot, which became more pronounced (stronger) with the A2 strategy whereas it became less pronounced (weaker) with the A1 strategy.

There is a significant penalty in BSFC at the most extreme conditions for both approaches. Preliminary sets of experiments were performed to determine whether some of this penalty could be recovered while still maintaining low $NO_x$ and reasonable PM emissions. Preliminary recovery results at 2000 rpm and 2.0 bar BMEP are summarized in Table 1. Using A1, the 47% EGR condition was chosen as a starting point and various injection parameters were manipulated in an attempt to recover BSFC. The BSFC penalty for A1 was recovered by advancing injection timing while maintaining an order of magnitude decrease in $NO_x$ and a factor of two decrease in PM. HC emissions and exhaust temperature were still higher than the production conditions, which may actually be

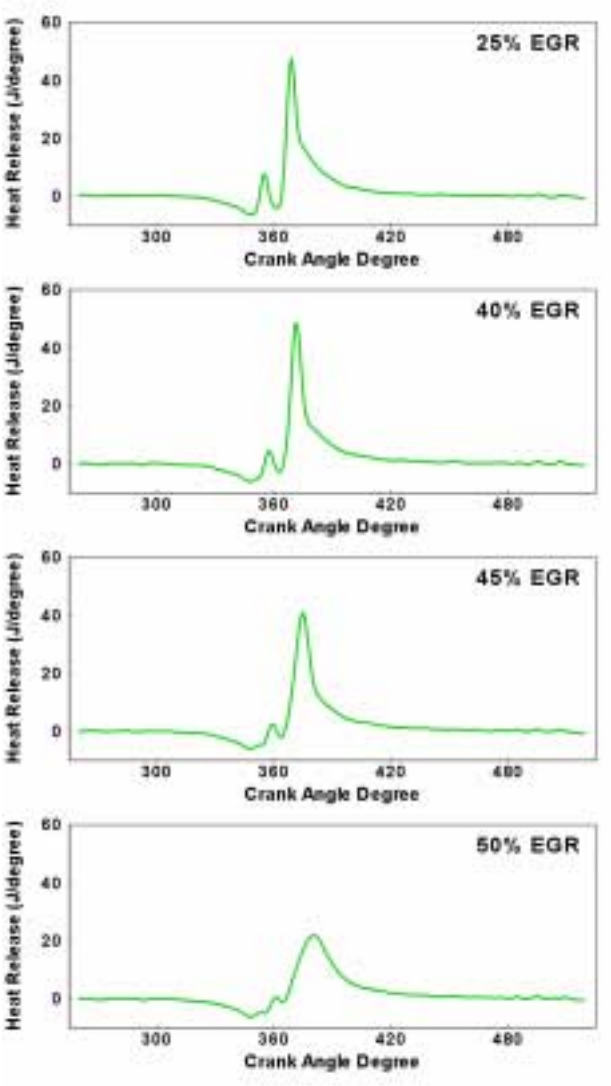


**Figure 5.** A significant shift in heat release was observed at higher EGR levels (1500 rpm, 2.6 bar BMEP).

beneficial to the regeneration of aftertreatment devices. Using A2, the $0^{o}$ injection timing condition was chosen as a starting point. The BSFC penalty for A2 was decreased to 6% by increasing rail pressure while maintaining an order of magnitude decrease in $NO_x$ and a factor of three decrease in PM. As was seen for A1, HC emissions and exhaust temperature were still higher than the production conditions. COV in IMEP for the recovered A1 and A2 conditions was similar to that seen for the production condition. Similar results were also seen for the 1500 rpm and 2.6 bar BMEP point but with a slight

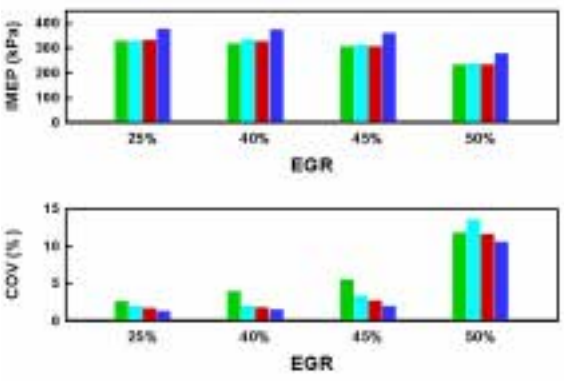


**Figure 6.** Cylinder-to-cylinder variations in combustion parameters were significant for all EGR levels (1500 rpm, 2.6 bar BMEP).

increase in the COV in IMEP for A1 and A2 as compared to the production conditions.

## Conclusions

The experiments and corresponding analysis performed on a Mercedes 1.7-L CIDI engine revealed new combustion regimes exhibiting the desirable properties of simultaneous low $NO_x$ and PM. While there is a penalty operating in these regimes, preliminary experiments indicate that manipulating injection parameters can minimize this penalty. Both strategies used in this investigation showed promise. Further data reduction and analysis is necessary to determine if one approach has a distinct advantage over the other.

Further analysis of the extensive data collected during this investigation is expected to improve our understanding of these new combustion regimes and perhaps reveal information that will help us exploit these conditions further for improved emissions. Continued development of the virtual sensor concept is also on-going with the new data, and recent results have showed promise. The combination of operating in this new combustion regime in conjunction with more advanced control is expected to lower the performance requirements of combustion emissions controls.

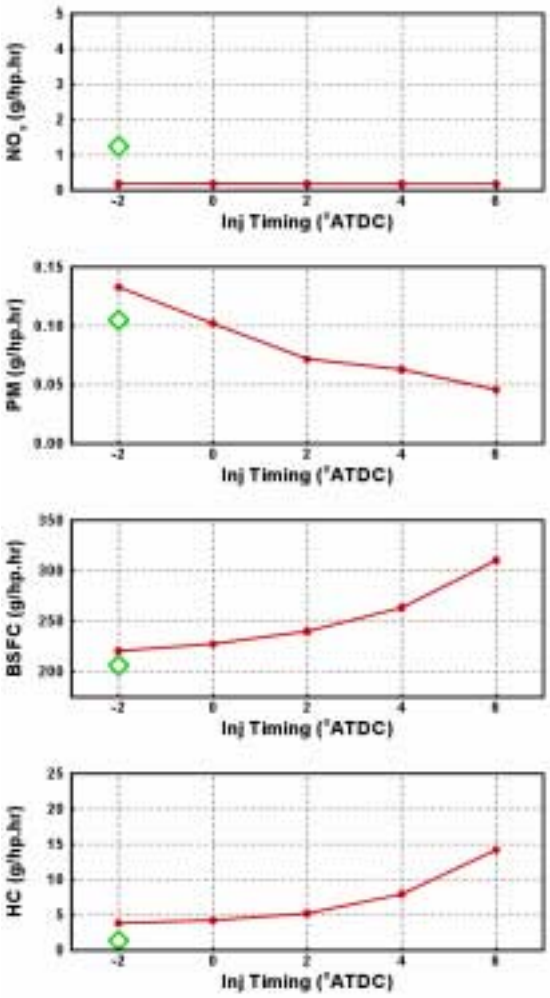


**Figure 7.** Lower engine-out $NO_x$ and PM were also observed using retarded injection timing (A2). EGR rate is fixed at 44% (1500 rpm, 2.6 bar BMEP).

## FY 2002 Publications/Presentations

1. J. B. Green Jr., R. M. Wagner, and C. S. Daw, "Model Based Control of Cyclic Dispersion in Lean Spark Ignition Combustion", Technical Meeting of the Central States Section of the Combustion Institute (Knoxville, TN USA; March 2002).

2. R. M. Wagner, C. S. Daw, and J. B. Green Jr., "Low-Order Map Approximations of Lean Cyclic Dispersion in Premixed Spark Ignition Combustion", SAE Paper No. 2001-01-3559.

3. R. M. Wagner, "Low-Order Map Approximations of Cyclic Combustion Variations in Lean Fueled Spark Ignition Engines", invited seminar at the University of Missouri-Rolla (Rolla, MO USA; November 2001).

## Invention Disclosure

1. J. B. Green Jr., R. M. Wagner, and C. Stuart Daw, "A Combustion Diagnostic for Active Engine Feedback Control". UT-Battelle is pursuing a patent on this invention disclosure.

# B. Resolving EGR Distribution and Mixing

*Bill Partridge (Primary Contact) and Sam Lewis*
*Oak Ridge National Laboratory*
*Engineering Science and Technology Division*
*2360 Cherahala Boulevard*
*Knoxville, TN 37932*

*DOE Technology Development Manager: Gurpreet Singh*

*Main Subcontractor: Cummins, Inc., Columbus, IN*

This project addresses the following DOE R&D Plan barriers and tasks:

*Barriers*

A. $NO_x$ Emissions

*Tasks*

4e. R&D on $NO_x$ Reducing Technologies

## Objectives

- Assess the performance of two exhaust gas recirculation (EGR) hardware designs in terms of (1) EGR-air mixture uniformity and (2) port-to-port charge uniformity at select engine conditions.

## Approach

- Assess the two designs at four steady-state engine conditions indicative of a modalized Federal Test Procedure (FTP). Use Spatially Resolved Capillary Inlet Mass Spectrometry to quantify $CO_2$ distributions. Infer EGR distributions from $CO_2$ distributions.

## Accomplishments

- Identified hardware design that produces better EGR/air-mixture and charge uniformity.
- Established a map of the two designs in terms of flow characteristic and limitations. This serves as a database for identifying non-uniformity barriers and origins, and for developing computational fluid dynamics (CFD) models for follow-on design improvements.

## Future Direction

- Compare model and experimental results to improve hardware design and modeling tool.
- Implement similar approach to investigate EGR performance on the Cummins B-series engine.

---

## Introduction

Exhaust gas recirculation (EGR) is a methodology for reducing $NO_x$ emissions based on the engine system rather than aftertreatment. To implement EGR, exhaust gas is added as a diluent to the intake air charge to reduce the peak flame temperature, thereby reducing the $NO_x$ emissions. Based on the temperature dependence of the dominant $NO_x$ mechanism, EGR can have a dramatic effect on $NO_x$ emissions.

Efficient EGR implementation requires the EGR/air charge to be both well mixed and uniform from cylinder-to-cylinder. Degraded mixture uniformity can result in high particulate matter emissions. Non-

uniform cylinder-to-cylinder (or intake port-to-port, P-T-P) charge distribution reduces the potential EGR dynamic range.

Cummins is developing a new V-8 engine with cooled EGR for the light truck automotive market. The EGR system design incorporates an EGR/air mixing section immediately upstream of the intake manifold. Two mixing-section designs were evaluated at select engine conditions in terms of EGR/air charge uniformity at the intake manifold input flange and P-T-P uniformity.

Specific Objectives

- Characterize the EGR/air mixture uniformity at the intake manifold intake flange at select engine conditions.
- Characterize the EGR-charge P-T-P uniformity at select engine conditions.
- Determine if intake port 2 is EGR starved relative to the other intake ports.

Experimental Apparatus and Method

The evaluated engine system was a V-8 engine being developed for the light truck automotive market, with cooled EGR. Figure 1 shows an EGR/air mixing hardware design immediately upstream of the intake manifold, and the intake manifold ports (or runners) associated with cylinders 2 (closest to the input flange) and 4. SwageLok fittings for the measurement probes are apparent in Figure 1 at the intake manifold inlet flange and the individual ports. Notice that the EGR/air charge flow path to port 2 requires a dramatic, >90 turn. There was of specific interest in determining if this geometry caused port 2 to be EGR starved.

The EGR uniformity was assessed at the four steady-state engine conditions (EC) listed as EC1-4 in Table 1, which were selected as representative of a modalized federal test procedure (FTP). EC1-2 are low and high load at low speed, respectively and EC3-4 are low and high load at high speed, respectively. A fifth engine condition was used for the P-T-P evaluation and corresponds to EC4 but with the intake throttle fully open to achieve maximum mass air flow (MAF). The Table 1 notes indicate MAF increases from the previous EC, revealing a monotonically increasing MAF with

**Figure 1.** EGR/air mixing section and intake manifold. Fittings for measurement probes are apparent.

increasing EC number. The MAF increase is consistently 20-32%, except for the EC3-4 transition where it is a dramatically different at 63%; effects on the EGR-air mixing associated with this difference might be expected. EC5 is not part of the modalized FTP but was included to assess if increasing MAF would enhance mixing and EGR- mixing and EGR-charge uniformity.

| Engine Condition | Speed (RPM) | Load | Mass Air Flow (lbs/hr) | Note |
|---|---|---|---|---|
| 1 | 1400 | 77 | 262 | |
| 2 | 1400 | 153 | 345 | +32% MAF |
| 3 | 1800 | 119 | 412 | +19% MAF |
| 4 | 1800 | 238 | 671 | +63% MAF |
| 5 | 1800 | 238 | 825 | +23% MAF |

**Table 1.** Engine conditions used for evaluation of the EGR system. EC1-4 are the major constituents of a set of steady-state engine conditions representative of a modalized FTP.

The local instantaneous EGR load was quantified by corresponding $CO_2$ concentrations. The local $CO_2$ concentration was measured with a spatially resolving capillary-inlet mass spectrometer,

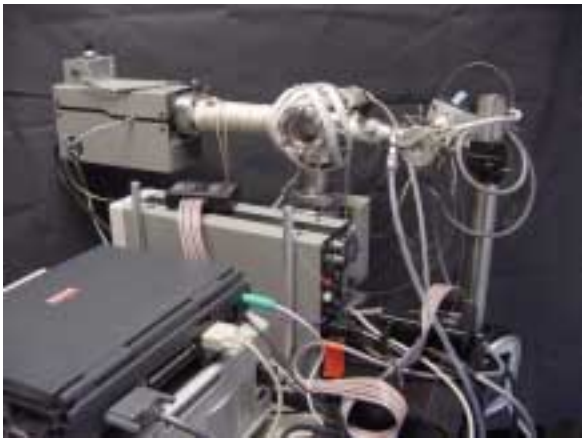

**Figure 2.** SpaciMS Mounted on a Portable 12-in x 24-in Breadboard

SpaciMS, which is shown in Figure 2 and is described in Reference 2. Fused silica capillaries are used to extract and transport small quantities of undiluted sample from the probed location to the instrument. Various capillary sampling locations are selected via a multi-port valve which is connected to the mass spectrometer inlet. The SpaciMS head uses electron ionization, quadrupole mass filtering, and user-selectable Faraday cup or continuous-dynode electron-multiplier detection. The detector output is monitored via a multi-channel data acquisition (DAQ) system to allow synchronization of $CO_2$ dynamics with other experimental parameters, such as triggers (e.g., engine top-dead-center), instrument pressure, etc. The instrument is easily transportable to user facilities. The instrument was calibrated based on a standard addition procedure.

The probe end of a sampling capillary is shown in Figure 3. The inner diameter (ID) of the sampling and transporting capillary is 50-µm ID, the outer diameter (OD) is approximately 180-µm, and it extracts 10-µL/min of undiluted sample. A 1/16-in OD stainless steel capillary is used to house and provide mechanical support to the fused silica capillary. To mitigate flow disturbances, the fused silica capillary is extended about 15 mm beyond the support capillary end. A SwageLok probe mount is easily installed in the intake manifold, and non-swaging ferrules are used to allow probe translation. Despite its use of a physical probe, the SpaciMS is a minimally invasive diagnostic because of the small capillary size and sampling rate, and the probe access


**Figure 3.** Minimally Invasive Capillary Sampling Probe

method; specifically, the probe requires little modification of test hardware compared to some optical techniques (e.g., planar laser-induced fluorescence). The minimally invasive aspects of the capillary probe also prevent capillary clogging in environments with high water and particulate matter concentrations, and hence allow for direct sampling of undiluted diesel exhaust and EGR.

Carbon dioxide transients, associated with a temporally varying EGR load, remain temporally aligned like boxcars of a train as they travel through the sampling capillary. By tuning the capillary length and diameter, excellent instrument response of about 100-ms T90 (time between the 10% and 90% full-step response) can be achieved. For the EGR work reported here, capillaries of 50-µu ID and 9.8-ft length were used, resulting in T90 response time of 950 ms. With cycle periods of 86- and 66-ms for the low- and high-speed ECs, respectively, this setup did not resolve intra-cycle EGR dynamics. Rather, the results presented here represent the ensemble-averaged EGR performance.

The data acquisition system monitored six channels at 400 Hz for 1 minute. In addition to the SpaciMS, the DAQ system monitored an engine cycle trigger, exhaust $CO_2$ and EGR levels based on conventional non-dispersive infrared (NDIR) $CO_2$ analyzers, and the temperature and internal vacuum of the SpaciMS. A high DAQ rate was dictated to capture the cycle trigger. In keeping with assessments ensemble-averaged EGR performance, the local EGR results were averaged over 700 and 900 cycles for the low- and high-speed results, respectively.

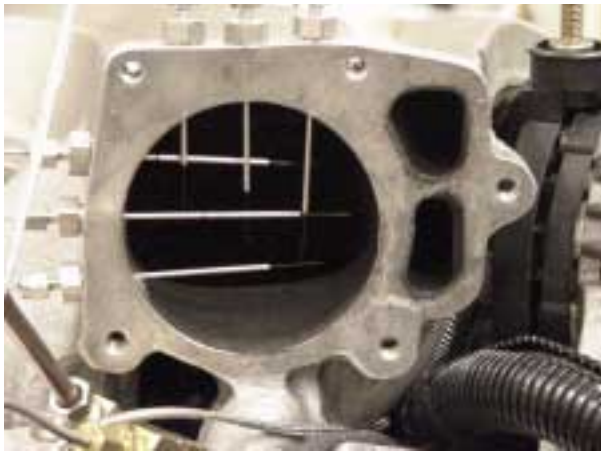

**Figure 4.** Location of Six Sampling Capillaries in the Plane of the Intake Manifold Inlet Flange

Figure 4 shows the six capillary probes used for resolving the EGR distribution in the plane of the intake manifold inlet flange. Only one probe was positioned in the flow at a time during measurements to mitigate flow disturbance. The probes are spaced at 0.75-intervals with the center horizontal and vertical probes approximately bisecting the flow passage. The inlet-flange EGR distribution was characterized with twenty discrete SpaciMS measurements, located as indicated in the results maps. Each capillary probe sampled four locations, except the outer vertically translating probes which sampled only two locations each. The order of the sampling locations corresponded to increasing probe penetration of the flow for each individual probe, and cycling through the probes clockwise in Figure 4 starting at the lowest horizontal probe. Because of the crossed pattern of the probes and the time between sampling locations, the measured field distribution is validated by consistency of the various capillary probes; i.e., the various horizontal and vertical capillaries check each other.

## Results

Intake Flange Uniformity

Figure 5 shows the EGR loading distribution in the intake flange flow passage, normalized to the maximum value in the field, for the eight hardware-EC combinations investigated. The normalization was based on the discrete data, and the images were formed via interpolation. At the top of each

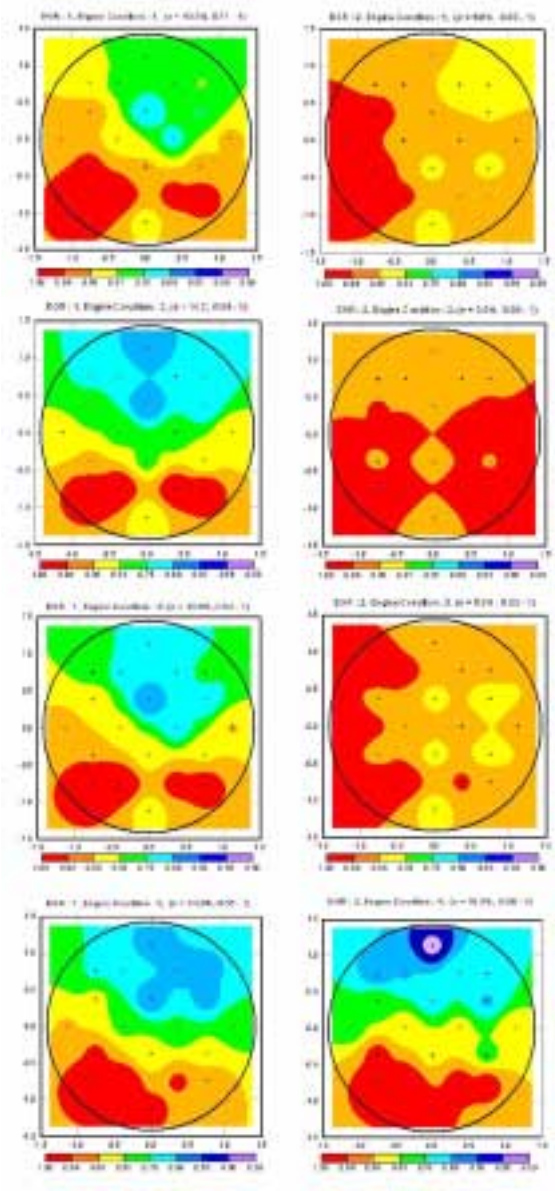

**Figure 5.** Normalized EGR distribution for EGR1 and EGR2 hardware designs at EC1-4. The flow-passage diameter and location of twenty SpaciMS measurements ( • ) are indicated. Hardware EGR1 and EGR2 results are in the left and right columns, respectively, with EC1-4 proceeding from

distribution the specific hardware and EC are specified; the standard deviation and range of the twenty normalized measurements are specified parenthetically.

In Figure 5, perfect EGR charge uniformity would be indicated by a single color. For EC1-3 the

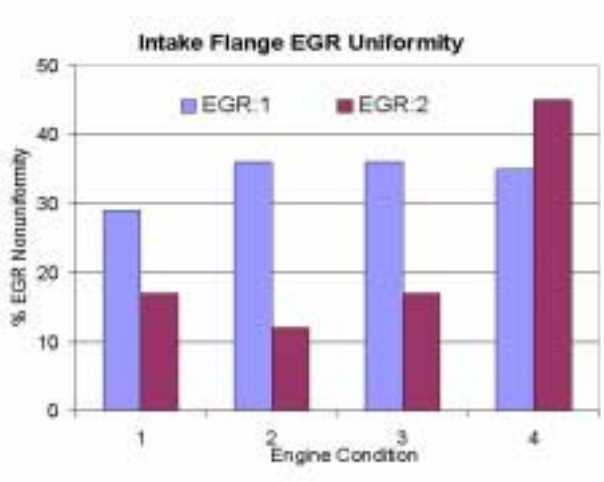


**Figure 6.** Percent EGR Non-Uniformity at the Intake Flange Flow Passage for the Eight Hardware-EC Combinations

EGR2 hardware consistently produces a more uniform EGR charge. For instance, the most uniform EGR field was produced by EGR2 at EC2 and had only 12% variation (a range of 0.88 to 1); at this same EC, EGR1 produced 36%, or 3X more, nonuniformity. The excellent performance of EGR2 collapses at EC4, where the EGR charge is strongly biased to the bottom of the flow passage and the distribution nonuniformity rises dramatically to 45%. This performance degradation of EGR2 is coincident with the dramatic MAF increase associated with the EC3-4 transition; possibly, this design has reached some critical MAF for charge separation. Hardware EGR1 consistently produces a charge distribution biased to the bottom of the flow passage.

There are limitations and anomalies in the EGR distribution images associated with the discrete nature of the measurements and the interpolation method. For instance, it is unclear if EGR1 actually produces two EGR lobes at EC1-3 as indicated rather method. For instance, it is unclear if EGR1 actually produces two EGR lobes at EC1-3 as indicated rather than a single high EGR band. The interpolation produces likely anomalous distribution curvature, for instance with EGR2 at EC4 around 75%, 85% and 50% normalized EGR loading. Nevertheless, the images clearly identify the general biasing of the EGR for the various combinations, and they strike an appropriate balance between measurement mesh density and hardware-EC combinations investigated.

Figure 6 is a reduction of the data in Figure 5, it shows the range of normalized EGR distribution for the various hardware-EC combinations. For EC1-3, the average non-uniformities are approximately 54% less for EGR2 compared to EGR1; the average uniformity is 47% better with EGR2 over EC1-4. EGR2 experiences a 3X increase in the non-uniformities at EC4 compared to EC1-3. This is synchronous with the MAF increase noted earlier, and a similar trend is observed with the P-T-P measurements. Overall, EGR2 produces better performance despite its degraded performance at EC4.

Port-to-Port Uniformity

Figure 7 shows the deviation in the P-T-P EGR charge from the average value for the two hardware designs at EC1-5. Perfect P-T-P EGR charge uniformity would have zero deviation across the eight ports. Positive and negative deviations indicate rich and lean EGR charge, respectively, relative to the average value for that hardware-EC combination. For example, with EGR1 at EC1, ports 1 and 3-5 are somewhat EGR rich, port 2 receives an average EGR charge, and ports 6-8 are somewhat EGR lean.

The most apparent feature of Figure 7 is the behavior at EC5, which is the same speed and load as EC4 but with maximum MAF. It was thought that increasing the MAF might enhance mixing and P-T-P uniformity. However, just the opposite occurred; increasing MAF destroyed the P-T-P uniformity. The deviations for both hardware designs at EC5 hit the rails of Figure 7 for multiple ports, and are up to 18%. The residence time may be too short to allow adequate mixing. This speculation is similar to the critical MAF discussed earlier.

Figure 7 demonstrates that port 2 is not uniquely EGR starved for either design. Rather, port 2 is on average somewhat EGR rich. For EGR2 at EC1-3, where its performance is as desired, port 2 has close to zero deviation on average.

Figure 7 affords several comparisons between the performance of the two hardware designs. It is apparent that the deviations are significantly less for EGR2; there are many cases, e.g., EC2-4 for port 1, where the EGR1 deviations are more than 100% greater than the corresponding deviations with

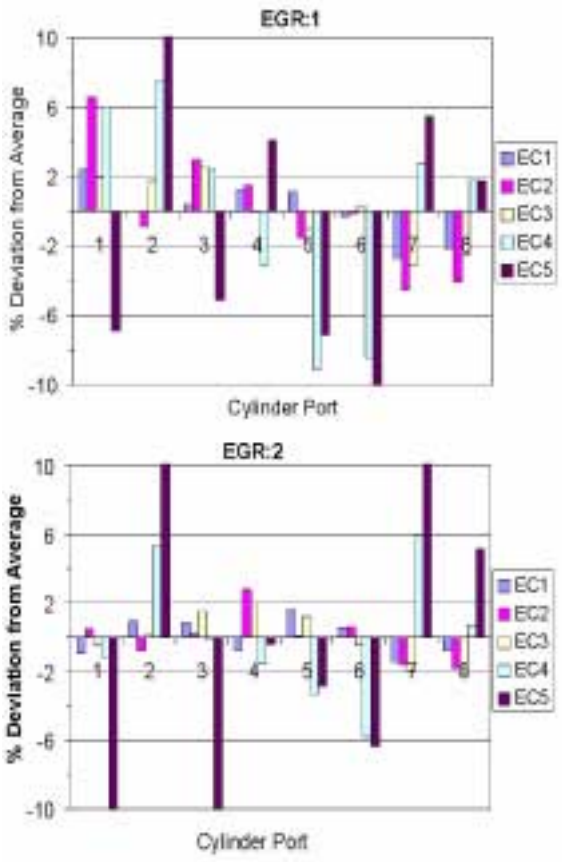


**Figure 7.** Percent Deviation in the P-T-P EGR Distributions for Hardware EGR1 and EGR2 at EC1-5

EGR2. EGR1 produces significant biasing of the EGR charge to the front cylinders (ports 1-4), as evident from the sinusoidal average distribution of the deviations. This data will be valuable to modeling efforts to investigate the origins of separation and non-uniformities. Specifically, the relationship between the distinct biasing of the EGR charge to the bottom of the intake flange and front cylinders with EGR1 will benefit the modaling efforts. There is less clear front-to-back biasing with EGR2, even at EC4 where the distribution was strongly biased to the bottom of the inlet flange flow passage.

Figure 8 is a reduction of Figure 7, and displays the maximum spread of deviation for the eight hardware-EC combinations. For instance, the maximum and minimum deviation for EGR2 at EC4 is +6% and -6%, respectively, as defined by ports 7

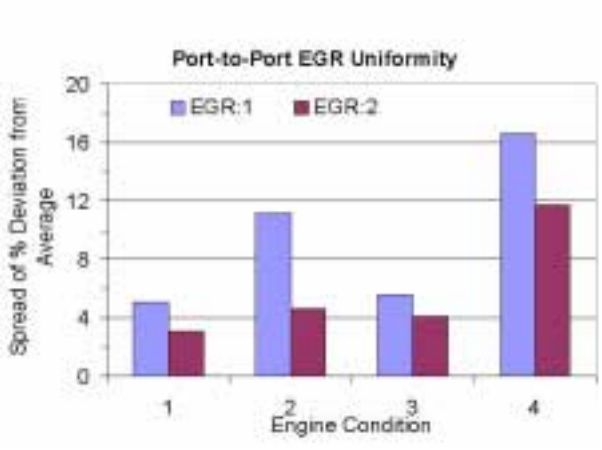


**Figure 8.** Maximum Spread in the Percent Deviation of the P-T-P EGR Distributions

and 6; this produces a spread of deviation of 12% for this same case as indicated in Figure 8. The scale of the P-T-P deviations in Figure 8 is 2-5X less than that of the corresponding non-uniformities at the intake flange. This indicates some mitigation in the intake flange non-uniformities (Figure 6).

Figure 8 also indicates several consistencies between the intake flange and P-T-P results. It demonstrates that EGR2 consistently produces better P-T-P performance for EC1-4, even though it produced the lesser intake flange uniformity at EC4. The average P-T-P uniformity for EC1-4 is 42% better with EGR2. This shows some consistency with the 47% improvement with EGR2 at the intake flange. EGR2 experiences the same 3X degradation in EGR uniformity in Figure 8 as was observed in Figure 6. Again, this is data useful in modeling studies for identifying the fundamental origin of this degraded performance.

## Conclusions

Two EGR-system hardware designs for the Cummins medium-duty V-8 diesel engine were assessed in terms of EGR charge uniformity. A minimally invasive SpaciMS instrument was used to quantify EGR charge uniformity at the intake manifold inlet flange and ports. The results identified the better hardware design, as well as the limitations and flow characteristics of both designs.

The minimally invasive nature of the SpaciMS proved critical to characterizing the EGR distributions in the inlet flange flow passage of the intake manifold. The probe access methodology required little modification of the base hardware designs, and hence provided a more realistic assessment of actual hardware performance. The P-T-P work did not directly utilize the minimally invasive nature of the SpaciMS, although it was used indirectly to assess the effects of more invasive extractive and optical-based diagnostics.

The EGR2 hardware design provides significantly better average performance. Specifically, the average intake flange and P-T-P EGR-charge uniformity are 40-50% better with the EGR2 design compared to EGR1. Despite the superior performance of EGR2, there is room for improvement at the high-speed, high-load EC, EC4, where a 300% degradation in both the intake flange and P-T-P EGR uniformity is observed relative to EC1-3.

Systematic biasing of the P-T-P EGR charge distributions was investigated. Port 2, which requires a more dramatic flow path, is not uniquely EGR starved for either design over the range of ECs investigated.

In addition to identifying the better design, characterization of EGR-air mixing behavior is valuable to understanding non-uniformity barriers and origins. Specifically, even the behavior of the lesser-performing EGR1 design is valuable for elucidating the causes of this performance. Such efforts will incorporate models of the mixing process. The current effort has identified several characteristics useful for such an effort. The EGR1 design biases the EGR charge to the bottom of the intake flange and to the front cylinders. The EGR2 design shows little P-T-P biasing, but there is some biasing to the left side of the intake flange at low loads and the right side at high loads. Increasing the MAF at EC3-4 severely compromises the intake flange and P-T-P EGR uniformity for the EGR2 design. Further increasing the MAF, EC4-5, destroys the P-T-P uniformity for both designs. Nevertheless, there is significant mitigation of non-uniformities between the intake flange and the individual ports.

## References

1. Stang, J.H., Koeberlein, D.E., Ruth, M.J. (2001). "Cummins Light Truck Diesel Engine Progress Report," SAE Paper No. 2001-01-2065.

2. Partridge, W.P., Storey, J.M.E., Lewis, S.A, Smithwick, R.W., DeVault, G.L., Cunningham, M.J., Currier, N.W., Yonushonis, T.M. (2000). "Time-Resolved Measurements of Emission Transients By Mass Spectrometry," SAE Paper No. 2000-01-2952.

# VI. CIDI COMBUSTION AND MODEL DEVELOPMENT

## A. Using Swirl to Improve Combustion in CIDI Engines

*Paul Miles (Primary Contact)*
*Sandia National Laboratories*
*P.O. Box 969, MS 9053*
*Livermore, CA 94551-0969*

*DOE Technology Development Manager: Kathi Epping*

*Main Subcontractors: University of Wisconsin Engine Research Center (UW ERC), Madison, WI and Wayne State University (WSU), Detroit, MI*

This project addresses the following DOE R&D Plan barriers and tasks:

*Barriers*

B. PM Emissions

C. Cost

*Tasks*

1a. Advanced Fuel Systems

3a. Identification of Advanced Combustion Systems

### Objectives

- Provide the physical understanding of the in-cylinder combustion processes needed to meet future diesel engine emissions standards while retaining the inherent efficiency and low $CO_2$ emissions of the direct-injection diesel engine.
- Improve the multi-dimensional models employed in engine design and optimization, and validate the model predictions against in-cylinder measurements and tailpipe emissions.

### Approach

- Measurements of flow and thermophysical properties are obtained in an optically-accessible engine using laser-based measurement techniques.
- Engine performance, fuel economy, and emissions are measured in a traditional, non-optical test engine with the identical geometry.
- Optical and traditional test engine measurements are compared against model predictions, and the model is refined accordingly.

### Accomplishments

- Elucidated previously unknown mechanism by which the interaction of the fuel jets with the swirling flow creates an unstable flow, resulting in large increases in late-cycle turbulence.
- Investigated the late-cycle turbulence generation process for variable levels of flow swirl and injection pressure.

- Acquired detailed characterization of turbulent velocity field, including Reynolds stress, mean flow gradients, turbulent kinetic energy, and length scale (dissipation). These were the first measurements of Reynolds stress in a fired diesel, the first determination of length scales in a fired diesel, and the first direct estimate of turbulence production.
- Determined the principal reasons for the failure of current engine turbulence models to predict the late-cycle turbulence, by comparison with detailed measurements.
- Measured engine-out emissions with varying levels of EGR, injection pressure, and swirl ratio. Established detailed database for assessment of model predictions.

### Future Directions

- Further investigate the interaction of the fuel jets and the mean in-cylinder flow to find conditions for optimal enhancement of turbulence and mixing. Extend measurements to late-injection, low-temperature combustion regimes where enhanced mixing may significantly extend the applicable load/speed range.
- Map engine-out emissions at various loads, swirl ratios, and injection pressures to establish, in conjunction with optical engine measurements and computations, the influence of enhanced late-cycle turbulence on engine-out emissions. Investigate emissions and performance for late-injection operating regimes to establish applicable speed/load range.

---

## Introduction

Direct-injection diesel engines have the highest fuel conversion efficiency of any reciprocating internal combustion engine technology, with concomitant low emissions of $CO_2$. This efficiency comes at the cost, however, of $NO_x$ and particulate matter (PM) emissions which are high in relation to proposed future emission standards. Introduction of flow swirl in direct-injection diesel combustion systems is an established technique for reducing engine-out PM emissions, and enabling reduced $NO_x$ emissions by permitting injection timing retardation and increasing the combustion system EGR tolerance. Swirl influences PM emissions through two paths: reduced formation of PM and more rapid destruction of the PM formed via enhanced flow turbulence and mixing. The ability of swirl to enhance turbulence and mixing is also very important for alternative, low-temperature diesel combustion regimes. These regimes, which are characterized by very low $NO_x$ and PM emissions, are limited in their range of application by the ability to introduce and mix the fuel in a short time period.

In spite of their clear potential for enhancing diesel combustion, the physics of swirl-supported combustion systems is still poorly understood. Furthermore, recent measurements have demonstrated that multi-dimensional models employed in engine design and optimization do not adequately capture the turbulence enhancement that can be achieved with flow swirl. This work focuses on providing the physical understanding and the sophisticated modeling tools required to achieve the lowest possible engine-out emissions from swirl-supported diesel combustion systems, through an integrated approach combining measurement and modeling of the combustion and emissions formation processes.

## Approach

A three-pronged approach is taken toward obtaining the required physical understanding and validated modeling capabilities: detailed measurements of the flow and combustion processes are made in an optically-accessible laboratory test engine; emissions, performance and fuel consumption measurements are made in a traditional single-cylinder test engine; and computer simulations are performed and compared to the data obtained in both the optical and traditional test engines. Natural synergies emerge among these three areas. For example, the comparison of the computed and the experimental results serves to establish the validity of the various sub-models in the codes, to verify the ability of the codes to accurately predict global

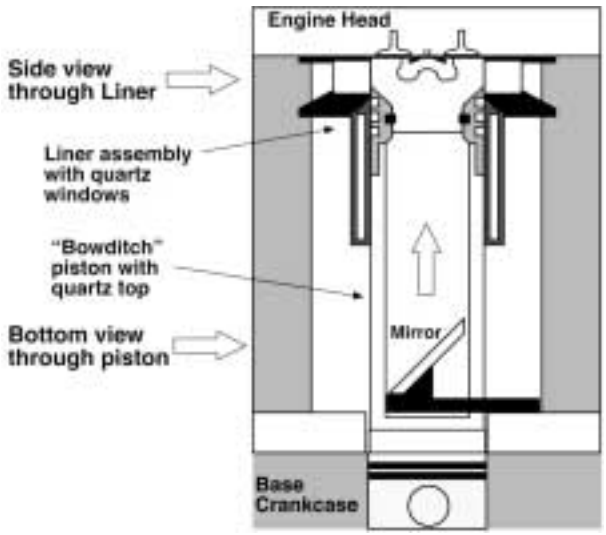


**Figure 1.** Schematic View of the Optical Engine Facility

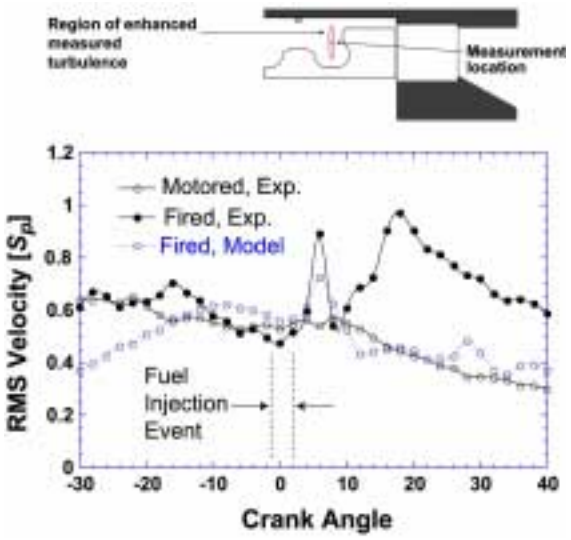


**Figure 2.** RMS radial velocity fluctuations measured at a simulated idle condition. The 'motored' data were acquired without fuel injection.

parameters such as emissions, and to assist in the interpretation of the experimental data. Similarly, traditional test engine measurements serve to identify interesting operating parameter trade-offs that bear further investigation either numerically or experimentally in the optical engine.

## Results

The optically-accessible diesel engine facility is depicted in Figure 1. This facility employs a slotted, extended piston assembly with a quartz combustion chamber that permits the progress of combustion to be visualized from below. In addition, the upper region of the cylinder liner is equipped with quartz windows that allow a lateral view of the combustion process to be obtained. This lateral view capability, in a configuration that maintains the faithful combustion chamber geometry, is a unique aspect of this facility. The engine bowl geometry, bore, stroke, and fuel injection equipment are typical of state-of-the-art direct-injection diesel engines for passenger car applications. Variable cylinder swirl levels can be achieved through throttling of one of the intake ports.

Research performed in FY2002 in the optical engine focused on clarifying the physics of the production of late-cycle turbulence. Figure 2 depicts the large increase in late-cycle RMS velocity fluctuations seen within the central bowl, as well as

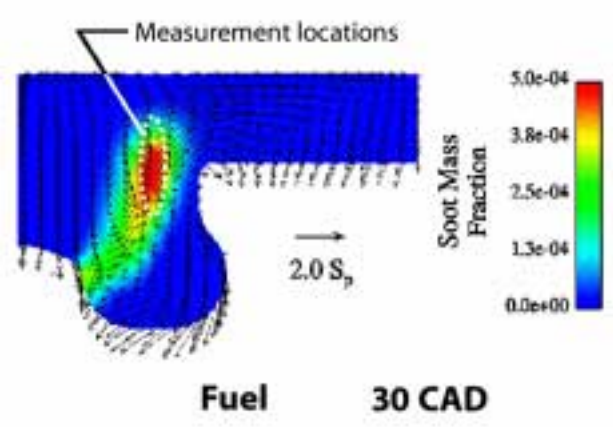


**Figure 3.** Illustration of the Location of PM (Soot) within the Cylinder at 30 CAD ATDC.

the inability of the model to adequately capture the measured fluctuations. The location at which these increased fluctuations are measured coincides well with the predicted locations of unburned fuel and PM-as shown in Figure 3. Cycle-resolved analysis of the velocity data has demonstrated that the increased fluctuations coincide with increased small-scale turbulence capable of influencing the in-cylinder mixing processes. Furthermore, data obtained with fuel injection into a $N_2$ environment (no combustion

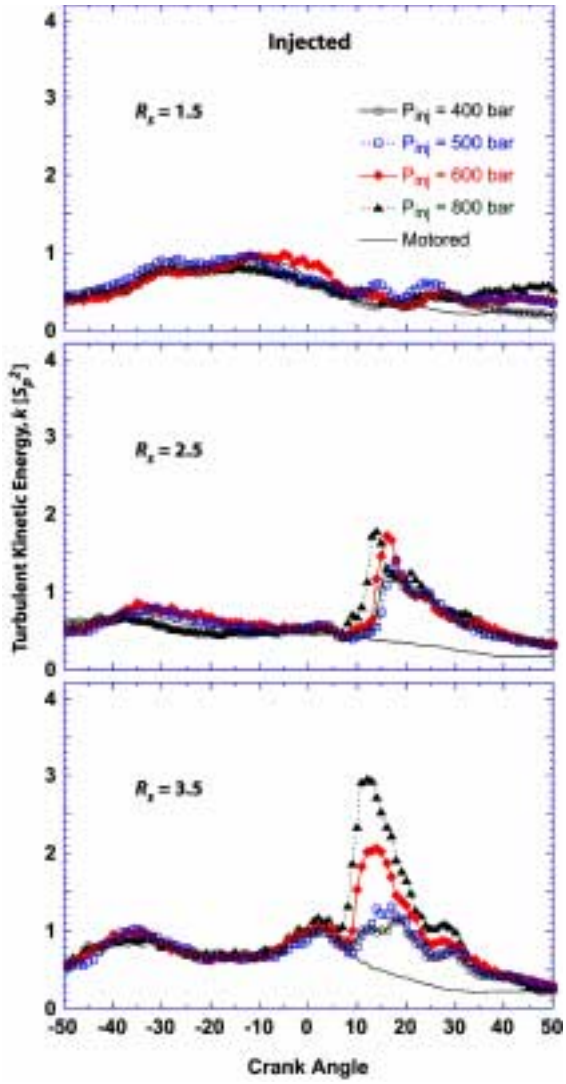


**Figure 4.** The variation of turbulent kinetic energy with swirl ratio and injection pressure. The measurement location is the same as that shown in Figure 2.

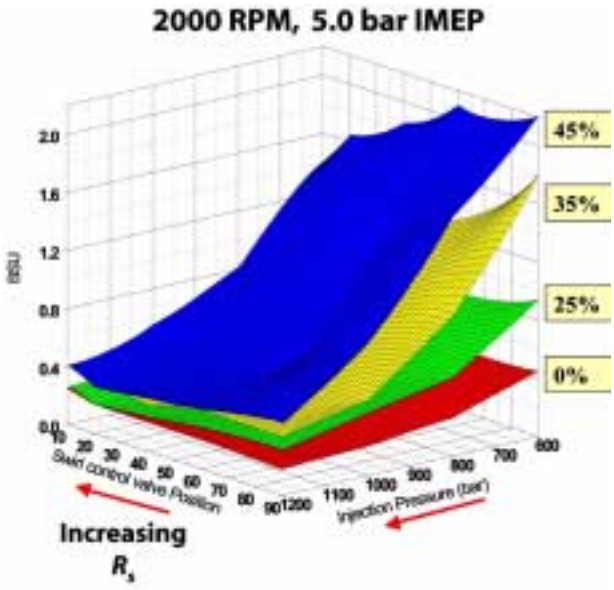


**Figure 5.** The Variation of In-Cylinder Particulate Matter, Expressed in Bosch Smoke Units (BSU), as Swirl, Injection Pressure and EGR Rate Are Varied

occurs) have established that the increased turbulence is predominantly related to the interaction between the fuel sprays and the swirling flow, not to the actual combustion and heat release process.

Figure 4 exhibits the extreme sensitivity of the late-cycle turbulence to flow swirl and to injection pressure. At the lowest swirl ratio it is seen that significant late-cycle turbulence cannot be generated regardless of injection pressure. At the higher swirl ratios, however, the turbulence generated is very strongly influenced by injection pressure. Closer examination of Figure 4 reveals that the swirl level and injection pressure must be balanced -- at low injection pressure, more turbulence can be generated by an intermediate than by a high swirl level. This behavior is consistent with turbulence generation due to formation of an unstable distribution of angular momentum in the cylinder, caused by entrainment and the enhanced r-z plane vortical structures generated by the fuel jet. At low swirl, there is insufficient angular momentum to form an unstable distribution regardless of injection pressure. At high swirl, more energetic injection events are required to counteract the stronger centrifugal forces acting on the fluid elements and displace them inwards. Inward displacement of high angular momentum fluid is required to form the unstable momentum distribution that releases the mean flow energy into turbulence. For this reason more moderate swirl ratios are preferred for less energetic injection events.

In a parallel research effort conducted in the traditional test engine, measurement of engine-out emissions and performance has resulted in a detailed database from which the model performance can be assessed. An example of these measurements is

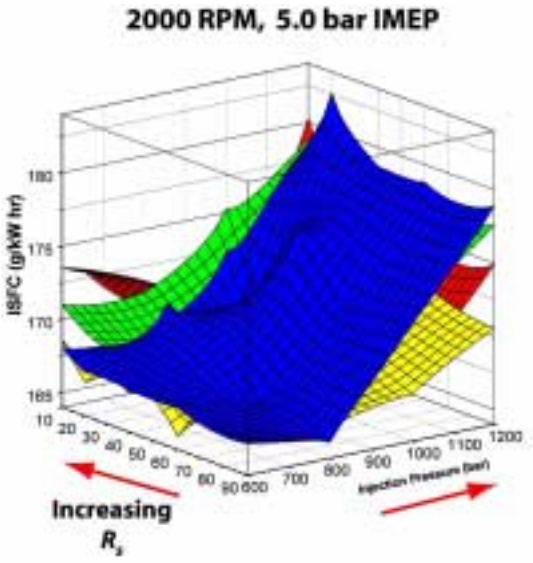


**Figure 6.** Fuel Consumption Measured for Various Levels of Swirl, Injection Pressure and EGR Rate

shown in Figure 5, which depicts the variation in engine-out PM as swirl, injection pressure and EGR rate is varied. The beneficial effect of both swirl and injection pressure on reducing PM at a fixed EGR rate are readily apparent. Although the benefits of increased injection pressure seem to exceed the benefits of increased swirl, there is a significant fuel economy penalty associated with the high injection pressures, as shown in Figure 6.

## Conclusions

Measurements of the turbulent velocity field in a CIDI engine have identified a turbulence production mechanism that significantly enhances late-cycle flow turbulence and may speed the oxidation of unburned fuel and PM. The effects of variations in flow swirl and injection pressure have been investigated, and work is proceeding to clarify the effects of engine speed and load. Current engine models do not accurately capture this increased turbulence. Detailed measurements of the characteristics of the turbulence field have clarified the reasons behind the model and will lead to more accurate model predictions.

A comprehensive mapping of performance, fuel consumption, and engine-out emissions has also been performed in a single-cylinder test engine. The results allow the effects of various combustion parameters on engine operation to be thoroughly examined. Understanding the complex reasons behind changes in emissions, fuel economy, and performance as different parameters are varied is key to rational optimization of CIDI engines.

## FY 2002 Publications/Presentations

1. Lee, T., and Reitz, R.D. "Response Surface Method Optimization of a HSDI Diesel Engine Equipped with a Common Rail Injection System," Accepted ASME Journal of Gas Turbines and Power, 2002.

2. Miles, P., Megerle, M., Sick, V., Richards, K., Nagel, Z., and Reitz, R.D., "The Evolution of Flow Structures and Turbulence in a Fired HSDI Diesel Engine," SAE Paper 2001-01-3501, 2001.

3. Miles, P., Megerle, M., Sick, V., Richards, K., Nagel, Z., and Reitz, R.D., "Measurement and Modeling of Large-Scale Flow Structures and Turbulence in a High-Speed Direct-Injection Diesel Engine," Proceedings of COMODIA 2001, July 10-12, Japan.

4. Miles, P., Megerle, M., Hammer, S., Nagel, Z., Reitz, R.D., Sick, V., "Late-Cycle Turbulence Generation in Swirl-Supported, Direct-Injection Diesel Engines," SAE Paper 2002-01-0891, 2002.

5. Miles, P.C., Megerle, M., Nagel, Z., Reitz, R.D., and Sick, V., "Turbulence Production and Reynolds Stress Modeling in Swirl-Supported, Direct-Injection Diesel Engines," Accepted, 29th International Symposium on Combustion, July 21-26, 2002.

6. Miles P.C., Megerle, M., Nagel, Z., Liu, Y., Lai. M.-C., Reitz, R.D, and Sick, V. "The Influence of Swirl and Injection Pressure on Post-Combustion Turbulence in a HSDI Diesel Engine," Accepted for presentation at Thermo- and Fluid-Dynamic Processes in Diesel Engines-THIESEL 2002, Sept. 11-13, 2002.

# B. Effects of Injector and In-cylinder Conditions on Soot Formation in Diesel Sprays

*Dennis L. Siebers (Primary Contact)*
*MS 9053*
*Sandia National Laboratories*
*P.O. Box 969*
*Livermore, CA 94551-9053*

*DOE Technology Development Managers: Kathi Epping and Gurpreet Singh*

This project addresses the following DOE R&D Plan barriers and tasks:

*Barriers*

B. PM Emissions

C. Cost

*Tasks*

1a. Advanced Fuel Systems

3a. Identification of Advanced Combustion Systems

## Objectives

- Investigate the effects of engine and injector parameters on soot forming processes in direct-injection (DI) diesel sprays:
  - Develop line-of-sight extinction and laser-induced incandescence (LII) techniques for measuring soot concentrations and visualizing soot distributions.
  - Determine the changes in soot concentration in DI diesel sprays in response to changes in engine and injector parameters, including the effects of EGR.
  - Provide a database for validating combustion and soot models in the multidimensional, computational models being developed for diesel engine design and optimization.

## Approach

- Utilize advanced optical diagnostics coupled with a unique optically-accessible diesel combustion simulation facility (DCSF) to conduct these investigations.
  - Measure soot concentrations and visualize soot distributions using line-of-sight extinction and laser-induced incandescence techniques.
  - Simultaneously with the soot measurements, acquire luminosity and OH-chemiluminescence images to characterize the spray combustion region.
  - Conduct experiments over a wide range of conditions, including those in current, as well as proposed advanced diesel engines.

## Accomplishments

- Completed a comprehensive database on the effects of in-cylinder, injector, and EGR conditions on soot in diesel sprays using #2 diesel fuel.

- Confirmed via direct soot concentration measurements that there is a strong link between fuel-air premixing upstream of the lift-off length and soot formation.
- Showed premixing upstream of the lift-off length is such that no soot is formed for orifices with 50 μm and smaller diameters for moderate-load diesel conditions.
- Initiated measurements of soot concentration as a function of in-cylinder, injector, and EGR conditions using low-sooting, oxygenated fuels.

### Future Directions

- Extend the soot concentration measurements to include data for low-sooting, oxygenated fuels. (These results, coupled with the recently completed #2 diesel fuel results, will provide a comprehensive picture of the effects of various parameters on soot formation in DI diesel sprays.)
- Develop a capability to investigate wall impingement effects on the evolution of diesel combustion and emissions processes.
- Initiate investigation of wall impingement effects on the evolution of diesel combustion and emissions processes.
- Investigate injection rate modulation and orifice geometry effects on diesel combustion and emissions processes.

## Introduction

Improving our understanding of in-cylinder combustion and emission formation processes in diesel engines is critical to developing advanced, low-emission diesel engines. The goal of this research is to investigate the soot formation processes in DI diesel sprays and determine how various engine and injector parameters affect these processes. Research completed during the previous year showed that fuel-air premixing upstream of the lift-off length plays an important role in the soot formation process. The research this year focused on developing a more detailed understanding of soot formation processes in DI diesel sprays through direct soot volume fraction measurements and visualization of soot distributions downstream of the lift-off length. The understanding of lift-off and its impact on soot formation previously developed was critical to the interpretation of the new soot concentration measurements.

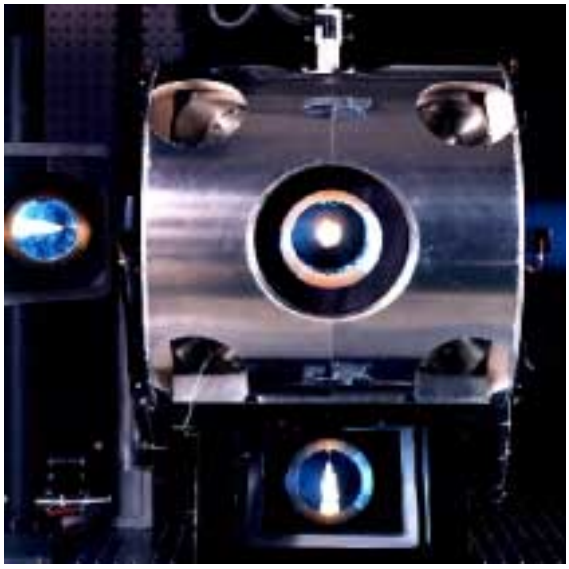

**Figure 1.** Photograph of the DCSF in operation demonstrating the optical access to the diesel spray. The bright spot in the center of the front window is a burning diesel spray penetrating toward the viewer. Mirrors at 45° next to the bottom and left-side windows show side views of the burning spray.

## Approach

The research was performed in the DCSF using an electronically controlled, common-rail diesel fuel injector. The range of conditions that can be covered in this facility is unique in the world. They include conditions in current and proposed advanced diesel engines. Figure 1 shows a picture of the DCSF in operation. Parameters varied in the investigation included: injection pressure; orifice diameter; and ambient gas temperature, density and oxygen concentration. Changes in the ambient gas oxygen concentration are one of the primary effects of EGR

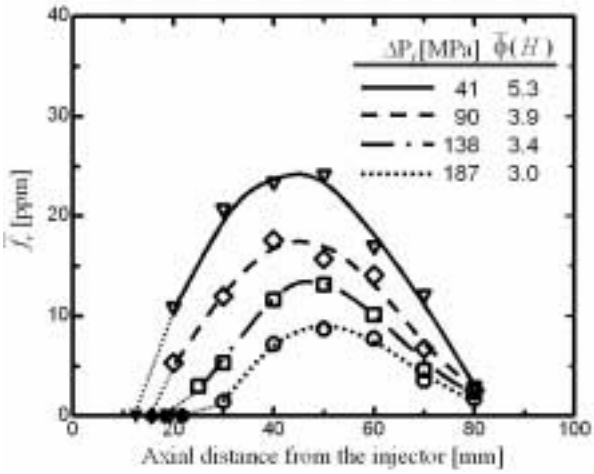


**Figure 2.** The average soot volume fraction along the path length of the soot measurement as a function of axial distance from the injector for four orifice pressure drops. The orifice diameter was 100 μm.

in an engine. The fuel used for all experiments over the past year was a #2 diesel fuel.

Soot volume fraction measurements and visualization of the soot distributions in diesel fuel jets were used to investigate the evolution of soot in the diesel sprays. Soot volume fraction was measured at various axial and radial locations downstream of the lift-off length using a line-of-sight extinction technique. Soot distributions were visualized with laser-induced incandescence (LII). Simultaneous images of OH chemiluminescence and visible light emission were also acquired and used to characterize the location of flame lift-off and the path length through the sooting region in the spray (needed for the soot volume fraction measurements), respectively [Siebers and Pickett, 2002; Pickett and Siebers, 2002].

## Results

The effects of injection pressure; orifice diameter; and ambient gas temperature, density and oxygen concentration on soot in DI diesel sprays were investigated. Figures 2 and 3 present example results that show the effects of injection pressure and orifice diameter on the axial distribution of soot in a diesel fuel jet, respectively. Figure 2 presents axial distributions of soot volume fraction ($\bar{f}_v$) in fuel jets from a 100 μm orifice for four orifice pressure drops ($\Delta P_f$ = 41, 90, 138, 187 MPa). Figure 3 presents axial distributions of soot volume fraction for an orifice pressure drop of 138 MPa and for four different orifice diameters (d = 50 μm, 71 μm, 100 μm, and 180 μm). The ambient gas density, temperature, and oxygen concentration for the data in each figure were 14.8 kg/m$^3$, 1000 K, and 21%, respectively. The solid symbols on the x-axes in the figures give the location of the lift-off lengths measured using OH-chemiluminescence imaging. Also presented in the figure legends are the cross-sectional average equivalence ratio, $\bar{\phi}(H)$, at the lift-off length, *H*.

The axial soot profiles for different orifice pressure drops in Figure 2 show that the soot level in the fuel jet decreases with increasing pressure drop across the injector orifice. Analysis of the peak soot volume fraction in each profile indicates that the peak soot decreases linearly with increasing injection velocity. The results also show that the axial location of the first soot is pushed downstream with increasing orifice pressure drop. This latter trend is due to the increase in lift-off length with increasing injection pressure.

The data in Figure 3 show that orifice diameter also has a strong effect on soot in a diesel spray. Figure 3 shows that as orifice diameter decreases the level of soot in the fuel jet decreases. The decrease is such that while the sooting region for the 180 μm orifice is optically thick and measurements cannot be made beyond an axial distance of 60 mm, the 50 μm orifice produces no detectable soot at all.

A contributing factor to the decreasing level of soot with increasing orifice pressure drop or decreasing orifice diameter is the increase in air entrainment that occurs upstream of the lift-off length. Siebers and Higgins [2001] showed that as the air entrainment upstream of the lift-off length (relative to the amount of fuel injected) increases, the total soot present in a fuel jet decreases. The increase in air entrainment with increasing injection velocity or decreasing orifice diameter is reflected in the cross-sectional average equivalence ratios shown in the legend of each figure.

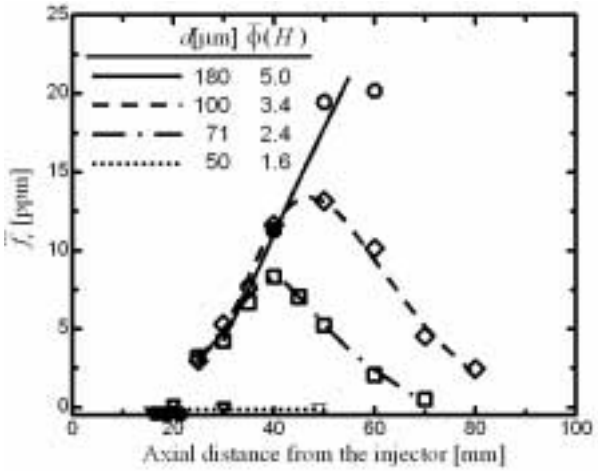


**Figure 3.** The average soot-volume fraction along the path length of the soot measurement as a function of axial distance from the injector for four orifice diameters. The orifice pressure drop was 138 MPa.

Ambient gas temperature, density, and oxygen concentration were also found to affect soot in a diesel spray. The peak soot in the diesel spray was found to dramatically increase with increasing ambient temperature. However, soot oxidation increased as well with increasing temperature. The net effect of increasing temperature was an increase in the peak soot level in a spray, but faster oxidation in the downstream region of the spray. Soot was also found to strongly increase with increasing ambient gas density, increasing in proportion to the density squared. On the other hand, reduced oxygen concentration (a primary effect of EGR) had little affect on the peak soot level; however, as oxygen concentration decreased, the soot formation and oxidation processes are pushed downstream and stretched out in the spray. Thus, more time is required to oxidize the soot that is formed under reduced oxygen conditions. As the EGR level is increased in an engine, this will result in soot being exhausted before complete oxidation, if other parameters such as injection timing are not modified.

## Conclusions

The soot concentration measurements completed over the past year provide the first comprehensive database on soot in DI diesel fuel sprays over a wide range of conditions relevant to diesel engines. The results show that peak soot concentrations in DI diesel sprays decrease with increasing injection pressure, decreasing orifice diameter, and decreasing ambient gas temperature and density; however, decreasing temperature also decreases the oxidation rate of soot. The results also show that the ambient gas oxygen concentration does not affect peak soot concentrations to a significant degree, but does delay the soot formation and oxidation processes. Finally, the direct soot measurements confirmed that there is a strong link between the amount of soot formed in a fuel spray and the amount of fuel-air premixing upstream of the lift-off length.

## References

1. L. Pickett and D. Siebers, "An Investigation of Diesel Soot Formation Processes Using Micro-Orifices," *Accepted* at the Twenty-Ninth International Symposium on Combustion, Sapporo, Japan, July 2002.

2. D. Siebers and L. Pickett, "Injection Pressure and Orifice Diameter Effects on Soot in DI Diesel Fuel Jets," *Accepted* at the Conference on Thermofluidynamic Processes in Diesel Engines (Thiesel 2002), Valencia, Spain, September, 2002.

3. D. Siebers and B. Higgens, "Flame Lift-Off on Direct-Injection Diesel Sprays Under Quiescent Conditions," Paper No. 2000-01-0530, SAE International Congress, Detroit, MI, March, 2001.

## FY 2002 Publications/Presentations

1. L. M. Pickett and D. L. Siebers, "An Investigation of Diesel Soot Formation Processes Using Micro-Orifices," *Accepted* at the Twenty-Ninth International Symposium on Combustion, Sapporo, Japan, July 2002.

2. D. L. Siebers, "Diesel Fuel Jets Under Quiescent Engine Conditions," *Submitted* as a chapter for Flow and Combustion in Automotive Engines (Ed. C. Arcoumanis), Springer-Verlag, Heidelberg, Germany.

3. D. L. Siebers, "Some Recent Development in the Understanding of DI Diesel Fuel Jets," Invited

paper at ILASS Americas, 15th Annual Conference on Liquid Atomization and Spray Systems, Madison, WI, May 2002.

4. D. L. Siebers and L. M. Pickett, "Injection Pressure and Orifice Diameter Effects on Soot in DI Diesel Fuel Jets," *Accepted* at the Conference on Thermofluidynamic Processes in Diesel Engines (Thiesel 2002), Valencia, Spain, September, 2002.

5. D. L. Siebers, B. Higgens and L. M. Pickett, "Flame Lift-Off on Direct-Injection Diesel Fuel Jets: Oxygen Concentration Effects," SAE Paper No. 2002-01-0890, SAE International Congress, Detroit, MI, March, 2002.

6. L. Pickett and D. L. Siebers, "Orifice Diameter Effects on Diesel Fuel Jet Flame Structure," *Submitted* to Journal for Gas Turbines and Power.

7. L. Pickett and D. L. Siebers, "Orifice Diameter Effects on Diesel Fuel Jet Flame Structure," Internal Combustion Engine Division of the ASME 2001 Fall Technical Conference, Chicago, IL, September, 2001.

8. P. J. O'Rourke, D. L. Siebers and S. Subramaniam, "Some Implications of a Mixing-Controlled Vaporization Model for Multidimensional Modeling of Diesel Sprays," *Submitted* to Atomization and Sprays.

9. D. L. Siebers and B. Higgens, "Effects of Injector Conditions on the Flame Lift-Off Length of DI Diesel Sprays," Thermo- and Fluid-dynamic Processes in Diesel Engines, Springer-Verlag, Heidelberg, Germany, 2002.

10. D. L. Siebers, "Progress on the Investigation of Diesel Fuel Jet Soot Formation Processes," Diesel Combustion/Alternative Fuels CRADA Meeting, USCAR, Detroit, MI, June, 2002.

11. D. L. Siebers, "Some Recent Development in the Understanding of DI Diesel Fuel Jets," Invited paper at ILASS Americas, 15th Annual Conference on Liquid Atomization and Spray Systems, Madison, WI, May, 2002.

12. D. Siebers, "Effects of Injector and In-Cylinder Conditions on Soot Formation in Diesel Fuel Jets," Combustion and Emission Control for Advanced CIDI Engines: 2002 Annual Review, U. S. Department of Energy, Chicago, IL, May, 2002.

13. D. Siebers, "Effects of Injector and In-Cylinder Conditions on Soot Formation in Diesel Fuel Jets," OAAT Mid-Year Review, Sandia National Laboratories, Livermore, CA, March, 2002.

14. D. L. Siebers, "Flame Lift-Off on Direct-Injection Diesel Fuel Jets: Oxygen Concentration Effects," SAE Paper No. 2002-01-0890, SAE International Congress, Detroit, MI, March, 2002.

15. D. L. Siebers, "Progress on the Investigation of Diesel Fuel Jet Soot Formation Processes," Diesel Combustion/Alternative Fuels CRADA Meeting, Sandia National Laboratories, Livermore, CA, January 2002.

16. L. Pickett and D. L. Siebers, "Orifice Diameter Effects on Diesel Fuel Jet Flame Structure," Fall Technical Conference of the Internal Combustion Engine Division of the ASME, Chicago, IL, September 2001.

17. D. Siebers, "Progress on DI Diesel Spray Soot Investigations," Diesel Combustion/Alternative Fuels CRADA Meeting, University of Wisconsin, Madison, WI, June, 2001.

18. D. Siebers, "Diesel Combustion Cross-Cut Research," CIDI Combustion, Emission Control & Fuels R&D Laboratory Merit Review & Peer Evaluation, Oak Ridge National Laboratory, Oak Ridge, TN, June, 2001.

# C. Effects of Fuel Parameters and Diffusion Flame Lift-Off on Soot Formation in a Heavy-Duty Diesel Engine

*Mark P. B. Musculus (Primary Contact)*
*Combustion Research Facility*
*Sandia National Laboratories*
*P.O. Box 969, MS9053*
*Livermore, CA 94551-0969*

*DOE Technology Development Manager: Gurpreet Singh*

*Main Subcontractor: Sandia National Laboratories, Livermore, CA*

This project addresses the following DOE R&D Plan barriers and tasks:

*Barriers*

B. PM Emissions

C. Cost

*Tasks*

1. Fuel Systems R&D

3a. Identification of Advanced Combustion Systems

## Objectives

- The overall objective of this project is to advance the understanding of diesel engine combustion and emissions formation through the application of advanced laser-based diagnostics in an optically-accessible diesel engine that is capable of operating under conditions typical of real diesel engines.
- Specific objectives for FY 2002 include:
  - Quantification of the effects of fuel-bound oxygen on in-cylinder soot formation over a wide range of fuel oxygen content.
  - Quantification of the effects of the aromatic molecules in real diesel fuels on in-cylinder soot formation compared to paraffinic research fuels that contain no aromatic molecules.
  - Evaluation of the importance of air entrainment on soot formation though direct measurements of the diffusion flame lift-off for a wide range of fuels.

## Approach

- Investigation of the effects of fuel-bound oxygen and aromatic molecules on soot formation:
  - Improve the accuracy and dynamic range of a previous laser-based line-of-sight (LOS) extinction technique for measurement of both soot within the reacting jet and deposition of soot on in-cylinder surfaces.
  - Compare the in-cylinder soot levels and/or soot deposition rates on in-cylinder surfaces for a wide range of fuels to understand the influence of the differences in fuel chemistry on in-cylinder soot formation.
- Investigation of the effects of air entrainment on soot formation:

- Use a hydroxyl radical (OH) chemiluminescence imaging technique to measure the diffusion flame lift-off length for a wide range of fuels.
- Using measured diffusion flame lift-off lengths, estimate the influence of air entrainment on soot reduction for a wide range of fuels.

### Accomplishments

- Conducted a detailed investigation of the correlation between in-cylinder soot formation and both fuel oxygen content and fuel aromatic content.
  - Improved a laser-based absorption technique for accurate measurement of in-cylinder soot, both within the reacting diesel jet and deposited on in-cylinder surfaces. Although this diagnostic technique was developed for diesel environments, it is transferable to other high pressure, high temperature transient environments.
  - Established that in-cylinder soot formation decreases linearly with increasing fuel oxygen content over a wide composition range of an oxygenated fuel blend.
  - Demonstrated that fuel aromatic content significantly affects in-cylinder soot formation, and that conventional diesel fuels with aromatic molecules produce twice the in-cylinder soot of primary reference fuel mixture, which has no aromatic molecules.
- Examined the air entrainment mechanism of soot reduction for a wide range of fuels.
  - Measured diffusion flame lift-off lengths for five (5) different paraffinic, oxygenated fuel blends and two (2) conventional diesel fuels at two (2) operating conditions.
  - Showed that there is little difference in the diffusion flame lift-off length and corresponding air entrainment for two typical operating conditions between the fuels studied, indicating that differences in air entrainment is not an important mechanism of soot reduction for these oxygenated fuels.
  - Provided evidence that fuel-bound oxygen may reduce soot formation more effectively than an equivalent quantity of entrained oxygen, which has significant implications for future strategies for soot reduction with both oxygenated fuels and conventional diesel fuels.

### Future Directions

- Continue to examine the structure of diffusion flames by combining side-on OH planar laser-induced fluorescence (PLIF) with OH chemiluminescence imaging to understand the behavior of the diffusion flame lift-off length and soot formation in realistic diesel engine environments.
- Implement state-of-the-art common-rail diesel fuel injection technology in the optical diesel engine so that advanced, multi-mode combustion strategies for emissions reduction may be examined.

---

## Introduction

Numerous studies have shown that engine-out soot emissions may be reduced by fueling with oxygenated fuels [e.g., 1, 2]. Other optical studies in simulated diesel environments have shown that in-cylinder soot formation may be reduced by increasing air entrainment via increased diffusion flame lift-off length with conventional diesel fuel [3, 4]. Both of these developments are encouraging because they demonstrate two separate strategies that have the potential to reduce or even eliminate diesel soot emissions. However, integration of these data into a coherent view of in-cylinder diesel soot formation is difficult because of differences in the fuels used and in the parameters that were measured. Thus, there is a need for a comprehensive study to simultaneously examine the effects of oxygenated fuels and diffusion flame lift-off on in-cylinder soot

formation, so that the ultimate potential of these two strategies for soot reduction can be better understood.

Over the past decade, laser diagnostics have been used to improve the understanding of in-cylinder diesel combustion and pollutant formation processes [5]. To better understand the mechanisms by which both oxygenated fuels and/or increased diffusion flame lift-off can reduce in-cylinder soot formation, it is desirable to measure both diffusion flame lift-off and in-cylinder soot formation for a wide range of fuels. In this study, the chemical and physical parameters affecting soot formation are studied in an optically accessible, heavy-duty diesel engine. The specific objectives of this study are as follows:

- Examine soot formation within the reacting diesel jet for oxygenated, paraffinic fuel blends having a wide range of fuel oxygen content, as well as for real diesel fuels.
- Investigate the potential of OH chemiluminescence imaging to quantify diffusion flame lift-off in engines, and examine the physical effects of flame lift-off and fresh air entrainment on soot formation.

This investigation, and all of the work on this project, is conducted in cooperation with our Cooperative Research & Development Agreement (CRADA) partners (Cummins, Caterpillar, and Detroit Diesel), and the results are presented at the cross-cut diesel CRADA meetings.

## Approach

In the current study, a previously-developed line-of-sight (LOS) continuous wave (CW) laser-absorption technique was improved and employed to measure both "jet-soot" within the reacting diesel jet and "wall-soot" deposited on the piston bowl-rim. The relative importance of (1) gradient-index beam steering, (2) photoelastic properties of the optical windows, and (3) coherent beam interference on the performance of this diagnostic were quantified. These factors were addressed using necessary optical techniques to yield a more robust and accurate soot extinction diagnostic for diesel engines. The knowledge gained in developing this diagnostic for diesel engines may also be applied to extinction measurements in other high pressure, high temperature transient environments.

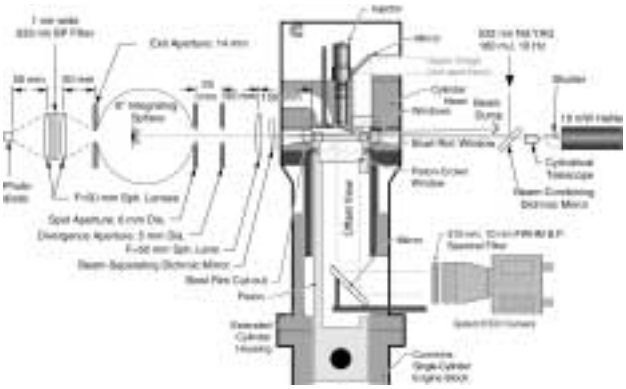

**Figure 1.** Schematic Diagram Showing Optical Engine, Elements of LOS Extinction Technique, and OH Chemiluminescence Imaging Camera

This soot extinction diagnostic was applied to a realistic diesel environment in the Sandia/Cummins optically accessible heavy-duty diesel engine, as shown in Figure 1. A portion of the piston bowl-rim was replaced with a quartz window, upon which soot was deposited during combustion. A HeNe-laser beam passed through the combustion chamber to measure extinction from either jet-soot during fired cycles, or wall-soot during the motored cycles between skip-fired cycles. For the jet-soot measurements only, a high power Nd:YAG laser was aligned co-axially with the LOS beam and was pulsed at an appropriate time to ablatively remove soot deposits from the window surface. Crank-angle resolved jet-soot extinction data were obtained for five (5) different oxygenated paraffinic fuel blends and for 2 conventional No. 2 diesel fuels, which contained about 25% aromatics, at two diesel operating conditions, representative of both low- and high-load operation. Additionally, cycle-resolved measurements of wall-soot deposition rates were acquired for each of these fuels at both operating conditions.

Previous studies have shown that the natural OH chemiluminescence emission from the diffusion flame can be used to determine the diffusion flame lift-off length [3]. Thus, for each fuel at both operating conditions, OH chemiluminescence from the diffusion flame was imaged through the piston crown window as shown in Figure 1, using appropriate spectral filters. Due to inherent and unavoidable scattering interference present in the OH

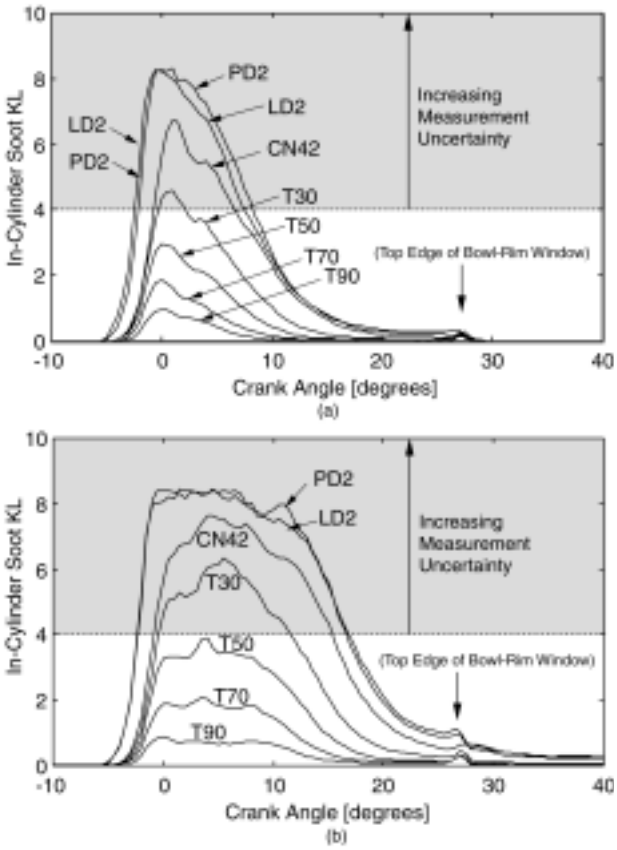


**Figure 2.** Jet-soot KL factors for seven fuels at (a) low-load and (b) high-load operating conditions. KL factors below 4 have measurement uncertainty of 5% or less. The fuel oxygen content of the oxygenated, paraffinic fuels increases from 0% to 27% (by weight) in the order CN42→T30→T50→ T70→T90. LD2 and PD2 are conventional diesel fuels, which contain aromatic molecules.

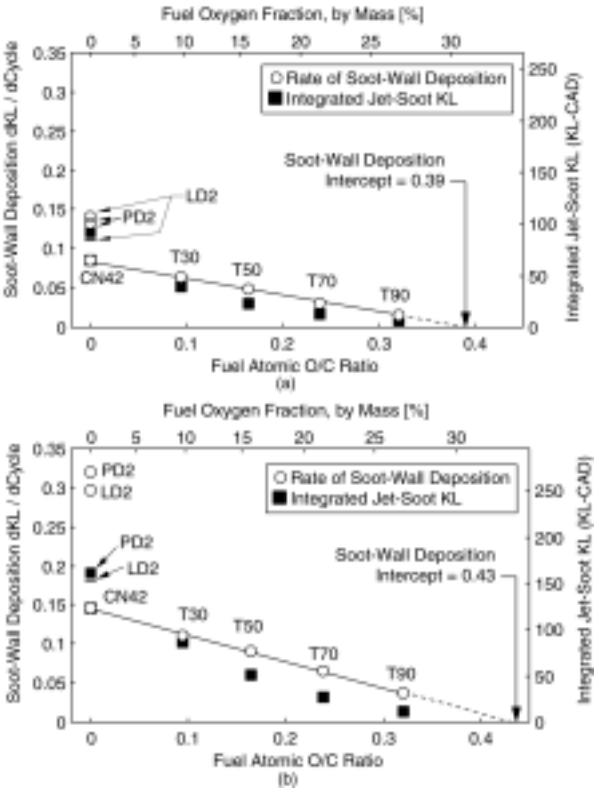


**Figure 3.** Rate of soot-wall deposition on bowl-rim window (open circles) and integrated jet-soot KL (filled squares) at (a) low-load and (b) high-load operating condition for seven fuels. The scales of the two y-axes have been adjusted so that the soot-wall deposition and integrated jet-soot data points for CN42 overlie each other. The fuel oxygen content of the oxygenated, paraffinic fuels increases from 0% to 27% (by weight) in the order CN42→T30→T50→T70→T90. LD2 and PD2 are conventional diesel fuels, which contain aromatic molecules.

chemiluminescence images from the engine, a straightforward image-processing scheme was used to spatially filter and smooth the images so that the diffusion flame liftoff length could be objectively extracted from instantaneous images, using a simple intensity thresholding scheme.

## Results

Shown in Figure 2 are the crank-angle-resolved jet-soot extinction "KL" values (which are roughly proportional to the mass of soot in the path off the LOS laser beam), at both operating conditions, for all seven fuels. In Figure 2, PD2 and LD2 are conventional diesel fuels, and CN42 is a blend of 62% heptamethylnonane [HMN] and 38% normal hexadecane (nC16), having a defined Cetane Number of 42. The oxygenated fuels are denoted as T##, where "##" represents the percentage volume fraction of TetraEthOxyPropane [TEOP] (e.g., T30 has 30% TEOP). The balance of each oxygenated fuel is composed of HMN and nC16, which were blended with the TEOP to achieve a cetane number near 42 for each oxygenated fuel blend. Thus, the oxygen content for the oxygenated fuel blends increases from 0% to 27% (by weight) in the order CN42→T30→T50→T70→T90 (also see top axes of plots in Figure 3). For all fuels, the in-cylinder soot

forms very quickly after the end of the diesel premixed burn, remains relatively constant during the fuel injection event, and then decreases more slowly after the end of injection. As shown in Figure 2, the peak in-cylinder soot decreases as the fuel oxygen content increases for the oxygenated fuels. Note that the peak jet-soot extinction for the conventional diesel fuels is artificially truncated because the soot concentrations exceed the measurement capabilities of this part of the extinction diagnostic.

Shown in Figure 3 as filled squares are the integrated jet-soot data (area under each of the curves in Figure 2) for each of these fuels. Note that the integrated jet-soot for the conventional diesel fuels (PD2 and LD2) reported in Figure 3 is underestimated because the jet-soot extinction data is truncated at the maximum resolvable jet-soot (see discussion in paragraph above). Also plotted in Figure 3 as open circles is the rate of deposition of wall-soot on the piston bowl rim for each fuel. For the oxygenated fuels, the wall-soot measurements correlate well with the jet-soot extinction measurements, indicating that wall-soot can be used as an indirect measurement of in-cylinder jet-soot. Note also that the wall-soot deposition rates for PD2 and LD2 do not exceed the measurement capabilities of the wall-soot extinction technique, so this part of the extinction diagnostic can provide a more accurate measurement of the soot formation rates for these highly sooting fuels and conditions. Since the jet-soot and wall-soot measurements agree well, a combined technique using direct jet-soot measurements at low-sooting conditions, with indirect measurement of jet-soot via wall-soot measurements at highly-sooting conditions, provides a wide measurement range that is necessary for soot measurements in diesel engines. Finally, for the zero-oxygen-content fuels, the wall-soot deposition rate for PD2 and LD2 (which contain aromatics) exceeds that of CN42 (which contains no aromatics) by a factor of 2, indicating the strong influence of fuel molecular structure on in-cylinder soot formation.

Sample instantaneous OH chemiluminescence images acquired at the high-load operating condition are shown in Figure 4. These images are representative of the average diffusion flame

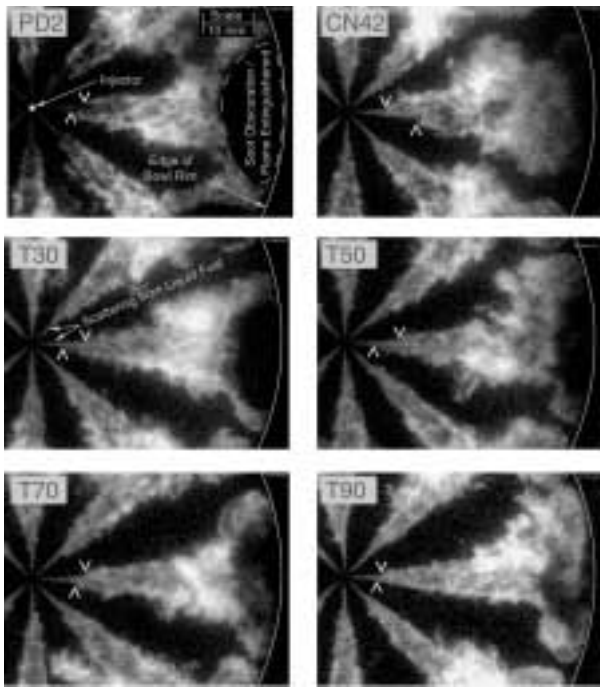


**Figure 4.** Representative instantaneous images of OH chemiluminescence for six fuels acquired from the high-load operating condition, at 2 crank angle degrees after top dead center. The upstream extent of the diffusion flame on each side of the jet is indicated by the white carats.

structure during the injection event for each fuel. The diffusion flame lift-off length was extracted from each of these images and is indicated on each "side" of the jet by white carats. As shown in Figure 4, the diffusion flame lift-off length is very similar for all of the fuels at the operating conditions of this study. As a result, the rates of air entrainment and subsequent fuel-air premixing prior to combustion are very similar between fuels, indicating that the potential physical effects of differences in air-entrainment between fuels is not an important mechanism for soot reduction.

Finally, by integrating data gathered from this study and other studies [3, 4], it appears that soot formation is reduced with increasing fuel oxygen content much more dramatically than with air entrainment. This suggests that fuel-bound oxygen reduces soot more effectively than an equivalent quantity of oxygen from entrained in-cylinder gases, but more data is required to confirm this hypothesis.

## Conclusions

Two important in-cylinder diesel soot reduction mechanisms were examined in a heavy-duty diesel engine with extensive optical access. Using a line-of-sight laser extinction diagnostic and OH chemiluminescence imaging, the effects of (1) fuel oxygen content and (2) the rates of air entrainment on in-cylinder soot formation were quantified for a wide range of oxygenated and conventional diesel fuels. In-cylinder soot formation decreased linearly with increasing fuel-bound oxygen content, and the aromatic molecules in typical diesel fuel increased soot formation by a factor of 2 over a diesel reference fuel containing no aromatic molecules. The diffusion flame lift-off length and resulting air entrainment rates were similar for all fuels tested, indicating that the degree of fuel-air premixing prior to combustion was not a significant mechanism for differences in soot formation among these fuels. The data also suggest that fuel-bound oxygen in oxygenated fuels may reduce in-cylinder soot formation more effectively than an equivalent quantity of entrained oxygen from the in-cylinder gases.

The results of this investigation improve our understanding of the effects of (1) fuel-bound oxygen and (2) pre-combustion air entrainment on in-cylinder soot formation. This study provides engine developers with more detailed information on the combined potential of these two approaches for reducing or eliminating diesel soot emissions.

## References

1. Nabi, M. N., Minami, M., Ogawa, H., and Miyamoto, N., "Ultra Low Emission and High Performance Diesel Combustion with Highly Oxygenated Fuel," SAE Paper 2000-01-0231, 2000.

2. Miyamoto, N., Ogawa, H., Nabi, M. N., Obata, K., and Arima, T., "Smokeless, Low NOx, Higher Thermal Efficiency, and Low Noise Diesel Combustion with Oxygenated Agents as Main Fuel," SAE Paper 980506, 1998.

3. Higgins, B. and Siebers, D., "Measurement of the Flame Lift-Off Location on DI Diesel Sprays Using OH Chemiluminescence," SAE Technical Paper no. 2001-01-0918, 2001.

4. Siebers, D. and Higgins, B., "Flame Lift-Off on Direct-Injection Diesel Sprays under Quiescent Conditions," SAE Paper 2001-01-0530, 2001.

5. Dec, J. E., "A Conceptual Model of D.I. Diesel Combustion Based on Laser-Sheet Imaging," SAE Paper 970873, 1997.

## FY 2002 Publications/Presentations

1. Musculus, M.P., Dec, J. E. and Tree, D. R. "Effects of Fuel Parameters and Diffusion Flame Lift-Off on Soot Formation in a Heavy-Duty DI Diesel Engine," SAE paper no. 2002-01-0889, 2002.

2. Musculus, M. P., "Effects of Fuel Parameters and Diffusion Flame Lift-Off on Soot Formation," Cross-Cut Diesel CRADA Meeting, January, 2001.

3. Dec, J. E. "An Understanding of DI Diesel Combustion and Emission based on Laser-Sheet Imaging," Advances in Engine Combustion Symposium at the Royal Institute of Technology, Stockholm, Sweden, April 11, 2002.

4. Musculus, M. P., "Effects of Fuel Parameters and Diffusion Flame Lift-Off on Soot Formation in a Heavy-Duty DI Diesel Engine," DOE CIDI Combustion, Emission Control, and Fuels Peer Review, May 14-16, 2001.

5. Dec, J. E., Siebers, D. L., and Musculus, M., "Diesel Engine Combustion and the Effects of Flame Lift-Off on Soot Formation," Invited seminar, International Truck and Engine Co., Melrose Park, IL, May 2002.

6. Musculus, M. P., "Progress on Flame Lift-Off Measurements in a Realistic Heavy-Duty DI Diesel Engine Environment," Cross-Cut Diesel CRADA Meeting, June 2002.

# D. KIVA Modeling Activities

*David J. Torres (Primary Contact), Peter O'Rourke, Mario F. Trujillo*
*Group T-3, MS B216*
*Los Alamos National Laboratory*
*Los Alamos, NM 87544*

*DOE Technology Development Manager: Gurpreet Singh*

This project addresses the following DOE R&D Plan barriers and tasks:

*Barriers*

A. $NO_x$ Emissions

B. PM Emissions

*Tasks*

3. Fundamental Combustion R&D

3a. Identification of Advanced Combustion Systems

## Objectives

- Develop a multicomponent fuel model for diesel applications.
- Implement a phase equilibrium model in KIVA-3V for high pressures to govern fuel droplet evaporation.
- Implement phase equilibrium for non-ideal liquid fuel mixtures in sprays and wall films to increase understanding of Laser Induced Fluorescence (LIF) techniques.
- Implement a high pressure equation-of-state in gas dynamics of KIVA-3V.
- Compare high pressure implementation and ideal gas implementation to access departures from ideal behavior.
- Begin testing KIVA-AC (Arbitrary-Connectivity), which is a parallel version of KIVA written in Fortran-90. KIVA-AC also has the meshing flexibility to include prisms, tetrahedrals, and hexahedra in its engine meshes.

## Approach

- Find a suitable diesel surrogate and add fuel properties of its constituents to the KIVA-3V fuel library.
- Implement a high pressure equation of state (EOS) in KIVA-3V. The Peng-Robinson equation-of-state (EOS) is considered by many to be the most accurate EOS for high pressure phase equilibrium calculations. We decided it would be the most suitable for diesel sprays.
- Quantify the degree to which gases at high pressures (as found in diesel engines) depart from the behavior predicted by the ideal gas law, and implement a high pressure equation of state into KIVA-3V's gas dynamics which could account for these deviations.
- Compare the high pressure model with the ideal gas model with regard to diesel sprays.
- Revive KIVA-AC and begin testing its speed against KIVA-3V and CHAD. A 3D adiabatic compression test was used to benchmark and begin the initial validation of KIVA-AC.

### Accomplishments

- Chose the IDEA fuel (62.5% n-decane and 37.5% alpha-methylnaphthalene by mass) was recommended to us as a diesel surrogate. Since n-decane was already included in the KIVA-3V fuel library, only properties of alpha-methylnaphthalene need to be found. IDEA fuel produces slightly less soot and $NO_x$ but gives very similar engine performance to diesel fuel. Our multicomponent model has successfully computed diesel fuel sprays using this diesel surrogate. Other diesel surrogates' droplet lifetimes and temperatures have also been compared to this IDEA fuel.
- The Peng-Robinson EOS has been implemented in the phase-equilibrium submodel of KIVA-AC. Fugacities are equated on the liquid and vapor sides. The implementation also accounts for air solubility in the liquid phase.
- Spray as well as film calculations have been performed which model the non-ideal behavior of a mixture of iso-octane and 3-pentanone. The model is based on a paper supplied to us by Dick Steeper, "Evaporation characteristics of the 3-pentanone/isooctane binary system," which was submitted to Experiments in Fluids in 2001.
- The Peng-Robinson EOS has been implemented into the gas dynamics of KIVA-3V. The Peng-Robinson EOS involves numerous modifications since the ideal gas assumption occurs in over 20 subroutines. We determined that significant departures from the ideal gas law do occur in the fuel vapor under diesel pressures. However, the deviations from the ideal gas law were negligible for air (a mixture of 79% nitrogen and 21% oxygen). The amount by which a fuel-air mixture departs from ideality will be determined by the relative percentages of fuel and air.
- Diesel sprays have been modeled using the high pressure model and an ideal model. Under the limited set of conditions we have tested, both sprays behave similarly. We expect to continue testing under a broader range of conditions and search for any differences which may develop.
- Revived KIVA-AC and timed results for the 3D adiabatic compression test.

### Future Directions

- Continue our work with the high pressure model in studying diesel sprays and submit a paper to the International Journal of Engine Research.
- Continue our validation and testing of KIVA-AC.
- Develop a full engine cycle meshing strategy in KIVA-AC for diesel engine geometries.
- Implement a parallel spray model in KIVA-AC.
- Release an updated version of KIVA.

---

## Introduction

In the past year, we have transitioned from Computational Hydrodynamics for Advanced Design (CHAD) development to KIVA development. CHAD has been judged too slow and difficult to use but could be revisited if ways are found to speed up CHAD. Most companies are using KIVA and would like to see accelerated KIVA development. As a result, ICEM's work on CHAD has ceased. ICEM is a company which was subcontracted to write an interface for CHAD, enabling CHAD to compute with moving engine geometries. ICEM did produce an alpha version of the interface called CHAD-ICE which was successful in simulating a Caterpillar 3208 Engine.

We have refocused efforts on KIVA development. These include implementing and applying a multicomponent fuels model for diesel sprays; implementing a high pressure Peng-Robinson EOS in the phase equilibrium submodel of KIVA-AC; and implementing a high pressure Peng-Robinson EOS in the gas dynamics of KIVA-AC.

All these changes were undertaken in order to improve KIVA's ability to model high pressures and sprays, as encountered in diesel engines. We now have the ability to compute with sprays in full 3D engine geometries with the high pressure Peng-Robinson EOS. We have also made efforts to compute non-ideal behaviors of iso-octane and 3-pentanone, which were a topic of interest at the last January 2002 CRADA meeting.

We have also begun efforts in benchmarking and validating KIVA-AC, which is a Fortran-90 parallel version of KIVA. KIVA-AC has the meshing flexibility of CHAD, which will allow a user to create better quality meshes. Industry and academia will benefit from a parallel KIVA, as well as KIVA-AC's meshing flexibility.

## Approach

Our approach has been to direct our KIVA modeling efforts to areas which would be beneficial to industry and the general engine community. One limitation of engine codes has been the use of a single-component fuel. The application of multicomponent fuels would allow users to improve prediction of liquid and vapor fuel distribution. We also hoped to quantify the value of a high pressure EOS in computing under diesel-like conditions and evaluate differences between an ideal and high pressure EOS. Our work with KIVA-AC will focus on using the meshing flexibility of KIVA-AC to improve engine meshes, while keeping the single processor speed of KIVA-AC comparable with KIVA-3V.

## Results

Figure 1 compares a droplet lifetime in the ideal model and the Peng-Robinson EOS (PREOS) at difference pressures. In Figure 1, the ambient temperature is fixed. IDEA fuel is used for the fuel as a diesel surrogate. The initial droplet radius is 5 microns, and the initial droplet temperature is 363 K. The relative velocity between the droplet and the gas is 100 m/s. The ideal gas behavior overestimates the droplet lifetime. In Figure 2, the same droplet is evaporated once again. However, in Figure 2, the ambient temperatures are modified as the ambient pressures are modified to reflect how an engine

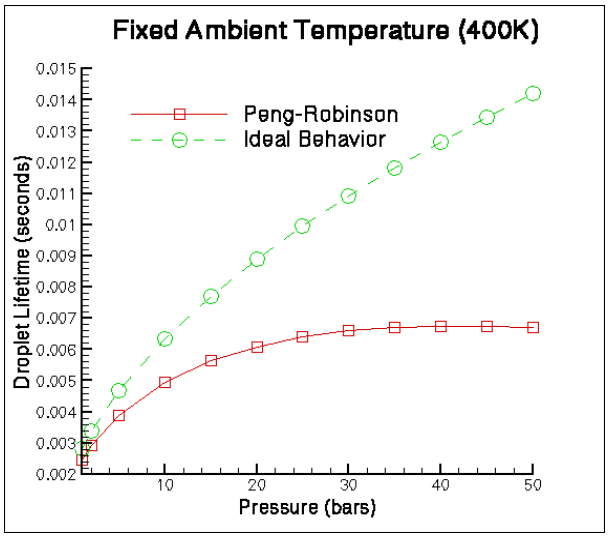


**Figure 1.** Droplet Lifetime Comparison of Peng-Robinson EOS and Ideal Behavior at Fixed Temperature as Pressure Increases

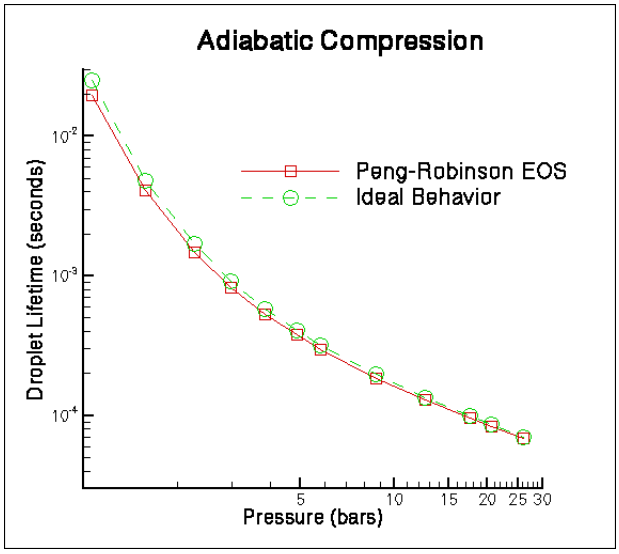


**Figure 2.** Droplet Lifetime Comparison of Peng-Robinson EOS and Ideal Behavior as Temperature Adiabatically Increases with Pressure

piston would adiabatically (with no heat loss) compress the air inside the cylinder. The initial ambient pressure and temperature at the start of the adiabatic process are 344.8 K and 1.06 bars. Figure 2 shows little difference in the PREOS and the ideal gas EOS. However, actual engines may use engine

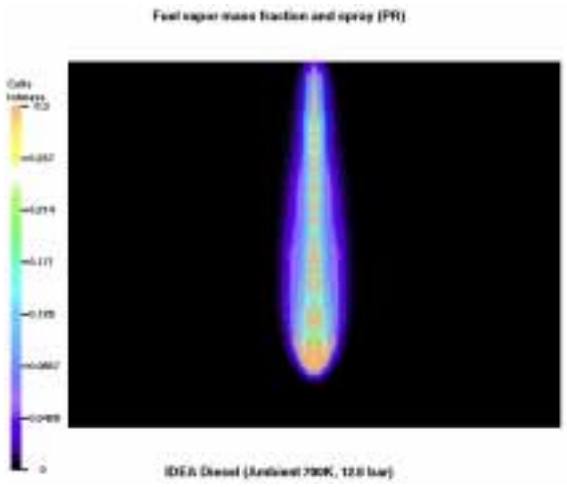

**Figure 3.** Liquid Spray Particles and Total Vapor Fuel Mass Fraction Contours for IDEA Fuel Using the Peng-Robinson Equation-of-State

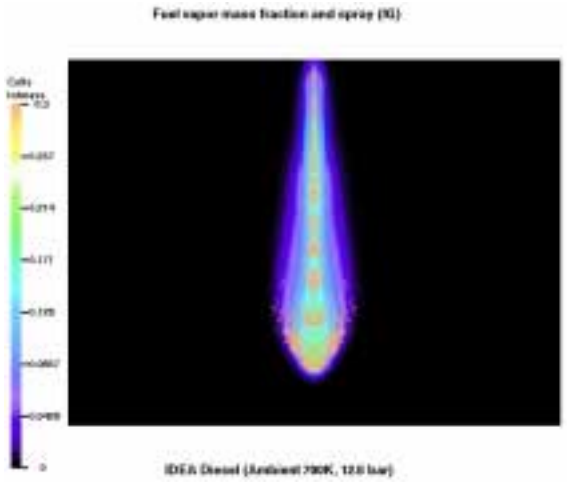

**Figure 4.** Liquid Spray Particles and Total Vapor Fuel Mass Fraction Contours for IDEA Fuel Using the Ideal Model

gas recirculation (EGR) or turbocharging, and do incur wall heat losses which could cause deviations from Figure 2. We hope to explore other engine conditions to determine if deviations from ideal behavior are significant.

Figure 3 computes an IDEA diesel spray with the PREOS, and Figure 4 computes the spray with the ideal model. The leading spray angle is narrower in PREOS than the ideal spray. The ambient

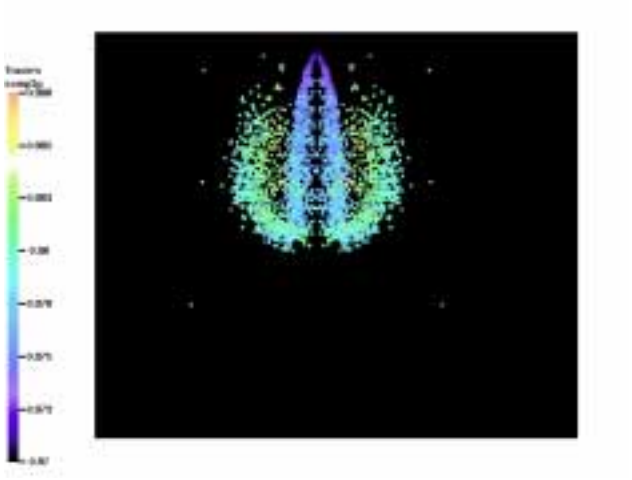

**Figure 5.** Spray particles are color coded to reflect the mass fraction of iso-octane. Despite the slightly lower boiling point of iso-octane ($3^{o}$C), 3-pentanone is preferentially vaporized.

temperature is 700 K and the ambient pressure is 12.6 bars. The spray particles are injected at 250 m/s. Overall, the ideal behavior seems not to be such a bad approximation even at high pressures, qualitatively matching the liquid spray and vapor fuel distribution. This is due to the fact that in engines the temperature also rises with pressure during compression.

Figure 5 shows the percentage of 3-pentanone in a binary mixture of 3% 3-pentanone and 97% iso-octane. The non-ideal behavior of the polar/non-polar mixure causes the 3-pentanone to be preferentially vaporized. This occurs despite the fact that 3-pentanone and iso-octane have similar boiling points. The ambient pressure is 2.64 bar and the ambient temperature is 393 K. Such effects should be accounted for in determining a fuel/tracer mix in LIF imaging.

Figure 6 shows the percentage of 3-pentanone in a binary mixture of 3% 3-pentanone and 97% iso-octane in a wall film. Again the concentration of 3-pentanone decreases relative to iso-octane.

## Conclusions

We have improved KIVA-3V's ability to model diesel sprays and pressures by implementing the Peng-Robinson EOS into the phase equilibrium and

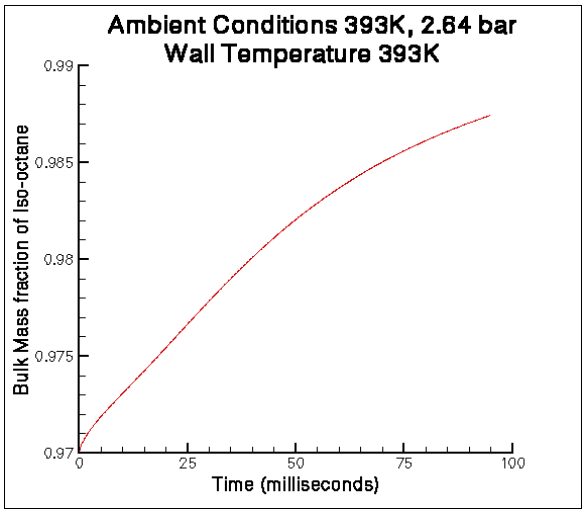


**Figure 6.** Film Mass Fraction of Iso-Octane Increases as 3-Pentanone is Preferentially Vaporized

gas dynamics of KIVA-3V. KIVA-3V can now model full 3D engine geometries with spray using a Peng-Robinson EOS which can account for departures from ideal behavior. At present, we do not see significant differences between the high pressure implementation and the ideal gas implementation, but we plan on exploring a broader range of engine conditions.

We have modeled non-ideal behavior of 3-pentanone and iso-octane in sprays and wall films. Our results show that 3-pentanone is preferentially vaporized, which is consistent with experimental results. We also show that it is important to account for the fact that 3-pentanone and iso-octane do not evaporate at the same rate in sprays and wall films in LIF imaging. The gradients in 3-pentanone tracer concentration are significant enough to falsely represent the fuel distribution.

## FY 2002 Publications/Presentations

1. Multicomponent Fuel Vaporization at High Pressures, D. J. Torres and P. J. O'Rourke, published in the 12th International Multidimensional Engine Modeling User's Group Meeting at SAE Congress.

2. A Discrete Multicomponent Fuel Model, D.J. Torres, P.J. O'Rourke, and A. A. Amsden, submitted to Atomization and Sprays, December 2001.

3. Efficient Multicomponent Fuel Algorithm, submitted to Combustion Theory and Modeling, May 2002.

4. Energy Distribution and Crown Development in Droplet Splashing, M.F. Trujillo and C. F. Lee, ILASS Americas, 15th Annual Conference on Liquid Atomization and Spray Systems, Madison, WI, May 2002.

5. Modeling Film Dynamics and Spray Impingement, M.F. Trujillo and C.F. Lee, to appear in J. Fluids Eng.

6. Generalizing the Thermodynamic State Relationships in KIVA-3V, LANL Technical Report, In Preparation.

7. KIVA Modeling Activities, D. J. Torres, January 2002 CRADA meeting, Livermore, CA.Generalizing the Thermodynamic State Relationships in KIVA-3V, Mario Trujillo, January 2002 CRADA meeting, Livermore CA.

8. Multicomponent Fuel Vaporization at High Pressures, D.J. Torres, 12th International Multidimensional Engine Modeling User's Group Meeting at SAE Congress, Detroit, March 2002.

9. Energy Distribution and Crown Development in Droplet Splashing, M. F. Trujillo, ILASS Americas, 15th Annual Conference on Liquid Atomization and Spray Systems, Madison, WI, May 2002.

10. Toward Improved Computer Models for Thick Sprays, P. J. O'Rourke, ILASS Americas, 15th Annual Conference on Liquid Atomization and Spray Systems, Madison, WI, May 2002

11. KIVA Modeling Activities, D. J. Torres, June 2002 CRADA meeting, Detroit, MI.

12. Extending the Thermodynamic State Relationships in KIVA-3V for High Pressure Environments, Mario Trujillo, June 2002 CRADA meeting, Detroit, MI.

# E. Diesel Fuel Spray Measurement Using X-Rays

*Jin Wang (Primary Contact), Roy Cuenca*
*Argonne National Laboratory*
*9700 S. Cass Ave*
*Argonne, IL 60439*

*DOE Technology Development Manager: Kathi Epping*

This project addresses the following DOE R&D Plan barriers and tasks:

*Barriers*

B. PM Emissions

*Tasks*

1. Fuel Systems R&D

## Objectives

- Understand diesel fuel spray structure and dynamics in the region close to the nozzle with small orifice diameters operated at high injection pressures.
- Develop highly quantitative and time-resolved methods characterize diesel fuel sprays.
- Establish a knowledge base regarding spray breakup mechanism and droplet interactions as a key to realistic computational modeling.

## Approaches

- Stage 1. Use synchrotron-based, monochromatic x-radiography to image diesel fuel sprays in a time-resolved and quantitative manner.
- Stage 2. Develop and utilize 2-dimensional (2-D) x-ray detectors for collecting the x-radiographic data more efficiently.
- Stage 3. Analyze the image data to qualitatively evaluate the spray characteristics such as structure (time-resolved fuel mass volume-fraction distribution) and dynamics (speed of spray core, supersonic properties associated with the sprays).
- Stage 4. Understand high-pressure sprays by theoretical modeling and computational approaches based on physical models best describing high-pressure injections.

## Accomplishments

- Imaged shock waves (Mach cones) generated by high-pressure and high-speed diesel fuel sprays directly using time-resolved x-radiography and analyzed fill-gas distribution quantitatively across the Mach cone.
- Studied diesel fuel sprays systematically as a function of fuel injection pressure, types of the nozzle finish, and density of the fill gas.
- Finished the fuel mass calibration against another independent mass measurement.
- Performed x-radiography measurement of diesel fuel sprays in a pressurized injection chamber.
- Developed multiphase models for simulating high-pressure, supersonic sprays in one dimension.
- Received several awards, published several technical papers and carried out an educational outreach program.

### Future Directions

- Assemble and test a wide-bandpass focusing multiplayer monochromator that provides improved x-ray intensity by one to two orders of magnitude. Continue to assist with the development of a fast framing x-ray detector (at Cornell University) suited for 2-D data collection so that the spray test using x-rays can be performed routinely at the 1-BM (bending magnet) beamline at the Advanced Photon Source (APS). The combination of the x-ray optics and the detector will allow a minimum set-up time and 2-5 hour (per injection condition) testing time.
- Conduct the diesel spray measurements under the conditions similar to a realistic cylinder pressure (2 MPa) and temperature (500°C transient) progressively.
- Develop 2-D multiphase models for realistically simulating the spray core and atomization near the injection nozzles.

## Introduction

In most cases, high-pressure diesel fuel sprays are optically dense, or the liquid droplets generated by the sprays scatter light so strongly that the detailed structure of the sprays cannot be resolved by conventional optical means. This is especially true in the region near the injection nozzle, which is often the region of greatest interest in understanding the structure and the dynamics of the spray. The lack of quantitative, time-resolved analysis on the structure and dynamics of sprays limits the accuracy of spray modeling and creates obstacles to improving spray technology. The synchrotron x-rays generated at the APS offers a new paradigm in engine fuel spray diagnostics. Experiments conducted by Argonne scientists and engineers in the areas of diesel fuel-spray characteristics using x-rays (Science, 295, p1261, 2002) have shown that x-rays can go far beyond the limits of lasers in combustion diagnostics. By using fast a 2-D x-ray detector and appropriate x-ray optics, we have proved that the x-ray measurement can be performed efficiently and the technique is practical for industrial applications in nozzle diagnosis and spray modeling. With more efficient experimental methods, it is possible now to study the sprays under various injection conditions in a single experiment run. In addition, the advantage of x-ray-based research to the study of fuel sprays has been clearly shown at atmospheric pressure. The need to perform the spray test under realistic engine conditions has become eminent.

## Approach

This research will quantify diesel fuel spray characteristics using monochromatic x-radiography. In the past, we used point-by-point measurement of monochromatic x-ray absorption to quantitatively characterize the dynamics and structure of high-pressure diesel spray jets with unprecedented resolution. However, this point-scanning method would be laborious if it were necessary to scan the much more spatially extended sprays or image shockwaves, which are typically a few centimeters across yet exhibit evolving submillimeter structures. In addition, without two-dimensional imaging capability, it is impractical to perform tomographic-type measurements to interrogate the asymmetric and highly transient sprays, which require many images taken from various orientations. The fuel spray was generated using a high-pressure injector typical of that in current diesel engines. In most of cases, the diesel fuel used in the test was doped with a cerium-containing additive in order to increase its x-ray absorption. Injection was performed into a spray chamber filled with inert gas at atmospheric pressure and at room temperature. Sulfur hexafluoride ($SF_6$), a very heavy gas, was used to create a relatively dense ambient environment in the injection chamber. Testing was also done using nitrogen in a pressurized chamber at 2 bar and room temperature. The pressurized chamber was fitted with x-ray transparent windows. The experiments were performed at either the 1-BM beamline of the Synchrotron Radiation Instrumentation Collaborative Access Team (SRI-CAT) at APS or the D-1 line at the CHESS (Cornell High Energy Synchrotron Source) with 6 keV x-ray beams.

## Results

The direct imaging and the quantitative analysis of the shock waves have become possible with highly

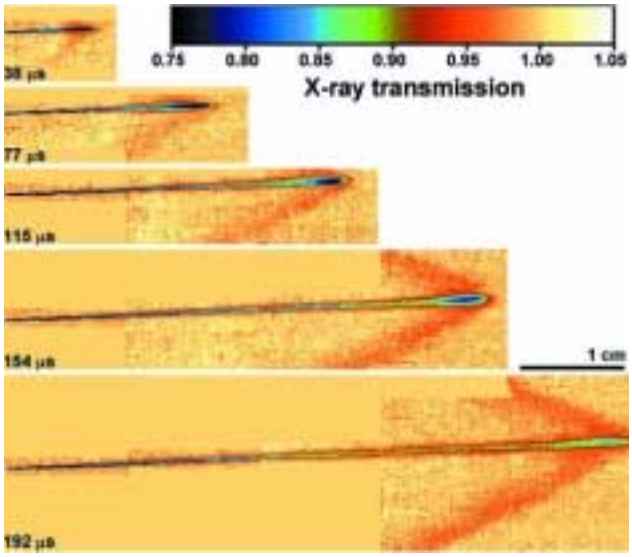


**Figure 1.** Time-resolved radiographic images of fuel sprays and the shock waves generated by the sprays for time instances of 38, 77, 115, 154 and 192 μs after the starting of the injection (of the 168 frames taken). The imaged area shown in the largest panel is 61.7 mm (horizontal) x 17.5 mm (vertical) with data corrected for the divergence of the x-ray beam.

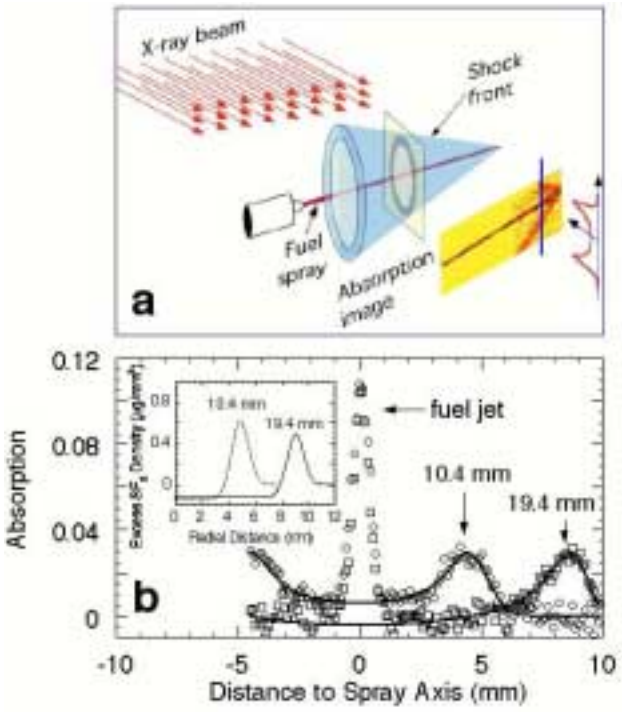


**Figure 2.** Quantitative analysis of the radiographic images of the Mach cone: the method of the data collection (a), and deconvolution of data by the line-of-sight approach (b). The absorption data were taken at two vertical lines at 10.4 (squares) and 19.4 mm (circles) behind the spray leading edge while it arrived at 60 mm from the nozzle at the instance of 192 μs after the injection. The peak at 0 mm is due to the absorption of the fuel jet and was ignored for the deconvelution modeling.

brilliant synchrotron x-ray sources and the advent of the pixel array detector (PAD). Figure 1 shows a series of x-radiographs of the fuel spray for times ranging from 38 to 192 μs after the beginning of the injection process. Here, the fuel injection pressure was set to 135 MPa, resulting in maximum leading edge speeds of 345 m/s. The leading-edge speed exceeds the sonic speed upon emergence. The shock wave front, or the so-called Mach cone, is clearly observed as emanating from the leading edge of the fuel jet soon after emergence with an x-ray absorption of up to 3% in the shock front.

The quantitative nature of the x-radiograph technique allows us not only to observe the qualitative dynamic evolution of the shock waves but also to derive thermodynamic parameters of interest such the mass density distribution of gas near and inside the Mach cone. Although radiography has long been used to study shocks in laser/solid interactions, to the best of our knowledge, this is first time that x-radiography has been applied to directly image and quantify the thermodynamic parameters of shock waves generated by liquid jets in a gaseous medium. A schematic showing the principle of the deconvolution analysis is shown in Figure 2a, and the model-dependent data fitting is highlighted in Figure 2b, along with the best fitting model (inset to Figure 2b). The model shows that, in the plane perpendicular to the jet axis, the shocked region is a cone with an excess density in the $SF_6$ of 0.7 μg/mm$^3$, measured 10.4 mm from the spray tip. Behind the high-density region, the interior of the cone has a small but observable reduction in the gas density from the ambient, which implies that the temperature should be high enough to generate the pressure higher than the ambient (0.1 MPa). Although an independent measurement of the pressure and temperature near the Mach cone is needed to completely characterize the shock waves, the mass distribution of gas near the shock front has never

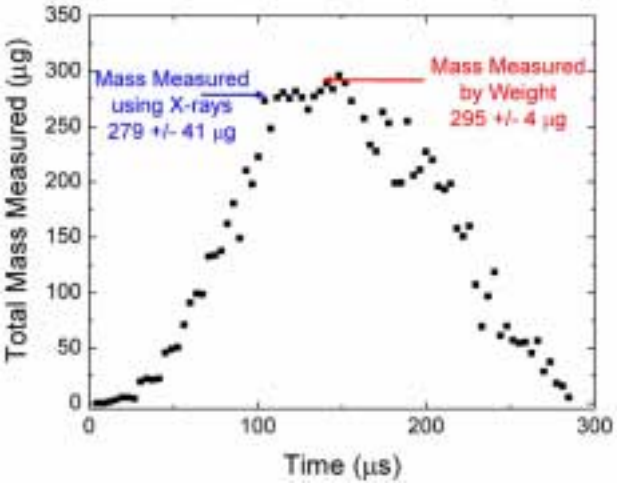


**Figure 3.** Fuel mass evaluated by x-radiography and a simple weighing method. The mass value from the latter is a result of the average of 1000 injection. Note that after 150 µs, spray starts to evaporate and leave the x-ray measuring scope.

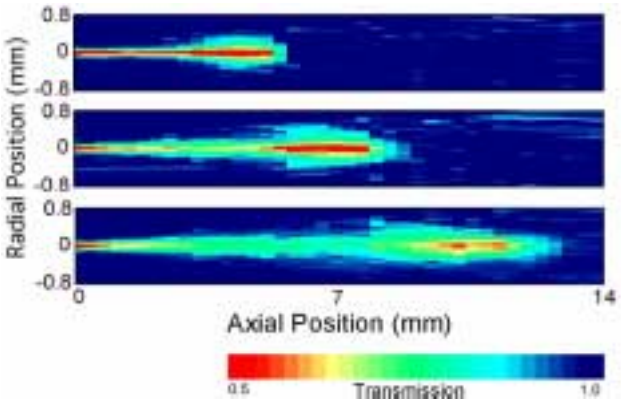


**Figure 4.** X-radiographs of diesel fuel jet injected to the pressurized chamber (2-bar) collected through the x-ray transparent window. Injection pressure was set at 1000 bar. Similar measurement was also performed at 1-bar ambient pressure, in which spray traveled at significantly higher speed.

been measured by any other means. The properties of shock waves have been studied at various injection conditions, such as different injection pressures (20 to 100 MPa), different ambient gas in the injection chamber, and different fuel compositions.

Time-resolved x-radiography determines the mass flow rate and the total mass of a spray. However, the quantitativeness and accuracy of the measurement had not been verified by an independent method. In a recent study, we measured the fuel mass distribution and fuel mass flow by using the x-ray method after the diesel fuel was injected. In the meantime, the total injected fuel mass was measured by simply weighing after each injection at same conditions as the x-ray measurement was performed. The mass value measured by x-radiography agrees with the value by weighing within 5% accuracy (Figure 3). The sensitivity and selectivity of the measurement to the spray core has been demonstrated.

By using a pressurized chamber equipped with an x-ray-transparent window (developed with ANL internal funding), an x-radiographic measurement of fuel sprays using nitrogen at 2-bar pressure was conducted successfully for the first time, as shown in Figure 4. A drastic difference in the dynamics of the spray, such as reduction in spray speed compared to the results obtained in the spray chamber with 1-bar fill gas, was observed. More detail data analysis is in progress and will be completed within FY 2002.

## Conclusions

We have demonstrated that the high-pressure fuel sprays are supersonic and that the Mach cone generated by the supersonic sprays in the gaseous medium can be directly imaged and quantitatively analyzed by x-radiography. Although the mannerin which the shock waves affect the atomization of the fuel and the combustion processes are currently unknown, the results will likely draw the attention of spray and combustion researchers to investigate the effects. To address the quantitativeness and the accuracy of the x-radiographic technique in determining fuel mass, the mass value has been compared to that obtained by an independent method with a discrepancy smaller than 5%. Most importantly, in FY 2002, we demonstrated that the x-radiography of fuel sprays is possible in a pressurized chamber. More systematic study of fuel sprays are being conducted and will become the focus of research in the next few years.

## FY 2002 Publications

1. Quantitative Measurements of Diesel Fuel Spray Characteristics in the Near-Nozzle Region by Using X-Ray Absorption, Y. Yue, C.F. Powell, R. Poola, and J. Wang, J.K. Schalle, Atomization Sprays, Vol. 11, 471 (2001).

2. X-ray Imaging of Shock Waves Generated by High-Pressure Fuel Sprays, A.G. MacPhee et al., Science, Vol. 295, 1261 (2002).

3. Shock Waves Generated by High-Pressure Fuel Sprays Directly Imaged by X-rays, SAE Paper 2002-01-1892.

## Awards

1. National Laboratory Combustion & Emissions Control R&D Award, U.S. DOE, May 2002.

2. Outstanding Mentor, Siemens Foundation, March 2002.

3. Mentor recognition, The College Board, February 2002.

# F. Design and Development of a Pressure Reactive Piston (PRP) to Achieve Variable Compression Ratio

*John Brevick (Primary Contact)*
*Ford Motor Company*
*Transmission/Driveline Research & Development*
*Fairlane Program Center-B, Cube 2CE11, MD 55*
*Dearborn, Michigan 48126-2720*

*DOE Technology Development Manager: Ken Howden*

*Main Subcontractors: University of Michigan, Ann Arbor, Michigan and Federal-Mogul Corporation, Plymouth, Michigan*

This project addresses the following DOE R&D Plan barriers and tasks:

*Barriers*

A. NOx Emissions

C. Costs

*Tasks*

2. Sensors and Controls

3a. Identification of Advanced Combustion Systems

## Objectives

- Develop and demonstrate a pressure reactive piston for a spark-ignited (SI) engine
- Develop and demonstrate a pressure reactive piston for a compression-ignited (CI) engine
- Quantify engine efficiency and emission effects due to the pressure reactive piston (PRP)

## Approach

- SI and CI engine simulation analysis
- SI and CI single cylinder engine baseline testing
- PRP spring design
- PRP dynamic analysis
- PRP design
- PRP component mechanical, thermal, and dynamic stress analysis
- SI and CI PRP prototype manufacture
- SI and CI PRP single cylinder engine testing

## Accomplishments:

- SI and CI baseline engine simulation analysis
- SI and CI baseline engine simulation correlation to test data complete
- SI and CI engine simulation code modified to include the PRP degree of freedom

- SI and CI engine simulation efficiency predictions with the PRP, piston limits and desired spring rates/ pre-load determined
- Baseline single-cylinder engine dynamometer installation complete
- SI PRP spring design complete
- PRP dynamic analysis initiated
- SI and CI PRP design and analysis complete
- Baseline SI and CI single-cylinder engine testing complete
- SI PRP hardware complete
- SI PRP testing completed with two different spring sets (two different pre-loads); engine efficiency, emissions and noise recorded
- CI PRP hardware expected mid-September 2002

### Future Directions

- CI PRP prototype manufacture
- Refine and iterate the dynamic model
- Refine and iterate engine simulation models
- CI PRP single-cylinder engine testing

---

## Introduction

The pressure reactive piston technology is based on Ford Motor Company U.S. Patent #5,755,192 (Variable Compression Ratio Piston) granted in 1998. The PRP is a two-piece piston separated by a spring system (see Figure 1). The patent is based on work in the late 1980s to early 1990s, which resulted in hardware being run in one cylinder of a multi-cylinder engine. Although this work was promising, the efficiency and emission effects were not quantified.

Many variable compression ratio piston designs have been patented and developed to varying degrees over the history of the internal combustion engine. Most designs control the compression ratio throughout the engine cycle and vary the compression ratio on demand (e.g., through controlling the oil volume in an upper versus lower chamber in the piston). A limitation on these designs is that the rate of compression ratio change may not be adequate at times when rapid load changes are demanded on the engine. A unique feature of PRP technology is that the upper piston reacts to cylinder pressure during the power stroke of the engine; during the rest of the engine cycle, the upper piston remains in the high compression position.

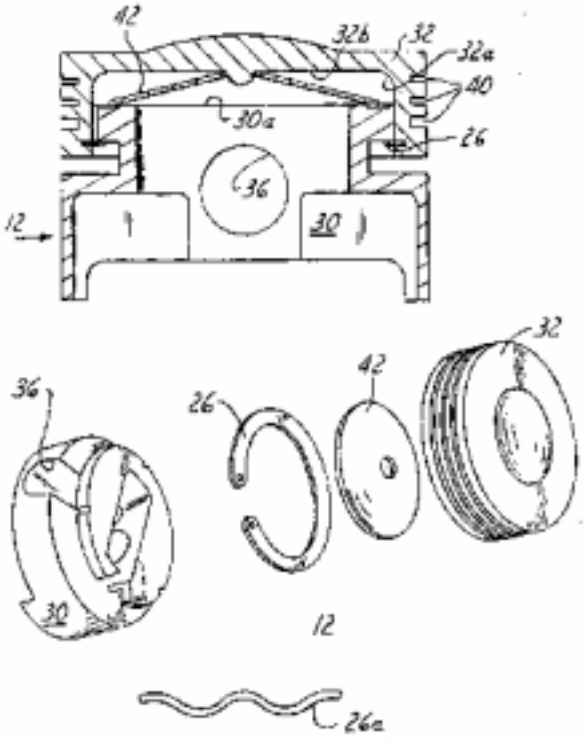


**Figure 1.** Drawing of the Pressure Reactive Piston Components

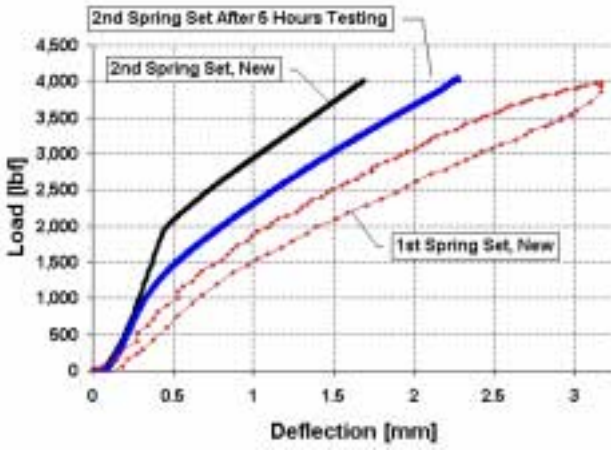


**Figure 2.** Load vs. Deflection for Two SI Spring Sets

The PRP operation strategy for an SI engine is to set the spring system preload to allow high compression (13:1) operation during partial load operation. During high engine load operation the spring system and piston geometry allow the effective compression ratio to drop (upper piston deflects relative to the piston pin) to prevent detonation or spark knock. Detonation is prevented because the peak cylinder pressure is limited by the deflection of the upper piston, controlled by the spring system. The expected result is higher engine efficiency at part load, which is typical operation for automotive engine applications. Reduced high load engine noise is also anticipated.

The PRP operation strategy for a CI engine is to set the spring system preload to allow high compression (19:1) for start-up operation. Firing loads, even light engine load operation, deflect the PRP spring system; however, high engine load operation deflects the upper piston further. This upper piston deflection controlled by the spring system reduces the peak cylinder pressure and gas temperature. The expected result is lower engine-out $NO_x$ at the same engine efficiency and power output. Lower engine friction and noise are also expected.

## Approach

For engine simulation, University of Michigan Diesel Engine Simulation and Spark Ignition Simulation codes are being utilized. The PRP dynamic modeling is being done with University of Michigan code. Spring design configuration analysis has been accomplished with University of Michigan code, based on SAE Belleville spring references. Federal Mogul (F-M) is performing finite element analysis (FEA) on the PRP, including thermal, mechanical, and dynamic loads. Functional prototypes will allow any major issue to be discovered and will accelerate resolution. Single-cylinder engine testing will correlate the engine simulation models as well as demonstrate the capabilities of the PRP. Ricardo SI and CI Hydra engines (as well as associated emission, fuel, and torque instrumentation) will be used for experimental testing at the University of Michigan.

## Results

The Ricardo Hydra spark and compression ignition single-cylinder engines, with double ended motoring dynamometer, have been installed at the University of Michigan - Lay automotive building. The SI and CI engine baseline testing have been completed, summarized and reported. The engine test data has been used to tune and correlate the engine simulation analysis.

F-M has completed the analysis and design of the SI and CI pressure reactive pistons. Detail drawings have been completed for all PRP components. All SI PRP hardware has been completed, including: upper and lower piston, spring set, retaining ring, piston pin, and rod. F-M manufactured the upper and lower piston; Associated Spring manufactured the Belleville spring set, spacer ring, and retaining ring. A second SI spring set (and revised retaining ring) was manufactured also to allow testing of two different pre-loads. Ford modified the Ricardo Hydra piston pin and rod to be compatible with the PRP.

Two spring sets were run on the SI PRP. A comparison of the load deflection characteristics of the two spring sets is shown in Figure 2. Note that the pre-load on the second spring set was approximately 2,000 lbs, where on the first spring set the pre-load was negligible. As will be shown below the second spring set with higher pre-load showed efficiency improvement over the first spring set (with negligible pre-load). The 2nd spring set was run in the engine for approximately 5 hours, and the load

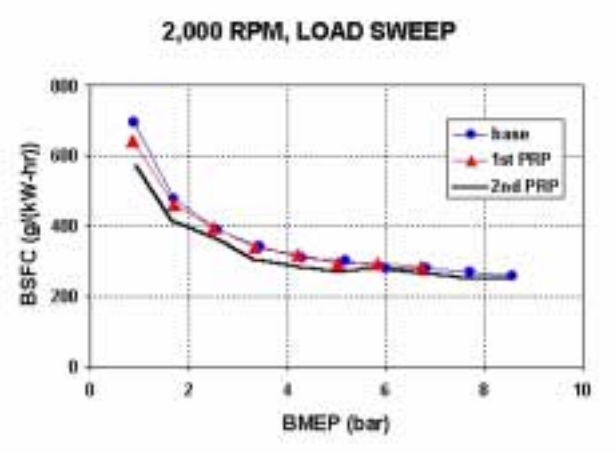


**Figure 3.** BSFC for the Base SI Engine and with the Two PRP Spring Sets

deflection characteristic was again measured. The pre-load dropped to the 1,000 lb range. The following test results were run as the "2nd spring set", with approximately a 1,000 lb pre-load.

Table 1 lists the speeds and loads used for engine testing.

**Table 1.** Engine Test Speed/Load Points

| Mode | Speed (rpm) | Load (bar) |
|---|---|---|
| 2 | 1,500 | 2.66 |
| 3 | 2,000 | 2.0 |
| 4 | 2,300 | 4.16 |

Engine test results with the second spring set show BSFC improvement over the base engine (PRP with the first spring set is shown for reference) through the 2,000 rpm load sweep up to 60% load and are shown in Figure 3. The BSFC improvement over base with the SI PRP (second spring set) ranged from 7 to 18%. For example, the engine efficiency at 10% load is 11.7% (BSFC 697 g/kW-hr) with the base piston, but 14.3% efficient (BSFC 573 g/kW-hr) with the PRP. At 50% load the engine efficiency is 25.6% (BSFC 320 g/kW-hr) with the base piston, but 28.9% efficient (BSFC 283 g/kW-hr) with the PRP. Note that efficiency improvements at these light loads are very significant in automotive applications, as most of the time is spent driving at light load conditions.

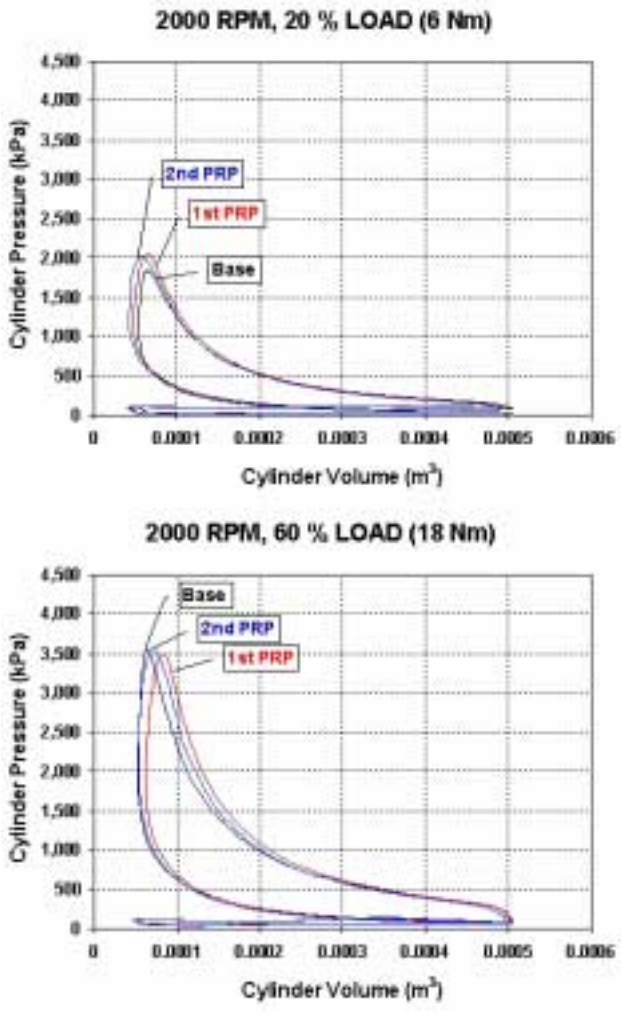


**Figure 4.** Cylinder Pressure vs. Volume Graphs

Engine testing demonstrated the capability of the SI PRP to develop full torque (at least at 2,000 rpm), similar to the base engine. This is very significant, in proving the PRP concept, as both part load efficiency and full load torque has now been demonstrated. Digital sound was recorded on the base SI engine as well as the SI PRP during the 2,000 rpm load sweep. No identifiable noise associated with the SI PRP was noted. A jury tape will be made to allow direct sound comparison of the base to the PRP.

Pressure versus volume curves of the base, and the SI PRP with the first and second spring sets are shown in Figure 4 at 2,000 rpm 20 and 60% load. Note that both PRP runs have higher peak pressure than baseline at 20% load, but very similar peak

pressures at 60% load. Note also that the cylinder volume versus crankshaft position relationship changes with the PRP and the plots shown include this additional PRP degree of freedom. The peak pressure occurs later from TDC on the 2nd PRP spring set than baseline, however BSFC is improved. Peak pressure is even farther from TDC on the 1st PRP spring set, however BSFC is not improved from baseline. These PV curves were developed with test fuel (Indolene Clear) and typical ambient conditions (no extremes to induce spark knock), and MBT was not ignition timing spark knock limited. The test engine responded well to a 1,000 lb pre-load, there is potential for further improvement in BSFC with a higher pre-load (i.e., the original intent 2,500 lb pre-load). Clearly, the most desirable pre-load with the PRP must be developed for a given engine, increasing the pre-load until unacceptable spark retard is required to prevent spark knock.

Compression ignition engine analysis has been initiated and utilized to characterize the spring set requirements. An initial spring set has been developed to provide the desired pre-load and maximum deflection load (see Figure 5). The spring loads desired for the CI engine (6,500 lbs pre-load) are much higher than the SI engine (2,500 lbs pre-load); however, the deflection of the piston is less on the CI engine (1.8 mm) than the SI engine (3.3 mm). The spring package size is very restricted on the CI engine because of the combustion bowl. To reduce spring stress and achieve the desired load deflection characteristics (6,500 lb pre-load, 8,500 lbs w/ 1.8 mm deflection), the Belleville springs were configured with stepped inner diameter (ID) and thickness. The compressive stresses are still very high and, therefore, the pre-load may have to be reduced to 4,500 lbs. The highest stress is on the top spring at the ID. Profile changes to the spring seat area of the upper piston are being considered to address these higher stresses.

The initial design of the CI PRP is shown in Figure 6. The upper piston will be made from steel, and the lower piston will be made from aluminum. The piston pin will be longer than base and used to retain the upper and lower piston. The racetrack shaped piston pin bore in the upper piston will control the compression ratio limit, and prevent the combustion bowl from rotating. Caps on the piston

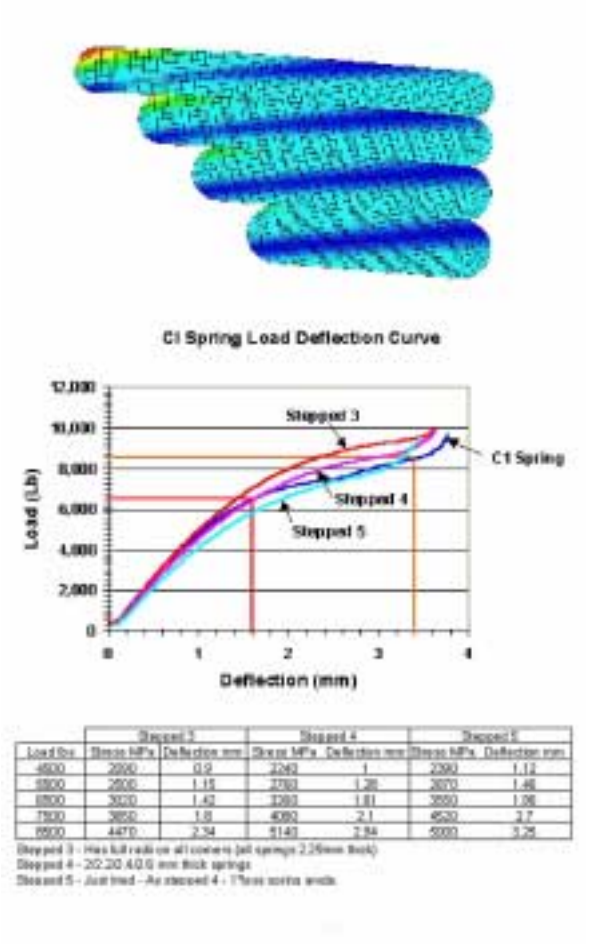


| | Stepped 3 | | Stepped 4 | | Stepped 5 | |
|---|---|---|---|---|---|---|
| Load lbs | Stress MPa | Deflection mm | Stress MPa | Deflection mm | Stress MPa | Deflection mm |
| 4500 | 2000 | 0.9 | 2240 | 1 | 2390 | 1.12 |
| 6500 | 2900 | 1.15 | 3760 | 1.28 | 3970 | 1.46 |
| 8500 | 3920 | 1.42 | 5260 | 1.81 | 5550 | 1.96 |
| 7500 | 3850 | 1.8 | 4980 | 2.1 | 4520 | 2.7 |
| 6500 | 4470 | 2.34 | 5140 | 2.84 | 5000 | 3.25 |

Stepped 3 - Has full radius on all corners (all springs 2.25mm thick)
Stepped 4 - 2@.20 4@.0 mm thick springs
Stepped 5 - Just tried - As stepped 4 - Three works well

**Figure 5.** CI PRP Spring Set Analysis

pin will utilize the cylinder bore to retain the pin in position. Features in the piston pin bore on the upper piston will provide the soft landing feature that the wavy retainer ring provides on the SI piston.

An engineering cost analysis to produce PRP pistons was completed. The variable cost increase over a standard SI piston is estimated to be in the $5.00 - $6.00 range (includes the effects of casting, machining, spring system, and piston assembly). This estimate does not include the engineering or investment costs necessary to implement this technology in production. This estimate assumes high volume production levels typical of the automotive industry.

## Conclusions/Future Directions

Initial SI PRP testing indicates 7 to 18% BSFC improvement up to 60% load. This was

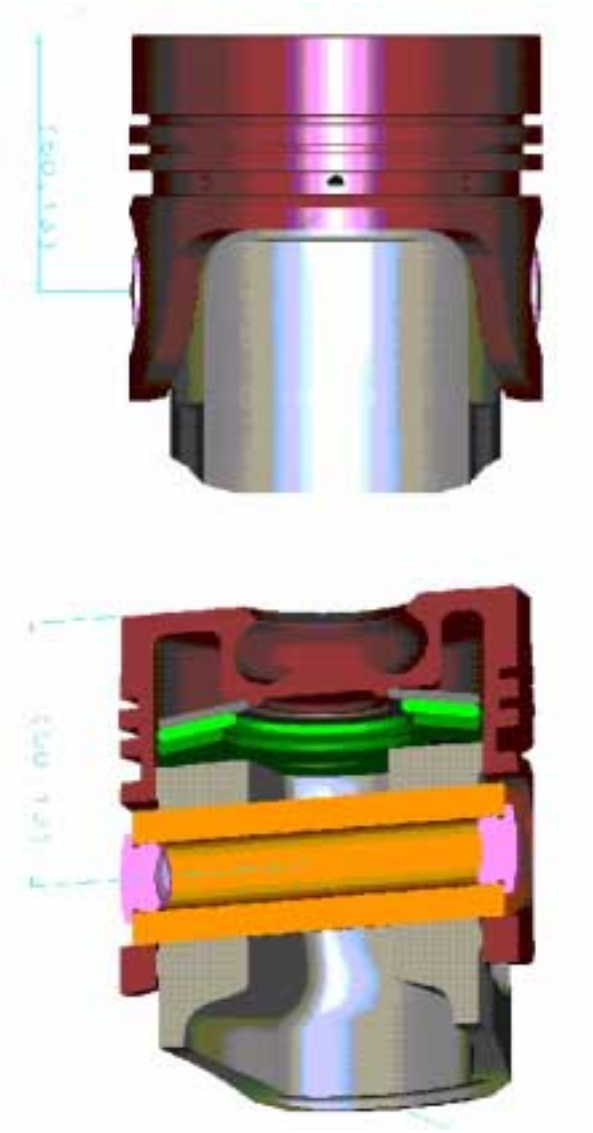

**Figure 6.** CI PRP Design

accomplished with a higher spring pre-load. Full-load capability has been demonstrated with the SI PRP. The PRP spring environment peak operating temperature can now be estimated because the upper piston was instrumented with Temp-plugs. The results of temperature measurements will be included in the final report.

We have asked for a one-year, no cost extension to the contract (September 30, 2002), and it has been approved. With this time we plan to complete the CI PRP prototype hardware and initial engine testing.

Further work (beyond the current contract) should concentrate on the spring geometry and materials. Now that the PRP has been proven in concept, lightweight and durability need to be addressed. Spring development initially needs to utilize finite element analysis to establish load/ deflection characteristics, and stress for the large number of geometries and materials possible. Producing springs and testing the durability of this springs is needed and multiple CI PRP spring pre-loads need to be tested to quantify their effect on $NO_x$ emissions. Further funding is necessary to accomplish this work.

## References

1. 2000 and 2001 DOE annual reports on the Pressure Reactive Piston

## FY2002 Publications/Presentations

1. "Simulation and Development of a Pressure Reactive Piston for Spark Ignition and Compression Ignition Engines", Jason Martz, Ryan Nelson, Jeff Sanko, University of Michigan Graduate Program

2. "Characterization of a Single Cylinder Port Fuel Injection Spark Ignition Engine", Jason Mart, University of Michigan Graduate Program

# G. Measurements of the Fuel/Air Mixing and Combustion in the Cylinder of a High Speed Direct-Injection Diesel Engine

*Chia-fon F. Lee (Primary Contact)*
*University of Illinois at Urbana-Champaign*
*1206 West Green Street*
*Urbana, IL 61801*

*DOE Technology Development Managers: Kathi Epping and Gurpreet Singh*

This project addresses the following DOE R&D Plan barriers and tasks:

*Barriers*

A. $NO_x$ Emissions

B. PM Emissions

*Tasks*

3. Identification of Advanced Combustion Systems

## Objectives

- Study fuel spray penetration, mixing, and interaction with the bowl geometry
- Visualize ignition and combustion processes
- Analyze development of soot during combustion

## Approach

- Use a previously developed optical engine to perform laser-diagnostic studies on mixing and combustion
- Apply exciplex planar laser-induced fluorescence (PLIF) to study fuel/air mixing
- Image combustion events using natural flame emission
- Apply laser-induced incandescence (LII) to study soot formation

## Accomplishments in the third year

- Performed exciplex PLIF measurements for various operating conditions
- Imaged combustion cycles for various operating conditions
- Performed LII measurements at various locations in the engine

## Future Directions

- Perform the PLIF, LII and combustion imaging measurements for a wider range of load and speed conditions and for various injection strategies

## Introduction

High-speed direct injection diesel engines must reduce $NO_x$ and soot emissions in order to meet future emissions regulations. Simultaneous reduction can be achieved through multiple injection strategies in heavy-duty diesel engines. Studies show that either simultaneous reduction of $NO_x$ and soot is possible, or the reduction of one without significant increase in the other is possible [1-4]. Similar efforts are being extended to smaller diesel engines [5, 6].

Laser diagnostics provide the means to visualize in-cylinder processes non-intrusively. The use of exciplex PLIF to track liquid and vapor phases of fuel during injection processes is a valuable resource [7, 8]. Imaging of natural flame luminosity from combustion events has garnered widespread use [9-11]. Laser-induced incandescence has been used to locate soot formation locations and concentrations [12-14]. By combining these laser diagnostics, an entire combustion event from start to finish can be analyzed.

## Approach

The optical engine was built from a single-cylinder DIATA engine supplied by Ford Motor Company. Access to the combustion chamber is attained through a side window or a fused silica piston top attached to a Bowditch piston extension. The documented results from typical operating conditions for this engine are listed in Table 1. Case 1 is for single injection operation and Cases 2 and 3 are for multiple injection operation. The corresponding in-cylinder pressure measurements are shown in Figure 1.

The engine is supplied with nitrogen and motored for all exciplex PLIF images. The first (pilot) injection event in Case 2 is imaged using an expanded laser beam. A laser sheet directed along the axis of injection is employed after 20° before top dead center (BTDC).

Combustion imaging conditions are case dependent. A combination of camera gating, lens aperture size and neutral density filters is used to keep perceived intensities from saturating the cameras.

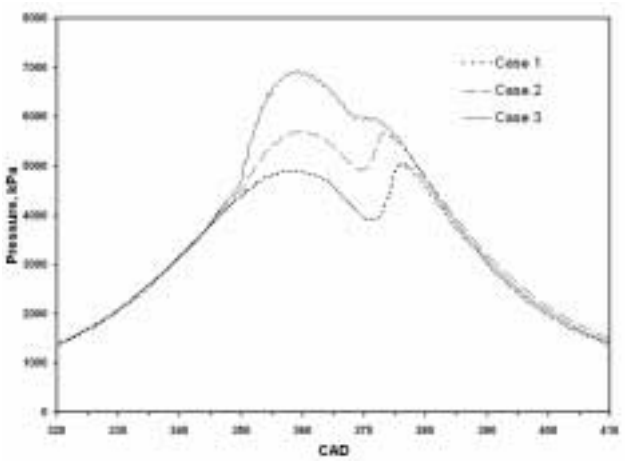


**Figure 1.** In-cylinder Pressure Traces for the Three Operating Conditions

**Table 1.** Operating Conditions for the Reported Test Cases

| | |
|---|---|
| Engine Speed | 1500 RPM |
| Rail Pressure | 600 bar |
| SOI Case 1 | $4^o$ ATDC |
| Case 1 Duration | 6 CAD |
| SOI1 Case 2 | $-30^o$ ATDC |
| Case 2 Duration 1 | 4 CAD |
| SOI1 Case 2 | $4^o$ ATDC |
| Case 2 Duration 2 | 5 CAD |
| SOI1 Case 3 | $-30^o$ ATDC |
| Case 3 Duration 1 | 5 CAD |
| SOI2 Case 3 | $4^o$ ATDC |
| Case 3 Duration 2 | 4.5 CAD |

LII is reported for Case 3. A laser sheet is directed into the opposite squish region for early timings. Late combustion soot distributions are imaged with a horizontal laser sheet.

## Results

### Exciplex Planar Laser-Induced Fluorescence

Figures 2 and 3 show the resulting exciplex images for Cases 1 and 2 respectively.

Case 1

Liquid spray impingement upon the piston is observed at 9° after top dead center (ATDC). The impingement region grows as injection continues. At

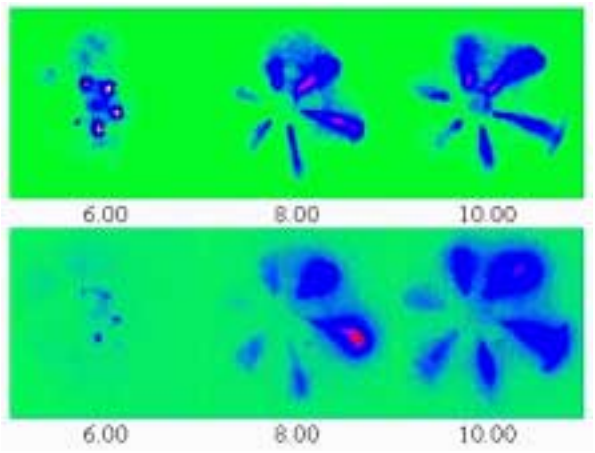


**Figure 2.** Liquid (top) and Vapor (bottom) images for Case 1. All images are the average of four separate injection events.

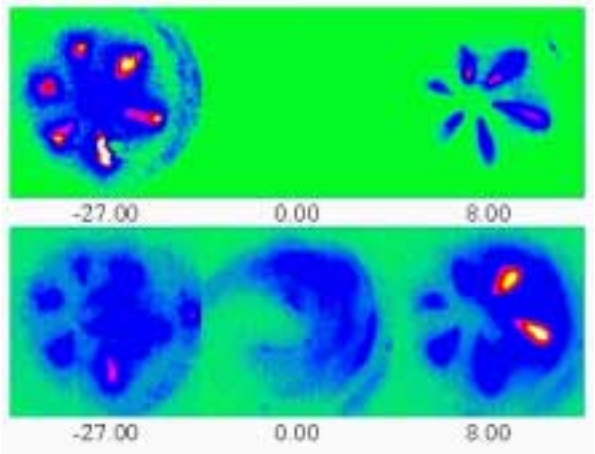


**Figure 3.** Liquid (Figure 3 - Liquid (top) and Vapor (bottom) images for Case 2. All images are the average of four separate injection events.

later times, the liquid signal in the region of impingement dissipates due to vaporization.

Early vapor images show vapor throughout the liquid jet cross-section. The structure of the vapor is slightly wider and longer than the liquid because of diffusion of the vapor. The majority of the vapor seen in these images resides within the piston bowl.

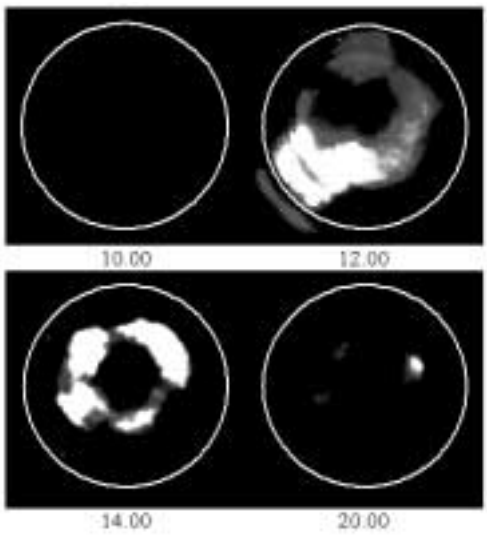


**Figure 4.** Natural flame emission images for Case 1. Circle shown is the field of view through the bottom of the piston. All images are the average of four separate injection events.

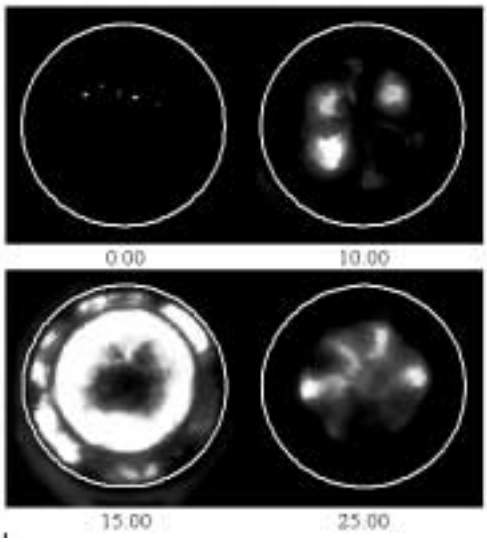


**Figure 5**. Natural flame emission images for Case 2. Circle shown is the field of view through the bottom of the piston. Top images are images of a single injection event and bottom images are the average of four separate injection events.

Case 2

Impingement on the top of the piston is observed at 25° BTDC. Total evaporation of this liquid occurs by top dead center (TDC). However, the second injection event is similar to Case 1 with noticeably less impingement.

Vapor is again seen throughout the liquid jet cross-section for both parts of the injection cycle. The vapor from the first injection event mixes prior to the second injection event and is relatively uniform near TDC. While the vapor remained within the bowl for Case 1, evidence of vapor outside of the bowl is seen for Case 2.

**Natural Flame Emission**

Figures 4, 5 and 6 show the resulting combustion images for Cases 1, 2 and 3 respectively.

Case 1

Ignition for Case 1 is seen at 9° ATDC. Flame luminosity is confined towards the leading edge of the vapor plume. The luminous combustion zone increases as the cycle continues, until the majority of the bowl region is illuminated. Luminous combustion throughout Case 1 is confined to the bowl region.

Case 2

Early luminosity is seen in Case 2 at 8° BTDC. This luminosity is visualized at spotty points occurring at various locations. Combustion from the second injection event begins slightly before 9° ATDC. Ignition occurs near the leading edge in a single jet, quickly spreading to other jets. Luminosity spreads throughout the combustion chamber including the squish region. Late cycle luminosity is found solely within the piston bowl.

Case 3

The spotty luminosity at the early time is observed similar to Case 2, and combustion from the second injection event begins slightly before 8.5° ATDC. Ignition and late cycle luminosity are also similar to Case 2. However, combustion spreads up the jet structure in a more diffusion-type burn for Case 3.

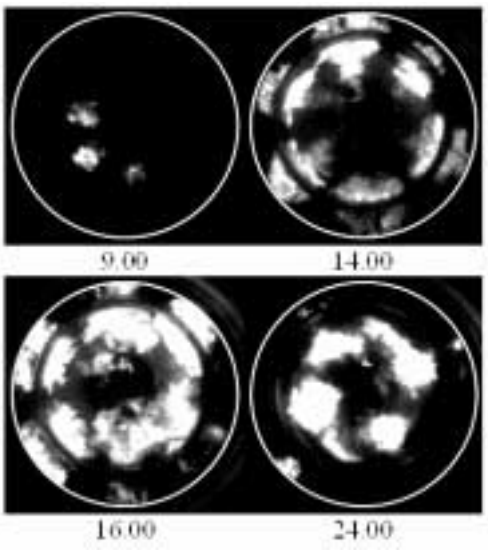


**Figure 6**. Natural flame emission images for Case 3. Circle shown is the field of view through the bottom of the piston. All images are of a single injection event.

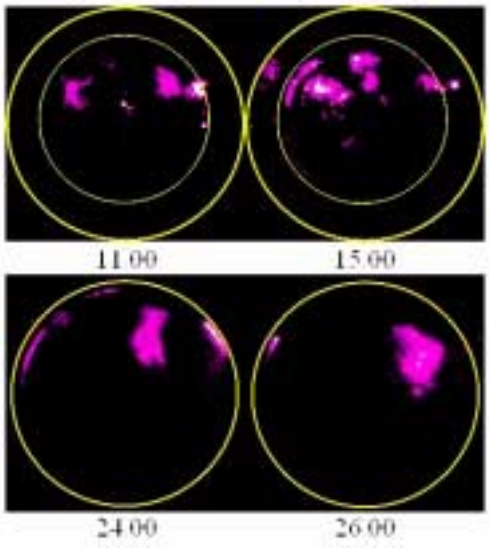


**Figure 7.** Laser-induced incandescence images for Case 3. Squish region images (top) have field of view (outside) and piston bowl region (inside) outlines. Horizontal images (bottom) have piston bowl region outlined.

**Laser-Induced Incandescence**

Figure 7 shows the resulting LII images for Case 3.

Case 3

Soot is seen to originate near the spray tip and progresses upstream near the injector. Evidence of soot is seen within the squish region. Late in the cycle, soot is seen to reside within the confines of the piston bowl.

## Conclusions

Case 1 combustion has low soot production because there is hardly any liquid remaining within the cylinder.

Case 3 combustion has higher soot production because it was a diffusion burning process.

Case 2 ignition occurs near the spray tip and slowly progresses inward, with no evidence of burning around the jet structures.

The main advantage to employing exciplex fluorescence over the other diagnostic techniques is that it allows for simultaneous imaging of liquid and vapor distributions. Most other techniques can't separate a vapor signal from a liquid signal.

Other techniques used to image soot distributions are often line-of-sight integrations and subsequently lack of spatial resolution. Laser-induced incandescence allows for a planar distribution of soot volume fractions to be measured.

This project indicates that for lowering PM, ignition occurring later in the cycle is preferable. This allows a longer time for fuel/air mixing and thus less locally rich regions burning in which to form soot.

## References

1. Nehmer, D. A. and Reitz, R. D., SAE Paper 940668, (1994)

2. Tow, T., Pierpont, A. and Reitz, R. D., SAE Paper 940897, (1994)

3. Pierpont, D. A., Montgomery, D. T. and Reitz, R. D., SAE Paper 950217, (1995)

4. Han, Z., Uludogan, A., Hampson, G. J. and Reitz, R. D., SAE Paper 960633, (1996)

5. Chen, S. K., SAE Paper 2000-01-3084, (2000)

6. Badami, M., Millo, F. and D'Amato, D. D., SAE Paper 2001-01-0657, (2001)

7. Bardsley, M. E. A., Felton, P. G. and Bracco, F. V., SAE Paper 880521, (1988)

8. Campell, P. H., Sinko, K. M. and Chehroudi, B., SAE Paper 950445, (1995)

9. Miles, P. C., SAE Paper 2000-01-1829, (2000)

10. Arcoumanis, C., Cho, S. T., Gavaises, M. and Yi, H. S., SAE Paper 2000-01-1183, (2000)

11. Winterbourne, D. E., Yates, D. A., Clough, E., Rao, K. K., Gomes, P. and Sun, J-H., Proc. Instn. Mech. Engrs., Pt. C, Vol. 208, pp. 223-240, (1994)

12. Dec, J. E., zur Loye, A. O. and Siebers, D., SAE Paper 910224, (1991)

13. Dec, J. E. and Espey, C., SAE Paper 922307, (1992)

14. Dec, J. E., SAE Paper 920115, (1992)

## FY 2002 Publications/Presentations

1. Mathews, W. S., R. E. Coverdill, C. F. Lee, and R. A. White, "Effects of Multiple Injection on Liquid and Vapor Fuel Distribution in an HSDI Engine", Proceedings of the 15th Annual Conference on Liquid Atomization and Spray Systems, Madison, WI, May 2002.

2. Mathews, W. S., R. E. Coverdill, C. F. Lee, and R. A. White, "The Influence of Multiple Injection on HSDI Diesel Combustion", Proceedings of the 15th Annual Conference on Liquid Atomization and Spray Systems, Madison, WI, May 2002.

3. Mathews, W. S., R. E. Coverdill, C. F. Lee, and R. A. White, "Liquid and Vapor Fuel Distributions in a Small-Bore Direct-Injection Diesel Engine", SAE Paper 2002-01-2666, Powertrain & Fluid Systems Conference, San Diego, CA, Oct. 2002.

4. "Effects of Multiple Injection on Mixing and Soot Formation in a HSDI Engine", presented at DOE/University Meeting, Sandia National Laboratory, Livermore, CA, Jan. 2002.

5. "Combustion and Soot Visualization in an HSDI Diesel Engine", presented at DOE/University Meeting, USCAR, Southfield, MI, June 2002.

# H. Computational Studies of High Speed Direct Injection (HSDI) Diesel Engine Combustion

*Jay Keller (Primary Contact), Rolf D. Reitz and Chris Rutland*
*Combustion Research Facility MS 9053*
*Sandia National Laboratory*
*Livermore, California 94550*

*DOE Technology Development Manager: Gurpreet Singh*

This project addresses the following DOE R&D Plan barriers and tasks:

*Barriers*

A. $NO_x$ Emissions

B. PM Emissions

*Tasks*

3. Fundamental Combustion R&D

## Objectives

- The purpose of this project was to investigate turbulent combustion processes in a small bore CIDI engine. The project investigated the effect of multiple injections at high exhaust gas recirculation (EGR) levels for NOx control through the use of experiments and advanced chemistry models and turbulence models.
- Perform engine experiments for optimization of fuel injection as a function of engine operating conditions including various swirl levels.
- Develop computational models to simulate $NO_x$ formation. Test models against a wide range of engine results.
- Formulate and test turbulent combustion models with both global and detailed engine data.

## Approach

- Perform engine experiments on a high speed direct injection (HSDI) diesel engine to study the effect of multiple injections and swirl on emissions.
- Use the HSDI engine for optimization of fuel injection timing, boost pressure and EGR levels for $NO_x$ reduction.
- Determine the factors that control $NO_x$ formation using detailed chemistry and computational fluid dynamics (CFD) modeling.
- Use large eddy simulation (LES) turbulent combustion models with validation on both global and detailed engine data.

## Accomplishments

- A response surface method (RSM) was used with the engine experiments to identify boost pressure, EGR and late injection combustion parameters that lead to optimal low-emissions performance.
- The engine experiments revealed that flow field factors beyond engine swirl level influence engine emissions with multiple injection.

- Detailed chemistry modeling was coupled with CFD modeling to successfully predict low $NO_x$ engine operation with compression ignition combustion.
- A new large eddy turbulence model has been developed and successfully applied to predict diesel engine combustion.

## Introduction

This is the final report of a University of Wisconsin project that consisted of experiments and modeling work to provide a better understanding of direct-injection engine fluid motion, fuel/air mixing, and combustion. The work focused on compression ignited, direct injection (CIDI) engines. A goal of the research was to provide increased understanding of the important in-cylinder fluid dynamics and HSDI diesels. This understanding is critical to the performance of efficient, science based engine optimization.

## Approach

The project investigated the effect of various fuel injection strategies at high exhaust gas recirculation (EGR) levels for $NO_x$ control through the use of engine experiments and advanced chemistry and turbulence models. Emissions measurements were made using a 0.5 L HSDI diesel engine that features a common rail fuel injection system and intake flow port configurations with various combinations of tangential and helical port geometries for swirl control [1]. The CHEMKIN detailed chemistry model was combined with the KIVA code for the detailed emissions computations. A new LES model has been incorporated in the KIVA code and successfully applied for diesel combustion predictions.

## Results

Task 1: Engine experiments for HSDI engine optimization S Our previous response surface optimization studies have demonstrated the emission reduction capability of EGR on a HSDI diesel engine equipped with a common rail injection system [1]. The RSM optimization identified low-temperature and premixed combustion characteristics, i.e., the modified kinetics (MK) combustion region, resulting in simultaneous reductions in $NO_x$ and particulate matter (PM) emissions without sacrificing brake specific fuel consumption (BSFC).

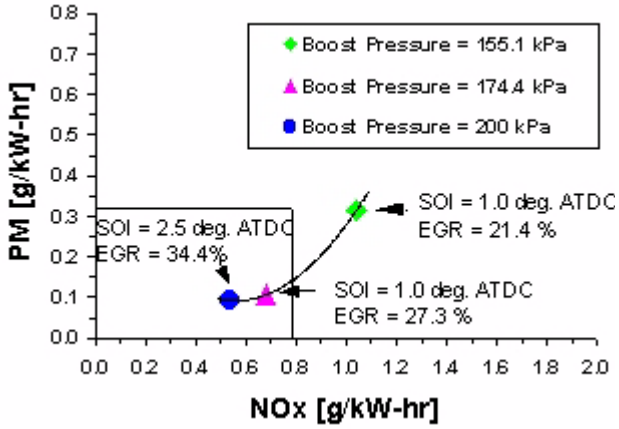


**Figure 1.** Measured Effect of Start of Ignition (SOI), Boost Pressure and EGR on HSDI Engine Emissions

The increase of intake boost pressure shortens ignition delay, which is not favorable for MK combustion, but it allows extension of the operability region. In the present study, $NO_x$ emissions were reduced by 74%, and even with heavy EGR and retarded injection timing, it was possible to keep PM emissions and BSFC at nearly the same levels. At the optimized operating conditions, CO and total hydrocarbon (THC) emissions were 4.79 and 0.21 g/kW-hr, respectively. These levels are also within the EPA Tier II 2004 automotive diesel mandates (6.72 g/kW-hr CO and 0.49 g/kW-hr THC). Figure 1 shows that higher intake boost pressure requires the use of more EGR and later injection timings, which intensifies the characteristics of MK combustion, i.e., lower-temperature and more thoroughly premixed combustion characteristics. It was found that application of the RSM was difficult in the vicinity of the late injection MK combustion region when the intake boost pressure was included as an independent factor in a factorial design, because misfire and unstable engine operation made it difficult for the RSM to locate a better optimum point in the MK combustion region under high boost conditions.

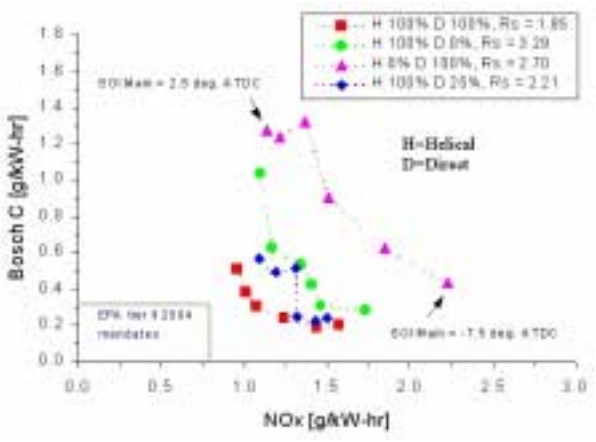


**Figure 2.** Measured Effect of Swirl on HSDI Engine Emissions

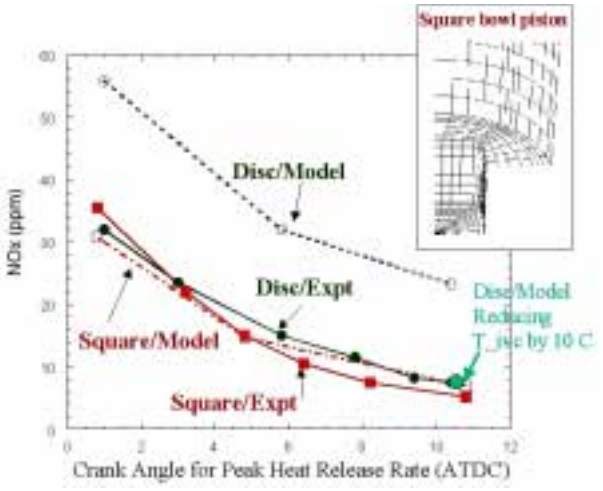


**Figure 3.** Experimental and Predicted $NO_x$ Emissions for Various Conditions

It has been recognized that engine emission levels depend greatly on swirl due to its mixing characteristics. Four different port variations were chosen to investigate the effects of swirl ratio on engine emissions and BSFC. Injection pressure, EGR rate, dwell between injections, and the amount of fuel in the pilot injection were kept at an optimum level. The results show that intake generated flows have a significant effect on emissions. In particular, Figure 2 indicates that flow effects on engine emissions cannot be correlated simply by a single parameter, such as a swirl ratio (Rs).

Task 2: Develop computational models to simulate $NO_x$ formation S In order to determine the factors that control $NO_x$ formation, detailed chemistry modeling was applied to homogeneous charge compression ignition (HCCI) engine combustion. The KIVA/CHEMKIN model was applied to simulate combustion in a premixed HCCI engine using iso-octane [2]. The experiments studied the effects of turbulence on HCCI combustion by using two pistons with different geometry, namely a disc shape and a square bowl piston (see Figure 3). The square bowl piston is known to generate more turbulence. The engine was operated at 1200 revolutions/min and with equivalence ratio of 0.4 under various heated intake conditions. An iso-octane mechanism with $NO_x$ chemistry consisting of 101 species and 499 rea ctions was used. The present model is capable of simulating HCCI combustion by considering the effect of flow turbulence on reaction chemistry. The turbulence levels and the combustion phasing in both geometries were predicted reasonably well. The trend in the $NO_x$ emission was also reproduced by the model, as shown in Figure 3. The computations show that the high turbulence in the square bowl case enhances the wall heat flux and consequently prolongs the combustion duration. The results indicate that it is necessary to integrate detailed chemistry to the CFD code for combustion simulations so that the flow and combustion can be coupled. It was also found that the ignition timing is very sensitive to the wall heat flux predictions as well as the initial conditions such as initial mixture temperature. As can be seen from Figure 3, a 10 K decrease in the initial temperature resulted in a large reduction in predicted $NO_x$ emissions. An accurate estimate of initial mixture conditions is also crucial to the model predictions.

Task 3: Formulate and test turbulent combustion models S Large eddy simulation (LES) models were developed and adapted for use in diesel in-cylinder CFD calculations in this task. The general approach was based on the dynamic structure LES approach developed by Pomraning and Rutland [3]. The work under the current project focused on combustion models and the scalar transport models that support the combustion modeling. The general approach in the combustion models is called the 'flamelet time scale' (FTS) model. This is a combination of flamelet approaches and the time scale approach. The flamelet component provides the capability for

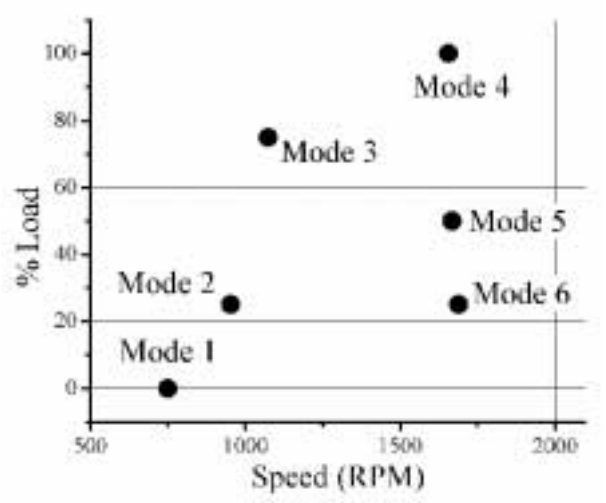


**Figure 4.** 6-Mode Emissions Test Speed/Load Points

more complex chemical reaction schemes, and the time scale component modifies the flamelet solution to account for unsteady, non-equilibrium effects. In the method, flamelet libraries are generated off-line using the OPPDIF code. These libraries require the mean mixture fraction, the mixture fraction variance, the scalar dissipation (or stretch rate), and the EGR rate. Scalar mixing models using the LES approach were developed for modeling the transport of the mean mixture fraction and its variance. An improved expression for the stretch rate in the flamelet solution was developed using the scalar dissipation rate from the mixture fraction equations and the LES formalism. Recent improvements have been made in the time scale so it is now obtained directly from the flamelet solution instead of from an Arrhenius expression. The result is a model that compares very well with experimental data over a wide range of operating conditions in a heavy-duty diesel engine, as shown in Figures 4, 5a, and 5b (Rao, Pomraning, and Rutland [4] and Rao and Rutland [5]).

## Conclusions

Task 1: Engine experiments for HSDI engine optimization S The engine experiments show that by using late injection and high EGR (MK-type combustion), $NO_x$ emissions could be reduced by 74% while keeping PM, CO and HC emissions consistent with EPA tier II 2004 automotive diesel mandates. In addition, the results show that intake

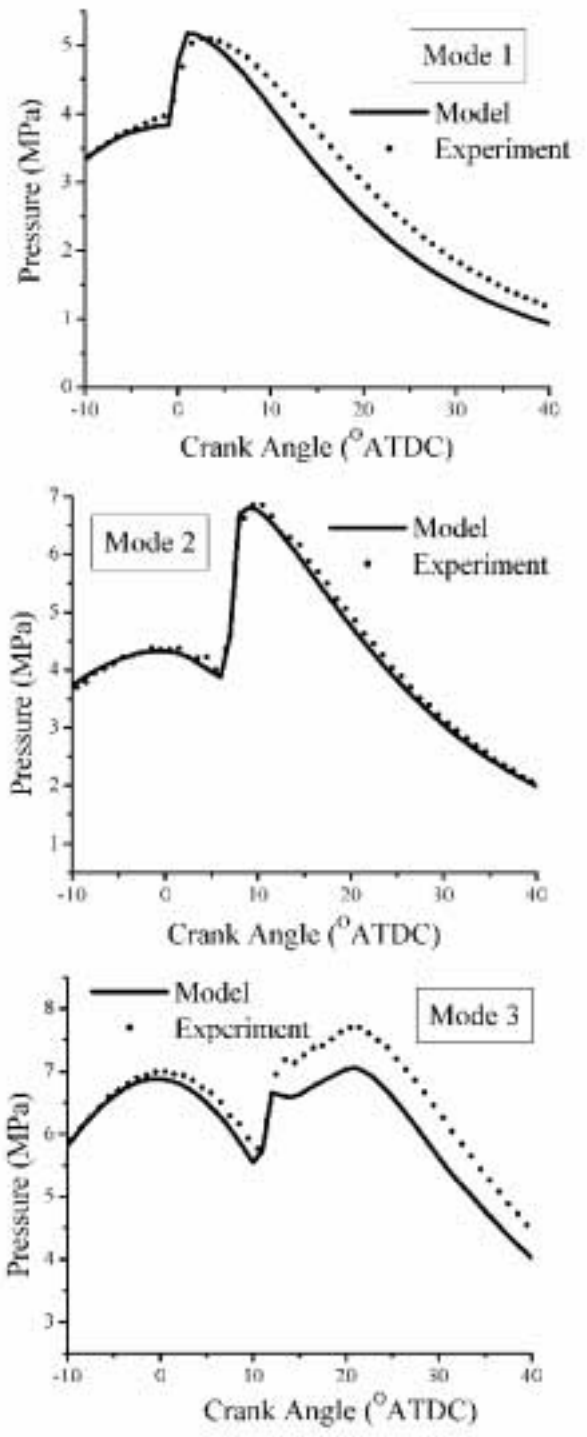


**Figure 5a.** 6-Mode Emissions Test S Comparison of Measured and Predicted Cylinder Pressure Traces Using an LES Turbulent Combustion Model (Modes 1, 2, & 3)

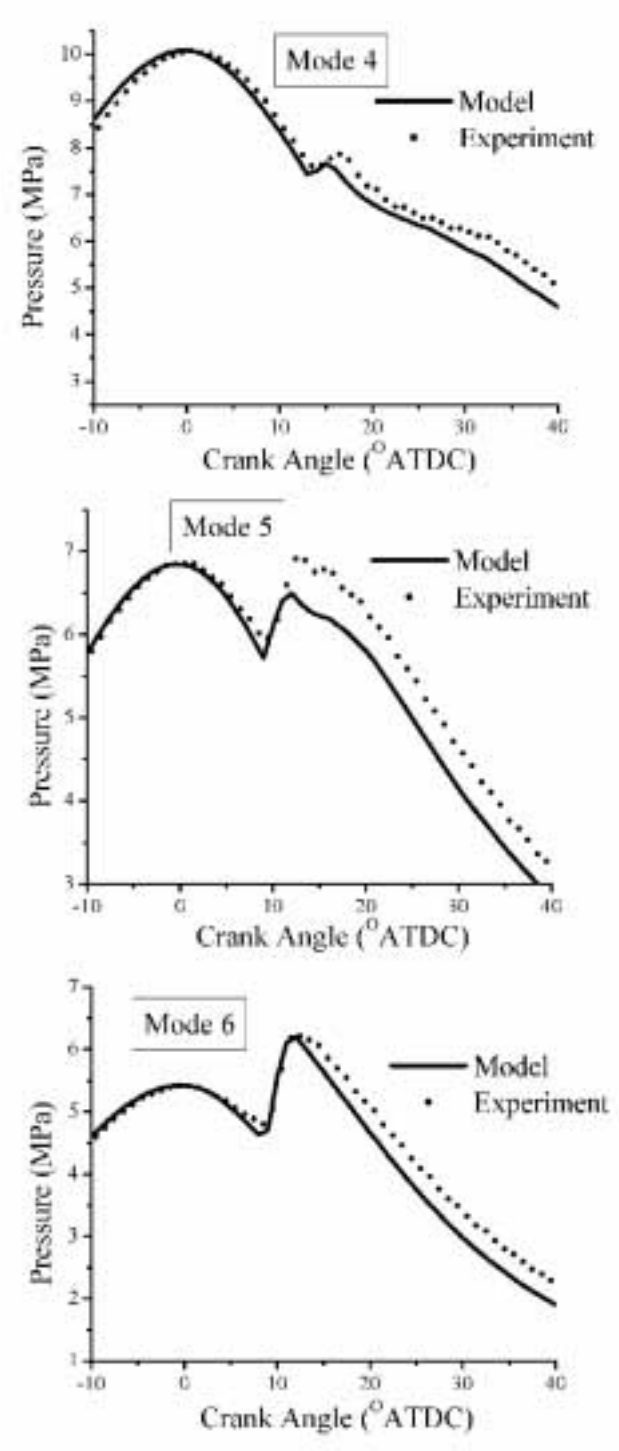


**Figure 5b.** 6-Mode Emissions Test S Comparison of Measured and Predicted Cylinder Pressure Traces Using an LES Turbulent Combustion Model (Modes 4, 5, & 6)

generated flows have a significant effect on emissions, and this requires further study.

Task 2: Develop computational models to simulate $NO_x$ formation S It was found that measured compression-ignition engine $NO_x$ emission data was well reproduced by the combined KIVA/ CHEMKIN model. It was also found that the ignition timing is very sensitive to the wall heat flux model, as well as to the initial conditions such as the initial mixture temperature.

Task 3: Formulate and test turbulent combustion models S A new LES model has been integrated into engine computations, and the model results compare very well with experimental data over a wide range of operating conditions in a heavy-duty diesel engine.

## References

1. Lee, T., and Reitz, R.D. "Response Surface Method Optimization of a HSDI Diesel Engine Equipped with a Common Rail Injection System," Accepted ASME Journal of Gas Turbines and Power, 2002.

2. Christensen, M. and Johansson, B. "The Effect of Combustion Chamber Geometry on HCCI Operation," SAE 2002-01-0425, 2002.

3. Pomraning, E. and Rutland, C.J, 2002, "A Dynamic One-Equation Non-Viscosity LES Model," AIAA Journal, Vol. 40, No. 4, pg. 689-701.

4. Rao, S., Pomraning, E., and Rutland, C. J., 2001, "Development of Advanced Combustion Models for Diesel Engines Using Large Eddy Simulation," Second Joint Meeting of the US Sections of the Combustion Inst., Oakland, CA March 26-28, 2001.

5. Rao, S. and Rutland, C.J., 2002, "A Flamelet Time Scale Model for Non-Premixed Combustion Including Unsteady Effects," submitted to Comb. and Flame.

## FY 2002 Publications/Presentations

1. Lee, T., and Reitz, R.D. "Response Surface Method Optimization of a HSDI Diesel Engine Equipped with a Common Rail Injection System," Accepted ASME Journal of Gas Turbines and Power, 2002.

2. Pomraning, E. and Rutland, C.J, 2002, "A Dynamic One-Equation Non-Viscosity LES Model," AIAA Journal, Vol. 40, No. 4, pg. 689-701.

3. Rao, S., Pomraning, E., and Rutland, C. J., 2001, "Development of Advanced Combustion Models for Diesel Engines Using Large Eddy Simulation," Second Joint Meeting of the US Sections of the Combustion Inst., Oakland, CA March 26-28, 2001.

4. Rao, S. and Rutland, C.J., 2002, "A Flamelet Time Scale Model for Non-Premixed Combustion Including Unsteady Effects," submitted to Comb. and Flame.

5. Kong, S.-C., and Reitz, R.D., "Application of Detailed Chemistry and CFD for Predicting Direct Injection HCCI Engine Combustion and Emissions" Accepted, Proceedings 29th International Symposium on Combustion, July 21-26, 2002.

# I. Understanding Direct-Injection Engine Combustion with Dynamic Valve Actuation and Residual-Affected Combustion

*Chris Edwards (Primary Contact)*
*Stanford University*
*Department of Mechanical Engineering*
*Stanford, CA 94305-3032*

*DOE Technology Development Manager: Kathi Epping*

This project addresses the following DOE R&D Plan barriers and tasks:

*Barriers*

A. $NO_x$ Emissions

B. PM Emissions

*Tasks*

3. Fundamental Combustion R&D

## Objective

- To establish and quantify the conditions under which dynamic valving can be used to implement residual-induced autoignition (a.k.a., homogeneous charge compression ignition, HCCI) or residual-affected combustion in direct-injection engines.

## Approach

- Use an electrohydraulic variable valve actuation (VVA) system developed at Stanford to enable hot exhaust to be re-inducted for use on the subsequent combustion cycle.
- Explore the regions of valve timing space in which autoignition can be induced.
- Measure the performance and emissions characteristics of HCCI combustion.
- Develop enhanced ways to use VVA for the implementation of HCCI in passenger car engines.

## Accomplishments

- Re-induction based HCCI using VVA has been demonstrated in both skip-fired and steady-state operating modes.
- The domain of valve timing which permits HCCI to occur has been quantified.
- The range of equivalence ratios and loads where HCCI can be made to occur has been quantified.
- The emissions and performance data for HCCI versus spark ignition (SI) combustion has been quantified.

## Future Directions

- To develop methods to reduce the rate of pressure rise for HCCI combustion.
- To develop ways to control set-point operation and combustion-mode transitions in HCCI.

## Introduction

Homogeneous charge compression ignition (HCCI) has shown the potential to provide combustion that is highly efficient and produces very low $NO_x$. This is brought about by causing combustion to occur under very dilute conditions -- more dilute than would normally be possible -- using a high sensible energy charge to ensure that reaction will occur. Since the peak temperature encountered during combustion is most strongly affected by the level of charge dilution, and $NO_x$ emission is most strongly affected by peak temperature, very low engine-out $NO_x$ emissions can be achieved despite high compression ratio and/or initial charge temperature. The high efficiency of HCCI combustion is a direct result of the dilute operating conditions -- under these conditions, the combustion gases can be expanded very effectively such that less energy is rejected with the exhaust gas than with conventional SI combustion.

## Approach

Figure 1 shows the electrohydraulic VVA system used in our studies. This system allows arbitrary lift profiles to be executed by both the intake and exhaust valves. Using this system, a single engine can operate as a conventional, spark-ignited engine on one operating cycle and execute a completely different mode of combustion (e.g., HCCI) on the next cycle. Exhaust reinduction occurs when the valve timing is modified such that the hot exhaust gas from the previous combustion cycle is drawn in (re-inducted) along with fresh charge during the intake stroke. In doing this, a dilute, high-sensible-energy mixture can be formed which is suitable for obtaining HCCI combustion. Two full-lift valving strategies have been employed to achieve HCCI combustion. The first is late exhaust valve closing (LEVC). Here the intake valve is operated under its native conditions but the exhaust valve closing time is delayed well into the intake stroke. The second, used in conjunction with LEVC, is late intake valve opening (LIVO). In this case, in addition to leaving the exhaust valve open during intake, the opening of the intake valve is delayed so that a greater fraction of exhaust can be reinducted.

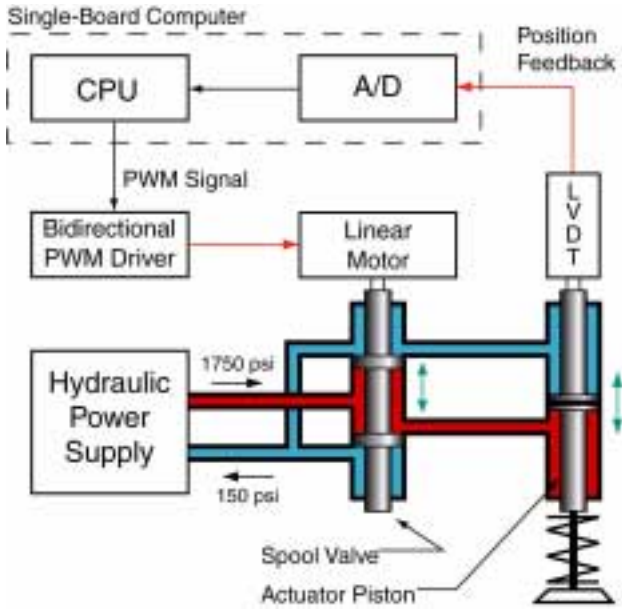


**Figure 1.** Schematic of the Stanford VVA System Used to Induce HCCI by Exhaust Reinduction

## Results

Figure 2 summarizes the potential benefits of reinduction-based HCCI over conventional SI combustion under the same conditions. The plot shows results for efficiency and emissions as a function of load for steady-state HCCI at 0.93 equivalence ratio (the center of the HCCI operating band) using propane as the fuel at a compression ratio of 13:1. This scatter plot shows the results from a matrix of 80 valving conditions spanning the range of valve conditions where reinduction-based HCCI can be achieved. For comparison, measured bands from operation of the same engine with stock valving, unity equivalence ratio, and conventional SI combustion via a throttle and spark are also shown. These data demonstrate the following observations about VVA-induced HCCI combustion:

- HCCI combustion is capable of achieving 25-60% of the load range of conventional SI combustion.
- At any given load, and for any valving condition explored, HCCI combustion is more efficient than conventional SI combustion.

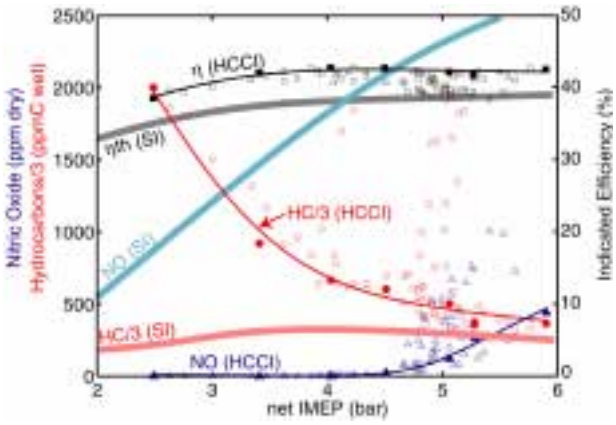


**Figure 2.** Scatter plot showing results from a matrix of 80 valving conditions used to explore the performance of reinduction-based HCCI. For comparison, data bands measured for the same engine operating in conventional, spark-ignited mode are also shown. The solid symbols and lines indicate a possible operating path through the valve timing space that provides near-optimum efficiency and emissions at all load conditions.

- Nitric oxide (NO) emissions from HCCI are, at most, half those from conventional combustion, and if valve timing is chosen judiciously, they are one to two orders of magnitude lower than SI values. We note that although it cannot be seen on this plot, for indicated mean effective pressure (IMEP) values of 4.2 bar and below, the NO emission is single-digit on a ppm basis (less than 10 ppm) and that for many conditions, the true value is below the detection limit of our analyzer (< 4 ppm).
- Depending on the choice of valve timing and the operating load, HC emissions for HCCI range from values comparable to SI operation to values an order of magnitude larger than those for SI.
- Although not shown, CO emissions from HCCI combustion are essentially invariant with load and valving conditions. They follow conventional SI trends with equivalence ratio and for these measurements were below 0.1% for all conditions.

There exist operating paths through the valve timing space that provide near-optimum emissions and efficiency performance at all loads. One such path is illustrated by the filled-in symbols and lines through the HCCI data in Figure 2. It should be noted that execution of such a path requires actuation and control of both valves S actuation of only a single valve cannot provide optimum performance.

## Conclusions

Variable valve actuation can be used to implement residual-affected combustion -- the most prominent example of which is HCCI. A comparison of performance characteristics between HCCI and SI combustion indicates that HCCI has a number of advantages over conventional combustion. A key drawback of HCCI is an excessive rate of pressure rise, which leads to a noisy engine. Preliminary studies based on the present results indicate that it may be possible to significantly reduce the rate of pressure rise through use of active control. This topic will be pursued in our upcoming research.

## FY 2002 Publications

1. Caton, P. A., Edwards, C. F., Simon, A. J., and Gerdes, J. C., "Residual-Effected Homogeneous Charge Compression Ignition at Low Compression Ratio Using Exhaust Reinduction," submitted to the Journal of Engine Research, June 2002.

# J. Late-Cycle Air Injection for Reducing Diesel Particulate Emissions

*Douglas E. Longman (Primary Contact), Sreenath Gupta, Roger Cole*
*Argonne National Laboratory*
*Energy Systems Division*
*9700 South Cass Avenue*
*Argonne, IL 60439*

*DOE Technology Development Manager: Gurpreet Singh*

*Subcontractors: University of Wisconsin Engine Research Center, Madison, WI*

*CRADA Partner: Caterpillar Inc., Peoria, IL*
*Ken Erdman (Primary Contact)*
*Caterpillar Inc.*
*Technical Center, Bldg F*
*P.O. Box 1875*
*Peoria, IL 61656-1875*

This project addresses the following DOE R&D Plan barriers and tasks:

*Barriers:*

A. $NO_x$ Emissions

B. PM Emissions

C. Cost

*Tasks:*

3a. Identification of Advanced Combustion Systems

## Objectives

- Reduce diesel particulate and $NO_x$ emissions through in-cylinder technologies.
- Maintain or improve diesel engine efficiency.

## Approach

- Modeling
  - Use the computational fluid dynamics (CFD) KIVA-III code at the University of Wisconsin's Engine Research Center (ERC) to conduct a parametric study of the effects of late-cycle gas injection on exhaust emissions.
  - Use the model to identify the dominant characteristics of gas injection that influence the engine exhaust emissions.
  - Determine the effects of gas composition on the gas injection's effectiveness for reducing emissions.
- Experimental
  - Generate experimental data using a Caterpillar 3401 research engine at Argonne National Laboratory (ANL) to validate the KIVA results.

## Accomplishments

- Modeling

- Parametric studies showed that the mixing caused by the jet momentum from the introduction of the gas jet is the dominant mechanism that controls the particulate oxidation during the diffusion phase of the combustion cycle. Altering the composition of the air being introduced (oxygen-enriched air) provided little additional benefit in reducing particulate matter. Only with low injection pressures were the effects of enriched injected air shown to have additional benefits.

- Experimental
  - Baseline engine data were taken and shown to be comparable with Caterpillar data.
  - A simple, continuous-flow air injector was installed in the cylinder head and tested at various air-injection pressures and fuel-injection timings.
  - A solenoid-controlled air injector was designed and is currently being fabricated.

### Future Directions

- Test the solenoid-controlled air injector at various air pressures, air-injection timings and durations, and fuel-injection timings to validate the modeling results.
- Experimentally explore optimization of air-injection parameters.

---

## Introduction

The desire and need to identify novel approaches for reducing diesel engine emissions has been well documented and recognized by DOE. The application of varying air composition techniques has been expanded to explore the area of an auxiliary gas injection. Such an auxiliary gas injection would introduce high-pressure gas (air or possibly oxygen-enriched air) late in the diffusion phase of the combustion cycle. The combination of turbulent mixing and increased localized oxygen content surrounding the oxidizing particulate matter in the combustion chamber is expected to reduce the overall generation of particulate matter (PM) in the engine exhaust. Also, by introducing this late in the combustion cycle, the formation of $NO_x$ should not be affected.

By combining this late-cycle injection technique with optimization of the fuel-injection timing, reduction of both PM and $NO_x$ simultaneously can become a possibility. This would ultimately lead to an improvement in the traditional PM/$NO_x$ tradeoff that exists with the majority of today's current in-cylinder emission reduction technologies.

## Approach

A KIVA-3 model developed by the University of Wisconsin-Madison used a centrally located gas injector to investigate gas-injection parameters such as pressure, timing, duration, orientation, and oxygen content. Optimization of this model showed that PM could be reduced to 30% of baseline, $NO_x$ could be reduced to 60% of baseline, and fuel consumption could be reduced to 95% of baseline quantities. However, this central location would require development of an injector that could handle both the fuel and the gas injections. Later modeling investigated off-center gas injection, which is a more likely mechanical configuration. The emissions reduction with side gas injection, though significant, was not as much as the fully optimized central gas injection.

A simple gas injector, shown in Figure 1, was fabricated and installed in a port in the cylinder head. This injector flows continuously whenever the gas pressure exceeds the cylinder pressure and has only a check valve near the orifice to prevent reverse flow when the gas is turned off. The gas jet is located near the edge of the combustion bowl with the jet angled 45° downward and inward at an angle of 45° to the radius of the cylinder. Thus, the jet has downward, inward, and swirl components to its velocity. This jet orientation is based on experimental results by Kurtz et al at the University of Wisconsin.

A more sophisticated gas injector, shown in Figure 2, is currently being fabricated for future tests. This gas injector uses a solenoid from a common-rail fuel injector and some additional valving to control the timing and the duration of the gas flow. Design

**Figure 1.** Simple, Continuous-Flow Air Injector Used for Current Tests

**Figure 2.** Solenoid-Operated Air Injector for Future Tests

calculations show that the gas injector will be able to fully open or fully close in less than 20 crank-angle degrees at the engine's maximum rated speed of 1800 rpm. This is fast enough for the planned tests.

## Results

The Caterpillar 3401E engine was operated at 1500 rpm and 192 Nm torque for all of the tests. The speed differs slightly from that modeled by KIVA (1600 rpm) because of drive-shaft resonance at 1600 rpm. The typical air consumption by the engine at these conditions is about 200 kg/hr. The air injection quantity is typically about 20 kg/hr. The air/fuel ratio was allowed to increase with the gas injection, but the particulate measurements were corrected for the exhaust dilution caused by the injected air.

Brake-specific PM (BSPM) is shown as a function of injection timing in Figure 3. This graph shows the results of Scanning Mobility Particle Sizer (SMPS) measurements. The simple, continuous-flow air injector can reduce particulate emissions by 30-50% for a fuel-injection timing of 0° before top dead center (BTDC). The effect of air injection is greater with fuel-injection timings close to top dead center than it is for advanced injection timings.

Figure 4 shows the effect of air-injection pressure on the quantity of PM. This figure shows that air injection decreases the quantity of PM

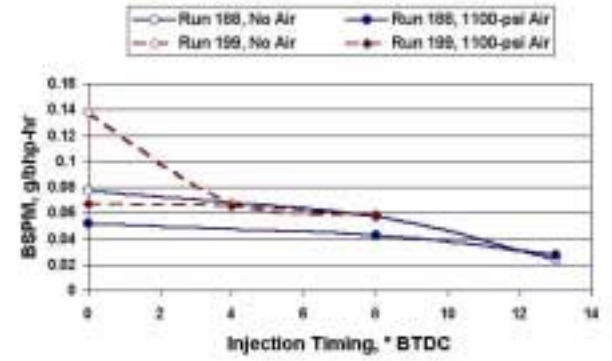


**Figure 3.** SMPS Measurements of PM Emissions with and without Air Injection as a Function of Fuel-Injection Timing

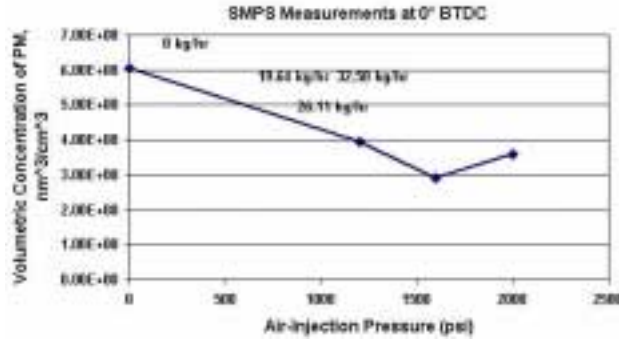


**Figure 4.** SMPS measurements of PM emissions as a function of air-injection pressure. The quantity of air flow is shown beside each point.

produced compared to the case of no air injection. However, after a quantity of air that is sufficient to reduce the quantity of PM produced is added, adding more air has little effect. The quantity of air at 1100 psi was 19.64 kg/hr; the quantity of air at 2000 psi was 32.58 kg/hr.

Figure 5 shows an SMPS trace of particle count vs particle size. This figure shows that air injection decreases the number of particles larger than about 70 nm but has less effect on the number of smaller particles. The most likely explanation is that with air injection all particles are reduced in size through oxidation. However, many of the smaller particles are replaced by particles that were formerly larger.

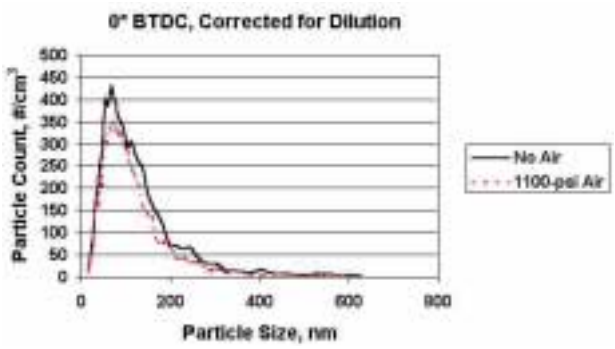


**Figure 5.** SMPS Particle Size Measurements with and without Air Injection

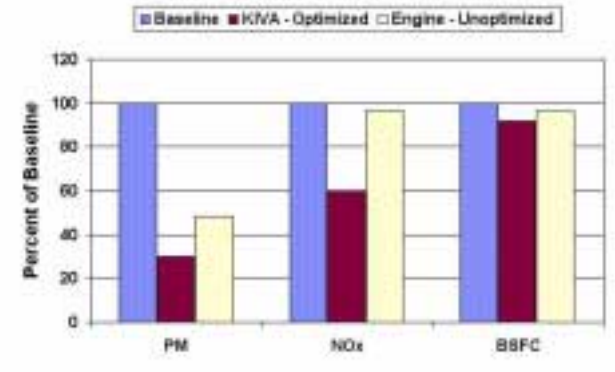


**Figure 6.** Comparison of baseline (without air injection), optimized KIVA calculations (with central air injection), and unoptimized engine measurements (with air injection) of PM, $NO_x$, and BSFC. Baseline engine measurements and engine measurements with air injection were made at a fuel-

With this process, the statistical mode of particle size is about 90 nm (same as without air injection), although the particle count at the mode is about 25% less than the case of no air injection.

Figure 6 shows a comparison of baseline, optimized KIVA calculations, and unoptimized engine measurements. The KIVA calculations are based on a central multi-jet air injector. The engine measurements use a single-jet air injector that flows continuously and is located near the edge of the piston bowl. Fuel-injection timing for the experimental measurements shown in Figure 6 is 0° BTDC for both the baseline and the air-injection case. With air injection, the PM emission is reduced to 48% of baseline, the $NO_x$ emission is reduced to 96% of baseline, and the brake-specific fuel consumption (BSFC) is reduced to 96% of baseline.

## Conclusions

The unoptimized, simple air injector can reduce PM and/or $NO_x$ emissions from a diesel engine compared to baseline measurements. The reduction in PM emissions can be as much as 50%. Fuel-injection timing can be used to favor PM or $NO_x$ reductions while retaining the overall reduction of emissions. Air injection is more effective at reducing PM emissions at retarded fuel-injection timing than it is at advanced fuel-injection timing. After an amount of air that is sufficient to effect a PM reduction is introduced into the cylinder, adding more air does not significantly affect the PM reduction.

SMPS measurements indicate that all sizes of particles are further oxidized by air injection, but the number density of particles larger than 70-nm diameter is reduced significantly while the number density of particles smaller than 70-nm diameter is relatively unchanged. The statistical mode, that is, the size of particle, which has the maximum number density, is about the same, 90 nm, with and without air injection. However, the number density at the mode is significantly reduced with air injection.

Future tests will investigate whether the sudden impulse from the controlled air injection is more effective at reducing PM than the continuously flowing air jet, as well as the economy of air consumption of the controlled injector vs. the simple injector, best timing and duration of the air injection, jet orientation, and the issue of fuel-injection timing.

## FY 2002 Publications

1. Mather, D.K., D.E. Foster, R.B. Poola, D.E. Longman, A. Chanda, T.J. Vachon. *Modeling the Effects of Late Cycle Oxygen Enrichment on Diesel Engine Combustion and Emissions*, SAE 2002-01158.

## FY 2002 Presentations

1. DOE OTT's OAAT CIDI Merit Review, May 16, 2002. *Diesel Engine PM Reduction Using Late Cycle Gas Injection*, by Doug Longman, Argonne National Laboratory.

# K. The Impact of Oxygenated Blending Compounds on PM and $NO_x$ Formation of Diesel Fuel Blends

*Charles K. Westbrook (Primary Contact), William J. Pitz*
*Lawrence Livermore National Laboratory*
*P. O. Box 808, L-091*
*Livermore, CA 94551*

*DOE Technology Development Manager: John Garbak*

This project addresses the following DOE R&D Plan barriers and tasks:

*Barriers*

B. PM Emissions

*Tasks*

5e. R&D on PM Reducing Technologies

## Objectives

- Characterize the role of oxygenated additives in reduction of particulate matter (PM) emissions from diesel engines
- Develop detailed chemical kinetics reaction models for oxygenated hydrocarbon fuel additives
- Compare soot reduction potential of different oxygenated additives

## Approach

- Identify potential diesel additives and their molecular structures
- Develop kinetic reaction mechanisms for the oxygenated additives
- Compute the ignition of each fuel mixture or model the flame structures for the fuel and additive mixtures
- Compare predicted levels of PM and $NO_x$ with and without additives and use a detailed chemical models to determine the mechanisms for the changes

## Accomplishments

- Predicted reductions in PM emissions for mixtures of diesel fuel with addition of biodiesel fuels, dibutyl maleate and tripropylene glycol monomethyl ether
- Established that newly proposed oxygenated additives suppressed PM production at approximately the same rate as previous additives studied
- Based on kinetic model predictions, determined limits of validity of existing correlation between amount of oxygen in diesel/additive fuel mixture and PM reduction that agreed with experimental results in diesel engines

## Future Directions

- Extend model capabilities to additional oxygenated blending compounds
- Increase collaborations with projects outside Lawrence Livermore National Laboratory (LLNL) dealing with diesel fuel issues

## Introduction

Experimental diesel engine studies have indicated that when oxygen is added to diesel fuel, soot production in the engine is reduced. The soot reduction appears to be largely independent of the way oxygen is incorporated into the reactants, including entrainment of additional air into the reacting gases or direct inclusion of oxygen atoms into the diesel fuel molecules.

The present study examines possible diesel fuels which have incorporated oxygen atoms into the molecular structure of the fuel itself. Following past studies of oxygenated diesel fuels such as methanol, dimethyl ether, and dimethoxy methane, this work studies oxygenated fuels which have been selected by industry consultants on the basis of potential for improving performance in diesel engines.

## Approach

Chemical kinetic modeling has been developed uniquely at LLNL to investigate combustion of hydrocarbon fuels in practical combustion systems such as diesel engines. The basic approach is to integrate chemical rate equations for chemical systems of interest, within boundary conditions related to the specific system of importance. This approach has been used extensively [1-4] for diesel engine combustion, providing understanding of ignition, soot production, and $NO_x$ emissions from diesel engines in fundamental chemical terms.

The underlying concept is that diesel ignition takes place at very fuel-rich conditions, producing a mixture of chemical species concentrations that are high in those species such as acetylene, ethene, propene and others which are well known to lead to soot production. Some changes in combustion conditions reduce the post-ignition levels of these soot precursors and reduce soot production, while other changes lead to increased soot emissions. The LLNL project computes this rich ignition using kinetic modeling, leading to predictions of the effect such changes might have on soot production and emissions.

Kinetic reaction models were developed for the oxygenated additives proposed by a DOE/industry panel of experts. We then computed diesel ignition and combustion using heptane [5] as a reasonable diesel fuel surrogate model, mixed with oxygenated additives. The impact of the additive on predicted levels of soot-producing chemical species was then assessed.

## Results

Using operational insights derived from recent diesel engine experiments by Dec [6], we assumed that soot production in diesel combustion occurs from reactions of chemical species created in fuel-rich ignition near the fuel injection location. Because there is insufficient oxygen in this region to burn the fuel completely, the hydrocarbon species remaining there react instead to produce soot. Our kinetics calculations show that when the fuel itself contains some oxygen, that oxygen helps convert more of the ignition products into chemical species that do not contribute to soot production.

During the past year, the LLNL project has examined two important oxygenated hydrocarbon species that have been proposed as possible diesel fuels. These are dibutyl maleate (DBM) and tripropylene glycol monomethyl ether (TPGME), both of which include significant amounts of oxygen imbedded in the primarily hydrocarbon fuel molecule. Schematic diagrams of the structures of these two species are shown Figure 1. Detailed chemical kinetic reaction mechanisms were developed for both of these fuels, and the resulting models were used to assess their sooting tendencies.

The model calculations indicate that the distribution of oxygen atoms within the fuel molecule can have a significant influence on the anti-sooting effects of the oxygen atoms. Our work supports a view that oxygen atoms within a fuel molecule form C-O bonds that remove the C atom from the pool of species which can eventually produce soot. Each O atom removes one C atom from the sooting environment, and TPGME is an excellent example of a fuel in which this mechanism can be seen.

However, in DBM, the available oxygen atoms are less well distributed, and in some cases two oxygen atoms produce $CO_2$ directly from the decomposition of the additive. As a result, the total

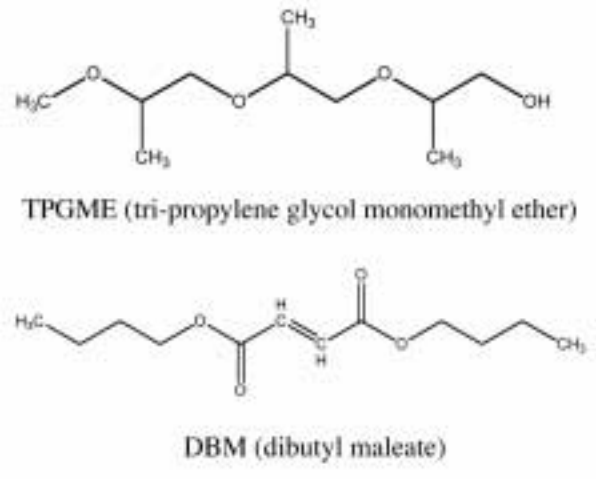


**Figure 1.** Schematic Chemical Structure Diagrams for Proposed oxygenated Diesel Fuel Components Tripropylene Glycol Monomethyl Ether and Dibutyl Maleate

population of O atoms in the fuel are not as effective at sequestering carbon atoms as in TPGME, so DBM is less effective as a soot reduction fuel additive than TPGME. This analysis is consistent with recent experimental results from Sandia National Laboratories in Livermore. Ongoing kinetic analyses are examining the implications of these results and may lead to new definitions of potentially important diesel fuels for engine combustion. In addition, this work may lead to better analyses of the soot reduction capacities of other alternative diesel fuels. In particular, these kinetic results suggest that biodiesel fuels may have the same reduction in oxygen additive effectiveness as that noted above for DBM. The methyl ester group in biodiesel fuels has the potential to produce $CO_2$ directly, making the oxygen content of the biodiesel fuel less able to capture one C atom for every O atom in the fuel and reducing the proportional effectiveness of the fuel-bound oxygen.

## Conclusions

Kinetic modeling provides a unique tool to analyze combustion properties of potential alternative fuels for diesel engines. This can provide a way to screen proposed new fuel classes or types that may be important in applied studies. A kinetic model can be very cost-effective as an alternative to experimental analyses, and computations can also provide a fundamental explanation of the reasons for the observed results.

## References

1. Fisher, E. M., Pitz, W. J., Curran, H. J., and Westbrook, C. K., "Detailed Chemical Kinetic Mechanisms for Combustion of Oxygenated Fuels", Proc. Combust. Inst. 28: 1579-1586 (2000).

2. Curran, H. J., Fisher, E. M., Glaude, P.-A., Marinov, N. M., Pitz, W. J., Westbrook, C. K., Layton, D. W., Flynn, P. F., Durrett, R. P., zur Loye, A. O., Akinyemi, O. C., and Dryer, F. L., "Detailed Chemical Kinetic Modeling of Diesel Combustion with Oxygenated Fuels," Society of Automotive Engineers paper SAE-2001-01-0653 (2001).

3. Flynn, P.F., Durrett, R.P., Hunter, G.L., zur Loye, A.O., Akinyemi, O.C., Dec, J.E., and Westbrook, C.K., "Diesel Combustion: An Integrated View Combining Laser Diagnostics, Chemical Kinetics, and Empirical Validation", Society of Automotive Engineers paper SAE-1999-01-0509 (1999).

4. Curran, H. J., Fisher, E. M., Glaude, P.-A., Marinov, N. M., Pitz, W. J., Westbrook, C. K., Layton, D. W., Flynn, P. F., Durrett, R. P., zur Loye, A. O., Akinyemi, O. C., and Dryer, F. L., "Detailed Chemical Kinetic Modeling of Diesel Combustion with Oxygenated Fuels," Society of Automotive Engineers paper SAE-2001-01-0653 (2001).

5. Curran, H. J., Gaffuri, P., Pitz, W. J., and Westbrook, C. K., "A Comprehensive Modeling Study of n-Heptane Oxidation," Combustion and Flame 114, 149-177 (1998).

6. Dec, J.E., "A Conceptual Model of DI Diesel Combustion Based on Laser-Sheet Imaging," SAE publication SAE-970873 (1997).

# L. Fabrication of Small Fuel Injector Orifices

*George R. Fenske (Primary Contact), John Woodford*
*Argonne National Laboratory*
*9700 South Cass Avenue*
*Argonne, IL 60439*

*DOE Technology Program Manager: Nancy Garland*

This project addresses the following DOE R&D Plan barriers and tasks:

*Barriers*

B. PM Emissions

*Tasks*

5d. Advanced PM Reducing Systems

## Objectives

- Develop a methodology for reducing the diameter of fuel injector orifices to 50 μm by applying material to the interior diameter (ID) of the orifice.
- Characterize the spray and combustion properties of the fuel injector systems so treated.
- Transfer the technology to an industrial partner.

## Approach

- Identify and rate potential thin- and thick-film deposition technologies for reducing the diameter of diesel engine fuel injector orifices.
- Perform laboratory-scale evaluations of the most promising technology(ies).

## Accomplishments

- Identified and rated potential deposition technologies.
- Selected electroless nickel (EN) plating as the primary candidate, with electroplating and/or physical vapor deposition (PVD) as possible secondary candidates.
- Reduced orifice diameter from 200 μm to 100μm with EN plating.
- Identified critical role of particulates in EN orifice plating quality.

## Future Directions

- Complete construction of forced-circulation multicomponent plating system.
- Measure spray characteristics of coated injectors.
- Provide coated injector tips to Argonne National Laboratory Energy Systems personnel for combustion tests.
- Determine vulnerability of EN-plated injectors to deposit formation. If necessary, vary plating chemistry to ameliorate vulnerability.

## Introduction

Recent work on the control of particulate matter (PM) emissions and improvement of engine combustion efficiency in diesel engines has shown the effectiveness of reduced injector orifice diameter in promoting fuel atomization, leading to more complete combustion and reduction in soot formation[1,2]. Using electrodischarge machining (EDM), the current method for fabricating injector orifices, the minimum achievable orifice diameter is on the order of 125 μm. To see significant improvement, the orifice diameter should be 50 μm or less. Work towards refining EDM techniques to allow economical large-scale fabrication of 100 μm orifices is ongoing. In addition, there are two other technologies that may be used for the manufacture of small orifices: laser drilling and LIGA (Lithographie, Glavanoformung, and Abformung). Both technologies have disadvantages precluding their commercial use in the near- to mid-term. Therefore, we propose another method.

There are currently a wide variety of techniques for the deposition of moderately thick (>10 μm) films onto various surfaces. It may be possible to reduce the diameter of an extant orifice by depositing material onto the interior of the orifice (Figure 1). We will select and evaluate an appropriate technique for this, and if it appears that this approach is successful, we will develop a method and transfer it to an industrial partner. We are currently working with Siemens, and they have provided us with sample injector tips and information.

## Approach

As mentioned above, there are a large number of coating techniques to be considered. Our first step, therefore, is to perform a survey of deposition methods and determine which may be used to coat orifice IDs. We will then rank those methods taking into account coating cost, start-up cost, environmental friendliness, etc.

With the ranked list in hand, we will work towards implementing the easiest method on a laboratory scale, while examining the feasibility of working on others. Our criteria for a successful technique are as follows:

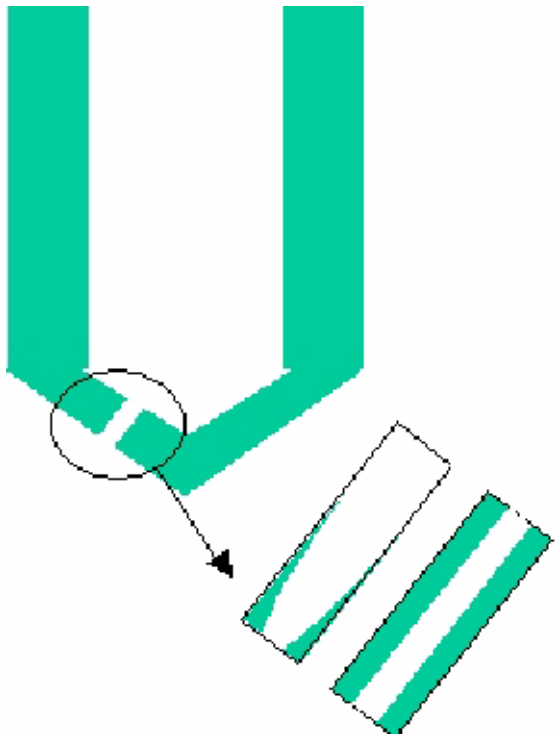

**Figure 1.** Schematic Illustration Showing Proposed Method of Reducing Orifice Diameter

- Allows reduction in orifice diameter to at least 50 μm.
- Coating adheres well to substrate.
- Coating is at least as damage-resistant as substrate.

In addition, we will consider it a limited success if the surface chemistry of the (adherent, damage-resistant) coating is such that deposit formation is minimized, even if we are unable to achieve the 50 μm goal.

As part of the evaluation process, we will examine the flow-through and spray characteristics of coated nozzles and provide them to industrial partners or other collaborators for combustion studies. Although our focus in this project is on deposition methods, the overall goal is to improve fuel combustion in diesel engines.

Following a successful lab-scale demonstration of the coating technology, we will work with Siemens or another industrial partner to transfer the technology.

## Results

We completed a process comparison in the second quarter (Table 1). The most promising candidate method was EN plating, which offered a combination of rapid deposition rate, ability to coat inside diameters, ready scalability, overall maturity level, low-expense facilities, and durability of coating. We then set out to evaluate the process according to the criteria described above.

**Table 1. Process Comparison**

| Process | Inexpensive? | Reliable? | Green? | Adherent? | Uniform? |
|---|---|---|---|---|---|
| **MOCVD (vacuum)** | **No** | Yes | Variable | Yes | Unknown |
| **PVD** | No | Variable | Yes | Variable | Probably Not |
| **MOCVD (atm.)** | Variable | Yes | Variable | Yes | Unknown |
| **Thermal Spray** | Yes | Yes | Yes | Variable | No |
| **EP** | Yes | Yes | Variable | Yes | Unknown |
| **EN** | Yes | Yes | Variable | Variable | Yes |

MOCVD = metallorganic vapor deposition
PVD = physical vapor deposition
EP = electroplating

EN plating is a method of depositing nickel/phosphorus (or nickel/boron) alloys (usually Ni-P or Ni-B solid solutions, with NiP or NiB precipitates) onto metallic surfaces from an aqueous solution. Samples are placed in a plating bath of the appropriate composition, the bath is heated to ca. 70 - 95°C, and the nickel/phosphorus coating grows directly from the bath via a surface-catalyzed chemical reaction.

Initial results are quite promising. We have coated the orifice IDs on sample injector tips provided by Siemens (Figure 2) with reasonable uniformity (Figure 3). We have also established the adherence of the EN plating on the injector tips. Although we have not yet achieved reduction to 50 µm, we have deposited ca. 50µm thick EN plate onto the ID of 200 µm diameter orifices, reducing them to 100 µm diameter.

In order to obtain greater uniformity, better adhesion on the interior of the injector tip, and more rapid deposition, we began to plate injector tips by forcing the plating bath through the injector orifices during the coating process. This approximately doubled the deposition rate to ca. 50 µm/hour. However, we found that the bath needed to be filtered to prevent clogging of the nozzles with small Ni particles. In fact, if the bath is not filtered the Ni particles nucleate the growth of metallic threads inside the body of the injector tip. In addition, the pump we were using did not develop enough pressure to force the bath through the orifices once

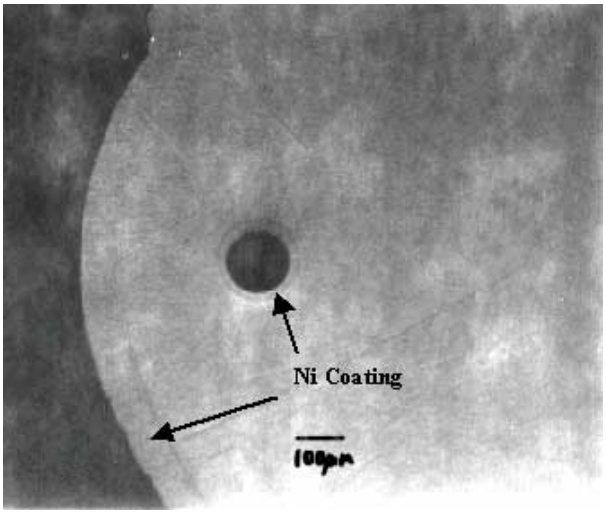


**Figure 2.** Micrograph, cross-section of coated fuel injector tip orifice. The nickel plate is the lighter-colored ring around the orifice ID.

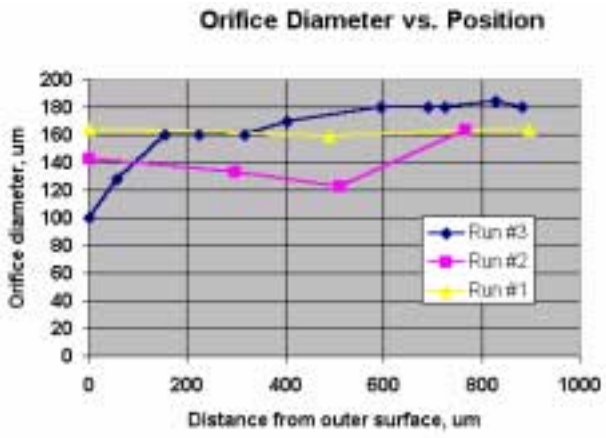


**Figure 3.** Graph of Coating Thickness as a Function of Position along the Length of the Orifice

they had closed to ca. 100 μm in diameter. We are currently in the process of constructing a larger-scale plating bath with a capacity of several gallons, a more powerful pump, a filter on the supply line, and a manifold for coating multiple injector tips at a time.

## Conclusions

EN plating has been shown to be an effective method of reducing the inside diameter of fuel injector tip orifices. Further work towards improving the method is ongoing.

## References

1. Heywood, John B., Internal Combustion Engine Fundamentals, McGraw-Hill, 1988.

2. Pickett, Lyle M. and Siebers, Dennis L., Paper No. 2001-ICE-399, ICE-Vol. 37-1, 2001 Fall Technical Conference, ASME 2001, Ed.: V. W. Wong.

# M. World Direct Injection Emission Technology Survey

*Brad Adelman (PrimaryContact), Jeff Moore, Simon Edwards, Marc Vigar*
*Ricardo, Inc.*
*7850 South Grant Street*
*Burr Ridge IL 60527*

*DOE Technology Development Manager: Ken Howden*

*Main Subcontractors: Ricardo Consulting Engineers, Shoreham-by-Sea, United Kingdom*

This project addresses the following DOE R&D Plan barriers and tasks:

*Barriers*

A. NOx Emissions

B. PM Emissions

*Tasks*

1. Fuel Systems R&D
2. Sensors and Controls
3. Fundamental Combustion R&D
4. NOx Control Device R&D
5. Particulate Matter Control Device R&D

## Objective

- Analyze and assess the status of direct injection (DI) emission control technology for transportation applications outside the U.S.
- Collect data from public and private sources.
- Compare data with future legislated emission and fuel efficiency targets for the U.S.

## Approach

- The project is divided into four main stages: data definition, data gathering, analysis of data and reporting. These include the following activities:
- Stage 1, Data Definition: Identify key concepts, technologies and companies involved in the development of DI emission control technologies. Define technology roadmaps and interview template for company visits. Define and set up interactive knowledge management tool.
- Stage 2, Data Gathering: Contact companies and other organizations, and visit as needed. Study information available on companies from public sources. Extract Ricardo internal research results. Insert data into the interactive knowledge management storage medium.
- Stage 3, Analysis of Data: Divide data into business/economic aspects and technical/manufacturing aspects. Evaluate the size and scope of corporate research and development efforts.
- Stage 4, Reporting: Draw conclusions on which technologies are technically promising and will be acceptable to the major producers in the world marketplace. Divide marketplace into base engine and aftertreatment for light-duty compressed ignition direct injection (CIDI), heavy-duty CIDI, large DI

engines (over 6-inch bore) and spark ignition direct injection (SIDI). Statement on fuels and their relevance to engine and aftertreatment.

### Accomplishments

- Data Definition is complete. "Mind Map" created as a guide.
- Data Gathering is currently on-going. An internal website for information exchange between participants has been created. Interview trips to OEMs are being scheduled. Interview results are being stored. Liaison with participants is ongoing

### Future Directions

- Continue with Data Gathering
- Analyze Data
- Report Results

---

## Introduction

The objective of this project is to assess the state-of-the-technology of DI engine emission control outside of the United States for comparison with the technology that is currently available in the United States. The purpose of the comparison is to determine whether the foreign technologies studied are capable of yielding significant benefits in fuel economy and meeting U.S. emission regulations. The work will also address the question of what will be needed in the U.S. in the future in order to meet the overall fuel economy goals consistent with the ambient air quality legislation.

In particular, the current work will identify companies engaged in DI engine emission control technology development, demonstration and/or commercialization. Moreover, Ricardo will characterize these companies in terms of size, manufacturing effort, and research and development effort, among other criteria. This analysis will relate DI technology to the future legislated emission and fuel economy targets for the U.S. It will identify the degree to which these technologies are commercially available and any developmental requirements needed to bring them to market will be assessed.

## Approach

The major issues involved in this work are the collection of the necessary data, the analysis of the data, and drawing of conclusions from it. The initial phase of the project involves identifying target companies, scheduling interview visits and creating a "Mind Map" to be used as a reference guide for the entire project. The "Mind Map" is depicted in Figure 1, it demonstrates the internal website established to allow project participants to store the results of company interviews and to access the data.


**Figure 1.** "Mind Map" for Project and Example of the Internal Website

The work plan is divided into four main parts: data definition, data gathering, analysis of data, and reporting. Data definition has been performed with direct consultation with representatives from the DOE. Regarding technology, several engine types have been selected: DI gasoline (motorcycles, passenger vehicles), DI light-duty diesel (passenger vehicles), medium- and heavy-duty diesel (vans, trucks, buses), large engine (rail applications) and DI natural gas engines (passenger vehicles, buses). In particular, the study will assess the following technical aspects:

- Engine specific performance
- Engine design
- Air handling systems
- Fuel injection systems
- Combustion systems
- Catalytic emission control systems (ECS)
- Controls systems
- Fuels and lubes requirements.

Data will be gathered from public domain information and the Ricardo database, Powerlink™. In addition to information available from database searches, Ricardo will also perform a series of technical discussions with several companies involved in research and development in the area of direct injection, e.g. engine, vehicle, and automotive parts manufacturers as well as emission control systems (ECS) and petroleum companies.

Data analysis will assess the effect the technology has on fuel economy, engine-out and tail pipe emissions, cost to manufacture, cost to create/ maintain infrastructure, and end-user costs. With regards to business aspects, the data will be gathered in relation to market locations and sizes, growth potential, competition and new opportunities. The latter data will be taken from the public domain.

## Future Directions

This project is currently ongoing and is in the data gathering stage.

# VII. HOMOGENEOUS CHARGE COMPRESSION IGNITION

## A. Natural Gas Homogeneous Charge Compression Ignition R&D

*Salvador Aceves (Primary Contact), J. Ray Smith, Daniel Flowers, Joel Martinez-Frias, Robert Dibble*
*Lawrence Livermore National Laboratory*
*7000 East Ave. L-644*
*Livermore, CA 94550*

*DOE Technology Development Managers: Gurpreet Singh and Stephen Goguen*

*Main Subcontractor: University of California Berkeley, Berkeley, CA*

This project addresses the following DOE R&D Plan barriers and tasks:

*Barriers*

A. $NO_x$ Emissions

B. PM Emissions

C. Cost

*Tasks*

1a. Advanced Fuel Systems

3. Fundamental Combustion R&D

### Objectives

- Obtain controlled low-emission, high-efficiency operation of homogeneous charge compression ignition (HCCI) engines.
- Advance analysis techniques to learn the fundamentals of HCCI combustion and to make accurate predictions of combustion and emissions.
- Use our capabilities to determine and evaluate control and startability strategies.

### Approach

- Conduct experiments on a 4-cylinder Volkswagen TDI engine and on a single-cylinder Caterpillar 3401 engine to evaluate startability and control strategies.
- Develop and use single-zone and multi-zone chemical kinetics models for analysis of HCCI combustion and for evaluation of possible control strategies.

### Accomplishments

Part 1. Analysis

- We have developed the most advanced and accurate analysis tools for HCCI combustion. During this year we have performed a detailed analysis of experiments conducted at the Lund Institute of Technology, where different engine geometries were studied. Our analysis results indicate that we can

successfully predict the effect of cylinder geometry on HCCI combustion. This opens the door to conducting computer-based engine optimization studies in a way that was never before possible.

- We have considerably reduced our computation time by developing a segregated solver and by developing a reduced chemical kinetic mechanism with only 200 species that can successfully predict iso-octane HCCI combustion.
- We have discovered that improving the resolution of the multi-zone method (increasing the number of zones) considerably improves the quality of our prediction of carbon monoxide emissions. CO emissions are well known to be very sensitive to operating conditions and therefore are extremely difficult to predict in HCCI engines.

Part 2. Experimental

- The 4-cylinder Volkswagen TDI has been run without an intake heater, by adjusting the equivalence ratio and EGR to obtain satisfactory combustion.
- We have balanced combustion between the cylinders of the VW TDI engine by using small electric heaters at the intake ports and by independently throttling the exhaust of the individual cylinders.
- We conducted a laser absorption experiment on the Caterpillar 3401 engine to determine the effect of fuel-air mixing on HCCI engine emissions.

### Future Directions

- Two fundamental problems of HCCI engines are difficulty in controlling the engine and low maximum power. In this project, the analytical and experimental work are dedicated to solving these two problems.
- We will use our analysis techniques to study the details of the combustion process in the Volkswagen TDI engine.
- We will also use our analytical capabilities and experimental facilities to achieve a satisfactory method of starting the engine under any environmental condition that may exist.
- The Caterpillar 3401 engine gives us an ideal test bed for heavy truck engine applications. Engine data for the 3401 will be generated and analyzed.

---

## Introduction

This work addresses the need to develop a new combustion concept that allows both high efficiency and low emissions for trucks and SUVs. The high efficiency of diesel engines is highly desirable for improving the fuel economy of light-duty trucks and SUVs. However, diesel engines are well known as significant sources of $NO_x$ and particulate matter emissions. The use of HCCI combustion systems represents a promising approach that needs further research and development.

### HCCI Engine Analysis

We have applied our advanced analysis capabilities to study the effect of engine geometry on HCCI combustion and emissions. We did this by performing a detailed analysis of experiments conducted at the Lund Institute of Technology, where different engine geometries were studied. Three geometries were used with different crevice widths (0.26 mm, 1.3 mm and 2.1 mm) and a fixed compression ratio (17:1). Figure 1 shows hydrocarbon emissions as a function of the air-fuel equivalence ratio. The figure shows that the model does a reasonable job at predicting the absolute values of HC emissions. The maximum difference between the numerical and experimental values for HC emissions is approximately 40%, but in many cases agreement is within 10% or better, especially for the wider crevices (1.3 and 2.1 mm). In addition to this, the model does an excellent job at predicting trends. For the piston with a 0.26-mm crevice, the model predicts that the HC emissions decrease monotonically as air/fuel equivalence ratio

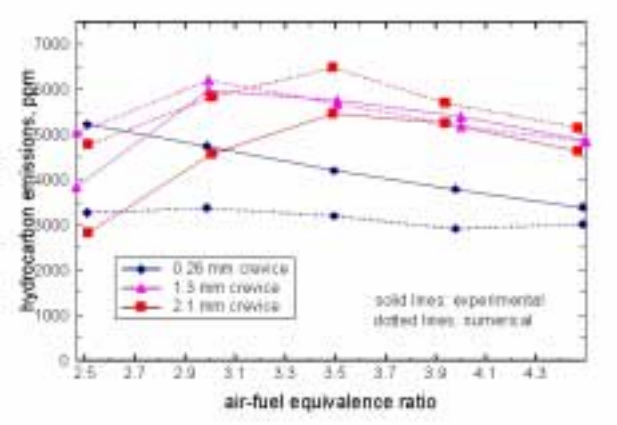


**Figure 1.** Comparison between experimental and numerical hydrocarbon (HC) emissions as a function of the air-fuel equivalence ratio (λ), for the three cylinder geometries considered.

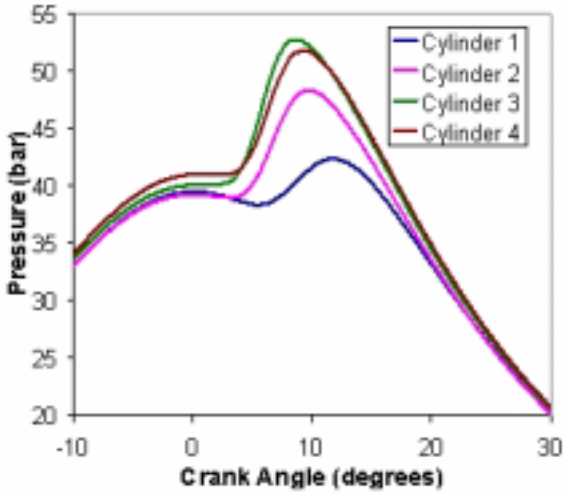


**Figure 2.** Pressure traces for the four cylinders of the TDI engine before balancing. Cylinder 1 is the coldest and cylinder 3 is the hottest.

increases, in agreement with the experimental results. For the wider crevices, the trend is not monotonic, but rather HC emissions reach a peak at an intermediate value of λ. This maximum is reached at λ=3 for the 1.3 mm crevice engine, and at λ=3.5 for the 2.1 mm crevice engine. As the figure indicates, the model predicts the non-monotonic behavior of the HC emissions as a function of λ. In addition to this, the model exactly predicts the value of λ for maximum HC emissions. The fact that the multi-zone model can predict all the trends for hydrocarbon emissions, as well as the equivalence ratio for peak hydrocarbon emissions is a great success for this methodology.

The results presented in Figure 1 show that the multi-zone model can accurately predict the magnitude and the functional form of the HC emissions as a function of λ and cylinder geometry. Considering that HCCI combustion is very sensitive to temperature and equivalence ratio, the accurate results are an indication that the model is capturing the dependence between reaction rates and temperature distributions. These results show the great potential of multi-zone analysis for computer design and optimization of HCCI engines. Combustion chamber geometry and engine operating parameters can be analyzed and optimized for maximum efficiency, low emissions and low peak cylinder pressure with an accuracy never before possible.

## HCCI Experiments

This year we have been able to operate the Volkswagen TDI engine without an electric intake heater. Electric heaters are desirable fro use on laboratory HCCI engines, because they can be easily controlled. However, electric heaters are not a viable option for an engine that has to deliver power, because the electric heater may consume a larger portion of the power generated by the engine than is desirable. We accomplished heater-free operation by controlling the equivalence ratio and the EGR of the engine to obtain satisfactory combustion.

We have also been able to balance the cylinders in the TDI engine by using electric trim heaters in each of the intake ports. The results are shown in Figures 2 and 3. Figure 2 shows the pressure traces for the 4 cylinders of the TDI engine before balancing the cylinders. The figure shows big differences in the pressure traces. HCCI combustion is extremely sensitive to temperature and composition, and the hotter cylinders burn significantly earlier than the cold cylinders. Figure 3 shows the engine after balancing the combustion with trim heaters. Very little electric power (slightly over 100 W) was necessary to balance this engine at this operating condition.

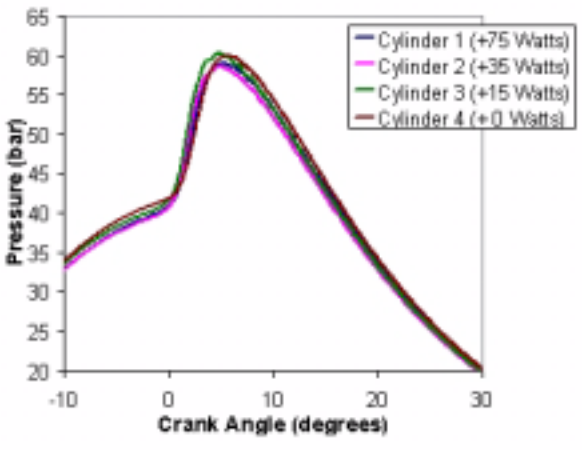


**Figure 3.** Pressure Traces for the Four Cylinders of the TDI Engine after Balancing

## Conclusions

During the present year we have achieved significant progress in evaluating HCCI combustion, both by analysis and experiments. In analysis, we have demonstrated that our multi-zone methodology can successfully predict the effect of engine geometry and operating conditions on HCCI engine combustion and emissions. In experimental work we have run the VW TDI engine with no intake electric heater, and we have successfully balanced the cylinders using minimal electrical power. Our future work is dedicated to study the fundamentals of HCCI combustion, as well as to identify optimum strategies for HCCI engine control, and startability and to increase the engine power output.

## FY 2002 Publications/Presentations

1. Prediction of Carbon Monoxide and Hydrocarbon Emissions in Isooctane HCCI Engine Combustion Using Multi-Zone Simulations, Daniel Flowers, Salvador M. Aceves, Joel Martinez-Frias, Robert W. Dibble, Proceedings of the Combustion Institute, 2002.

2. Thermal Charge Conditioning for Optimal HCCI Engine Operation, Joel Martinez-Frias, Salvador M. Aceves, Daniel Flowers, J. Ray Smith, Robert Dibble, Accepted for publication, Journal of Energy Resources Technology, Vol. 124, pp. 67-75, 2002.

3. Detailed Chemical Kinetic Simulation of Natural Gas HCCI Combustion: Gas Composition Effects and Investigation of Control Strategies, Daniel Flowers, Salvador M. Aceves, Charles Westbrook, J. Ray Smith and Robert Dibble, Journal of Engineering for Gas Turbines and Power, Vol. 123, pp. 433-439, 2001.

4. The Potential of HCCI Combustion for High Efficiency and Low Emissions, Kathi Epping, Salvador M. Aceves, Richard L. Bechtold, John E. Dec, SAE Paper 2002-01-1923.

5. An Investigation of the Effect of Fuel-Air Mixedness on the Emissions from an HCCI Engine, James W. Girard, Robert W. Dibble, Daniel L. Flowers, Salvador M. Aceves, SAE Paper 2002-01-1758.

6. Equivalence Ratio-EGR Control of HCCI Engine Operation and the Potential for Transition to Spark-Ignited Operation, Joel Martinez-Frias, Salvador M. Aceves, Daniel Flowers, J. Ray Smith, Robert Dibble, SAE Paper 2001-01-3613.

7. A Decoupled Model of Detailed Fluid Mechanics Followed by Detailed Chemical Kinetics for Prediction of Iso-Octane HCCI Combustion, Salvador M. Aceves, Joel Martinez-Frias, Daniel L. Flowers, J. Ray Smith, Robert W. Dibble, John F. Wright, Randy P. Hessel, SAE Paper 2001-01-3612.

8. Current Research in HCCI Combustion at UC Berkeley and LLNL, Robert Dibble, Michael Au, James Girard, Salvador M. Aceves, Daniel L. Flowers, Joel Martinez-Frias, SAE Paper 2001-01-2511.

9. HCCI Combustion: Analysis and Experiments, Salvador M. Aceves, Daniel L. Flowers, Joel Martinez-Frias, J. Ray Smith, Robert Dibble, Michael Au, James Girard, SAE Paper 2001-01-2077.

# B. HCCI Combustion with GDI Fuel Injection

*John E. Dec (Primary Contact)*
*Sandia National Laboratories*
*MS 9053, P.O. Box 969*
*Livermore, CA 94551-9699*

*DOE Technology Development Managers: Kathi Epping and Gurpreet Singh*

*Main Subcontractor: Sandia National Laboratories, Livermore, CA*

This project addresses the following DOE R&D Plan barriers and tasks:

*Barriers*

A. $NO_x$ Emissions

B. PM Emissions

C. Cost

*Tasks*

1a. Advanced Fuel Systems

3c. Identification of Advanced Combustion Systems

## Objectives

- Develop a fundamental understanding of homogeneous charge compression ignition (HCCI) combustion processes to overcome the technical barriers to the development of practical HCCI engines.
- Establish an HCCI engine research laboratory (multi-year task).
  - Bring all-metal HCCI engine to full operational status, and complete detailed design and parts fabrication for the optically accessible engine.
- Map-out operation of the HCCI engine over a range of operating conditions, evaluate engine performance and operational limits, and compare trends with single-zone model predictions.
- Investigate low-load operation, the completeness of bulk-gas reactions, and the sources of emissions and combustion inefficiencies.
- Conduct an initial investigation of partial charge stratification using a gasoline direct injection (GDI) fuel injector.

## Approach

- Build a versatile HCCI engine laboratory with both all-metal and optically accessible engines to allow investigations of various fueling, mixing, and control strategies.
- Operate the metal HCCI engine over a wide range of intake temperatures, intake pressures, fueling rates, and engine speeds using well-mixed fuel.
  - Systematically vary operating parameters about a baseline operating condition.
  - Perform single-zone, kinetic-rate modeling computations (using CHEMKIN) over this operational range and compare trends with experimental results.

- Conduct detailed experiments of engine performance and emissions at low loads to determine the cause of poor combustion efficiency and high emissions at these conditions, and perform complementary CHEMKIN computations.
- Use late-cycle fuel injection with a GDI fuel injector to obtain partial charge stratification, and investigate its potential to mitigate poor performance at low loads.

### Accomplishments

- The all-metal HCCI engine is fully operational, including both the premixed and GDI fueling systems. Complete exhaust-gas analysis equipment has been installed and is fully operational.
- Other laboratory capabilities have been advanced and are on track as planned.
  - Optical engine design is complete, and preparation of machine drawings and parts fabrication is underway.
  - Design and hardware fabrication of a variable valve actuation (VVA) system has been completed with the help of the International Truck and Engine Co.
- Completed a parametric investigation of the metal-engine performance and emissions over a wide range of intake temperatures, intake pressures, fueling rates, and engine speeds.
  - Determined operating limits and tradeoffs between various engine operating parameters.
- Showed that the high emissions and poor combustion efficiencies at low fuel loads are due to incomplete bulk-gas reactions, providing the first known experimental verification of previous modeling predictions.
- Showed that partial charge stratification obtained by late GDI fuel injection (80°- 60° before top dead center [BTDC]) can substantially improve combustion efficiencies and emissions at low-loads without significantly affecting $NO_x$ and smoke.

### Future Directions

- Complete set-up of optically accessible engine and conduct initial experiments.
  - Use natural emission imaging to investigate well-mixed and partially stratified combustion.
- Investigate the effects of fuels on intake temperature requirements and the completeness of bulk-gas reactions over a range of engine speeds and loads, using a combination of experiments and computations (for a variety of reference-fuel mixtures and commercial-grade gasoline).
- Investigate diesel-fueled HCCI. Explore the potential of late-cycle GDI fuel injection for diesel-fueled HCCI. Install a high-pressure, common-rail direct injection diesel fuel injector to investigate various injection and mixing strategies.
- Investigate various partial charge stratification concepts that provide different degrees of fuel/air/residual mixing and/or thermal stratification, as a means of slowing the combustion rate to extend operation to higher loads and to improve combustion efficiency at low loads.

---

## Introduction

Homogeneous charge, compression ignition (HCCI) is an alternative engine combustion process that can provide high diesel-like efficiencies and very low emissions of $NO_x$ and particulates. However, research is required to overcome the technical barriers to producing a practical HCCI engine, such as controlling ignition timing over the load/speed map, slowing the heat-release rate at higher loads, controlling hydrocarbon (HC) and carbon monoxide (CO) emissions, maintaining combustion stability, cold starting, and responding to rapid transients.

The objective of this project is to develop the fundamental understanding necessary to overcome these barriers. To achieve this objective, an HCCI engine laboratory has been established that is being

**Figure 1.** Photograph of the All-Metal HCCI Engine

equipped with two HCCI engines of the same basic design: 1) an all-metal engine is being used to establish operating points, develop combustion-control strategies, and investigate emissions, and 2) an optically accessible engine will be used to apply advanced laser diagnostics to the in-cylinder processes. In addition, the project includes a modest computational modeling effort using the CHEMKIN single-zone model with time-varying compression, to guide the experiments and provide fundamental understanding of selected HCCI processes.

This research project is being conducted in close cooperation with both the automotive and heavy-duty diesel engine industries. Results are presented at the Cross-Cut Diesel CRADA meetings, and the project will be included in the new Compression-Ignition Engine CRADA, beginning in FY03.

## Approach

A versatile HCCI engine laboratory is being built that allows investigations of a wide range of operating conditions and various fuel injection, fuel/air/residual mixing, and control strategies that have the potential to overcome the technical barriers to HCCI. Both the all-metal and optical engines are derived from Cummins B-series diesel engines, SUV-sized engines (0.98 liters/cylinder) that can provide an operating range relevant to both automotive and heavy-duty manufacturers. The engines are converted for balanced, single-cylinder operation, and are equipped with a variety of special features for HCCI research.

After bringing the all-metal engine to full operational status, three investigations were performed: 1) The operational limits and performance characteristics of the engine were determined by systematically mapping out its operation over a wide range of operating conditions using well-mixed fueling. Complementary CHEMKIN computations were made over the same operating range and used to assist in understanding the engine behavior. 2) To determine the cause of poor combustion efficiency and high emissions under low-load operation, a detailed experimental and computational investigation was made of engine performance and emissions at these conditions. 3) Late-cycle GDI fuel injection was examined as a means of achieving partial charge stratification to overcome the poor performance associated with low-load operation.

## Results

The all-metal engine, shown in Figure 1, and its supporting subsystems were brought to full operational status. In addition, a complete exhaust gas analysis system for $CO_2$, $O_2$, CO, HC, $NO_x$, and smoke was acquired and installed.

To verify that this new HCCI engine with its custom piston design was functioning well, initial studies involved mapping its performance over a wide range of intake temperatures and pressures, fuel loadings, and speeds, and comparing the results with CHEMKIN computations. Iso-octane was used as the fuel for these initial studies because it is a reasonable surrogate for gasoline [1], it minimizes experimental uncertainties, and it facilitates comparison with the model. Figures 2 - 4 show examples of the engine's performance at a typical

fully combusting condition, with a well-mixed charge obtained by early GDI fuel injection. Shown on the x-axes of these plots is the intake temperature, which adjusts the combustion phasing. For this operating condition, combustion phasing is near optimal for intake temperatures of 109° to 122°C, and the data show that at these intake temperatures, the engine is performing very well relative to other HCCI engines. Combustion and thermal efficiencies are high, on the order of 95% and 49%, respectively; combustion stability is excellent (standard deviation of the gross indicated mean effective pressure [IMEPg] is < 1%); CO and HC emissions are about 60 and 35 g/kg-fuel, respectively; $NO_x$ is extremely low at 50 mg/kg-fuel (1 ppm); and smoke was not detectable.

Our previous CHEMKIN modeling results [2] had indicated that as fueling was reduced below an equivalence ratio ($\phi$) of about 0.2 towards idle ($\phi$ = 0.1 to 0.12), the bulk-gas reactions would become progressively less complete. To determine whether the prediction from this simple model holds for a real HCCI engine, a combined experimental and modeling study was conducted of low-load operation. Figure 5 presents the CHEMKIN modeling results which represent the behavior of the bulk-gases for an idealized, adiabatic version of the engine with the same 18:1 compression ratio and 1200 rpm speed used in the experiment. These results show that as fueling is reduced below $\phi$ = 0.16, the CO emissions begin to rise dramatically while $CO_2$ levels fall, indicating incomplete combustion due to the combustion temperatures being too low [2]. The corresponding experimental results, presented in Figure 6, show remarkably similar trends. For the experiment, the onset of the rise in CO occurs at a somewhat higher equivalence ratio than the model, which would be expected considering the heat transfer in the real engine. However, the experimental CO levels rise to a value that is nearly identical to the model (about 65% of the fuel carbon), showing that the cause of this behavior is incomplete combustion throughout the bulk gases. Experiments conducted with the fully premixed fueling system and at a lower engine speed (600 rpm) showed similar results.

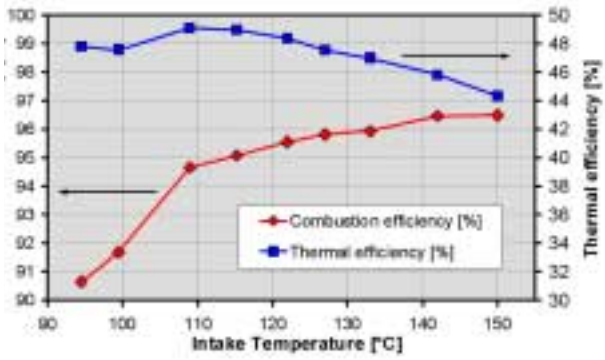


**Figure 2.** Combustion and thermal efficiencies as a

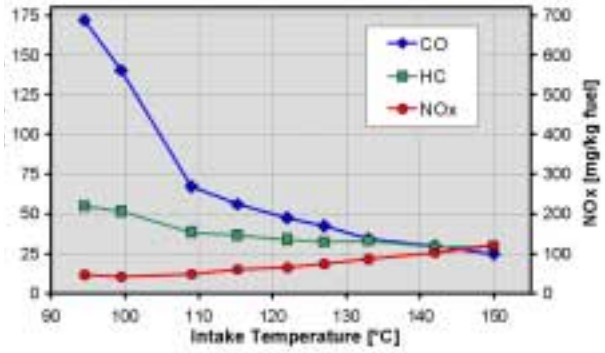


**Figure 3.** CO, HC, and $NO_x$ Emissions as a

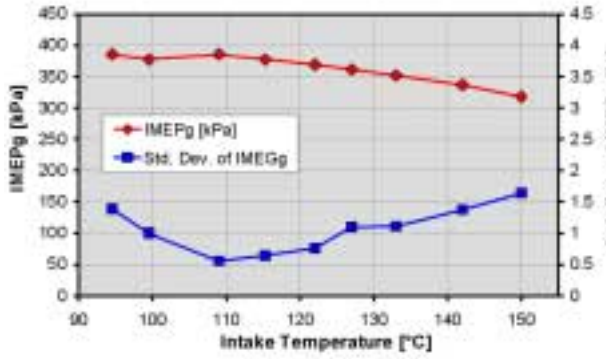


**Figure 4.** IMEPg and Standard Deviation of the IMEPg as a Function of Intake Temperature for a Typical Fully

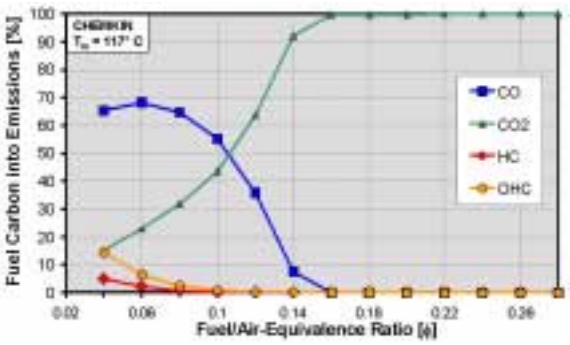


**Figure 5.** HCCI emissions as a function of equivalence ratio for the CHEMKIN single-zone adiabatic model. An intake temperature of 117°C was used to match combustion phasing with that of the experiment, which is shown in Figure 6.

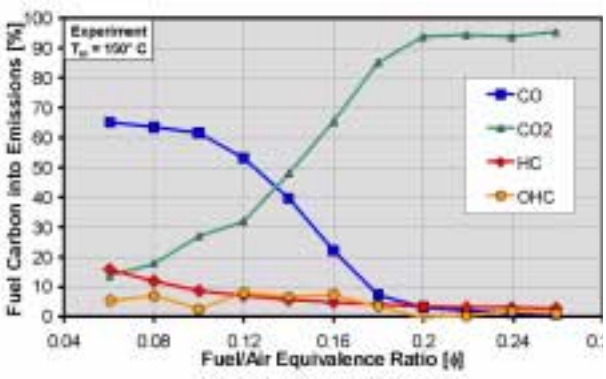


**Figure 6.** HCCI emissions as a function of equivalence ratio for the metal engine. An intake temperature of 150°C was required to maintain combustion phasing near top dead center (TDC). This temperature is

Late GDI fuel injection offers a potential solution to this problem of incomplete bulk-gas reactions at lower fuel loads because it can be used to partially stratify the fuel-air mixture. Figure 7 shows the results of varying the injection timing from early in the intake stroke to well up the compression stroke for $\phi = 0.1$. Early injection provides a well-mixed charge with high CO levels in agreement with the data for $\phi = 0.1$ in Figure 6. As the injection timing is retarded, the charge becomes more stratified which increases local equivalence ratios and, hence, local combustion temperatures. These higher temperatures cause the CO emissions to drop and the combustion efficiency to improve significantly. Although the charge eventually becomes so stratified that local combustion temperatures become sufficiently high to start producing $NO_x$, substantial improvements in the combustion can be realized prior to this point. For example, an injection timing of 290° (70° BTDC) dramatically reduced the CO and HC emissions and increased combustion efficiency from 61% to 83% while producing only 4 ppm $NO_x$.

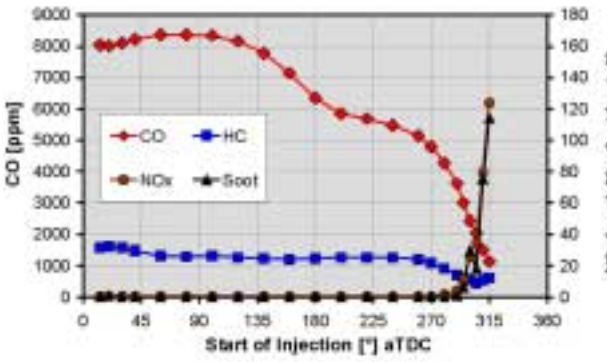


**Figure 7.** Engine-out emissions as a function of fuel injection timing for a low fuel load corresponding to an average equivalence ratio ($\phi$) of 0.1. 0° is TDC intake and 360°

## Conclusions

A parametric study of the metal-engine operation has shown that with an appropriate combustion chamber, HCCI engines operating at fully combusting conditions can provide diesel-like thermal efficiencies, HC and CO emission levels similar to spark-ignition engines, and extremely low $NO_x$ and smoke emissions.

As the fuel loading is reduced below $\phi = 0.2$ down to idle ($\phi \approx 0.1$), combustion efficiency drops and CO emissions rise dramatically along with a lesser rise in HC and oxygenated hydrocarbon (OHC) emissions. Comparison of these experimental results with the idealized adiabatic CHEMKIN model shows that this low-load behavior is caused by incomplete combustion reactions throughout the bulk gases due to excessively low combustion temperatures.

Partial charge stratification, achieved by late-cycle GDI fuel injection, can substantially improve the combustion efficiency at low loads. For an idle-like fuel loading ($\phi = 0.1$), injecting well into the compression stroke (70° BTDC) improved the combustion efficiency from 61% to 83% without producing significant $NO_x$.

## References

1. Kelly-Zion, P. L. and Dec, J. E., "A Computational Study of The Effect of Fuel Type on Ignition Time in HCCI Engines," Proceedings of the Combustion Institute, Vol. 28, Part 1, pp. 1187-1194, 2000.

2. Dec. J. E., "A Computational Study of the Effects of Low Fuel Loading and EGR on Heat Release Rates and Combustion Limits in HCCI Engine," SAE paper no. 2002-01-1309, 2002.

## FY 2002 Publications/Presentations

1. Dec. J. E., "A Computational Study of the Effects of Low Fuel Loading and EGR on Heat Release Rates and Combustion Limits in HCCI Engine," SAE paper no. 2002-01-1309, 2002.

2. Dec, J. E. "HCCI Combustion Research using Liquid-Phase Fuels," presented at and published in the proceedings of the Diesel Engine Emissions Reduction Workshop (DEER01), Portsmouth, VA, August 2001.

3. Epping, K., Aceves, S., Bechtold, R., and Dec, J., "The Potential of HCCI Combustion for High Efficiency and Low Emissions," SAE paper no. 2002-01-1923, SAE Future Car Conference, June 2002.

4. Epping, K., Aceves, S., Bechtold, R., and Dec, J., Homogeneous Charge Compression Ignition (HCCI), a Report to Congress, report prepared for the United States Congress, released September 2001.

5. Dec, J. E. and Keller, J. O., "HCCI Combustion Research at Sandia National Laboratories," International Energy Agency, Task Leaders Meeting, September 2001.

6. Dec, J. E., "HCCI Engines - the Promise and the Challenges," Energy Frontiers International, Clean Fuels and Advanced Engine Symposium, San Francisco, October 2001.

7. Dec, J. E. and Sjöberg, M., "HCCI Combustion with GDI Fuel Injection" Cross-Cut Diesel CRADA Meeting, January 16-17, 2002.

8. Dec, J. E. and Sjöberg, M., "HCCI Combustion Research at Sandia National Laboratories," Advances in Engine Combustion Symposium at the Royal Institute of Technology, Stockholm, Sweden, April 11, 2002.

9. Dec, J. E. and Sjöberg, M., "HCCI Combustion with GDI Fuel Injection" DOE CIDI Combustion and Aftertreatment Peer Review, May 14-16, 2002.

10. Dec, J. E. and Sjöberg, M., "HCCI Combustion Research at Sandia National Laboratories," Invited seminar, International Truck and Engine Co., Melrose Park, IL, May 2002.

11. Dec, J. E. and Sjöberg, M., "A Parametric Study of HCCI Combustion and the Sources of Emissions at Low Loads," HCCI Working Group Meeting, June 11, 2001 and Cross-Cut Diesel CRADA Meeting, June 13, 2002.

# C. HCCI Light-Duty Engine Studies: Fuel/Tracer Mixtures for Quantitative PLIF Measurements

*Richard Steeper (Primary Contact), Donghee Han*
*Sandia National Laboratories, MS 9053*
*P.O. Box 969*
*Livermore, CA 94551-0969*

*DOE Technology Development Manager: Kathi Epping*

This project addresses the following DOE R&D Plan barriers and tasks:

*Barriers*

A. $NO_x$ Emissions

B. PM Emissions

C. Cost

*Tasks*

1a. Advanced Fuel Systems

3c. Identification of Advanced Combustion Systems

## Objectives

- Develop a method to identify laser-induced fluorescence (LIF) tracers that properly co-evaporate with selected fuel components to enable quantitative fuel distribution measurements. Use the improved fuel/tracer mixtures to measure in-cylinder equivalence ratios.
- Characterize the in-cylinder fuel-air mixing process in the homogeneous charge compression ignition (HCCI) light-duty optical engine through measurements of direct-injection sprays, wall-spray interactions, and fuel-vapor distributions at the time of ignition.

## Approach

- Quantify the evaporative behavior of fuel/tracer mixtures used for LIF imaging using a bench-top batch evaporation experiment. Compare the evaporation characteristics of the commonly used LIF fuel/tracer blend isooctane/3-pentanone with other isooctane/ketone blends formulated to improve co-evaporation.
- Use the improved fuel/tracer mixtures in direct-injection optical engine experiments to obtain quantitative equivalence ratio distributions. Compare the measurements with those made using the conventional 3-pentanone/isooctane mixture.

## Accomplishments

- Collected data demonstrating the mismatch in volatility of the tracer 3-pentanone in solution with isooctane.
- Identified several alternative fuel/tracer mixtures providing more closely matched volatilities, thereby improving the accuracy of the LIF imaging diagnostic.
- In collaboration with University College London, applied vapor-liquid equilibrium theory to successfully model evaporation of simple fuel/tracer mixtures.

- Measured equivalence ratio distributions and probability density functions (PDFs) in the fired optical engine.

### Future Directions

- Modify the light-duty optical engine to support a wider range of HCCI operating conditions.
- Record late-compression-stroke equivalence ratio PDFs for a range of injection timings, injector cone angles, piston-top geometries, and operating conditions. Use the data to aid interpretation of emissions data.

---

## Introduction

Understanding and controlling the preparation of fuel/air mixtures in HCCI engines is essential to overcoming barriers facing the technology. As has been revealed by tests performed in engines at Sandia and elsewhere, emissions from HCCI engines are strongly coupled with injection timing. This dependence indicates the important role of fuel/air mixing on formation of emissions. Furthermore, control of ignition timing and combustion over a range of loads in the HCCI engine may well require advanced fuel/air mixing strategies (i.e., not necessarily homogeneous) S strategies that will require further understanding of the fuel/air mixing process.

LIF imaging is an appropriate and commonly used diagnostic to monitor fuel/air mixing; however, work is still needed to make the diagnostic quantitative. Typically, the diagnostic relies on a tracer that fluoresces, mixed with a fuel that does not fluoresce. In order for the tracer to properly track the fuel component in the vapor phase, the two must co-evaporate. The simplistic (and common) approach of selecting fuel/tracer components by matching boiling points and heats of vaporization is inadequate and can lead to significant errors in reported fuel distributions. An improved method of formulating fuel/tracer mixtures is developed in this work.

## Approach

Two activities have been pursued during FY02. First, a bench-top experiment has been used to characterize the evaporative behavior of several LIF fuel/air mixtures. Second, direct-injection engine tests have provided data to compare the performance of the various mixtures in making LIF measurements of late-compression-stroke equivalence ratios.

## Results

Results of the bench-top experiment shown in Figure 1 demonstrate the evaporation behavior of several LIF tracers in solution with isooctane. The graph plots the vapor-phase LIF signal recorded as the fuel/tracer solution evaporates. The progress variable plotted on the x-axis is the amount of liquid that has not yet evaporated, with time progressing from right to left. The lower data points represent the commonly used mixture isooctane + 10% 3-pentanone (initial concentration in volume %). If 3-pentanone correctly evaporated with isooctane, the liquid-phase concentrations would not change, and the LIF signal would remain constant through the experiment. But instead, the signal drops off dramatically with time-clearly indicating that the 3-pentanone is too volatile.

From the upper data points in Figure 1, it is also clear that the next heavier ketone, hexanone, is not volatile enough. It evaporates too slowly, increasing in concentration during the experiment, and producing an LIF signal that improperly increases with time.

But a combination of these two ketone tracers behaves as desired. The LIF signal from a mix of isooctane + 3-pentanone + 3-hexanone (the middle data points of Figure 1) is reasonably steady during the experiment. The conclusion is that this combination of tracers correctly co-evaporates, ensuring that the mixture will correctly track the fuel in the vapor phase.

Success in finding tracer combinations to track single-component fuels like isooctane led to experiments to find tracers that could track more complex fuels containing more than one fuel component. Figure 2 presents results for a mixture of

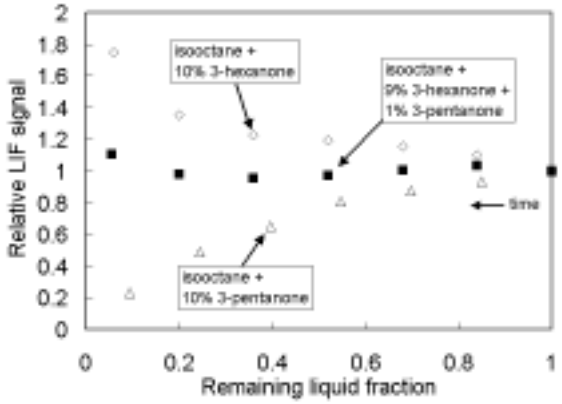


Figure 1. Relative vapor-phase fluorescence signal histories of fuel-tracer mixtures as a function of remaining liquid fraction during batch evaporation. Initial concentrations indicated in volume percent.

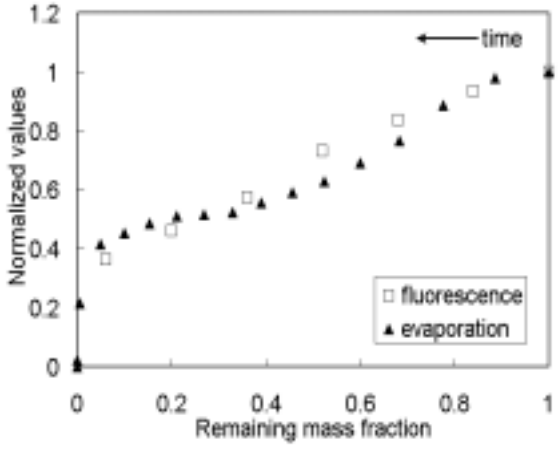


**Figure 2.** Normalized evaporation rate and LIF signal for a 2-fuel-component mixture. Initial concentrations: fuels: 70% isooctane, 20% cyclopentane; tracers: 4.5% 3-hexanone, 4% 3-pentanone, 1.5% 2-butanone.

2 fuels plus 3 ketone tracers. The filled symbols represent the instantaneous evaporation rate of the mixture. With two fuel components, the evaporation rate is no longer constant, so the desired LIF signal must decrease with time as well. Trial and error tests with many tracers and tracer concentrations yielded the LIF curve shown (open symbols), which tracks the evaporation curve reasonably well. This mixture therefore can be expected to properly co-evaporate

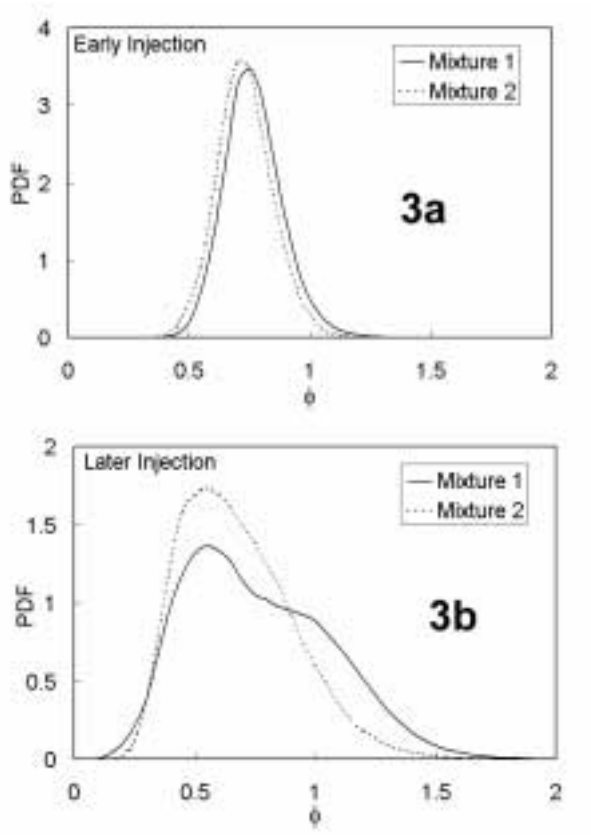


**Figures 3a. and 3b.** PDFs of equivalence ratio recorded near the end of the compression stroke in a plane close to the fire deck. The curves represent two co-evaporating fuel/ tracer mixtures injected early (a) and late (b) in the intake stroke. Initial composition of Mixture 1: see Figure 2 caption; Mixture 2: 90% cyclohexane plus 10% 3-pentanone.

and provide an LIF signal proportional to the local concentration of fuel vapor.

Several of the developed fuel/tracer mixtures were tested in an optical engine. Figure 3 presents data for two co-evaporating fuel/tracer mixtures in the form of PDFs of equivalence ratio recorded late in the compression stroke. The PDFs provide a measure of the probability of finding a given equivalence ratio value somewhere in the plane interrogated by the LIF diagnostic: the narrower the PDF, the more homogeneous the fuel/air mixture. Figure 3a represents an early injection case, and the PDFs for Mixtures 1 and 2 are both narrow since there is plenty of time for mixing. In Figure 3b, the

injection timing is delayed so that mixing is less complete, producing broader PDFs.

## Conclusions

An important conclusion can be drawn from the results of Figure 3. Although the PDFs are nearly identical for early injection (Figure 3a), in the case of late injection (Figure 3b), the PDFs for the two mixtures are distinctly different. This means that the fuel/air mixing process occurs at a different rate for complex fuels (more than one fuel component) compared to simple fuels (a single fuel component). This result casts doubt on the common practice of using a simple fuel of average volatility to model a more complex fuel in engine experiments.

## FY 2002 Publications/Presentations

1. D. Han and R. R. Steeper, "Examination of Iso-octane/Ketone Mixtures for Quantitative LIF Measurements in a DISI Engine," SAE Paper 2002-01-0837, 2002.

2. D. Han and R. R. Steeper, "An LIF Equivalence Ratio Imaging Technique for Multicomponent Fuels in an IC Engine," Proc. Combust. Inst. 29, 2002.

3. M. Davy, P. Williams, D. Han, and R. R. Steeper, "Evaporation Characteristics of the 3-Pentanone/ Isooctane Binary System," submitted to Experiments in Fluids, 2001.

4. R. R. Steeper, "Tracer Selection for Quantitative PLIF Measurements," DOE CRADA Meeting, Sandia National Laboratories, Livermore, CA, Jan. 2002.

5. R. R. Steeper, "Examination of Iso-octane/Ketone Mixtures for Quantitative LIF Measurements in a DISI Engine," SAE 2002 World Congress, Detroit, MI, Mar. 2002.

6. R. R. Steeper, "Light-Duty HCCI Laboratory: Fuel/Tracer Mixtures for PLIF Measurements," DOE Annual Review, Argonne National Laboratory, Chicago, IL, May, 2002.

7. R. R. Steeper, "HCCI Light-Duty Optical Engine Experiments," DOE CRADA Meeting, USCAR, Detroit, MI, June, 2002.

8. R. R. Steeper, "An LIF Equivalence Ratio Imaging Technique for Multicomponent Fuels in an IC Engine," 29th International Symposium on Combustion, Sapporo, Japan, July, 2002.

# D. HCCI Engine Optimization and Control Using Diesel Fuel

*Rolf D. Reitz (Primary Contact), Dave Foster, Kevin Hoag and Chris Rutland*
*University of Wisconsin*
*1500 Engineering Drive*
*Madison, WI 53706*

*DOE Technology Development Manager: Gurpreet Singh*

*Subcontractor: Professor D. Haworth, State College, PA*

This project addresses the following DOE R&D Plan barriers and tasks:

*Barriers:*

A. $NO_x$ Emissions

B. PM Emissions

C. Cost

*Tasks:*

1a. Advanced Fuel Systems

3. Fundamental Combustion R&D

## Objectives

- Develop methods to optimize and control Homogeneous-Charge Compression Ignition (HCCI) engines, with emphasis on diesel-fueled engines.
- Use engine experiments and detailed modeling to study factors that influence combustion phasing, unburned hydrocarbon (UHC) and CO emissions.
- Provide criteria for transition to other engine operation regimes (e.g., standard diesel combustion).

## Approach

- Use 2 fully-instrumented engines with prototype fuel injection systems and combustion sensors to map and define HCCI combustion regimes, and apply optimization techniques.
- Develop and apply engine performance models, including zero- and 1-dimensional global models for control system development.
- Use homogeneous charge Coordinating Fuels Research (CFR) engine experiments to document fuel effects on HCCI ignition.
- Develop and apply modeling tools, including multi-dimensional codes (e.g., KIVA with state-of-the-art turbulent combustion and detailed chemistry models) to reveal combustion mechanisms.

## Accomplishments

- Engine operation at both very early and very late start-of-injection timings has been shown to produce low emissions with HCCI-like combustion.
- A combustion control criterion based on the ignition/injection time delay has been formulated for low emissions operation.
- A multidimensional model has been developed and applied successfully to model early and late injection cases.

- HCCI ignition has been shown to be controlled by effects beyond fuel octane number.
- Computationally efficient methods to incorporate detailed chemistry submodels have been formulated.

### Future Directions

- A prototype high pressure hydraulic unit injector will be implemented to assess the effects of multiple injections on diesel HCCI combustion regimes.
- Use of cylinder pressure-based sensing for engine control will be analyzed.
- Ignition characteristics of diesel fuel will be explored in engine experiments.
- Efficient methods for including detailed kinetics in multidimensional models will be implemented and tested.

---

## Introduction

Advantages of Homogeneous Charge Compression Ignition (HCCI) operation include significantly reduced $NO_X$ and particulate emissions. However, there are significant challenges associated with the successful operation of HCCI engines. One of the major difficulties is to control the combustion phasing—mainly the assurance of autoignition at appropriate timings over a wide range of operating conditions. Another obstacle of HCCI engine operation is the relatively high emissions of unburned hydrocarbon (HC) and carbon monoxide (CO) due to incomplete combustion with low-temperature lean burn. The power output of the HCCI engine is also limited since the combustion can become unstable, and knock-like cylinder pressure oscillations can occur as the mixture approaches stoichiometric.

## Approach

In order to control the engine, it is necessary to know what variables to control. The technical tasks of the present work provide information about HCCI combustion mechanisms for use in knowledge-based engine control schemes. The experiments use a fully instrumented Caterpillar 3401 engine that features electronically controlled fuel injection systems to map combustion regimes. Combustion sensors are also being developed and adapted for engine control including crankshaft speed observers, and spark plug ionization and fiber optic detectors. Combustion diagnostics include engine-out HC and other gaseous emissions measurements.

Computer modeling, coupled with innovative engine experiments, is used to devise strategies for optimizing and controlling HCCI engine performance and reducing emissions over the speed-load range of interest. Engine performance models include zero- and one-dimensional global models for control system development. Data for chemical kinetics model validation is obtained using a CFR engine operated on a variety of fuels. The influence of turbulence, temperature, and mixture inhomogeneities is revealed with highly resolved computational fluid dynamics (CFD) predictions and laser-based engine experiments.

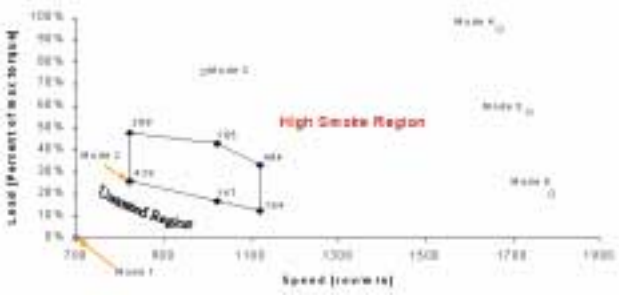


**Figure 1.** Late Start-of-Injection Operating Regime for PCCI Combustion (Numbers represent the emissions "merit" at each test data point. Low numbers represent low emissions; high numbers represent high emissions.)

## Results

HCCI engine combustion regime mapping – The Caterpillar 3401 engine with an electronic unit injector (EUI) injection system was tested over a wide range of speeds and loads. As shown in Figure 1, low emissions operation could be achieved with late injection timings [i.e., start-of-injection (SOI) after top dead center (TDC)] up to about 1200 rev/

min. At higher engine speeds, particulate matter (PM) levels increased significantly. Figure 1 also shows baseline 6-mode steady-state test points of the Federal Test Procedure (FTP) transient test procedure for reference. It is seen that Premixed Charge Compression Ignition (PCCI) operation was also limited to light load conditions. In PCCI combustion, heat release rate analysis indicates that diffusion burning is minimal, and most of the combustion process occurs in a premixed combustion mode. The engine tests were ranked using a merit function that is based on $NO_x$, PM and brake-specific fuel consumption (BSFC) as where the target values in the denominator reflect Environmental Protection Agency (EPA) 2002/2004 emissions mandates. The corresponding merit values are also indicated on Figure 1 for each engine test point.

$$Merit = \frac{1000}{\left(\frac{NOx + HC}{2.682\frac{g}{kW-hr}}\right) + \left(\frac{PM}{0.107\frac{g}{kW-hr}}\right) + \frac{BSFC}{200\frac{g}{kW-hr}}}$$

Early injection results (i.e., SOI 10-25 degrees before TDC) are shown in Figure 2. In this case, satisfactory engine operation was achieved for all engine speeds up to 40% load.

Combustion modeling and control - Cylinder pressure, heat release and fuel injection rate data are shown in Figure 3, together with the merit values for several early injection cases. As can be seen, cases whose start-of-combustion occurs after the injection has ended have the highest merit. The longer time available for mixing in these cases favors premixed burning, with dramatically reduced PM emissions. KIVA computations of the fuel/air equivalence ratio ($\phi$) distributions in the engine at the experimental start of combustion times are shown in Figures 4 and 5 for two early injection cases. Figure 5 shows that with sufficiently early SOI, rich regions ($\phi > 2$) are all but eliminated. This supports the experimental finding that particulate is reduced under these conditions, since it is known that PM does not form when $\phi<2$. These results indicate that the ignition delay time after the end of injection may be a suitable parameter for engine control.

Ignition chemistry - A CFR research engine was run in the HCCI combustion mode for a range of

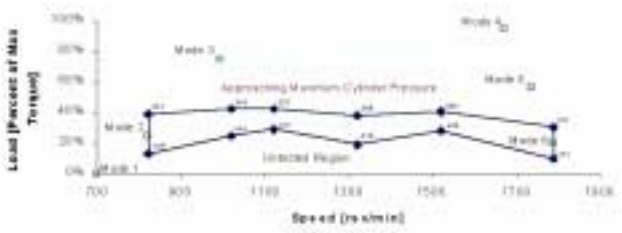

**Figure 2.** Early Start-of-Injection Operating Regime for PCCI Combustion (Numbers represent the emissions "merit" at each test data point. Low numbers represent low emissions, high numbers represent high emissions.)

temperatures and fuel compositions. The data indicate that the best HCCI operation occurs at or near the rich limit of operation. Analysis of the pressure and heat release histories indicated the presence, or absence, and impact of the fuel's negative temperature curvature (NTC) ignition behavior on establishing successful HCCI operation. The auto-ignition trends observed were in complete agreement with previous results found in the literature. Furthermore, analysis of the importance of the fuel's octane sensitivity, through assessment of an octane index, successfully explained the changes in the fuel's auto-ignition tendency with changes in engine operating conditions. For practical HCCI application it will be important to have an optimal phasing of the energy release with the piston motion. If the fuels being used do not have strong NTC behavior, this phasing appears to be most readily obtained through intake temperature control. If the fuel being used exhibits strong NTC behavior, the interaction between the in-cylinder temperature, pressure and engine speed becomes significantly more complicated. Under such conditions, it seems that some mechanism to trigger the start of HCCI combustion will be needed.

Multidimensional modeling - Work has focused on using 'i*n-situ* adaptive tabulation' (ISAT) for detailed chemistry in an HCCI application, together with detailed intake flow modeling to understand its impact on HCCI mixture preparation, ignition, and combustion. ISAT potentially reduces the computational time required to simulate complex hydrocarbon oxidation chemistry in HCCI ignition and combustion by automatically tabulating and reusing data. Initial tests for HCCI have shown reduction in computational time by as much as a

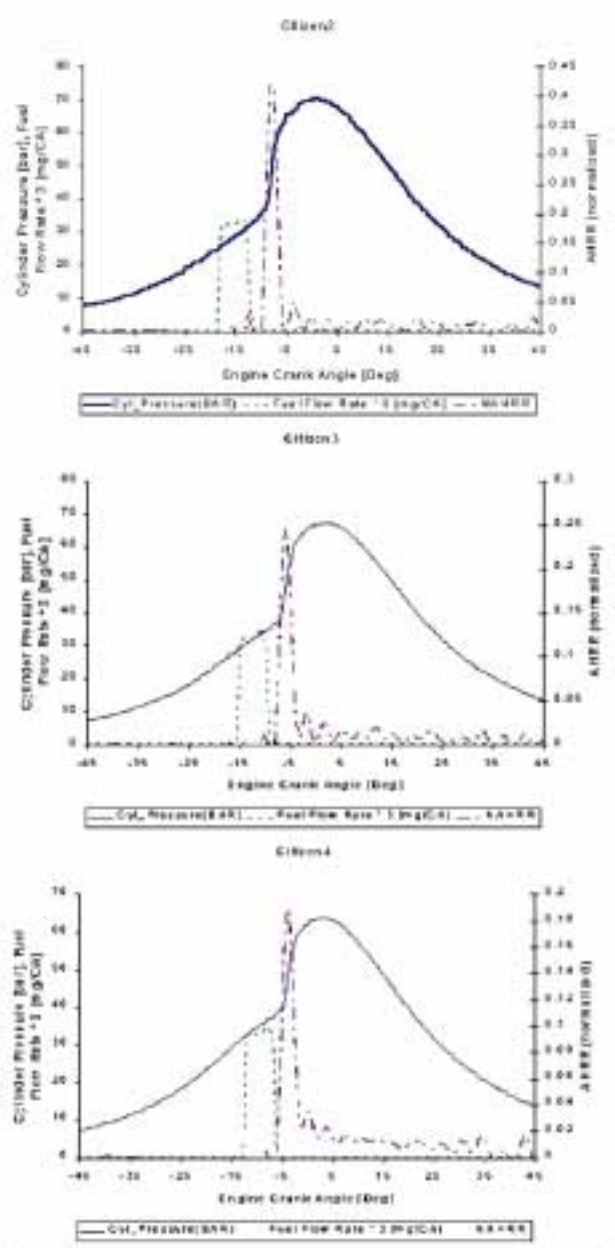

| Citizen | SOI | PM | NOx | Merit |
|---|---|---|---|---|
| 2 | -18 | 0.058 | 0.772 | 592 |
| 3 | -15 | 0.286 | 0.570 | 118 |
| 4 | -12 | 0.717 | 0.457 | 22 |

**Figure 3.** Measured Cylinder Pressure, Normalized Apparent Heat Release Rate (NAHHR) and Fuel Injection Rate as a Function of Start-of-Injection Timing for Early Injection Cases

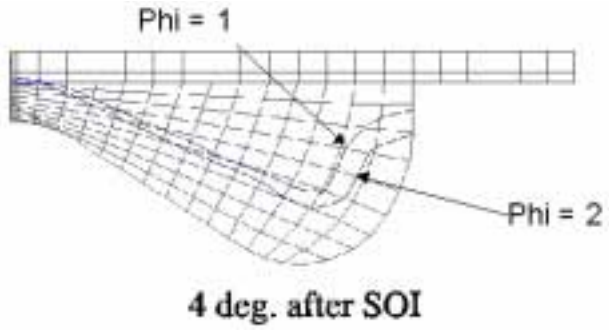


**Figure 4.** Predicted Fuel/Air Equivalence Ratio Contours for SOI S 9 after TDC at the Experimental Start of Combustion Time

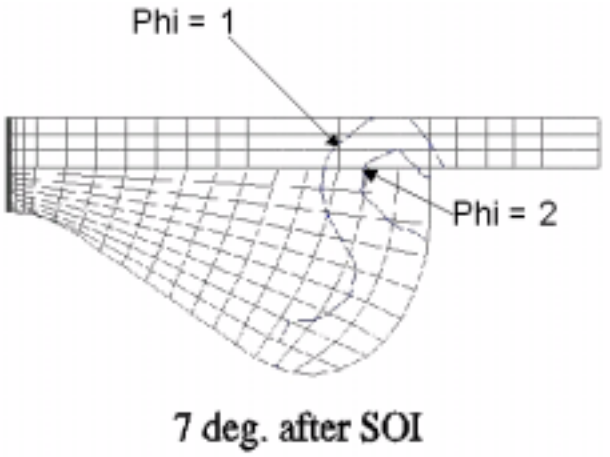


**Figure 5.** Predicted Fuel/Air Equivalence Ratio Contours for SOI S 18 after TDC at the Experimental Start of Combustion Time

factor of ten. Part of this was due to a variation on the basic ISAT approach of choosing a subset of parameters to characterize the tabulation. Additional work on CFD modeling has focused on intake flow simulations. These are being used to establish baseline Reynolds Averaged Navier Stokes (RANS) calculations of different intake air temperature and exhaust gas recirculation (EGR) cases before moving to large eddy sumulation (LES) models. The initial simulations show good comparison with experimental values of the pressure traces.

## Conclusions

The engine tests have shown that operation at both very early and very late start-of-injection timings is effective for low emissions. In particular, adequate dwell between the end-of-injection and the start of combustion allows time for fuel/air mixing. Low local equivalence rations are beneficial for particulate reduction and result in HCCI-like combustion. A combustion control criterion based on the ignition/injection time delay is being formulated for low emissions operation. A multidimensional model was applied successfully to help explain the experimental trends for both early and late injection cases. Combustion modeling is in progress, and the fuel chemistry experiments show that HCCI ignition is controlled by effects beyond fuel octane number. This indicates that detailed chemical kinetic models will require further validation by comparison with the present experiments.

## FY 2002 Publications/Presentations

1. DOE HCCI Presentations Meetings: Feb. 19, 2002 and June 11-12, 2002.

# E. HCCI Engine Optimization and Control Using Gasoline

*Dennis Assanis (Primary Contact)*
*University of Michigan (UM), Department of Mechanical Engineering*
*2045 W.E.Lay Auto. Lab.*
*1231 Beal Avenue*
*Ann Arbor, MI 48109-2121*

*DOE Technology Development Manager: Kathi Epping*

*Subcontractors: Massachusetts Institute of Technology (MIT); Stanford University (SU); University of California, Berkeley (UCB); Texas A&M University (TAMU)*

This project addresses the following DOE R&D Plan barriers and tasks:

*Barriers:*

A. $NO_X$ Emissions

B. PM Emissions

C. Cost

*Tasks:*

1a. Advanced Fuel Systems

3. Fundamental Combustion R&D

## Objectives

- Develop a homogeneous charge compression ignition (HCCI) engine control system
- Develop a multi-zonal thermo-kinetic cycle and system simulation of HCCI engine
- Experimentally and analytically investigate detailed and reduced chemical kinetic reaction mechanisms required to model the HCCI combustion processes
- Develop detailed HCCI process models using computational fluid dynamics (CFD) codes including spray dynamics and complex chemistry, validated with optical diagnostic engine experiments

## Approach

- Balance fundamental and applied work for maximum effectiveness
- Capitalize on university facilities and resources (both personnel and equipment) which are unique to the UM HCCI consortium
- Investigate critical chemical kinetic rates and mechanisms for gasoline, and develop and validate reduced kinetic mechanisms
- Develop a simple thermo-kinetic model of an HCCI engine to use in system simulations as well as more complex multi-zone / CFD codes
- Employ a range of chemical reaction computation methodologies in these models
- Test models with engine experiments and combine models and experiments to develop a workable engine control system

### Accomplishments

- Demonstrated use of variable valve actuation (VVA) as a means to achieve HCCI
- Demonstrated several approaches for generating reduced chemical reaction sets for gasoline
- Developed a thermo-kinetic model of HCCI for rapid computation in engine system simulations; the model has been validated against HCCI engine data for natural gas
- Developed a multi-zone model of HCCI operation which is initiated by detailed CFD computations of the breathing process; the model has been applied to investigate exhaust gas recirculation (EGR) mixing and VVA as control strategies
- Obtained benchmark ignition data on simple hydrocarbon fuels via rapid compression facility (RCF) experiments
- Isolated key elementary chemical reactions important in cool HCCI 'flames'

### Future Directions

- Chemical kinetic and computational studies along with shock tube and RCF experiments will continue to feed improved models of gasoline chemistry into the engine simulation tools
- Metal and optical engines and RCF experiments will provide benchmark data on control strategies (e.g. % EGR and/or residual gases) for specific ignition times and burn durations
- Engine experimental setups will contribute to the studies of heat transfer, transients and control methods
- Control algorithms will be developed and validated in engine experiments

---

## Introduction

Homogeneous Charge Compression Ignition (HCCI) has the potential to dramatically reduce NOx emissions from gasoline internal combustion engines, while achieving high thermal efficiencies characteristic of diesels, with lower particulate emissions. Because the ignition is not controlled by a spark plug as in conventional gasoline engines but occurs as a result of the compression heating of the charge, it has been difficult to implement HCCI in practical engines. Therefore, the primary objectives of this research program are to develop increased understanding of the physical and chemical processes important in HCCI engines and to apply this knowledge to identify, develop and assess control strategies and enabling technologies necessary to implement the HCCI combustion mode to a range of engines. To meet the program objectives, we have formed a Multi-University Research Consortium of experts in the areas of engines, optical diagnostics, numerical modeling, gas dynamics, chemical kinetics and combustion research from UM, MIT, SU, UCB, and TAMU.

## Approach

Our research approach combines experiments and modeling at various levels of complexity and resolution in order to acquire and utilize the knowledge and technology necessary to develop a robust control system for HCCI engines. Both single-cylinder and multi-cylinder engine experiments are addressing issues such as injection strategy, mixture homogeneity, valve timing, EGR, intake temperature, fuel properties, cooling strategy, transients and engine mode transitions (e.g. spark ignited to HCCI). Enabling technologies such as variable valve timing will also be explored as potential means to control auto-ignition. Extensive studies are underway to develop accurate and reliable chemical kinetic models for practical engine fuels relevant to HCCI application. At the same time, cycle simulation and CFD models are being developed using the experimental and chemical results to identify HCCI operating ranges and limits and to assist in the development and optimization of control strategies.

## Results

*Development of an HCCI Engine Control System* – At University of California Berkeley, a model of a single well-mixed reactor has been coupled with genetic algorithms for searching optimal intake conditions including temperature, pressure, equivalence ratio, and EGR. At MIT and UM, much of the work to mid-2002 has been on experimental setup. By the end of this first year we expect to be generating data on heat transfer, transient engine behavior and on practical control strategies. At Stanford, an existing setup has enabled measurements to be made of HCCI with exhaust re-induction via variable valve actuation (VVA) (1). Figure 1 shows a sequence of engine cycles in which HCCI combustion is induced in one cycle by leaving the exhaust valve open during intake.

*Full Cycle and System Modeling Tools* – Work at UM has produced a PC-based, computationally-efficient, quasi-dimensional simulation of HCCI engine performance and emissions (2). The model couples a detailed chemistry description, a core gas model, and a predictive boundary layer model. Performance predictions for a natural gas fueled Caterpillar 3500 engine were in satisfactory agreement with experimental data. The simulation also predicted emissions of unburned hydrocarbons (UHC) within 10-20%.

*Investigation of Chemical Kinetics for Gasoline HCCI* – Six detailed kinetic mechanisms for hydrocarbon oxidation have been compiled and examined at Stanford. These include mechanisms for butadiene, methane, propane, butane, heptane and neopentane. Shock tube studies at Stanford have determined ignition delay times and hydroxyl radical (OH) concentrations for several linear and branched alkanes, and they have been compared with extant models (3). MIT researchers are developing a methodology for estimating kinetic rate coefficients and their pressure dependence for large hydrocarbon molecules found in gasoline. The method relies on the group additivity technique for transition states. Using this method, substantially large reaction sets (~100,000) may be represented by a much reduced set of parameters (~100).

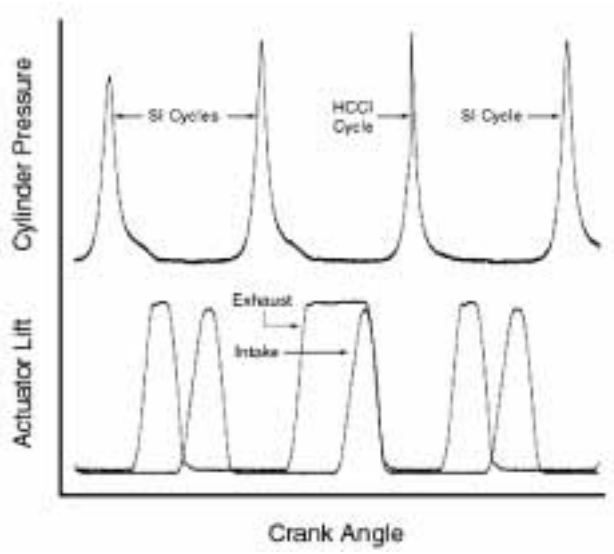


**Figure 1.** Cylinder Pressure and Valve Lift Showing Use of VVA to Achieve HCCI Combustion

At UM, computational modeling of the HCCI ignition process has been able to simulate the compression ignition process and unsteady counterflow ignition process to investigate the effect of flow strain and EGR mixing (4). Work on the Rapid Compression Facility to duplicate HCCI ignition conditions for simple hydrocarbon fuels is complete (5). Quantitative measurements of ignition delay times via pressure measurements and radical growth (OH) of complex hydrocarbon fuels are in progress. Tests at UCB on the detailed chemistry for HCCI suggest that a more robust detailed chemistry is needed for gasoline. Techniques to develop skeletal mechanisms with different approaches are being reviewed and developed.

*Detailed Modeling of Reaction, Mixing and Spray Dynamics Using CFD Codes and Experimental Validation* – At UM, a multi-dimensional fluid mechanics code (KIVA-3V) was used to simulate exhaust, intake and compression up to the point where chemical reactions become important (see Figure 2). The results were used to initialize the zones of a multi-zone code with detailed chemical kinetics (see Figure 3), which computes the combustion and expansion processes. The methodology was used to evaluate valve event strategies as a means of controlling HCCI by varying EGR and the degree of mixing (6). Results in Figure

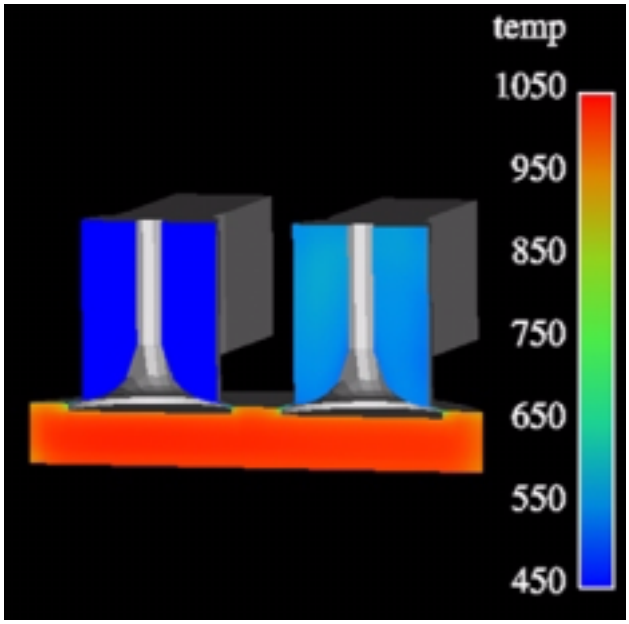


**Figure 2.** Temperature Field at End of Compression Calculated by KIVA-3V in Study of Valve Timing Effects and EGR Mixing

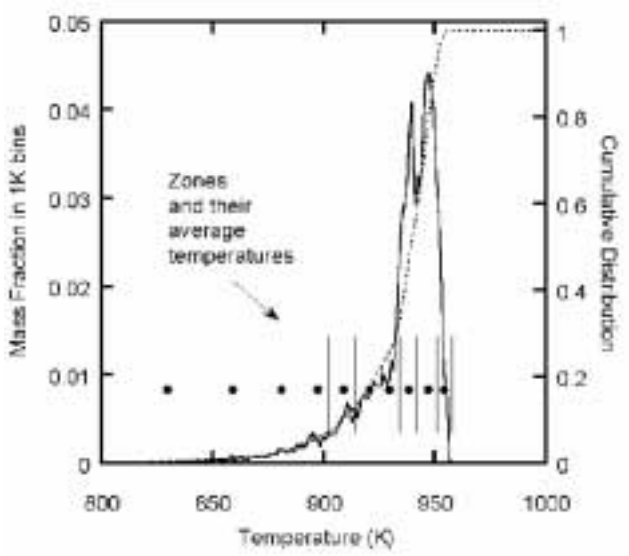


**Figure 3.** Temperatures from Figure 2 are Used to Define Input to Multi-Zone Kinetic Calculation

4 show that incomplete EGR mixing introduces corresponding variations in the temperature field prior to combustion. Preparation for optical diagnostic validation experiments with formaldehyde imaging by planar laser-induced fluorescence (PLIF) continues at UM. At Texas A&M University, triple-pump Coherent Anti-Stokes Raman Scattering

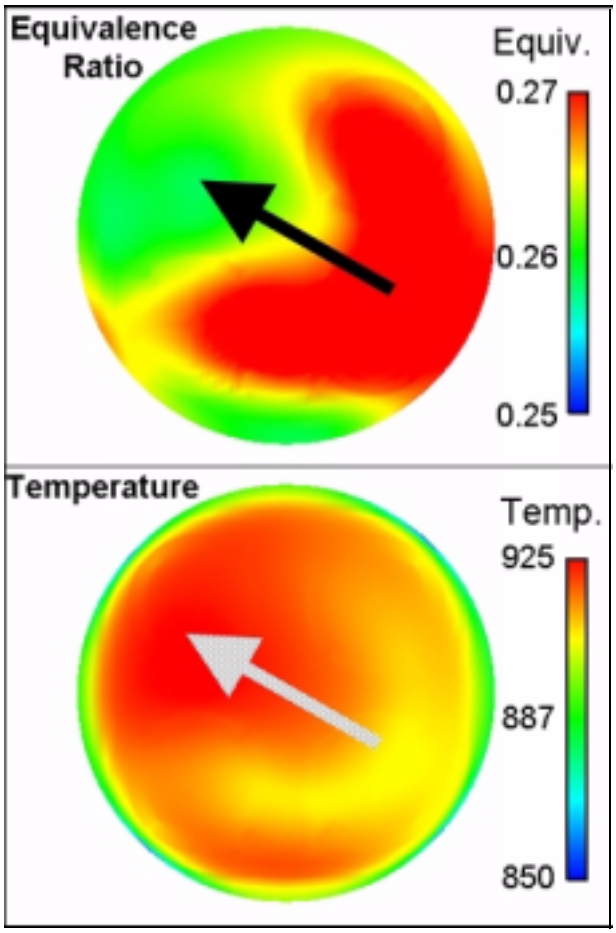


**Figure 4.** Equivalence ratio (a measure of EGR) correlates with temperature field at end of compression. Arrows point to higher EGR and higher temperature.

(CARS) work has demonstrated simultaneous single-laser-shot acquisition of triple-pump CARS signals from $H_2/N_2$ and $O_2/N_2$ spectral pairs, which will allow simultaneous *in situ* point measurements of T, $O_2$ and $CO_2$.

## Conclusions

Initial engine experiments have been completed on VVA for propane fuel. Additional experimental engine facilities will be generating key data for heat transfer, and transient and control studies by year's end.

Methods of developing a reduced chemical kinetics mechanism have been demonstrated and will be applied to the available detailed gasoline kinetics.

Areas of improvement needed in gasoline kinetics have been identified and will be examined in detail using shock tube studies.

Two models of HCCI engines have been developed: one employs detailed CFD calculations of the breathing process coupled with multi-zone, detailed chemical kinetics for the combustion period; a simpler model, much more computationally efficient, uses detailed chemical kinetics but fewer zones and a quasi-dimensional breathing process. The latter is intended to be used in full vehicle simulations.

## References/ FY 2002 Publications/ Presentations

1. Edwards, C.F. et al., "Residual-Effected Homogeneous Charge Compression Ignition at Low Compression Ratio Using Exhaust Re-induction," submitted to the International Journal of Engine Research (2002).

2. Fiveland, S. B., and Assanis, D. N., "Development and Validation of a Quasi-Dimensional Model for HCCI Engine Performance and Emissions Studies under Turbocharged Conditions," SAE Paper No. 2002-01-1757, 2002.

3. Oehlschlaeger M. A., Davidson, D. F., Herbon, J. T., and Hanson, R K., "Shock Tube Measurements of Branched-Alkane Ignition Times and OH Concentration Time Histories", in preparation.

4. Mason, S. D., Chen, J. H., Im, H. G., "Effects of Unsteady Scalar Dissipation Rate on Ignition of Non-Premixed Hydrogen/Air Mixtures in Counterflow," Proceedings of the Combustion Institute, v.29, in press (2002).

5. Donovan, M. T., Palmer, T., He, X., Wooldridge, M. S., and Atreya, A., "Demonstration of a Free-Piston Rapid Compression Facility to Produce Extended Duration High Temperature/Pressure Reaction Environments for Fundamental Combustion Studies," *2002 Spring Te*chnical Meeting of the Canadian Section of the Combustion Institute, May 12-15, 2002, Paper #5, pp. 1-6.

6. Babajimopoulos, A., Assanis, D. N., and Fiveland, S. B., "Modeling the Effects of Gas Exchange Processes on HCCI Combustion and an Evaluation of Potential Control through Variable Valve Actuation," Submitted to SAE for presentation at the Fall Fuels and Lubricants Meeting, 2002.

7. Flowers, D. L, Aceves, S.M., Martinez-Frias, J., and Dibble, R. W., "Prediction of Carbon Monoxide and Hydrocarbon Emissions in Isooctane HCCI Engine Combustion Using Multi-Zone Simulations," Proceedings of the Combustion Institute, v.29, in press (2002).

# ACRONYMS

| | |
|---|---|
| AC | Alternating Current |
| AHRR | Apparent Heat Release Rate |
| $Al_2O_3$ | Aluminum Oxide |
| AMST | Advanced Material Synthesis Technology |
| ANL | Argonne National Laboratory |
| APS | Advanced Photon Source |
| ATDC | After Top Dead Center |
| Au | Gold |
| BM | Bending Magnet |
| Bmep | Brake mean effective pressure |
| Bsfc | Brake specific fuel consumption |
| BSPM | Brake specific particulate matter |
| BSU | Bosch Smoke Unit |
| BTDC | Before Top Dead Center |
| CA | Crank Angle |
| CAD | Crank Angle Degrees |
| CAO | Chlorophyll *a* Oxygenase |
| CARS | Coherent Anti-Stokes Raman Scattering |
| CFD | Computational Fluid Dynamics |
| CFR | Coordinating Fuels Research |
| CHAD | Computational Hydrodynamics for Advanced Design |
| CHEMKIN | Name of Chemical-Kinetic Code |
| CHESS | Cornell High Energy Synchrotron Source |
| CI | Compression Ignition |
| CIDI | Compression Ignition Direct Injection |
| CN42 | Blend of 68% $C_{16}H_{34}$ [HMN] and 32% nC16 with a Cetane No. of 42 |
| CO | Carbon Monoxide |
| $CO_2$ | Carbon Dioxide |
| COV | Coefficient of Variation |
| $Cr_2O_3$ | Chromium Oxide |
| CRADA | Cooperative Research & Development Agreement |
| CV | Cyclic Voltammetry |
| CW | Continuous Wave |
| $C_x$ | Hydrocarbon containing x carbon atoms |
| DAQ | Data Acquisition System |
| DBM | Dibutyl Maleate |
| DC | Direct Current |
| DCSF | Diesel Combustion Simulation Facility |
| DEER | Diesel Engine Emissions Reduction Workshop |
| DI | Direct Injection |
| DO | Diesel oxidation catalyst |
| DOE | Department of Energy |
| DPF | Diesel Particulate Filter |
| DPS | Diesel Particle Scatterometer |
| ECM | Electronic Control Module |
| EDM | Electrodischarge Machining |
| EGR | Exhaust Gas Recirculation |
| ELS | Elastic Light Scattering |
| EMS | Engine Management System |
| EOS | Equation of State |
| EP | Electroplating |
| EPA | Environmental Protection Agency |
| ES | Energy Systems |
| EtOH | Ethanol |
| EUI | Electronic Unit Injector |
| FEA | Finite Elements Analysis |
| F-M | Federal–Mogul |
| FTIR | Fourier Transform Infrared |
| FTP | Federal Test Procedure |
| FY | Fiscal Year |
| g (or gm) | Gram |
| g/hp-h | Grams per horsepower-hour |
| GDI | Gasoline-type Direct Injector |
| h | Hours |
| H | Hydrogen |
| $H_2$ | Diatomic Hydrogen |
| $H_2O$ | Water |
| HC | Hydrocarbon |
| HCCI | Homogeneous Charge Compression Ignition |
| He | Helium |
| HELD | High-Energy Laser Diagnostics |
| HMN | 2,2,4,4,6,8,8 HeptaMethylNonane ($C_{16}H_{34}$) |
| HMO | Hydrous Metal Oxide |
| $HO_2$ | Hydroxyl Radicals |
| hr | Hour |
| HSDI | High Speed Direct Injection |
| HTO:Si | Silica-Doped Hydrous Titanium Oxide |
| Hz | Hertz |

| | |
|---|---|
| ID | Inner Diameter |
| IDE fuel | Diesel Surrogate |
| IMEP | Integrated Mean Effective Pressure |
| IMEPg | Integrated Mean Effective Pressure, gross |
| ISAT | *in-situ* adaptive tabulation |
| J/L | Joules per liter |
| K | Kelvin |
| kg | Kilogram |
| KL | Optical Density of Soot, Roughly Proportional to Mass of Soot in Path of Laser |
| kW | Kilowatt |
| L | Liter |
| LANL | Los Alamos National Laboratory |
| LBNL | Lawrence Berkeley National Laboratory |
| LD2 | Lubrizol Diesel Fuel No. 2 |
| LDT | Light-Duty Truck |
| LDV | Light-Duty Vehicle |
| LEP | Low Emissions Technologies Research and Development Partnership |
| LES | Large Eddy Simulation |
| LEVC | Late Exhaust Valve Opening |
| LIBS | Laser-Induced Breakdown Spectroscopy |
| LIDELS | Laser-Induced Desorption with Elastic Light Scattering |
| LIGA | Lithographie, Galvanoformung und Abformung |
| LII | Laser-Induced Incandescence |
| LIP | Laser-Induced Phosphorescence |
| LIVO | Late Intake Valve Opening |
| LLNL | Lawrence Livermore National Laboratory |
| LNT | Lean $NO_x$ Trap |
| LOS | Loss of Sight |
| MHz | Megahertz |
| mi | Mile |
| min | Minute |
| MIT | Massachusetts Institute of Technology |
| MK | Modified Kinetics |
| mm | Micron |
| mm | Millimeter |
| mmol | millimole |
| MOCVD | Metallorganic vapor deposition |
| MPa | Megapascal |
| ms | Microsecond |
| MVEG | European Driving Cycle for Emissions Certification |
| Mw-DPF | Microwave-regenerated diesel particulate filter |
| $N_2$ | Diatomic Nitrogen |
| $N_2O$ | Nitrous Oxide |
| NAHRR | Normalized Apparent Heat Release Rate |
| $nC_{16}$ | Normal Hexadecane ($C_{16}H_{34}$) |
| NCR | Combustion Research Group at the National Research Council |
| Nd:YAG | High Power Pulsed Laser Source |
| NDIR | Non Dispersive Infrared |
| $NH_3$ | Ammonia |
| $NH_4NO_3$ | Ammonium Nitrate |
| nm | Nanometer |
| Nm | Newton meter |
| NO | Nitric Oxide |
| $NO_2$ | Nitrogen Dioxide |
| $NO_x$ | Oxides of nitrogen |
| NRC | National Research Council |
| NREL | National Renewable Energy Laboratory |
| NTC | Negative temperature curvature |
| NTP | Non-Thermal Plasma |
| OAAT | Office of Advanced Automotive Technologies |
| $^oC$ | Degrees Celsius |
| OD | Outer Diameter |
| OFVT | Office of FreedomCAR and Vehicle Technologies |
| OH | Hydroxyl radical |
| OHC | Oxygenated Hydrocarbons |
| OHVT | Office of Heavy Vehicle Technologies |
| ORNL | Oak Ridge National Laboratory |
| PAD | Pixel Array Detector |
| PC | Personal computer |
| PCCI | Premixed Charge Compression Ignition |
| PDF | Probability Density Function |
| PLIF | Planar Laser-Induced Fluorescence |
| PM | Particulate Matter |
| PNGV | Partnership for a New Generation of Vehicles |
| PNNL | Pacific Northwest National Laboratory |

| | |
|---|---|
| PoxHC's | Partially Oxidized Hydrocarbons |
| ppm | Parts per million |
| PREOS | Peng-Robinson Equation of State |
| PRP | Pressure Reactive Piston |
| psi | Pounds per square inch |
| psia | Pounds per square inch absolute |
| P-T-P | Port-to-Port |
| PVD | Physical Vapor Deposition |
| QFD | Quality Function Deployment |
| R&D | Research and Development |
| RANS | Reynolds Averaged Navier Stokes |
| RCF | Rapid Compression Facility |
| RDG-PFA | Rayleigh-Debye-Gans polydisperse fractal aggregate |
| $RO_2$ | Hydrocarbon Radical Species |
| RPM | Revolutions Per Minute |
| s | Second |
| S:N | Signal/Noise Ratio |
| SAE | Society of Automotive Engineers |
| SBCE | Set Based Computer Engineering |
| SCP | Single-Cell Protein |
| SCR | Selective Catalytic Reduction |
| $SF_6$ | Sulfur Hexafluoride |
| SGB | Simulated Gas Bench |
| SI | Spark Ignition |
| SIDI | Spark Ignition Direct Injection |
| SMPS | Scanning Mobility Particle Sizer |
| SNL | Sandia National Laboratories |
| $SO_2$ | Sulfur Dioxide |
| $SO_3$ | Sulfur Trioxide |
| SOI | Start-of-Injection |
| $SO_x$ | Oxides of Sulfur |
| SRI-CAT | Synchrotron Radiation Instrumentation Collaborative Access |
| SU | Stanford University |
| SV | Space Velocity |
| T | Temperature |
| T30 | Oxygenated Fuel Blend of 30% TEOP with 53% HMN and 17% nC16 |
| T50 | Oxygenated Fuel Blend of 50% TEOP with 40% HMN and 10% nC16 |
| T70 | Oxygenated Fuel Blend of 70% TEOP with 30% HMN |
| T90 | Oxygenated Fuel Blend of 90% TEOP with 10% HMN (by volume) |
| TAMU | Texas A&M University |
| TDC | Top Dead Center |
| TDI | Turbocharged Direct Injection |
| TEOP | TetraEthOxyPropane (oxygenated fuel, $C_{11}H_{24}O_4$) |
| THC | Total Hydrocarbons |
| $TiO_2$ | Titanium dioxide |
| TPGME | Tripropylene Glycol Monomethyl Ether |
| TPM | Total Particulate Matter |
| UCB | University of California, Berkeley |
| UHC | Unburned Hydrocarbon |
| UM | University of Michigan |
| UW ERC | University of Wisconsin Engine Research Center |
| VOF | Volatile Organic Fraction |
| VVA | Variable Valve Actuation |
| WSU | Wayne State University |
| Wt | Weight |
| YSZ | Yttria-Stabilized Zirconia |